

6.1 THE CONCEPT OF STABILITY

When considering the design and analysis of feedback control systems, **stability** is of the utmost importance. From a practical point of view, a closed-loop feedback system that is unstable is of little value. As with all such general statements, there are exceptions; but for our purposes, we will declare that all our control designs must result in a closed-loop stable system. Many physical systems are inherently open-loop unstable, and some systems are even designed to be open-loop unstable. Most modern fighter aircraft are open-loop *unstable by design*, and without active feedback control assisting the pilot, they cannot fly. Active control is introduced by engineers to stabilize the unstable system—that is, the aircraft—so that other considerations, such as transient performance, can be addressed. Using feedback, we can stabilize unstable systems and then with a judicious selection of controller parameters, we can adjust the transient performance. For open-loop stable systems, we still use feedback to adjust the closed-loop performance to meet the design specifications. These specifications take the form of steady-state tracking errors, percent overshoot, settling time, time to peak, and the other indices discussed in Chapters 4 and 5.

We can say that a closed-loop feedback system is either stable or it is not stable. This type of stable/not stable characterization is referred to as **absolute stability**. A system possessing absolute stability is called a stable system—the label of absolute is dropped. Given that a closed-loop system is stable, we can further characterize the degree of stability. This is referred to as **relative stability**. The pioneers of aircraft design were familiar with the notion of relative stability—the more stable an aircraft was, the more difficult it was to maneuver (that is, to turn). One outcome of the relative instability of modern fighter aircraft is high maneuverability. A fighter aircraft is less stable than a commercial transport, hence it can maneuver more quickly. In fact, the motions of a fighter aircraft can be quite violent to the “passengers.” As we will discuss later in this section, we can determine that a system is stable (in the absolute sense) by determining that all transfer function poles lie in the left-half s -plane, or equivalently, that all the eigenvalues of the system matrix A lie in the left-half s -plane. Given that all the poles (or eigenvalues) are in the left-half s -plane, we investigate relative-stability by examining the relative locations of the poles (or eigenvalues).

A **stable system** is defined as a system with a bounded (limited) system response. That is, if the system is subjected to a bounded input or disturbance and the response is bounded in magnitude, the system is said to be stable.

A stable system is a dynamic system with a bounded response to a bounded input.

The concept of stability can be illustrated by considering a right circular cone placed on a plane horizontal surface. If the cone is resting on its base and is tipped slightly, it returns to its original equilibrium position. This position and response are said to be stable. If the cone rests on its side and is displaced slightly, it rolls with no tendency to leave the position on its side. This position is designated as the neutral stability. On the other hand, if the cone is placed on its tip and released, it falls onto its side. This position is said to be unstable. These three positions are illustrated in Figure 6.1.

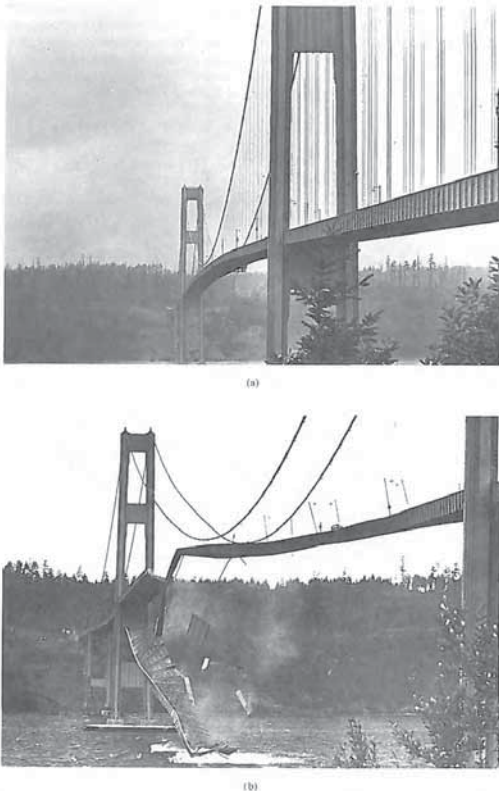


FIGURE 6.3
Tacoma Narrows Bridge (a) as oscillation begins (b) at catastrophic failure.

The Stability of Linear Feedback Systems

6.1	The Concept of Stability	387
6.2	The Routh–Hurwitz Stability Criterion	391
6.3	The Relative Stability of Feedback Control Systems	399
6.4	The Stability of State Variable Systems	401
6.5	Design Examples	404
6.6	System Stability Using Control Design Software	413
6.7	Sequential Design Example: Disk Drive Read System	421
6.8	Summary	424

P R E V I E W

Stability of closed-loop feedback systems is central to control system design. A stable system should exhibit a bounded output if the corresponding input is bounded. This is known as bounded-input–bounded-output stability and is one of the main topics of this chapter. The stability of a feedback system is directly related to the location of the roots of the characteristic equation of the system transfer function and to the location of the eigenvalues of the system matrix for a system in state variable format. The Routh–Hurwitz method is introduced as a useful tool for assessing system stability. The technique allows us to compute the number of roots of the characteristic equation in the right half plane without actually computing the values of the roots. This gives us a design method for determining values of certain system parameters that will lead to closed-loop stability. For stable systems, we will introduce the notion of relative stability, which allows us to characterize the degree of stability. The chapter concludes with a stabilizing controller design based on the Routh–Hurwitz method for the Sequential Design Example: Disk Drive Read System.

DESIRED OUTCOMES

Upon completion of Chapter 6, students should:

- Understand the concept of stability of dynamic systems.
- Be aware of the key concepts of absolute and relative stability.
- Be familiar with the notion of bounded-input, bounded-output stability.
- Understand the relationship of the s -plane pole locations (for transfer function models) and of the eigenvalue locations (for state variable models) to system stability.
- Know how to construct a Routh array and be able to employ the Routh–Hurwitz stability criterion to determine stability.

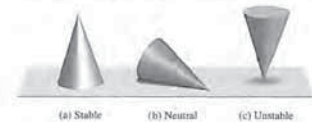


FIGURE 6.1
The stability of a cone.

The stability of a dynamic system is defined in a similar manner. The response to a displacement, or initial condition, will result in either a decreasing, neutral, or increasing response. Specifically, it follows from the definition of stability that a linear system is stable if and only if the absolute value of its impulse response $g(t)$, integrated over an infinite range, is finite. That is, in terms of the convolution integral Equation (5.2) for a bounded input, $\int_0^{\infty} |g(t)| dt$ must be finite.

The location in the s -plane of the poles of a system indicates the resulting transient response. The poles in the left-hand portion of the s -plane result in a decreasing response for disturbance inputs. Similarly, poles on the $j\omega$ -axis and in the right-hand plane result in a neutral and an increasing response, respectively, for a disturbance input. This division of the s -plane is shown in Figure 6.2. Clearly, the poles of desirable dynamic systems must lie in the left-hand portion of the s -plane [1–3].

A common example of the potential destabilizing effect of feedback is that of feedback in audio amplifier and speaker systems used for public address in auditoriums. In this case, a loudspeaker produces an audio signal that is an amplified version of the sounds picked up by a microphone. In addition to other audio inputs, the sound coming from the speaker itself may be sensed by the microphone. The strength of this particular signal depends upon the distance between the loudspeaker and the microphone. Because of the attenuating properties of air, a larger distance will cause a weaker signal to reach the microphone. Due to the finite propagation speed of sound waves, there will also be a time delay between the signal produced by the loudspeaker and the signal sensed by the microphone. In this case, the output from the feedback path is added to the external input. This is an example of positive feedback.

As the distance between the loudspeaker and the microphone decreases, we find that if the microphone is placed too close to the speaker, then the system will be unstable. The result of this instability is an excessive amplification and distortion of audio signals and an oscillatory squeal.

Another example of an unstable system is shown in Figure 6.3. The first bridge across the Tacoma Narrows at Puget Sound, Washington, was opened to traffic on July 1, 1940. The bridge was found to oscillate whenever the wind blew. After four

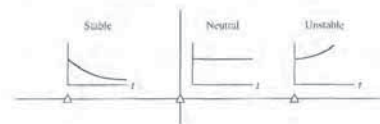


FIGURE 6.2
Stability in the s -plane.

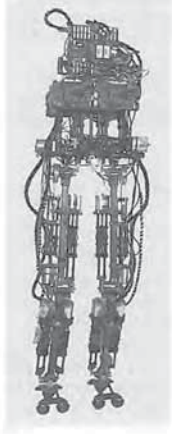


FIGURE 6.4 The M2 robot is more energy-efficient but less stable than many other designs that are well-balanced but consume much more power. (Courtesy of Professor Gill Pratt, Olin College.)

There are about one million robots in service throughout the world [10]. As the capability of robots increases, it is reasonable to assume that the numbers in service will continue to rise. Especially interesting are robots with human characteristics, particularly those that can walk upright. A class of robots that utilize series-elastic actuators as mechanical muscles emerged in the late 1990s. The M2 robot depicted in Figure 6.4 is more energy-efficient but less stable than many other designs that are well-balanced but consume much more power [21]. Examining the M2 robot in Figure 6.4, one can imagine that it is not inherently stable and that active control is required to keep it upright during the walking motion. In the next sections we present the Routh-Hurwitz stability criterion to investigate system stability by analyzing the characteristic equation without direct computation of the roots.

6.2 THE ROUTH-HURWITZ STABILITY CRITERION

The discussion and determination of stability has occupied the interest of many engineers. Maxwell and Vshnegradskii first considered the question of stability of dynamic systems. In the late 1800s, A. Hurwitz and E. J. Routh independently

Further rows of the schedule are then completed as

$$\begin{array}{c|ccc} s^n & a_n & a_{n-2} & a_{n-4} \\ s^{n-1} & a_{n-1} & a_{n-3} & a_{n-5} \\ s^{n-2} & b_{n-1} & b_{n-3} & b_{n-5} \\ s^{n-3} & c_{n-1} & c_{n-3} & a_{n-5} \\ \vdots & \vdots & \vdots & \vdots \\ s^0 & h_{n-1} & & \end{array}$$

where

$$b_{n-1} = \frac{a_{n-1}a_{n-2} - a_n a_{n-3}}{a_{n-1}}, \quad c_{n-1} = \frac{-1}{a_{n-1}} \begin{vmatrix} a_n & a_{n-2} \\ a_{n-1} & a_{n-3} \end{vmatrix},$$

$$b_{n-3} = \frac{-1}{a_{n-1}} \begin{vmatrix} a_n & a_{n-4} \\ a_{n-1} & a_{n-5} \end{vmatrix},$$

$$c_{n-1} = \frac{-1}{b_{n-1}} \begin{vmatrix} a_{n-1} & a_{n-3} \\ b_{n-1} & b_{n-3} \end{vmatrix},$$

and so on. The algorithm for calculating the entries in the array can be followed on a determinant basis or by using the form of the equation for b_{n-1} .

The Routh-Hurwitz criterion states that the number of roots of $q(s)$ with positive real parts is equal to the number of changes in sign of the first column of the Routh array. This criterion requires that there be no changes in sign in the first column for a stable system. This requirement is both necessary and sufficient.

Four distinct cases or configurations of the first column array must be considered, and each must be treated separately and requires suitable modifications of the array calculation procedure: (1) No element in the first column is zero; (2) there is a zero in the first column, but some other elements of the row containing the zero in the first column are nonzero; (3) there is a zero in the first column, and the other elements of the row containing the zero are also zero; and (4) as in the third case, but with repeated roots on the $j\omega$ -axis.

To illustrate this method clearly, several examples will be presented for each case.

Case 1. No element in the first column is zero.

EXAMPLE 6.1 Second-order system

The characteristic polynomial of a second-order system is

$$q(s) = a_2 s^2 + a_1 s + a_0.$$

The Routh array is written as

$$\begin{array}{c|cc} s^2 & a_2 & a_0 \\ s^1 & a_1 & 0 \\ s^0 & b_1 & 0 \end{array}$$

months, on November 7, 1940, a wind produced an oscillation that grew in amplitude until the bridge broke apart. Figure 6.3(a) shows the condition at the beginning of oscillation; Figure 6.3(b) shows the catastrophic failure [5].

In terms of linear systems, we recognize that the stability requirement may be defined in terms of the location of the poles of the closed-loop transfer function. The closed-loop system transfer function is written as

$$T(s) = \frac{p(s)}{q(s)} = \frac{K \prod_{i=1}^M (s + z_i)}{s^N \prod_{k=1}^O (s + \sigma_k) \prod_{m=1}^R [s^2 + 2\alpha_m s + (\alpha_m^2 + \omega_m^2)]} \quad (6.1)$$

where $q(s) = \Delta(s) = 0$ is the characteristic equation whose roots are the poles of the closed-loop system. The output response for an impulse function input (when $N = 0$) is then

$$y(t) = \sum_{k=1}^O A_k e^{-\sigma_k t} + \sum_{m=1}^R B_m \left(\frac{1}{\omega_m} \right) e^{-\alpha_m t} \sin(\omega_m t + \theta_m), \quad (6.2)$$

where A_k and B_m are constants that depend on $\sigma_k, z_i, \alpha_m, K$, and ω_m . To obtain a bounded response, the poles of the closed-loop system must be in the left-hand portion of the s -plane. Thus, a necessary and sufficient condition for a feedback system to be stable is that all the poles of the system transfer function have negative real parts. A system is stable if all the poles of the transfer function are in the left-hand s -plane. A system is not stable if not all the roots are in the left-hand plane. If the characteristic equation has simple roots on the imaginary axis ($j\omega$ -axis) with all other roots in the left half-plane, the steady-state output will be sustained oscillations for a bounded input, unless the input is a sinusoid (which is bounded) whose frequency is equal to the magnitude of the $j\omega$ -axis roots. For this case, the output becomes unbounded. Such a system is called marginally stable, since only certain bounded inputs (sinusoids of the frequency of the poles) will cause the output to become unbounded. For an unstable system, the characteristic equation has at least one root in the right half of the s -plane or repeated $j\omega$ roots; for this case, the output will become unbounded for any input.

For example, if the characteristic equation of a closed-loop system is

$$(s + 10)(s^2 + 16) = 0,$$

then the system is said to be marginally stable. If this system is excited by a sinusoid of frequency $\omega = 4$, the output becomes unbounded.

To ascertain the stability of a feedback control system, we could determine the roots of the characteristic polynomial $q(s)$. However, we are first interested in determining the answer to the question, Is the system stable? If we calculate the roots of the characteristic equation in order to answer this question, we have determined much more information than is necessary. Therefore, several methods have been developed that provide the required yes or no answer to the stability question. The three approaches to the question of stability are (1) the s -plane approach, (2) the frequency plane ($j\omega$) approach, and (3) the time-domain approach. The real frequency ($j\omega$) approach is outlined in Chapter 9, and the discussion of the time-domain approach is considered in Section 6.4.

published a method of investigating the stability of a linear system [6, 7]. The Routh-Hurwitz stability method provides an answer to the question of stability by considering the characteristic equation of the system. The characteristic equation in the Laplace variable is written as

$$\Delta(s) = q(s) = a_n s^n + a_{n-1} s^{n-1} + \dots + a_1 s + a_0 = 0. \quad (6.3)$$

To ascertain the stability of the system, it is necessary to determine whether any one of the roots of $q(s)$ lies in the right half of the s -plane. If Equation (6.3) is written in factored form, we have

$$a_n (s - r_1)(s - r_2) \dots (s - r_n) = 0, \quad (6.4)$$

where r_i is i th root of the characteristic equation. Multiplying the factors together, we find that

$$q(s) = a_n s^n - a_n (r_1 + r_2 + \dots + r_n) s^{n-1} + a_n (r_1 r_2 + r_2 r_3 + r_1 r_3 + \dots) s^{n-2} - a_n (r_1 r_2 r_3 + r_1 r_2 r_4 + \dots) s^{n-3} + \dots + a_n (-1)^n r_1 r_2 r_3 \dots r_n = 0. \quad (6.5)$$

In other words, for an n th-degree equation, we obtain

$$q(s) = a_n s^n - a_n (\text{sum of all the roots}) s^{n-1} + a_n (\text{sum of the products of the roots taken 2 at a time}) s^{n-2} - a_n (\text{sum of the products of the roots taken 3 at a time}) s^{n-3} + \dots + a_n (-1)^n (\text{product of all } n \text{ roots}) = 0. \quad (6.6)$$

Examining Equation (6.5), we note that all the coefficients of the polynomial must have the same sign if all the roots are in the left-hand plane. Also, it is necessary that all the coefficients for a stable system be nonzero. These requirements are necessary but not sufficient. That is, we immediately know the system is unstable if they are not satisfied; yet if they are satisfied, we must proceed further to ascertain the stability of the system. For example, when the characteristic equation is

$$q(s) = (s + 2)(s^2 - s + 4) = (s^3 + s^2 + 2s + 8), \quad (6.7)$$

the system is unstable, and yet the polynomial possesses all positive coefficients.

The Routh-Hurwitz criterion is a necessary and sufficient criterion for the stability of linear systems. The method was originally developed in terms of determinants, but we shall use the more convenient array formulation.

The Routh-Hurwitz criterion is based on ordering the coefficients of the characteristic equation

$$a_n s^n + a_{n-1} s^{n-1} + a_{n-2} s^{n-2} + \dots + a_1 s + a_0 = 0 \quad (6.8)$$

into an array or schedule as follows [4]:

$$\begin{array}{c|ccc} s^n & a_n & a_{n-2} & a_{n-4} \dots \\ s^{n-1} & a_{n-1} & a_{n-3} & a_{n-5} \dots \end{array}$$

approach zero after completing the array. For example, consider the following characteristic polynomial:

$$q(s) = s^5 + 2s^4 + 2s^3 + 4s^2 + 11s + 10. \quad (6.10)$$

The Routh array is then

$$\begin{array}{c|ccc} s^5 & 1 & 2 & 11 \\ s^4 & 2 & 4 & 10 \\ s^3 & \epsilon & 6 & 0 \\ s^2 & c_1 & 10 & 0 \\ s^1 & d_1 & 0 & 0 \\ s^0 & 10 & 0 & 0 \end{array}$$

where

$$c_1 = \frac{4\epsilon - 12}{\epsilon} = \frac{-12}{\epsilon} \quad \text{and} \quad d_1 = \frac{6c_1 - 10\epsilon}{c_1} \rightarrow 6.$$

There are two sign changes due to the large negative number in the first column, $c_1 = -12/\epsilon$. Therefore, the system is unstable, and two roots lie in the right half of the plane.

EXAMPLE 6.3 Unstable system

As a final example of the type of Case 2, consider the characteristic polynomial

$$q(s) = s^4 + s^3 + s^2 + s + K, \quad (6.11)$$

where we desire to determine the gain K that results in marginal stability. The Routh array is then

$$\begin{array}{c|ccc} s^4 & 1 & 1 & K \\ s^3 & 1 & 1 & 0 \\ s^2 & \epsilon & K & 0 \\ s^1 & c_1 & 0 & 0 \\ s^0 & K & 0 & 0 \end{array}$$

where

$$c_1 = \frac{\epsilon - K}{\epsilon} \rightarrow \frac{-K}{\epsilon}.$$

Therefore, for any value of K greater than zero, the system is unstable. Also, because the last term in the first column is equal to K , a negative value of K will result in an unstable system. Consequently, the system is unstable for all values of gain K . ■

Case 3. There is a zero in the first column, and the other elements of the row containing the zero are also zero. Case 3 occurs when all the elements in one row are zero or when the row consists of a single element that is zero. This condition occurs when the polynomial contains singularities that are symmetrically located about the origin of the s -plane. Therefore, Case 3 occurs when factors such as $(s + \sigma)(s - \sigma)$

where

$$b_1 = \frac{a_1 a_0 - (0)a_2}{a_1} = \frac{-1}{a_1} \frac{a_2}{a_1} = a_0.$$

Therefore, the requirement for a stable second-order system is simply that all the coefficients be positive or all the coefficients be negative. ■

EXAMPLE 6.2 Third-order system

The characteristic polynomial of a third-order system is

$$q(s) = a_3 s^3 + a_2 s^2 + a_1 s + a_0.$$

The Routh array is

$$\begin{array}{c|cc} s^3 & a_3 & a_1 \\ s^2 & a_2 & a_0 \\ s^1 & b_1 & 0 \\ s^0 & c_1 & 0 \end{array}$$

where

$$b_1 = \frac{a_2 a_1 - a_0 a_3}{a_2} \quad \text{and} \quad c_1 = \frac{b_1 a_0}{b_1} = a_0.$$

For the third-order system to be stable, it is necessary and sufficient that the coefficients be positive and $a_2 a_1 > a_0 a_3$. The condition when $a_2 a_1 = a_0 a_3$ results in a marginal stability case, and one pair of roots lies on the imaginary axis in the s -plane. This marginal case is recognized as Case 3 because there is a zero in the first column when $a_2 a_1 = a_0 a_3$. It will be discussed under Case 3.

As a final example of characteristic equations that result in no zero elements in the first row, let us consider the polynomial

$$q(s) = (s - 1 + j\sqrt{7})(s - 1 - j\sqrt{7})(s + 3) = s^3 + s^2 + 2s + 24. \quad (6.9)$$

The polynomial satisfies all the necessary conditions because all the coefficients exist and are positive. Therefore, utilizing the Routh array, we have

$$\begin{array}{c|cc} s^3 & 1 & 2 \\ s^2 & 1 & 24 \\ s^1 & -22 & 0 \\ s^0 & 24 & 0 \end{array}$$

Because two changes in sign appear in the first column, we find that two roots of $q(s)$ lie in the right-hand plane, and our prior knowledge is confirmed. ■

Case 2. There is a zero in the first column, but some other elements of the row containing the zero in the first column are nonzero. If only one element in the array is zero, it may be replaced with a small positive number, ϵ , that is allowed to

Consider the system with a characteristic polynomial

$$q(s) = (s + 1)(s + j)(s - j)(s + j)(s - j) = s^5 + s^4 + 2s^3 + 2s^2 + s + 1.$$

The Routh array is

$$\begin{array}{c|ccc} s^5 & 1 & 2 & 1 \\ s^4 & 1 & 2 & 1 \\ s^3 & \epsilon & \epsilon & 0 \\ s^2 & 1 & 1 & \epsilon \\ s^1 & \epsilon & 0 & \epsilon \\ s^0 & 1 & & \end{array}$$

where $\epsilon \rightarrow 0$. Note the absence of sign changes, a condition that falsely indicates that the system is marginally stable. The impulse response of the system increases with time as $t \sin(t + \phi)$. The auxiliary polynomial at the s^2 line is $s^2 + 1$, and the auxiliary polynomial at the s^4 line is $s^4 + 2s^2 + 1 = (s^2 + 1)^2$, indicating the repeated roots on the $j\omega$ -axis.

EXAMPLE 6.4 Fifth-order system with roots on the $j\omega$ -axis

Consider the characteristic polynomial

$$q(s) = s^5 + s^4 + 4s^3 + 24s^2 + 3s + 63. \quad (6.15)$$

The Routh array is

$$\begin{array}{c|ccc} s^5 & 1 & 4 & 3 \\ s^4 & 1 & 24 & 63 \\ s^3 & -20 & -60 & 0 \\ s^2 & 21 & 63 & 0 \\ s^1 & 0 & 0 & 0 \end{array}$$

Therefore, the auxiliary polynomial is

$$U(s) = 21s^2 + 63 = 21(s^2 + 3) = 21(s + j\sqrt{3})(s - j\sqrt{3}), \quad (6.16)$$

which indicates that two roots are on the imaginary axis. To examine the remaining roots, we divide by the auxiliary polynomial to obtain

$$\frac{q(s)}{s^2 + 3} = s^3 + s^2 + s + 21.$$

Establishing a Routh array for this equation, we have

$$\begin{array}{c|ccc} s^3 & 1 & 1 \\ s^2 & 1 & 21 \\ s^1 & -20 & 0 \\ s^0 & 21 & 0 \end{array}$$

or $(s + j\omega)(s - j\omega)$ occur. This problem is circumvented by utilizing the **auxiliary polynomial**, $U(s)$, which immediately precedes the zero entry in the Routh array. The order of the auxiliary polynomial is always even and indicates the number of symmetrical root pairs.

To illustrate this approach, let us consider a third-order system with the characteristic polynomial

$$q(s) = s^3 + 2s^2 + 4s + K, \quad (6.12)$$

where K is an adjustable loop gain. The Routh array is then

$$\begin{array}{c|cc} s^3 & 1 & 4 \\ s^2 & 2 & K \\ s^1 & \frac{8-K}{2} & 0 \\ s^0 & K & 0 \end{array}$$

For a stable system, we require that

$$0 < K < 8.$$

When $K = 8$, we have two roots on the $j\omega$ -axis and a marginal stability case. Note that we obtain a row of zeros (Case 3) when $K = 8$. The auxiliary polynomial, $U(s)$, is the equation of the row preceding the row of zeros. The equation of the row preceding the row of zeros is, in this case, obtained from the s^2 -row. We recall that this row contains the coefficients of the even powers of s , and therefore we have

$$U(s) = 2s^2 + Ks^0 = 2s^2 + 8 = 2(s^2 + 4) = 2(s + j2)(s - j2). \quad (6.13)$$

To show that the auxiliary polynomial, $U(s)$, is indeed a factor of the characteristic polynomial, we divide $q(s)$ by $U(s)$ to obtain

$$\frac{s^3 + 2s^2 + 4s + 8}{2s^2 + 8} = \frac{\frac{1}{2}s + 1}{s^2 + 4} + \frac{4s}{2s^2 + 8} = \frac{1}{2} \frac{s + 2}{s^2 + 4} + \frac{2s}{s^2 + 4}$$

When $K = 8$, the factors of the characteristic polynomial are

$$q(s) = (s + 2)(s + j2)(s - j2). \quad (6.14)$$

The marginal case response is an unacceptable oscillation.

Case 4. Repeated roots of the characteristic equation on the $j\omega$ -axis. If the $j\omega$ -axis roots of the characteristic equation are simple, the system is neither stable nor unstable; it is instead called marginally stable, since it has an undamped sinusoidal mode. If the $j\omega$ -axis roots are repeated, the system response will be unstable with a form $t \sin(\omega t + \phi)$. The Routh–Hurwitz criteria will not reveal this form of instability [20].

Table 6.1 The Routh–Hurwitz Stability Criterion

<i>n</i>	Characteristic Equation	Criterion
2	$s^2 + bs + 1 = 0$	$b > 0$
3	$s^3 + bs^2 + cs + 1 = 0$	$bc - 1 > 0$
4	$s^4 + bs^3 + cs^2 + ds + 1 = 0$	$bcd - d^3 - b^2 > 0$
5	$s^5 + bs^4 + cs^3 + ds^2 + es + 1 = 0$	$bcd + b - d^2 - b^2e > 0$
6	$s^6 + bs^5 + cs^4 + ds^3 + es^2 + fs + 1 = 0$	$(bcd + bf - d^2 - b^2e)e + b^2c - bd - bc^2f - f^2 + bfe + cdf > 0$

Note: The equations are normalized by $(\omega_n)^n$.

We divide through by ω_n^n and use $\bar{s} = s/\omega_n$ to obtain the normalized form of the characteristic equation:

$$\bar{s}^n + b\bar{s}^{n-1} + c\bar{s}^{n-2} + \dots + 1 = 0.$$

For example, we normalize

$$s^3 + 5s^2 + 2s + 8 = 0$$

by dividing through by $8 = \omega_n^3$, obtaining

$$\frac{\bar{s}^3}{\omega_n^3} + \frac{5}{2} \frac{\bar{s}^2}{\omega_n^2} + \frac{2}{4} \frac{\bar{s}}{\omega_n} + 1 = 0.$$

or

$$\bar{s}^3 + 2.5\bar{s}^2 + 0.5\bar{s} + 1 = 0,$$

where $\bar{s} = s/\omega_n$. In this case, $b = 2.5$ and $c = 0.5$. Using this normalized form of the characteristic equation, we summarize the stability criterion for up to a sixth-order characteristic equation, as provided in Table 6.1. Note that $bc = 1.25$ and the system is stable.

6.3 THE RELATIVE STABILITY OF FEEDBACK CONTROL SYSTEMS

The verification of stability using the Routh–Hurwitz criterion provides only a partial answer to the question of stability. The Routh–Hurwitz criterion ascertains the absolute stability of a system by determining whether any of the roots of the characteristic equation lie in the right half of the *s*-plane. However, if the system satisfies the Routh–Hurwitz criterion and is absolutely stable, it is desirable to determine the **relative stability**; that is, it is necessary to investigate the relative damping of each root of the characteristic equation. The relative stability of a system can be defined as the property that is measured by the relative real part of each root or pair of roots. Thus, root r_2 is relatively more stable than the roots r_1, \bar{r}_1 , as shown in Figure 6.6. The relative stability of a system can also be defined in terms of the relative damping coefficients ζ of each complex root pair and, therefore, in terms of the speed of response and overshoot instead of settling time.

Hence, the investigation of the relative stability of each root is clearly necessary because, as we found in Chapter 5, the location of the closed-loop poles in the *s*-plane determines the performance of the system. Thus, it is imperative that we

6.4 THE STABILITY OF STATE VARIABLE SYSTEMS

The stability of a system modeled by a state variable flow graph model can be readily ascertained. The stability of a system with an input–output transfer function $T(s)$ can be determined by examining the denominator polynomial of $T(s)$. Therefore, if the transfer function is written as

$$T(s) = \frac{p(s)}{q(s)},$$

where $p(s)$ and $q(s)$ are polynomials in *s*, then the stability of the system is represented by the roots of $q(s)$. The polynomial $q(s)$, when set equal to zero, is called the characteristic equation. The roots of the characteristic equation must lie in the left-hand *s*-plane for the system to exhibit a stable time response. Therefore, to ascertain the stability of a system represented by a transfer function, we investigate the characteristic equation and utilize the Routh–Hurwitz criterion. If the system we are investigating is represented by a signal-flow graph state model, we obtain the characteristic equation by evaluating the flow graph determinant. If the system is represented by a block diagram model we obtain the characteristic equation using the block diagram reduction methods. As an illustration of these methods, let us investigate the stability of the system of Example 3.2.

EXAMPLE 6.7 Stability of a system

The transfer function $T(s)$ examined in Example 3.2 is

$$T(s) = \frac{2s^2 + 8s + 6}{s^3 + 8s^2 + 16s + 6}. \tag{6.20}$$

The characteristic polynomial for this system is

$$q(s) = s^3 + 8s^2 + 16s + 6. \tag{6.21}$$

This characteristic polynomial is also readily obtained from either the flow graph model or block diagram model shown in Figure 3.11 or the ones shown in Figure 3.13. Using the Routh–Hurwitz criterion, we find that the system is stable and that all the roots of $q(s)$ lie in the left-hand *s*-plane. ■

We often determine the flow graph or block diagram model directly from a set of state differential equations. We can use the flow graph directly to determine the stability of the system by obtaining the characteristic equation from the flow graph determinant $\Delta(s)$. Similarly, we can use block diagram reduction to define the characteristic equation. An illustration of these approaches will aid in comprehending these methods.

EXAMPLE 6.8 Stability of a second-order system

A second-order system is described by the two first-order differential equations

$$\dot{x}_1 = -3x_1 + x_2 \quad \text{and} \quad \dot{x}_2 = +1x_2 - Kx_1 + Ku.$$

The two changes in sign in the first column indicate the presence of two roots in the right-hand plane, and the system is unstable. The roots in the right-hand plane are $s = +1 \pm j\sqrt{6}$. ■

EXAMPLE 6.5 Welding control

Large welding robots are used in today's auto plants. The welding head is moved to different positions on the auto body, and a rapid, accurate response is required. A block diagram of a welding head positioning system is shown in Figure 6.5. We desire to determine the range of K and a for which the system is stable. The characteristic equation is

$$1 + G(s) = 1 + \frac{K(s + a)}{s(s + 1)(s + 2)(s + 3)} = 0.$$

Therefore, $q(s) = s^4 + 6s^3 + 11s^2 + (K + 6)s + Ka = 0$. Establishing the Routh array, we have

s^4	1	11	Ka
s^3	6	$K + 6$	
s^2	b_3	Ka	
s^1	c_3		
s^0	Ka		

where

$$b_3 = \frac{60 - K}{6} \quad \text{and} \quad c_3 = \frac{b_3(K + 6) - 6Ka}{b_3}.$$

The coefficient c_3 sets the acceptable range of K and a , while b_3 requires that K be less than 60. Requiring $c_3 \geq 0$, we obtain

$$(K - 60)(K + 6) + 36Ka \geq 0.$$

The required relationship between K and a is then

$$a \leq \frac{(60 - K)(K + 6)}{36K}$$

when a is positive. Therefore, if $K = 40$, we require $a \leq 0.639$. ■

The general form of the characteristic equation of an *n*th-order system is

$$s^n + a_{n-1}s^{n-1} + a_{n-2}s^{n-2} + \dots + a_1s + a_0 = 0.$$

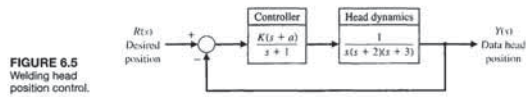


FIGURE 6.5 Welding head position control.

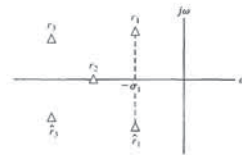


FIGURE 6.6 Root locations in the *s*-plane.

reexamine the characteristic polynomial $q(s)$ and consider several methods for the determination of relative stability.

Because the relative stability of a system is dictated by the location of the roots of the characteristic equation, a first approach using an *s*-plane formulation is to extend the Routh–Hurwitz criterion to ascertain relative stability. This can be simply accomplished by utilizing a change of variable, which shifts the *s*-plane axis in order to utilize the Routh–Hurwitz criterion. Examining Figure 6.6, we notice that a shift of the vertical axis in the *s*-plane to $-\sigma_1$ will result in the roots r_1, \bar{r}_1 appearing on the shifted axis. The correct magnitude to shift the vertical axis must be obtained on a trial-and-error basis. Then, without solving the fifth-order polynomial $q(s)$, we may determine the real part of the dominant roots r_1, \bar{r}_1 .

EXAMPLE 6.6 Axis shift

Consider the simple third-order characteristic equation

$$q(s) = s^3 + 4s^2 + 6s + 4. \tag{6.17}$$

As a first try, let $s_u = s + 1/2$ and note that we obtain a Routh array without a zero occurring in the first column. However, upon setting the shifted variable s_u equal to $s + 1$, we obtain

$$(s_u - 1)^3 + 4(s_u - 1)^2 + 6(s_u - 1) + 4 = s_u^3 + s_u^2 + s_u + 1. \tag{6.18}$$

Then the Routh array is established as

s_u^3	1	1
s_u^2	1	1
s_u^1	0	0
s_u^0	1	0

There are roots on the shifted imaginary axis that can be obtained from the auxiliary polynomial

$$U(s_u) = s_u^2 + 1 = (s_u + j)(s_u - j) = (s + 1 + j)(s + 1 - j). \tag{6.19}$$

The shifting of the *s*-plane axis to ascertain the relative stability of a system is a very useful approach, particularly for higher-order systems with several pairs of closed-loop complex conjugate roots.

or

$$\Delta(s) = (s - 1)(s + 3) + K = s^2 + 2s + (K - 3) = 0.$$

This confirms the results obtained using signal-flow graph techniques. ■

A method of obtaining the characteristic equation directly from the vector differential equation is based on the fact that the solution to the unforced system is an exponential function. The vector differential equation without input signals is

$$\dot{\mathbf{x}} = \mathbf{A}\mathbf{x}, \quad (6.22)$$

where \mathbf{x} is the state vector. The solution is of exponential form, and we can define a constant λ such that the solution of the system for one state can be of the form $x_i(t) = k_i e^{\lambda t}$. The λ_i are called the characteristic roots or eigenvalues of the system, which are simply the roots of the characteristic equation. If we let $\mathbf{x} = \mathbf{k}e^{\lambda t}$ and substitute into Equation (6.22), we have

$$\lambda \mathbf{k}e^{\lambda t} = \mathbf{A}\mathbf{k}e^{\lambda t}, \quad (6.23)$$

or

$$\lambda \mathbf{x} = \mathbf{A}\mathbf{x}. \quad (6.24)$$

Equation (6.24) can be rewritten as

$$(\lambda \mathbf{I} - \mathbf{A})\mathbf{x} = \mathbf{0}, \quad (6.25)$$

where \mathbf{I} equals the identity matrix and $\mathbf{0}$ equals the null matrix. This set of simultaneous equations has a nontrivial solution if and only if the determinant vanishes—that is, only if

$$\det(\lambda \mathbf{I} - \mathbf{A}) = 0. \quad (6.26)$$

The n th-order equation in λ resulting from the evaluation of this determinant is the characteristic equation, and the stability of the system can be readily ascertained. Let us consider again the third-order system described in Example 3.3 to illustrate this approach.

EXAMPLE 6.9 Closed epidemic system

The vector differential equation of the epidemic system is given in Equation (3.63) and repeated here as

$$\frac{d\mathbf{x}}{dt} = \begin{bmatrix} -\alpha & -\beta & 0 \\ \beta & -\gamma & 0 \\ \alpha & \gamma & 0 \end{bmatrix} \mathbf{x} + \begin{bmatrix} 1 & 0 \\ 0 & 1 \\ 0 & 0 \end{bmatrix} \begin{bmatrix} u_1 \\ u_2 \end{bmatrix}.$$

The characteristic equation is then

$$\begin{aligned} \det(\lambda \mathbf{I} - \mathbf{A}) &= \det \left\{ \begin{bmatrix} \lambda & 0 & 0 \\ 0 & \lambda & 0 \\ 0 & 0 & \lambda \end{bmatrix} - \begin{bmatrix} -\alpha & -\beta & 0 \\ \beta & -\gamma & 0 \\ \alpha & \gamma & 0 \end{bmatrix} \right\} \\ &= \det \begin{bmatrix} \lambda + \alpha & \beta & 0 \\ -\beta & \lambda + \gamma & 0 \\ -\alpha & -\gamma & \lambda \end{bmatrix} \end{aligned}$$

Section 6.5 Design Examples

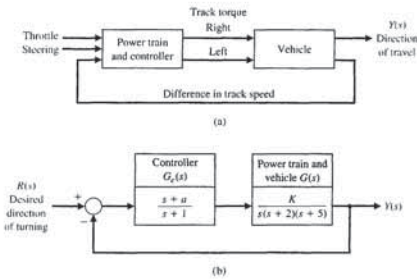


FIGURE 6.8 (a) Turning control system for a two-track vehicle. (b) Block diagram.

We must select K and a so that the system is stable and the steady-state error for a ramp command is less than or equal to 24% of the magnitude of the command.

The characteristic equation of the feedback system is

$$1 + G_c G_v(s) = 0,$$

or

$$1 + \frac{K(s+a)}{s(s+1)(s+2)(s+5)} = 0. \quad (6.27)$$

Therefore, we have

$$s(s+1)(s+2)(s+5) + K(s+a) = 0,$$

or

$$s^4 + 8s^3 + 17s^2 + (K+10)s + Ka = 0. \quad (6.28)$$

To determine the stable region for K and a , we establish the Routh array as

s^4	1	17	Ka
s^3	8	$K+10$	0
s^2	b_3	Ka	
s^1	c_3		
s^0	Ka		

where

$$b_3 = \frac{126 - K}{8} \quad \text{and} \quad c_3 = \frac{b_3(K+10) - 8Ka}{b_3}.$$

For the elements of the first column to be positive, we require that Ka , b_3 , and c_3 be positive. Therefore, we require that

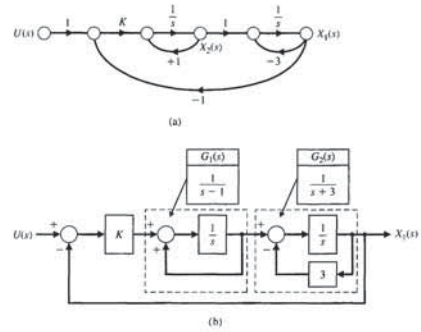


FIGURE 6.7 (a) Flow graph model for state variable equations of Example 6.8. (b) Block diagram model.

where the dot notation implies the first derivative and $u(t)$ is the input. The flow graph model of this set of differential equations is shown in Figure 6.7(a) and the block diagram model is shown in Figure 6.7(b).

Using Mason's signal-flow gain formula, we note three loops:

$$L_1 = s^{-1}, \quad L_2 = -3s^{-1}, \quad \text{and} \quad L_3 = -Ks^{-2},$$

where L_1 and L_2 do not share a common node. Therefore, the determinant is

$$\Delta = 1 - (L_1 + L_2 + L_3) + L_1L_2 = 1 - (s^{-1} - 3s^{-1} - Ks^{-2}) + (-3s^{-2}).$$

We multiply by s^2 to obtain the characteristic equation

$$s^2 + 2s + (K - 3) = 0.$$

Since all coefficients must be positive, we require $K > 3$ for stability. A similar analysis can be undertaken using the block diagram. Closing the two feedback loops yields the two transfer functions

$$G_1(s) = \frac{1}{s-1} \quad \text{and} \quad G_2(s) = \frac{1}{s+3},$$

as illustrated in Figure 6.7(b). The closed loop transfer function is thus

$$T(s) = \frac{KG_1(s)G_2(s)}{1 + KG_1(s)G_2(s)}.$$

Therefore, the characteristic equation is

$$\Delta(s) = 1 + KG_1(s)G_2(s) = 0,$$

$$\begin{aligned} &= \lambda[(\lambda + \alpha)(\lambda + \gamma) + \beta^2] \\ &= \lambda[\lambda^2 + (\alpha + \gamma)\lambda + (\alpha\gamma + \beta^2)] = 0. \end{aligned}$$

Thus, we obtain the characteristic equation of the system, and it is similar to that obtained in Equation (3.65) by flow graph methods. The additional root $\lambda = 0$ results from the definition of x_3 as the integral of $\alpha x_1 + \gamma x_2$, and x_3 does not affect the other state variables. Thus, the root $\lambda = 0$ indicates the integration connected with x_3 . The characteristic equation indicates that the system is marginally stable when $\alpha + \gamma > 0$ and $\alpha\gamma + \beta^2 > 0$. ■

As another example, consider again the inverted pendulum described in Example 3.4. The system matrix is

$$\mathbf{A} = \begin{bmatrix} 0 & 1 & 0 & 0 \\ 0 & 0 & -mg/M & 0 \\ 0 & 0 & 0 & 1 \\ 0 & 0 & gl & 0 \end{bmatrix}.$$

The characteristic equation can be obtained from the determinant of $(\lambda \mathbf{I} - \mathbf{A})$ as follows:

$$\det \begin{bmatrix} \lambda & -1 & 0 & 0 \\ 0 & \lambda & mg/M & 0 \\ 0 & 0 & \lambda & -1 \\ 0 & 0 & -gl & \lambda \end{bmatrix} = \lambda \left[\lambda \left(\lambda^2 - \frac{g}{l} \right) \right] = \lambda^2 \left(\lambda^2 - \frac{g}{l} \right) = 0.$$

The characteristic equation indicates that there are two roots at $\lambda = 0$: a root at $\lambda = +\sqrt{gl}$ and a root at $\lambda = -\sqrt{gl}$. Hence, the system is unstable, because there is a root in the right-hand plane at $\lambda = +\sqrt{gl}$. The two roots at $\lambda = 0$ will also result in an unbounded response.

6.5 DESIGN EXAMPLES

In this section we present two illustrative examples. The first example is a tracked vehicle control problem. In this first example, stability issues are addressed employing the Routh-Hurwitz stability criterion and the outcome is the selection of two key system parameters. The second example illustrates the stability problem robot-controlled motorcycle and how Routh-Hurwitz can be used in the selection of controller gains during the design process. The robot-controlled motorcycle example highlights the design process with special attention to the impact of key controller parameters on stability.

EXAMPLE 6.10 Tracked vehicle turning control

The design of a turning control for a tracked vehicle involves the selection of two parameters [8]. In Figure 6.8, the system shown in part (a) has the model shown in part (b). The two tracks are operated at different speeds in order to turn the vehicle.

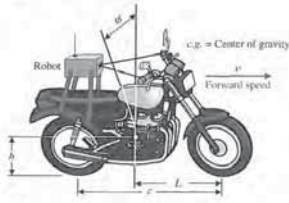


FIGURE 6.10 The robot-controlled motorcycle.

The design elements highlighted in this example are illustrated in Figure 6.11. Using the Routh–Hurwitz stability criterion will allow us to get to the heart of the matter, that is, to develop a strategy for computing the controller gains while ensuring closed-loop stability.

The control goal is

Control Goal

Control the motorcycle in the vertical position, and maintain the prescribed position in the presence of disturbances.

The variable to be controlled is

Variable to Be Controlled

The motorcycle position from vertical (ϕ).

Since our focus here is on stability rather than transient response characteristics, the control specifications will be related to stability only; transient performance is an issue that we need to address once we have investigated all the stability issues. The control design specification is

Design Specification

DS1 The closed-loop system must be stable.

The main components of the robot-controlled motorcycle are the motorcycle and robot, the controller, and the feedback measurements. The main subject of the chapter is not modeling, so we do not concentrate on developing the motorcycle dynamics model. We rely instead on the work of others (see [22]). The motorcycle model is given by

$$G(s) = \frac{1}{s^2 - \alpha_1} \tag{6.31}$$

where $\alpha_1 = g/h$, $g = 9.806 \text{ m/s}^2$, and h is the height of the motorcycle center of gravity above the ground (see Figure 6.10). The motorcycle is unstable with poles at $\pm \sqrt{\alpha_1}$. The controller is given by

$$G_c(s) = \frac{\alpha_2 + \alpha_3 s}{\tau s + 1} \tag{6.32}$$

Control is accomplished by turning the handlebar. The front wheel rotation about the vertical is not evident in the transfer functions. Also, the transfer functions assume a constant forward speed v which means that we must have another control system at work regulating the forward speed. Nominal motorcycle and robot controller parameters are given in Table 6.2.

Assembling the components of the feedback system gives us the system configuration shown in Figure 6.12. Examination of the configuration reveals that the robot controller block is a function of the physical system (h , c , and L), the operating conditions (v), and the robot time-constant (τ). No parameters need adjustment unless we physically change the motorcycle parameters and/or speed. In fact, in this example the parameters we want to adjust are in the feedback loop:

Select Key Tuning Parameters

Feedback gains K_P and K_D .

The key tuning parameters are not always in the forward path; in fact they may exist in any subsystem in the block diagram.

We want to use the Routh–Hurwitz technique to analyze the closed-loop system stability. What values of K_P and K_D lead to closed-loop stability? A related question that we can pose is, given specific values of K_P and K_D for the nominal system (that is, nominal values of α_1 , α_2 , α_3 , and τ), how can the parameters themselves vary while still retaining closed-loop stability?

Table 6.2 Physical Parameters

τ	0.2 s
α_1	9 1/s ²
α_2	2.7 1/s ²
α_3	1.35 1/s
h	1.09 m
V	2.0 m/s
L	1.0 m
c	1.36 m

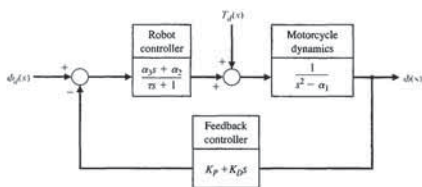


FIGURE 6.12 The robot-controlled motorcycle feedback system block diagram.

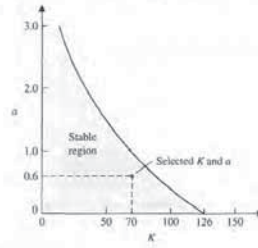


FIGURE 6.9 The stable region.

$$K < 126, \quad Ka > 0, \quad \text{and} \quad (K + 10)(126 - K) - 64Ka > 0. \tag{6.29}$$

The region of stability for $K > 0$ is shown in Figure 6.9. The steady-state error to a ramp input $r(t) = At$, $t > 0$ is

$$e_{ss} = A/Kv$$

where

$$K_v = \lim_{s \rightarrow 0} sG_c G = Ka/10.$$

Therefore, we have

$$e_{ss} = \frac{10A}{Ka} \tag{6.30}$$

When e_{ss} is equal to 23.8% of A , we require that $Ka = 42$. This can be satisfied by the selected point in the stable region when $K = 70$ and $a = 0.6$, as shown in Figure 6.9. Another acceptable design would be attained when $K = 50$ and $a = 0.84$. We can calculate a series of possible combinations of K and a that can satisfy $Ka = 42$ and that lie within the stable region, and all will be acceptable design solutions. However, not all selected values of K and a will lie within the stable region. Note that K cannot exceed 126. ■

EXAMPLE 6.11 Robot-controlled motorcycle

Consider the robot-controlled motorcycle shown in Figure 6.10. The motorcycle will move in a straight line at constant forward speed v . Let ϕ denote the angle between the plane of symmetry of the motorcycle and the vertical. The desired angle ϕ_d is equal to zero:

$$\phi_d(s) = 0.$$

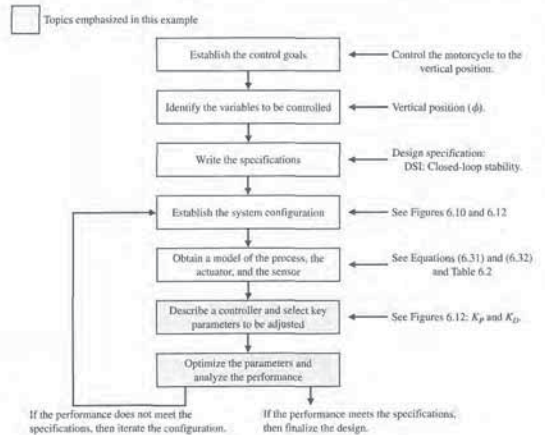


FIGURE 6.11 Elements of the control system design process emphasized in this robot-controlled motorcycle example.

where

$$\alpha_2 = v^2/(hc)$$

and

$$\alpha_3 = vL/(hc).$$

The forward speed of the motorcycle is denoted by v , and c denotes the wheel-base (the distance between the wheel centers). The length, L , is the horizontal distance between the front wheel axle and the motorcycle center of gravity. The time-constant of the controller is denoted by τ . This term represents the speed of response of the controller; smaller values of τ indicate an increased speed of response. Many simplifying assumptions are necessary to obtain the simple transfer function models in Equations (6.31) and (6.32).

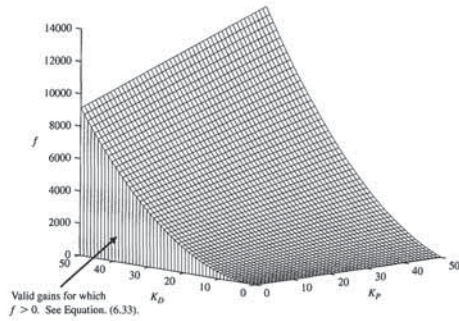


FIGURE 6.13 Region of valid gains (K_D, K_P) for which the inequality in Equation (6.33) is satisfied.

For this robot-controlled motorcycle, we do not expect to have to respond to nonzero command inputs (that is, $\phi_d \neq 0$) since we want the motorcycle to remain upright, and we certainly want to remain upright in the presence of external disturbances. The transfer function for the disturbance $T_d(s)$ to the output $\phi(s)$ without feedback is

$$\phi(s) = \frac{1}{s^2 - \alpha_1} T_d(s).$$

The characteristic equation is

$$q(s) = s^2 - \alpha_1 = 0.$$

The system poles are

$$s_1 = -\sqrt{\alpha_1} \text{ and } s_2 = +\sqrt{\alpha_1}.$$

Thus we see that the motorcycle is unstable; it possesses a pole in the right half-plane. Without feedback control, any external disturbance will result in the motorcycle falling over. Clearly the need for a control system (usually provided by the human rider) is necessary. With the feedback and robot controller in the loop, the closed-loop transfer function from the disturbance to the output is

$$\frac{\phi(s)}{T_d(s)} = \frac{\tau s + 1}{\tau s^3 + (1 + K_D \alpha_3) s^2 + (K_D \alpha_2 + K_P \alpha_3 - \tau \alpha_1) s + K_P \alpha_2 - \alpha_1}.$$

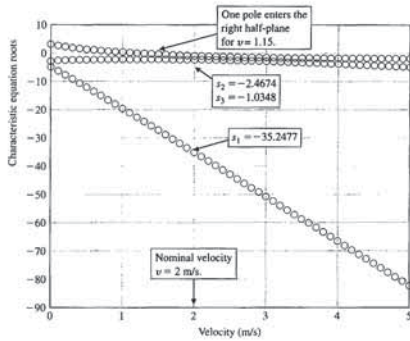


FIGURE 6.15 Roots of the characteristic equation as the motorcycle velocity varies.

6.6 SYSTEM STABILITY USING CONTROL DESIGN SOFTWARE

This section begins with a discussion of the Routh–Hurwitz stability method. We will see how the computer can assist us in the stability analysis by providing an easy and accurate method for computing the poles of the characteristic equation. For the case of the characteristic equation as a function of a single parameter, it will be possible to generate a plot displaying the movement of the poles as the parameter varies. The section concludes with an example.

The function introduced in this section is the function for, which is used to repeat a number of statements a specific number of times.

Routh–Hurwitz Stability. As stated earlier, the Routh–Hurwitz criterion is a necessary and sufficient criterion for stability. Given a characteristic equation with fixed coefficients, we can use Routh–Hurwitz to determine the number of roots in the right half-plane. For example, consider the characteristic equation

$$q(s) = s^3 + s^2 + 2s + 24 = 0$$

associated with the closed-loop control system shown in Figure 6.16. The corresponding Routh–Hurwitz array is shown in Figure 6.17. The two sign changes in the first column indicate that there are two roots of the characteristic polynomial in the right half-plane; hence, the closed-loop system is unstable. We can verify the Routh–Hurwitz result by directly computing the roots of the characteristic equation, as shown in Figure 6.18, using the pole function. Recall that the pole function computes the system poles.

Whenever the characteristic equation is a function of a single parameter, the Routh–Hurwitz method can be utilized to determine the range of values that the

The closed-loop transfer function from $\phi_d(s)$ to $\phi(s)$ is

$$T(s) = \frac{\alpha_2 + \alpha_3 s}{\Delta(s)},$$

where

$$\Delta(s) = \tau s^3 + (1 + K_D \alpha_3) s^2 + (K_D \alpha_2 + K_P \alpha_3 - \tau \alpha_1) s + K_P \alpha_2 - \alpha_1.$$

The characteristic equation is

$$\Delta(s) = 0.$$

The question that we need to answer is for what values of K_P and K_D does the characteristic equation $\Delta(s) = 0$ have all roots in the left half-plane?

We can set up the following Routh array:

$$\begin{array}{c|cc} s^3 & \tau & K_D \alpha_2 + K_P \alpha_3 - \tau \alpha_1 \\ s^2 & 1 + K_D \alpha_3 & K_P \alpha_2 - \alpha_1 \\ s & a & \\ 1 & K_P \alpha_2 - \alpha_1 & \end{array}$$

where

$$a = \frac{(1 + K_D \alpha_3)(K_D \alpha_2 + K_P \alpha_3 - \tau \alpha_1) - \tau(K_P \alpha_2 - \alpha_1)}{1 + K_D \alpha_3}.$$

By inspecting column 1, we determine that for stability we require

$$\tau > 0, K_D > -1/\alpha_3, K_P > \alpha_1/\alpha_2, \text{ and } a > 0.$$

Choosing $K_D > 0$ satisfies the second inequality (note that $\alpha_3 > 0$). In the event $\tau = 0$, we would reformulate the characteristic equation and rework the Routh array.

The computational difficulty arises in determining the conditions on K_P and K_D such that $a > 0$. We find that $a > 0$ implies that the following relationship must be satisfied:

$$f = \alpha_2 \alpha_3 K_D^2 + (\alpha_2 - \tau \alpha_1 \alpha_3 + \alpha_3^2 K_P) K_D + (\alpha_3 - \tau \alpha_2) K_P > 0. \quad (6.33)$$

Using the nominal values of the parameters $\alpha_1, \alpha_2, \alpha_3$, and τ (see Table 6.2), the stability region is shown in Figure 6.13. For all $K_D > 0$ and $K_P > 3.33$, the function $f > 0$, hence $a > 0$. Taking into account all the inequalities, a valid region for selecting the gains is $K_D > 0$ and $K_P > \alpha_1/\alpha_2 = 3.33$.

Selecting any point (K_P, K_D) in the stability region yields a valid (that is, stable) set of gains for the feedback loop. For example, selecting

$$K_P = 10 \text{ and } K_D = 5$$

yields a stable closed-loop system. The closed-loop poles are

$$s_1 = -35.2477, s_2 = -2.4674, \text{ and } s_3 = -1.0348.$$

Since all the poles have negative real parts, we know the system response to any bounded input will be bounded.

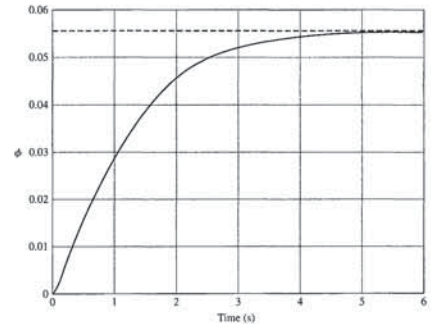


FIGURE 6.14 Disturbance response with $K_P = 10$ and $K_D = 5$.

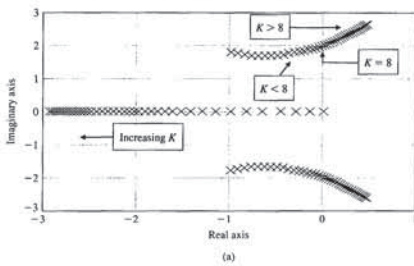
The response to a step disturbance

$$T_d(s) = \frac{1}{s}$$

is shown in Figure 6.14; the response is stable. The control system manages to keep the motorcycle upright, although it is tilted at about $\phi = 0.055$ rad = 3.18 deg.

It is important to give the robot the ability to control the motorcycle over a wide range of forward speeds. Is it possible for the robot, with the feedback gains as selected ($K_P = 10$ and $K_D = 5$), to control the motorcycle as the velocity varies? From experience we know that at slower speeds a bicycle becomes more difficult to control. We expect to see the same characteristics in the stability analysis of our system. Whenever possible, we try to relate the engineering problem at hand to real-life experiences. This helps to develop intuition that can be used as a reasonableness check on our solution.

A plot of the roots of the characteristic equation as the forward speed v varies is shown in Figure 6.15. The data in the plot were generated using the nominal values of the feedback gains, $K_P = 10$ and $K_D = 5$. We selected these gains for the case where $v = 2$ m/s. Figure 6.15 shows that as v increases, the roots of the characteristic equation remain stable (that is, in the left half-plane) with all points negative. But as the motorcycle forward speed decreases, the roots move toward zero, with one root becoming positive at $v = 1.15$ m/s. At the point where one root is positive, the motorcycle is unstable. ■



```
% This script computes the roots of the characteristic
% equation q(s) = s^3 + 2 s^2 + 4 s + K for 0 < K < 20
K=0:0.5:20;
for i=1:length(K)
    q=[1 2 4 K(i)];
    p=(-)roots(q);
end
plot(real(p),imag(p),'x'), grid
xlabel('Real axis'), ylabel('Imaginary axis')
```

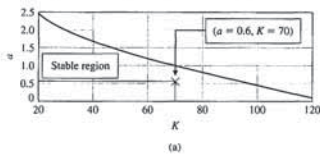
FIGURE 6.20 (a) Plot of root locations of $q(s) = s^3 + 2s^2 + 4s + K$ for $0 \leq K \leq 20$. (b) m-file script.

The script in Figure 6.20 contains the for function. This function provides a mechanism for repeatedly executing a series of statements a given number of times. The for function connected to an end statement sets up a repeating calculation loop. Figure 6.21 describes the for function format and provides an illustrative example of its usefulness. The example sets up a loop that repeats ten times. During the i th iteration, where $1 \leq i \leq 10$, the i th element of the vector a is set equal to 20, and the scalar b is recomputed.

The Routh–Hurwitz method allows us to make definitive statements regarding absolute stability of a linear system. The method does not address the issue of relative stability, which is directly related to the location of the roots of the characteristic equation. Routh–Hurwitz tells us how many poles lie in the right half-plane, but not the specific location of the poles. With control design software, we can easily calculate the poles explicitly, thus allowing us to comment on the relative stability.

EXAMPLE 6.12 Tracked vehicle control

The block diagram of the control system for the two-track vehicle is shown in Figure 6.8. The design objective is to find a and K such that the system is stable and the steady-state error for a ramp input is less than or equal to 24% of the command.



```
% The a-K stability region for the two track vehicle
% control problem
a=[0:1:0.01:3.0]; K=[20:1:120];
x=0*K; y=0*K;
n=length(K); m=length(a);
for i=1:n
    for j=1:m
        q=[1 8 17 K(i)+10, K(i)*a(j)];
        p=roots(q);
        if max(real(p)) > 0, x(i)=K(i); y(j)=a(j)-1; break; end
    end
end
plot(x,y), grid, xlabel('K'), ylabel('a')
```

FIGURE 6.22 (a) Stability region for a and K for two-track vehicle turning control. (b) m-file script.

Given the steady-state specification, $e_{ss} < 0.24A$, we find that the specification is satisfied when

$$\frac{10A}{aK} < 0.24A,$$

or

$$aK > 41.67. \quad (6.34)$$

Any values of a and K that lie in the stable region in Figure 6.22 and satisfy Equation (6.34) will lead to an acceptable design. For example, $K = 70$ and $a = 0.6$ will satisfy all the design requirements. The closed-loop transfer function (with $a = 0.6$ and $K = 70$) is

$$T(s) = \frac{70s + 42}{s^4 + 8s^3 + 17s^2 + 80s + 42}$$

The associated closed-loop poles are

$$s = -7.0767,$$

$$s = -0.5781,$$

$$s = -0.1726 + 3.1995i, \text{ and}$$

$$s = -0.1726 - 3.1995i.$$

FIGURE 6.16 Closed-loop control system with $T(s) = Y(s)/R(s) = 1/(s^3 + s^2 + 2s + 24)$.

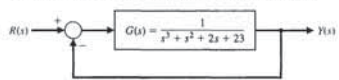
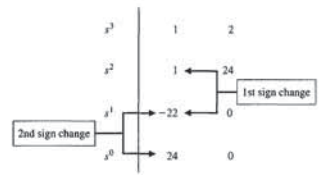


FIGURE 6.17 Routh array for the closed-loop control system with $T(s) = Y(s)/R(s) = 1/(s^3 + s^2 + 2s + 24)$.



parameter may take while maintaining stability. Consider the closed-loop feedback system in Figure 6.19. The characteristic equation is

$$q(s) = s^3 + 2s^2 + 4s + K = 0.$$

Using a Routh–Hurwitz approach, we find that we require $0 < K < 8$ for stability (see Equation 6.12). We can verify this result graphically. As shown in Figure 6.20(b), we establish a vector of values for K at which we wish to compute the roots of the characteristic equation. Then using the roots function, we calculate and plot the roots of the characteristic equation, as shown in Figure 6.20(a). It can be seen that as K increases, the roots of the characteristic equation move toward the right half-plane as the gain tends toward $K = 8$, and eventually into the right half-plane when $K > 8$.

```
>> numg=[1]; deng=[1 2 23]; sysg=tf(numg,deng);
>> sys=feedback(sysg,1);
>> pole(sys)

ans =

-3.0000
1.0000 + 2.6458i
1.0000 - 2.6458i
```

FIGURE 6.18 Using the pole function to compute the closed-loop control system poles of the system shown in Figure 6.16.

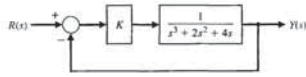


FIGURE 6.19 Closed-loop control system with $T(s) = Y(s)/R(s) = K/(s^3 + 2s^2 + 4s + 4)$.

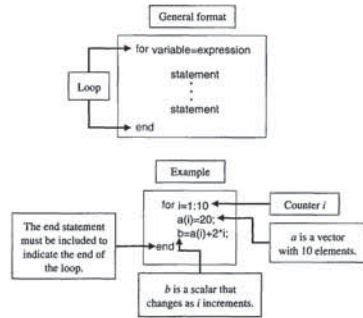


FIGURE 6.21 The for function and an illustrative example.

We can use the Routh–Hurwitz method to aid in the search for appropriate values of a and K . The closed-loop characteristic equation is

$$q(s) = s^4 + 8s^3 + 17s^2 + (K + 10)s + aK = 0.$$

Using the Routh array, we find that, for stability, we require that

$$K < \frac{126 - K}{8}(K + 10) - 8aK > 0, \text{ and } aK > 0.$$

For positive K , it follows that we can restrict our search to $0 < K < 126$ and $a > 0$. Our approach will be to use the computer to help find a parameterized a versus K region in which stability is assured. Then we can find a set of (a, K) belonging to the stable region such that the steady-state error specification is met. This procedure, shown in Figure 6.22, involves selecting a range of values for a and K and computing the roots of the characteristic polynomial for specific values of a and K . For each value of K , we find the first value of a that results in at least one root of the characteristic equation in the right half-plane. The process is repeated until the entire selected range of a and K is exhausted. The plot of the (a, K) pairs defines the separation between the stable and unstable regions. The region to the left of the plot of a versus K in Figure 6.22 is the stable region.

If we assume that $r(t) = At, t > 0$, then the steady-state error is

$$e_{ss} = \lim_{s \rightarrow 0} s \cdot \frac{s(s+1)(s+2)(s+5)}{s(s+1)(s+2)(s+5) + K(s+a)} \cdot \frac{A}{s^2} = \frac{10A}{aK},$$

where we have used the fact that

$$E(s) = \frac{1}{1 + G_c G(s)} R(s) = \frac{s(s+1)(s+2)(s+5)}{s(s+1)(s+2)(s+5) + K(s+a)} R(s).$$

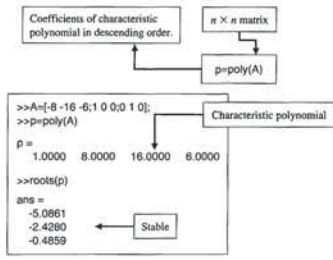


FIGURE 6.24 Computing the characteristic polynomial of A with the poly function.

the Routh-Hurwitz method to detect any unstable roots. Unfortunately, the manual computations can become lengthy, especially if the dimension of A is large. We would like to avoid this manual computation if possible. As it turns out, the computer can assist in this endeavor.

The poly function described in Section 2.9 can be used to compute the characteristic equation associated with A . Recall that poly is used to form a polynomial from a vector of roots. It can also be used to compute the characteristic equation of A , as illustrated in Figure 6.24. The input matrix A is

$$A = \begin{bmatrix} -8 & -16 & -6 \\ 1 & 0 & 0 \\ 0 & 1 & 0 \end{bmatrix}$$

and the associated characteristic polynomial is

$$s^3 + 8s^2 + 16s + 6 = 0.$$

If A is an $n \times n$ matrix, poly(A) is an $n + 1$ element row vector whose elements are the coefficients of the characteristic equation $\det(sI - A) = 0$.

EXAMPLE 6.13 Stability region for an unstable process

A jump-jet aircraft has a control system as shown in Figure 6.25 [16]. Assume that $z > 0$ and $p > 0$. The system is open-loop unstable (without feedback), since the characteristic equation of the process and controller is

$$s(s - 1)(s + p) = s[s^2 + (p - 1)s - p] = 0.$$

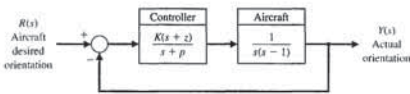


FIGURE 6.25 Control system for jump-jet aircraft. Assume that $z > 0$ and $p > 0$.

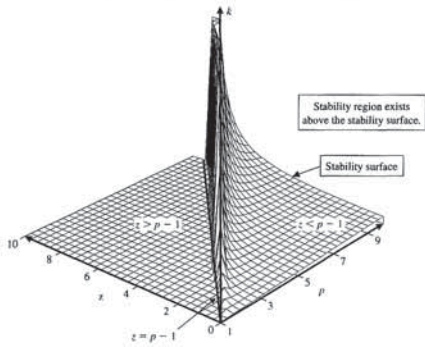


FIGURE 6.27 The three-dimensional region of stability lies above the surface shown.

6.7 SEQUENTIAL DESIGN EXAMPLE: DISK DRIVE READ SYSTEM



In Section 5.11, we examined the design of the head reader system with an adjustable gain K_a . In this section, we will examine the stability of the system as K_a is adjusted and then reconfigure the system.

Let us consider the system as shown in Figure 6.28. This is the same system with a model of the motor and load as considered in Chapter 5, except that the velocity

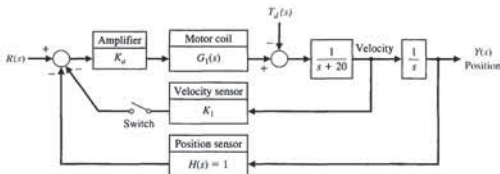


FIGURE 6.28 The closed-loop disk drive head system with an optional velocity feedback.

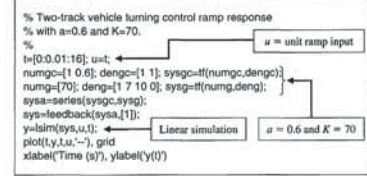
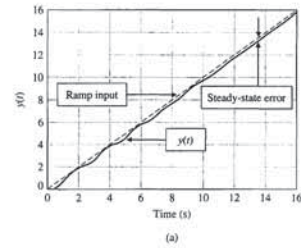


FIGURE 6.23 (a) Ramp response for $a = 0.6$ and $K = 70$ for two-track vehicle turning control. (b) m-file script.

The corresponding unit ramp input response is shown in Figure 6.23. The steady-state error is less than 0.24, as desired. ■

The Stability of State Variable Systems. Now let us turn to determining the stability of systems described in state variable form. Suppose we have a system in state-space form as in Equation (6.22). The stability of the system can be evaluated with the characteristic equation associated with the system matrix A . The characteristic equation is

$$\det(sI - A) = 0. \tag{6.35}$$

The left-hand side of the characteristic equation is a polynomial in s . If all of the roots of the characteristic equation have negative real parts (i.e., $\text{Re}(s_i) < 0$), then the system is stable.

When the system model is given in state variable form, we must calculate the characteristic polynomial associated with the A matrix. In this regard, we have several options. We can calculate the characteristic equation directly from Equation (6.35) by manually computing the determinant of $sI - A$. Then, we can compute the roots using the roots function to check for stability, or alternatively, we can use

Note that since one term within the bracket has a negative coefficient, the characteristic equation has at least one root in the right-hand s -plane. The characteristic equation of the closed-loop system is

$$s^3 + (p - 1)s^2 + (K - p)s + Kz = 0.$$

The goal is to determine the region of stability for K , p , and z . The Routh array is

$$\begin{array}{c|cc} s^3 & 1 & K - p \\ s^2 & p - 1 & Kz \\ s^1 & b_2 & \\ s^0 & Kz & \end{array}$$

where

$$b_2 = \frac{(p - 1)(K - p) - Kz}{p - 1}.$$

From the Routh-Hurwitz criterion, we find that we require $Kz > 0$ and $p > 1$. Setting $b_2 > 0$, we have

$$(p - 1)(K - p) - Kz = K[(p - 1) - z] - p(p - 1) > 0.$$

Consider two cases:

1. $z \geq p - 1$: there is no $0 < K < \infty$ that leads to stability.
2. $z < p - 1$: any $0 < K < \infty$ satisfying the stability condition for a given p and z will result in stability:

$$K > \frac{p(p - 1)}{(p - 1) - z}. \tag{6.36}$$

The stability conditions can be depicted graphically. The m-file script used to generate a three-dimensional stability surface is shown in Figure 6.26. This script uses mesh to create the three-dimensional surface and meshgrid to generate arrays for use with the mesh surface.

The three-dimensional plot of the stability region for K , p , and z is shown in Figure 6.27. One acceptable stability point is $z = 1$, $p = 10$, and $K = 15$. ■

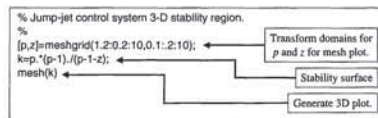
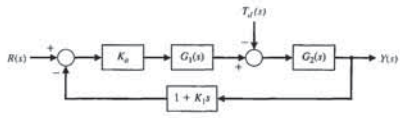


FIGURE 6.26 m-file script for stability region.

FIGURE 6.29 Equivalent system with the velocity feedback switch closed.



The characteristic equation is then

$$1 + [K_a G_1(s) G_2(s)](1 + K_1 s) = 0,$$

or

$$s(s + 20)(s + 1000) + 5000K_a(1 + K_1 s) = 0.$$

Therefore, we have

$$s^3 + 1020s^2 + [20000 + 5000K_a K_1]s + 5000K_a = 0.$$

Then the Routh array is

s^3	1	$20000 + 5000K_a K_1$	
s^2	1020	$5000K_a$	
s^1	b_1		
s^0	$5000K_a$		

where

$$b_1 = \frac{1020(20000 + 5000K_a K_1) - 5000K_a}{1020}$$

To guarantee stability, it is necessary to select the pair (K_a, K_1) such that $b_1 > 0$, where $K_a > 0$. When $K_1 = 0.05$ and $K_a = 100$, we can determine the system response using the script shown in Figure 6.30. The settling time (with a 2% criterion) is approximately 260 ms, and the percent overshoot is zero. The system performance is summarized in Table 6.3. The performance specifications are nearly satisfied, and some iteration of K_1 is necessary to obtain the desired 250 ms settling time.

Table 6.3 Performance of the Disk Drive System Compared to the Specifications

Performance Measure	Desired Value	Actual Response
Percent overshoot	Less than 5%	0%
Settling time	Less than 250 ms	260 ms
Maximum response to a unit disturbance	Less than 5×10^{-3}	2×10^{-3}



SKILLS CHECK

In this section, we provide three sets of problems to test your knowledge: True or False, Multiple Choice, and Word Match. To obtain direct feedback, check your answers with the answer key provided at the conclusion of the end-of-chapter problems. Use the block diagram in Figure 6.31 as specified in the various problem statements.

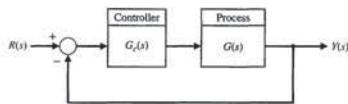


FIGURE 6.31 Block diagram for the Skills Check.

In the following True or False and Multiple Choice problems, circle the correct answer.

- A stable system is a dynamic system with a bounded output response for any input. True or False
- A marginally stable system has poles on the $j\omega$ -axis. True or False
- A system is stable if all poles lie in the right half-plane. True or False
- The Routh-Hurwitz criterion is a necessary and sufficient criterion for determining the stability of linear systems. True or False
- Relative stability characterizes the degree of stability. True or False
- A system has the characteristic equation

$$q(s) = s^3 + 4Ks^2 + (5 + K)s + 10 = 0.$$

The range of K for a stable system is:

- $K > 0.46$
- $K < 0.46$
- $0 < K < 0.46$
- Unstable for all K

- Utilizing the Routh-Hurwitz criterion, determine whether the following polynomials are stable or unstable:

$$p_1(s) = s^2 + 10s + 5 = 0,$$

$$p_2(s) = s^4 + s^3 + 5s^2 + 20s + 10 = 0.$$

- $p_1(s)$ is stable, $p_2(s)$ is stable
- $p_1(s)$ is unstable, $p_2(s)$ is stable
- $p_1(s)$ is stable, $p_2(s)$ is unstable
- $p_1(s)$ is unstable, $p_2(s)$ is unstable

- Consider the feedback control system block diagram in Figure 6.31. Investigate closed-loop stability for $G_c(s) = K(s + 1)$ and $G(s) = \frac{1}{(s + 2)(s - 1)}$ for the two cases where $K = 1$ and $K = 3$.

- Unstable for $K = 1$ and stable for $K = 3$

feedback sensor was added, as shown in Figure 6.28. Initially, we consider the case where the switch is open. Then the closed-loop transfer function is

$$\frac{Y(s)}{R(s)} = \frac{K_a G_1(s) G_2(s)}{1 + K_a G_1(s) G_2(s)}, \quad (6.37)$$

where

$$G_1(s) = \frac{5000}{s + 1000}$$

and

$$G_2(s) = \frac{1}{s(s + 20)}$$

The characteristic equation is

$$s(s + 20)(s + 1000) + 5000K_a = 0, \quad (6.38)$$

or

$$s^3 + 1020s^2 + 20000s + 5000K_a = 0.$$

We use the Routh array

s^3	1	20000
s^2	1020	$5000K_a$
s^1	b_1	
s^0	$5000K_a$	

where

$$b_1 = \frac{(20000)1020 - 5000K_a}{1020}$$

The case $b_1 = 0$ results in marginal stability when $K_a = 4080$. Using the auxiliary equation, we have

$$1020s^2 + 5000(4080) = 0,$$

or the roots of the $j\omega$ -axis are $s = \pm j141.4$. In order for the system to be stable, $K_a < 4080$.

Now let us add the velocity feedback by closing the switch in the system of Figure 6.28. The closed-loop transfer function for the system is then

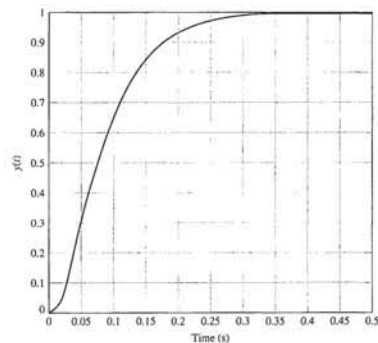
$$\frac{Y(s)}{R(s)} = \frac{K_a G_1(s) G_2(s)}{1 + [K_a G_1(s) G_2(s)](1 + K_1 s)}, \quad (6.39)$$

since the feedback path is equal to $1 + K_1 s$, as shown in Figure 6.29.

```

Ka=100; K1=0.05;
ng1=(5000); dg1=[1 1000]; sys1=tf(ng1,dg1);
ng2=[1]; dg2=[1 20 0]; sys2=tf(ng2,dg2);
nc=[K1 1]; dc=[0 1]; sysc=tf(nc,dc);
syso=series(Ka*sys1,sys2);
sys=feedback(syso,sysc); sys=minreal(sys);
t=[0:0.001:0.5];
y=step(sys,t); plot(t,y);
ylabel('y(t)'); xlabel('Time (s)'); grid
    
```

(a)



(b)

FIGURE 6.30 Response of the system with velocity feedback. (a) m-file script. (b) Response with $K_a = 100$ and $K_1 = 0.05$.

6.8 SUMMARY

In this chapter, we have considered the concept of the stability of a feedback control system. A definition of a stable system in terms of a bounded system response was outlined and related to the location of the poles of the system transfer function in the s -plane.

The Routh-Hurwitz stability criterion was introduced, and several examples were considered. The relative stability of a feedback control system was also considered in terms of the location of the poles and zeros of the system transfer function in the s -plane. The stability of state variable systems was considered.

In Problems 13 and 14, consider the system represented in a state-space form

$$\dot{\mathbf{x}} = \begin{bmatrix} 0 & 1 & 0 \\ 0 & 0 & 1 \\ -5 & -10 & -5 \end{bmatrix} \mathbf{x} + \begin{bmatrix} 0 \\ 0 \\ 20 \end{bmatrix} u$$

$$y = [1 \ 0 \ 1] \mathbf{x}$$

13. The characteristic equation is:
- $q(s) = s^3 + 5s^2 - 10s - 6$
 - $q(s) = s^3 + 5s^2 + 10s + 5$
 - $q(s) = s^3 - 5s^2 + 10s - 5$
 - $q(s) = s^3 - 5s + 10$
14. Using the Routh-Hurwitz criterion, determine whether the system is stable, unstable, or marginally stable.
- Stable
 - Unstable
 - Marginally stable
 - None of the above
15. A system has the block diagram representation as shown in Figure 6.31, where $G(s) = \frac{10}{(s+15)^2}$ and $G_c(s) = \frac{K}{s+80}$, where K is always positive. The limiting gain for a stable system is:
- $0 < K < 28875$
 - $0 < K < 27075$
 - $0 < K < 25050$
 - Stable for all $K > 0$

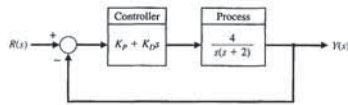
In the following Word Match problems, match the term with the definition by writing the correct letter in the space provided.

a. Routh-Hurwitz criterion	A performance measure of a system.	_____
b. Auxiliary polynomial	A dynamic system with a bounded system response to a bounded input.	_____
c. Marginally stable	The property that is measured by the relative real part of each root or pair of roots of the characteristic equation.	_____
d. Stable system	A criterion for determining the stability of a system by examining the characteristic equation of the transfer function.	_____
e. Stability	The equation that immediately precedes the zero entry in the Routh array.	_____
f. Relative stability	A system description that reveals whether a system is stable or not stable without consideration of other system attributes such as degree of stability.	_____
g. Absolute stability	A system possesses this type of stability if the zero input response remains bounded as $t \rightarrow \infty$.	_____

Exercises

FIGURE E6.13

Closed-loop system with a proportional plus derivative controller $G_c(s) = K_p + K_D s$.



- where a and b are constant parameters. Determine the necessary and sufficient conditions for the system to be stable. Is it possible to determine stability of a second-order system just by inspecting the coefficients of the characteristic equation?
- E6.13. Consider the feedback system in Figure E6.13. Determine the range of K_p and K_D for stability of the closed-loop system.
- E6.14. By using magnetic bearings, a rotor is supported contactless. The technique of contactless support for rotors becomes more important in light and heavy industrial applications [14]. The matrix differential equation for a magnetic bearing system is
- $$\dot{\mathbf{x}} = \begin{bmatrix} 0 & 1 & 0 \\ -3 & -1 & 0 \\ -2 & -1 & -2 \end{bmatrix} \mathbf{x}$$
- where $\mathbf{x}^T = [y, \dot{y}, i]$, y = bearing gap, and i is the electromagnetic current. Determine whether the system is stable.
- Answer: The system is stable.
- E6.15. A system has a characteristic equation
- $$q(s) = s^6 + 9s^5 + 31.25s^4 + 61.25s^3 + 67.75s^2 + 14.75s + 15 = 0.$$
- Determine whether the system is stable, using the Routh-Hurwitz criterion.
 - Determine the roots of the characteristic equation.
- Answer: (a) The system is marginally stable. (b) $s = -3, -4, -1 \pm 2j, \pm 0.5j$
- E6.16. A system has a characteristic equation
- $$q(s) = s^4 + 9s^3 + 45s^2 + 87s + 50 = 0.$$
- Determine whether the system is stable, using the Routh-Hurwitz criterion.
 - Determine the roots of the characteristic equation.
- E6.17. The matrix differential equation of a state variable model of a system has
- $$\mathbf{A} = \begin{bmatrix} 0 & 1 & -1 \\ -8 & -12 & 8 \\ -8 & -12 & 5 \end{bmatrix}$$

- Determine the characteristic equation.
 - Determine whether the system is stable.
 - Determine the roots of the characteristic equation.
- Answer: (a) $q(s) = s^3 + 7s^2 + 36s + 24 = 0$
- E6.18. A system has a characteristic equation
- $$q(s) = s^3 + 20s^2 + 5s + 100 = 0.$$
- Determine whether the system is stable, using the Routh-Hurwitz criterion.
 - Determine the roots of the characteristic equation.
- E6.19. Determine whether the systems with the following characteristic equations are stable or unstable:
- $s^3 + 4s^2 + 6s + 100 = 0$,
 - $s^4 + 6s^3 + 10s^2 + 17s + 6 = 0$, and
 - $s^2 + 6s + 3 = 0$.
- E6.20. Find the roots of the following polynomials:
- $s^3 + 5s^2 + 8s + 4 = 0$ and
 - $s^3 + 9s^2 + 27s + 27 = 0$.
- E6.21. A system has the characteristic equation
- $$q(s) = s^3 + 10s^2 + 29s + K = 0.$$
- Shift the vertical axis to the right by 2 by using $s = s_p - 2$, and determine the value of gain K so that the complex roots are $s = -2 \pm j$.
- E6.22. A system has a transfer function $Y(s)/R(s) = T(s) = 1/s$. (a) Is this system stable? (b) If $r(t)$ is a unit step input, determine the response $y(t)$.
- E6.23. A system is represented by Equation (6.22) where
- $$\mathbf{A} = \begin{bmatrix} 0 & 1 & 0 \\ 0 & 0 & 1 \\ -8 & -k & -4 \end{bmatrix}$$
- Find the range of k where the system is stable.
- E6.24. Consider the system represented in state variable form
- $$\dot{\mathbf{x}} = \mathbf{A}\mathbf{x} + \mathbf{B}u$$
- $$y = \mathbf{C}\mathbf{x} + \mathbf{D}u,$$
- where
- $$\mathbf{A} = \begin{bmatrix} 0 & 1 & 0 \\ 0 & 0 & 1 \\ -k & -k & -k \end{bmatrix}, \mathbf{B} = \begin{bmatrix} 0 \\ 0 \\ 1 \end{bmatrix}$$
- $$\mathbf{C} = [1 \ 0 \ 0], \mathbf{D} = [0].$$

- Unstable for $K = 1$ and unstable for $K = 3$
- Stable for $K = 1$ and unstable for $K = 3$
- Stable for $K = 1$ and stable for $K = 3$

9. Consider a unity negative feedback system in Figure 6.31 with loop transfer function where

$$L(s) = G_c(s)G(s) = \frac{K}{(1 + 0.5s)(1 + 0.5s + 0.25s^2)}$$

Determine the value of K for which the closed-loop system is marginally stable.

- $K = 10$
- $K = 3$
- The system is unstable for all K
- The system is stable for all K

10. A system is represented by $\dot{\mathbf{x}} = \mathbf{A}\mathbf{x}$, where

$$\mathbf{A} = \begin{bmatrix} 0 & 1 & 0 \\ 0 & 0 & 1 \\ -5 & -K & 10 \end{bmatrix}$$

The values of K for a stable system are

- $K < 1/2$
- $K > 1/2$
- $K = 1/2$
- The system is stable for all K

11. Use the Routh array to assist in computing the roots of the polynomial

$$q(s) = 2s^3 + 2s^2 + s + 1 = 0.$$

- $s_1 = -1; s_{2,3} = \pm \frac{\sqrt{2}}{2}j$
- $s_1 = 1; s_{2,3} = \pm \frac{\sqrt{2}}{2}j$
- $s_1 = -1; s_{2,3} = 1 \pm \frac{\sqrt{2}}{2}j$
- $s_1 = -1; s_{2,3} = 1$

12. Consider the following unity feedback control system in Figure 6.31 where

$$G(s) = \frac{1}{(s-2)(s^2+10s+45)} \text{ and } G_c(s) = \frac{K(s+0.3)}{s}$$

The range of K for stability is

- $K < 260.68$
- $50.06 < K < 123.98$
- $100.12 < K < 260.68$
- The system is unstable for all $K > 0$

EXERCISES

- E6.1. A system has a characteristic equation $s^3 + Ks^2 + (1 + K)s + 6 = 0$. Determine the range of K for a stable system.
- Answer: $K > 2$
- E6.2. A system has a characteristic equation $s^3 + 10s^2 + 2s + 30 = 0$. Using the Routh-Hurwitz criterion, show that the system is unstable.
- E6.3. A system has the characteristic equation $s^4 + 10s^3 + 32s^2 + 37s + 20 = 0$. Using the Routh-Hurwitz criterion, determine if the system is stable.
- E6.4. A control system has the structure shown in Figure E6.4. Determine the gain at which the system will become unstable.
- Answer: $K = 20/7$
- E6.5. A unity feedback system has a loop transfer function
- $$L(s) = \frac{K}{(s+1)(s+3)(s+6)}$$
- where $K = 20$. Find the roots of the closed-loop system's characteristic equation.
- E6.6. For the feedback system of Exercise E6.5, find the value of K when two roots lie on the imaginary axis. Determine the value of the three roots.
- Answer: $s = -10, \pm j5.2$
- E6.7. A negative feedback system has a loop transfer function
- $$L(s) = \frac{K(s+2)}{s(s-1)}$$
- Find the value of the gain when the ζ of the closed-loop roots is equal to 0.707.
 - Find the value of the gain when the closed-loop system has two roots on the imaginary axis.

- E6.8. Designers have developed small, fast, vertical-take-off fighter aircraft that are invisible to radar (stealth aircraft). This aircraft concept uses quickly turning jet nozzles to steer the airplane [16]. The control system for the heading or direction control is shown in Figure E6.8. Determine the maximum gain of the system for stable operation.
- E6.9. A system has a characteristic equation
- $$s^3 + 2s^2 + (K+1)s + 8 = 0.$$
- Find the range of K for a stable system.
- Answer: $K > 3$
- E6.10. We all use our eyes and ears to achieve balance. Our orientation system allows us to sit or stand in a desired position even while in motion. This orientation system is primarily run by the information received in the inner ear, where the semicircular canals sense angular acceleration and the otoliths measure linear acceleration. But these acceleration measurements need to be supplemented by visual signals. Try the following experiment: (a) Stand with one foot in front of another, with your hands resting on your hips and your elbows bowed outward. (b) Close your eyes. Did you experience a low-frequency oscillation that grew until you lost balance? Is this orientation position stable with and without the use of your eyes?
- E6.11. A system with a transfer function $Y(s)/R(s)$ is
- $$\frac{Y(s)}{R(s)} = \frac{24(s+1)}{s^4 + 6s^3 + 2s^2 + s + 3}$$
- Determine the steady-state error to a unit step input. Is the system stable?
- E6.12. A system has the second-order characteristic equation
- $$s^2 + as + b = 0.$$

FIGURE E6.4 Feedforward system.

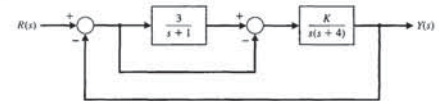
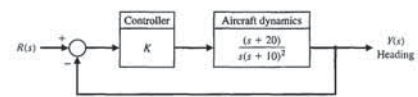


FIGURE E6.8 Aircraft heading control.



P6.2 An antenna control system was analyzed in Problem P4.5, and it was determined that, to reduce the effect of wind disturbances, the gain of the magnetic amplifier, k_m , should be as large as possible. (a) Determine the limiting value of gain for maintaining a stable system. (b) We want to have a system settling time equal to 1.5 seconds. Using a shifted axis and the Routh–Hurwitz criterion, determine the value of the gain that satisfies this requirement. Assume that the complex roots of the closed-loop system dominate the transient response. (Is this a valid approximation in this case?)

P6.3 Arc welding is one of the most important areas of application for industrial robots [11]. In most manufacturing welding situations, uncertainties in dimensions of the part, geometry of the joint, and the welding process itself require the use of sensors for maintaining weld quality. Several systems use a vision system to measure the geometry of the puddle of melted metal, as shown in Figure P6.3. This system uses a constant rate of feeding the wire to be melted. (a) Calculate the maximum value for K for the system that will result in a stable system. (b) For half of the maximum value of K found in part (a), determine the roots of the characteristic equation. (c) Estimate the overshoot of the system of part (b) when it is subjected to a step input.

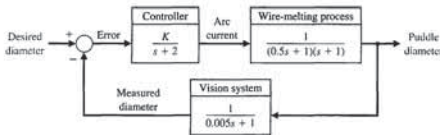


FIGURE P6.3 Welder control.

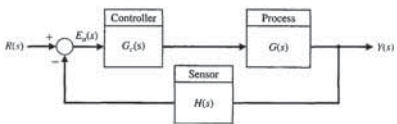


FIGURE P6.4 Nonunity feedback system.

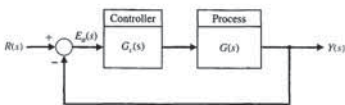


FIGURE P6.6 Unity feedback system.

Problems

433

(a) Determine the limiting gain for a stable system. (b) Determine a suitable gain so that the overshoot to a step command is approximately 5%.

P6.10 Robots can be used in manufacturing and assembly operations that require accurate, fast, and versatile manipulation [10, 11]. The open-loop transfer function of a direct-drive arm may be approximated by

$$G(s)H(s) = \frac{K(s+10)}{s(s+3)(s^2+4s+8)}$$

(a) Determine the value of gain K when the system oscillates. (b) Calculate the roots of the closed-loop system for the K determined in part (a).

P6.11 A feedback control system has a characteristic equation

$$s^3 + (1+K)s^2 + 10s + (5+15K) = 0.$$

The parameter K must be positive. What is the maximum value K can assume before the system becomes unstable? When K is equal to the maximum value, the system oscillates. Determine the frequency of oscillation.

P6.12 A system has the third-order characteristic equation $s^3 + as^2 + bs + c = 0$,

where a , b , and c are constant parameters. Determine the necessary and sufficient conditions for the system to be stable. Is it possible to determine stability of the system by just inspecting the coefficients of the characteristic equation?

P6.13 Consider the system in Figure P6.13. Determine the conditions on K , p , and z that must be satisfied for closed-loop stability. Assume that $K > 0$, $\zeta > 0$, and $\omega_n > 0$.

P6.14 A feedback control system has a characteristic equation

$$s^6 + 2s^5 + 12s^4 + 4s^3 + 21s^2 + 2s + 10 = 0.$$

Determine whether the system is stable, and determine the values of the roots.

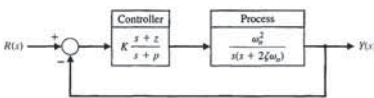


FIGURE P6.13 Control system with controller with three parameters K , p , and z .

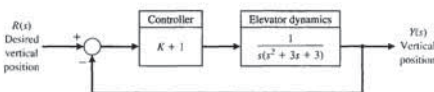


FIGURE P6.17 Elevator control system.

P6.4 A feedback control system is shown in Figure P6.4. The controller and process transfer functions are given by

$$G_c(s) = K \text{ and } G(s) = \frac{s+40}{s(s+10)}$$

and the feedback transfer function is $H(s) = 1/(s+20)$. (a) Determine the limiting value of gain K for a stable system. (b) For the gain that results in marginal stability, determine the magnitude of the imaginary roots. (c) Reduce the gain to half the magnitude of the marginal value and determine the relative stability of the system (1) by shifting the axis and using the Routh–Hurwitz criterion and (2) by determining the root locations. Show the roots are between -1 and -2 .

P6.5 Determine the relative stability of the systems with the following characteristic equations (1) by shifting the axis in the s -plane and using the Routh–Hurwitz criterion, and (2) by determining the location of the complex roots in the s -plane:

$$(a) s^3 + 3s^2 + 4s + 2 = 0.$$

$$(b) s^4 + 9s^3 + 30s^2 + 42s + 20 = 0.$$

$$(c) s^3 + 19s^2 + 110s + 200 = 0.$$

P6.6 A unity-feedback control system is shown in Figure P6.6. Determine the relative stability of the

430

Chapter 6 The Stability of Linear Feedback Systems

(a) What is the system transfer function? (b) For what values of k is the system stable?

E6.26 Consider the closed-loop system in Figure E6.26, where

$$G(s) = \frac{10}{s-10} \text{ and } G_c(s) = \frac{1}{2s+K}$$

(a) Determine the characteristic equation associated with the closed-loop system. (b) Determine the values of K for which the closed-loop system is stable.

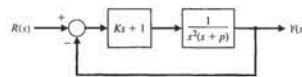


FIGURE E6.25 Closed-loop system with parameters K and ρ .

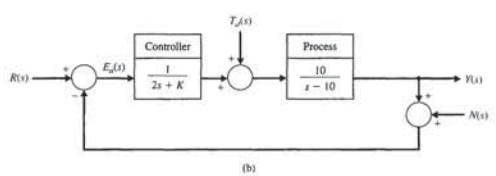
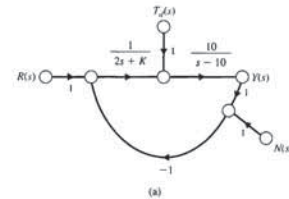


FIGURE E6.26 Closed-loop feedback control system with parameter K .

PROBLEMS

P6.1 Utilizing the Routh–Hurwitz criterion, determine the stability of the following polynomials:

$$(a) s^3 + 5s + 2$$

$$(b) s^3 + 4s^2 + 8s + 4$$

$$(c) s^3 + 2s^2 - 6s + 20$$

$$(d) s^4 + s^3 + 2s^2 + 12s + 10$$

$$(e) s^4 + s^3 + 3s^2 + 2s + K$$

$$(f) s^5 + s^4 + 2s^3 + s + 6$$

$$(g) s^5 + s^4 + 2s^3 + s^2 + s + K$$

Determine the number of roots, if any, in the right-half plane. If it is adjustable, determine the range of K that results in a stable system.

432

Chapter 6 The Stability of Linear Feedback Systems

system with the following transfer functions by locating the complex roots in the s -plane:

$$(a) G_c(s)G(s) = \frac{10s+2}{s^2(s+1)}$$

$$(b) G_c(s)G(s) = \frac{24}{s(s^3+10s^2+35s+50)}$$

$$(c) G_c(s)G(s) = \frac{(s+2)(s+3)}{s(s+4)(s+6)}$$

P6.7 The linear model of a phase detector (phase-locked loop) can be represented by Figure P6.7 [9]. The phase-locked systems are designed to maintain zero difference in phase between the input carrier signal and a local voltage-controlled oscillator. Phase-locked loops find application in color television, missile tracking, and space telemetry. The filter for a particular application is chosen as

$$F(s) = \frac{10(s+10)}{(s+1)(s+100)}$$

We want to minimize the steady-state error of the system for a ramp change in the phase information signal. (a) Determine the limiting value of the gain $K_1K_2 = K_c$ in order to maintain a stable system. (b) A steady-state error equal to 1° is acceptable for a

ramp signal of 100 rad/s. For that value of gain K_c , determine the location of the roots of the system.

P6.8 A very interesting and useful velocity control system has been designed for a wheelchair control system. We want to enable people paralyzed from the neck down to drive themselves in motorized wheelchairs. A proposed system utilizing velocity sensors mounted in a headgear is shown in Figure P6.8. The headgear sensor provides an output proportional to the magnitude of the head movement. There is a sensor mounted at 90° intervals so that forward, left, right, or reverse can be commanded. Typical values for the time constants are $\tau_1 = 0.5$ s, $\tau_2 = 1$ s, and $\tau_3 = \frac{1}{4}$ s.

(a) Determine the limiting gain $K = K_1K_2K_3$ for a stable system.

(b) When the gain K is set equal to one-third of the limiting value, determine whether the settling time (to within 2% of the final value of the system) is less than 4 s.

(c) Determine the value of gain that results in a system with a settling time of 4 s. Also, obtain the value of the roots of the characteristic equation when the settling time is equal to 4 s.

P6.9 A cassette tape storage device has been designed for mass-storage [1]. It is necessary to control the velocity of the tape accurately. The speed control of the tape drive is represented by the system shown in Figure P6.9.

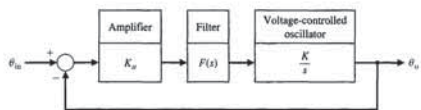


FIGURE P6.7 Phase-locked loop system.

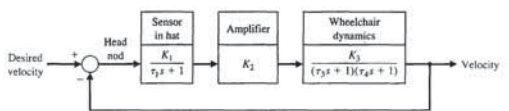


FIGURE P6.8 Wheelchair control system.

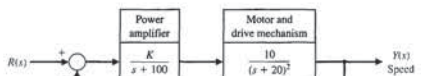


FIGURE P6.9 Tape drive control.

where $A = \begin{bmatrix} 0 & 1 \\ -k_1 & -k_2 \end{bmatrix}$, $B = \begin{bmatrix} 0 \\ 1 \end{bmatrix}$, and $C = [1 \quad -1]$, and where $k_1 \neq k_2$ and both k_1 and k_2 are real numbers.

ADVANCED PROBLEMS

AP6.1 A teleoperated control system incorporates both a person (operator) and a remote machine. The normal teleoperation system is based on a one-way link to the machine and limited feedback to the operator. However, two-way coupling using bilateral information exchange enables better operation [18]. In the case of remote control of a robot, force feedback plus position feedback is useful. The characteristic equation for a teleoperated system, as shown in Figure AP6.1, is $s^4 + 20s^3 + K_1s^2 + 4s + K_2 = 0$,



FIGURE AP6.1 Model of a teleoperated machine.

where K_1 and K_2 are feedback gain factors. Determine and plot the region of stability for this system for K_1 and K_2 .

AP6.2 Consider the case of a navy pilot landing an aircraft on an aircraft carrier. The pilot has three basic tasks. The first task is guiding the aircraft's approach to the ship along the extended centerline of the runway. The second task is maintaining the aircraft on the correct glide slope. The third task is maintaining the correct speed. A model of a lateral position control system is shown in Figure AP6.2. Determine the range of stability for $K = 0$.

AP6.3 A control system is shown in Figure AP6.3. We want the system to be stable and the steady-state error for a unit step input to be less than or equal to 0.05 (5%). (a) Determine the range of α that satisfies the error requirement. (b) Determine the range of α that meets both requirements.

AP6.4 A bottle-filling line uses a feeder screw mechanism, as shown in Figure AP6.4. The tachometer feedback is used to maintain accurate speed control. Determine and plot the range of K and p that permits stable operation.

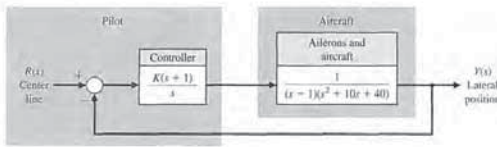


FIGURE AP6.2 Lateral position control for landing on an aircraft carrier.

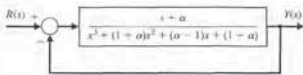


FIGURE AP6.3 Third-order unity feedback system.

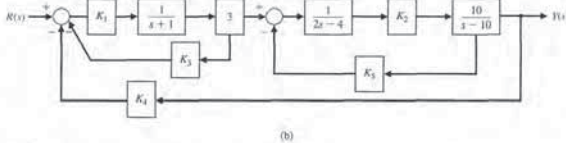
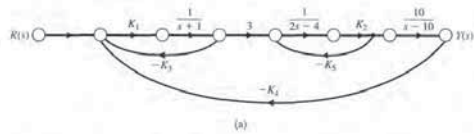


FIGURE AP6.5 Multiloop feedback control system. (a) Signal flow graph. (b) Block diagram.

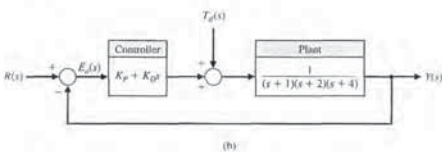
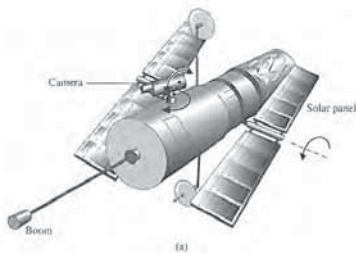


FIGURE AP6.6 (a) Spacecraft with a camera. (b) Feedback control system.

P6.18 Consider the case of rabbits and foxes in Australia. The number of rabbits is x_1 and, if left alone, it would grow indefinitely (until the food supply was exhausted) so that

$$\dot{x}_1 = kx_1$$

However, with foxes present on the continent, we have

$$\dot{x}_1 = kx_1 - ax_1x_2$$

where x_2 is the number of foxes. Now, if the foxes must have rabbits to exist, we have

$$\dot{x}_2 = -hx_2 + bx_1x_2$$

Determine whether this system is stable and thus decays to the condition $x_1(t) = x_2(t) = 0$ at $t = \infty$. What are the requirements on a, b, h , and k for a stable system? What is the result when k is greater than h ?

flight [16]. An aircraft taking off in a form similar to a missile (on end) is inherently unstable (see Example 3.4 for a discussion of the inverted pendulum). A control system using adjustable jets can control the vehicle, as shown in Figure P6.19. (a) Determine the range of gain for which the system is stable. (b) Determine the gain K for which the system is marginally stable and the roots of the characteristic equation for this value of K .

P6.20 A personal vertical take-off and landing (VTOL) aircraft is shown in Figure P6.20(a). A possible control system for aircraft altitude is shown in Figure P6.20(b). (a) For $K = 6$, determine whether the system is stable. (b) Determine a range of stability, if any, for $K > 0$.

P6.21 Consider the system described in state variable form by

$$\dot{\mathbf{x}}(t) = \mathbf{A}\mathbf{x}(t) + \mathbf{B}u(t) \\ y(t) = \mathbf{C}\mathbf{x}(t)$$

P6.19 The goal of vertical takeoff and landing (VTOL) aircraft is to achieve operation from relatively small airports and yet operate as a normal aircraft in level

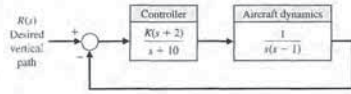


FIGURE P6.19 Control of a jump-jet aircraft.



FIGURE P6.20 (a) Personal VTOL aircraft. (Courtesy of Mirror Image Aerospace at www.skywalkervtol.com) (b) Control system.

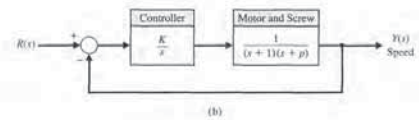
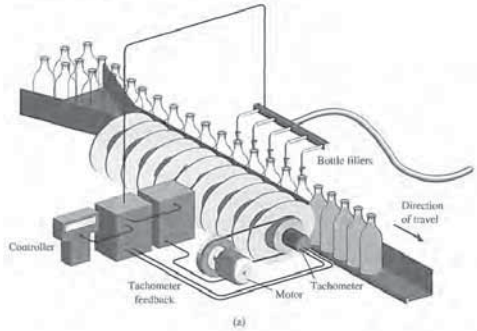
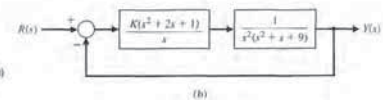


FIGURE AP6.4 Speed control of a bottle-filling line. (a) System layout. (b) Block diagram.

AP6.5 Consider the closed-loop system in Figure AP6.5. Suppose that all gains are positive, that is, $K_1 > 0$, $K_2 > 0$, $K_3 > 0$, $K_4 > 0$, and $K_5 > 0$.

- Determine the closed-loop transfer function $T(s) = Y(s)/R(s)$.
- Obtain the conditions on selecting the gains K_1, K_2, K_3, K_4 , and K_5 , so that the closed-loop system is guaranteed to be stable.
- Using the results of part (b), select values of the five gains so that the closed-loop system is stable, and plot the unit step response.

A proportional plus derivative controller is used in a system as shown in Figure AP6.6(b), where

$$G_c(s) = K_p + K_{pd}s$$

and where $K_p > 0$ and $K_{pd} > 0$. Obtain and plot the relationship between K_p and K_{pd} that results in a stable closed-loop system.

AP6.7 A human's ability to perform physical tasks is limited not by intellect but by physical strength. If, in an appropriate environment, a machine's mechanical power is closely integrated with a human arm's mechanical strength under the control of the human intellect, the resulting system will be superior to a loosely integrated combination of a human and a fully automated robot.

AP6.6 A spacecraft with a camera is shown in Figure AP6.6(a). The camera slews about 16° in a canted plane relative to the base. Reaction jets stabilize the base against the reaction torques from the slewing motors. Suppose that the rotational speed control for the camera slewing has a plant transfer function

$$G(s) = \frac{1}{(s+1)(s+2)(s+4)}$$

Extenders are defined as a class of robot manipulators that extend the strength of the human arm while maintaining human control of the task [23]. The defining characteristic of an extender is the transmission of both power and information signals. The extender is worn by the human; the physical contact between the extender

The parameter p is equal to 2 for many autos but can equal zero for those with high performance. Select a gain K that will result in a stable system for both values of p .

- DP6.2** An automatically guided vehicle on Mars is represented by the system in Figure DP6.2. The system has a steerable wheel in both the front and back of the vehicle, and the design requires that $H(s) = Ks + 1$. Determine (a) the value of K required for stability, (b) the value of K when one root of the characteristic equation is equal to $s = -5$, and (c) the value of the two remaining roots for the gain selected in part (b). (d) Find the response of the system to a step command for the gain selected in part (b).

- DP6.3** A unity negative feedback system with

$$G_c(s)G(s) = \frac{K(s+2)}{s(1+\tau s)(1+2s)}$$

has two parameters to be selected. (a) Determine and plot the regions of stability for this system. (b) Select τ and K so that the steady-state error to a ramp input is less than or equal to 25% of the input magnitude. (c) Determine the percent overshoot for a step input for the design selected in part (b).

- DP6.4** The attitude control system of a space shuttle rocket is shown in Figure DP6.4 [17]. (a) Determine

the range of gain K and parameter m so that the system is stable, and plot the region of stability. (b) Select the gain and parameter values so that the steady-state error to a ramp input is less than or equal to 10% of the input magnitude. (c) Determine the percent overshoot for a step input for the design selected in part (b).

- DP6.5** A traffic control system is designed to control the distance between vehicles, as shown in Figure DP6.5 [15]. (a) Determine the range of gain K for which the system is stable. (b) If K_m is the maximum value of K so that the characteristic roots are on the $j\omega$ -axis, then let $K = K_m/N$, where $6 < N < 7$. We want the peak time to be less than 2 seconds and the percent overshoot to be less than 18%. Determine an appropriate value for N .

- DP6.6** Consider the single-input, single-output system as described by

$$\dot{\mathbf{x}}(t) = \mathbf{A}\mathbf{x}(t) + \mathbf{B}u(t)$$

$$y(t) = \mathbf{C}\mathbf{x}(t)$$

where

$$\mathbf{A} = \begin{bmatrix} 0 & 1 \\ 2 & -2 \end{bmatrix}, \mathbf{B} = \begin{bmatrix} 0 \\ 1 \end{bmatrix}, \mathbf{C} = [1 \quad 0]$$

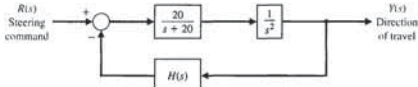


FIGURE DP6.2 Mars guided vehicle control.

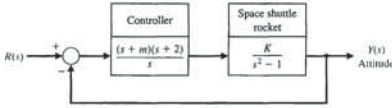


FIGURE DP6.4 Shuttle attitude control.

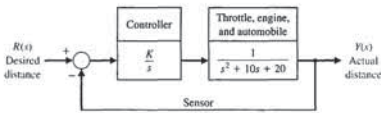


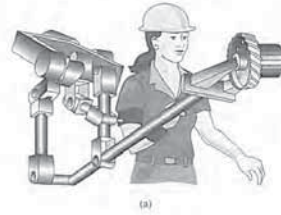
FIGURE DP6.5 Traffic distance control.

and the human allows the direct transfer of mechanical power and information signals. Because of this unique interface, control of the extender trajectory can be accomplished without any type of joystick, keyboard, or master-slave system. The human provides a control system for the extender, while the extender actuators provide most of the strength necessary for the task. The human becomes a part of the extender and "feels" a scaled-down version of the load that the extender is carrying. The extender is distinguished from a conventional master-slave system; in that type of system, the human

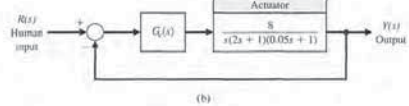
operator is either at a remote location or close to the slave manipulator, but is not in direct physical contact with the slave in the sense of transfer of power. An extender is shown in Figure AP6.7(a) [23]. The block diagram of the system is shown in Figure AP6.7(b). Consider the proportional plus integral controller

$$G_c(s) = K_P + \frac{K_I}{s}$$

Determine the range of values of the controller gains K_P and K_I such that the closed-loop system is stable.



(a)



(b)

FIGURE AP6.7 Extender robot control.

DESIGN PROBLEMS

- CDP6.1** The capstan drive system of problem CDP5.1 uses the amplifier as the controller. Determine the maximum value of the gain K_a before the system becomes unstable.

- DP6.1** The control of the spark ignition of an automotive engine requires constant performance over a wide range of parameters [15]. The control system is shown in Figure DP6.1, with a controller gain K to be selected.

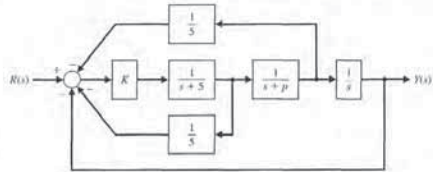


FIGURE DP6.1 Automobile engine control.

Develop an m-file to determine the closed-loop transfer function and show that the roots of the characteristic equation are $s_1 = -2.89$ and $s_{2,3} = -0.55 \pm j1.87$.

- CP6.4** Consider the closed-loop transfer function

$$T(s) = \frac{1}{s^5 + 2s^4 + 2s^3 + 4s^2 + s + 2}$$

- (a) Using the Routh-Hurwitz method, determine whether the system is stable. If it is not stable, how many poles are in the right half-plane? (b) Compute the poles of $T(s)$ and verify the result in part (a). (c) Plot the unit step response, and discuss the results.

- CP6.5** A "paper-pilot" model is sometimes utilized in aircraft control design and analysis to represent the pilot in the loop. A block diagram of an aircraft with a pilot "in the loop" is shown in Figure CP6.5. The variable τ represents the pilot's time delay. We can represent a slower pilot with $\tau = 0.6$ and a faster pilot with $\tau = 0.1$. The remaining variables in the pilot model are assumed to be $K = 1$, $\tau_1 = 2$, and $\tau_2 = 0.5$. Develop an m-file to compute the closed-loop system poles for the fast and slow pilots. Comment on the results. What is the maximum pilot time delay allowable for stability?

- CP6.6** Consider the feedback control system in Figure CP6.6. Using the for function, develop an m-file script

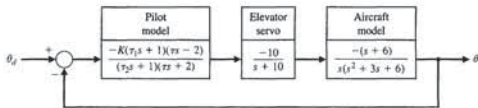


FIGURE CP6.5 An aircraft with a pilot in the loop.

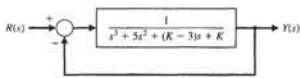


FIGURE CP6.6 A single-loop feedback control system with parameter K .

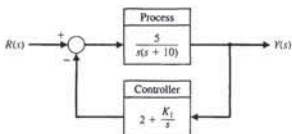


FIGURE CP6.8 Nonunity feedback system with parameter K_1 .

to compute the closed-loop transfer function poles for $0 \leq K \leq 5$ and plot the results denoting the poles with the "x" symbol. Determine the maximum range of K for stability with the Routh-Hurwitz method. Compute the roots of the characteristic equation when K is the minimum value allowed for stability.

- CP6.7** Consider a system in state variable form:

$$\dot{\mathbf{x}} = \begin{bmatrix} 0 & 1 & 0 \\ 0 & 0 & 1 \\ -12 & -14 & -10 \end{bmatrix} \mathbf{x} + \begin{bmatrix} 0 \\ 0 \\ 12 \end{bmatrix} u$$

$$y = [1 \quad 1 \quad 0] \mathbf{x}$$

- (a) Compute the characteristic equation using the poly function. (b) Compute the roots of the characteristic equation, and determine whether the system is stable. (c) Obtain the response plot of $y(t)$ when $u(t)$ is a unit step and when the system has zero initial conditions.

- CP6.8** Consider the feedback control system in Figure CP6.8. (a) Using the Routh-Hurwitz method, determine the range of K_1 resulting in closed-loop stability. (b) Develop an m-file to plot the pole locations as a function of $0 < K_1 < 30$ and comment on the results.

- CP6.9** Consider a system represented in state variable form

$$\dot{\mathbf{x}} = \mathbf{A}\mathbf{x} + \mathbf{B}u$$

$$y = \mathbf{C}\mathbf{x} + \mathbf{D}u$$

Assume that the input is a linear combination of the states, that is,

$$u(t) = -\mathbf{K}\mathbf{x}(t) + r(t),$$

where $r(t)$ is the reference input. The matrix $\mathbf{K} = [K_1 \quad K_2]$ is known as the gain matrix. If you substitute $u(t)$ into the state variable equation you will obtain the closed-loop system

$$\dot{\mathbf{x}}(t) = [\mathbf{A} - \mathbf{B}\mathbf{K}]\mathbf{x}(t) + \mathbf{B}r(t)$$

$$y(t) = \mathbf{C}\mathbf{x}(t)$$

For what values of \mathbf{K} is the closed-loop system stable? Determine the region of the left half-plane where the desired closed-loop eigenvalues should be placed so that the percent overshoot to a unit step input, $R(s) = 1/s$, is less than $P.O. < 5\%$ and the settling time is less than $T_s < 4s$. Select a gain matrix, \mathbf{K} , so that the system step response meets the specifications $P.O. < 5\%$ and $T_s < 4s$.

- DP6.7** Consider the feedback control system in Figure DP6.7. The system has an inner loop and an outer loop.

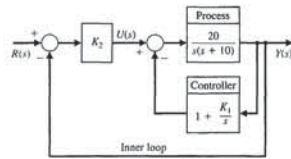


FIGURE DP6.7 Feedback system with inner and outer loop.

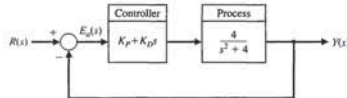


FIGURE DP6.8 A marginally stable plant with a PD controller in the loop.

COMPUTER PROBLEMS

- CP6.1** Determine the roots of the following characteristic equations:
 (a) $q(s) = s^3 + 3s^2 + 10s + 14 = 0$,
 (b) $q(s) = s^4 + 8s^3 + 24s^2 + 32s + 16 = 0$,
 (c) $q(s) = s^2 + 2s^2 + 1 = 0$.

Develop an m-file to compute the roots of the closed-loop transfer function characteristic polynomial for $K = 1, 2$, and 5 . For which values of K is the closed-loop system stable?

- CP6.2** Consider a unity negative feedback system with

$$G_c(s) = K \text{ and } G(s) = \frac{s^2 - s + 2}{s^2 + 2s + 1}$$

- CP6.3** A unity negative feedback system has the loop transfer function

$$G_c(s)G(s) = \frac{s+1}{s^3 + 4s^2 + 6s + 10}$$

- 7.1 Introduction 444
- 7.2 The Root Locus Concept 444
- 7.3 The Root Locus Procedure 448
- 7.4 Parameter Design by the Root Locus Method 467
- 7.5 Sensitivity and the Root Locus 473
- 7.6 PID Controllers 480
- 7.7 Negative Gain Root Locus 492
- 7.8 Design Examples 496
- 7.9 The Root Locus Using Control Design Software 510
- 7.10 Sequential Design Example: Disk Drive Read System 516
- 7.11 Summary 518

P R E V I E W

The performance of a feedback system can be described in terms of the location of the roots of the characteristic equation in the s -plane. A graph showing how the roots of the characteristic equation move around the s -plane as a single parameter varies is known as a root locus plot. The root locus is a powerful tool for designing and analyzing feedback control systems. We will discuss practical techniques for obtaining a sketch of a root locus plot by hand. We also consider computer-generated root locus plots and illustrate their effectiveness in the design process. We will show that it is possible to use root locus methods for controller design when more than one parameter varies. This is important because we know that the response of a closed-loop feedback system can be adjusted to achieve the desired performance by judicious selection of one or more controller parameters. The popular PID controller is introduced as a practical controller structure. We will also define a measure of sensitivity of a specified root to a small incremental change in a system parameter. The chapter concludes with a controller design based on root locus methods for the Sequential Design Example: Disk Drive Read System.

DESIRED OUTCOMES

Upon completion of Chapter 7, students should:

- Understand the powerful concept of the root locus and its role in control system design.
- Know how to obtain a root locus plot by sketching or using computers.
- Be familiar with the PID controller as a key element of many feedback systems.
- Recognize the role of root locus plots in parameter design and system sensitivity analysis.
- Be able to design controllers to meet desired specifications using root locus methods.

443

Section 7.2 The Root Locus Concept

445

and therefore it is necessary that

$$|KG(s)| = 1$$

and

$$\angle KG(s) = 180^\circ + k360^\circ, \quad (7.4)$$

where $k = 0, \pm 1, \pm 2, \pm 3, \dots$

The root locus is the path of the roots of the characteristic equation traced out in the s -plane as a system parameter varies from zero to infinity.

The simple second-order system considered in the previous chapters is shown in Figure 7.2. The characteristic equation representing this system is

$$\Delta(s) = 1 + KG(s) = 1 + \frac{K}{s(s+2)} = 0, \quad (7.5)$$

or, alternatively,

$$\Delta(s) = s^2 + 2s + K = s^2 + 2\zeta\omega_n s + \omega_n^2 = 0. \quad (7.5)$$

The locus of the roots as the gain K is varied is found by requiring that

$$|KG(s)| = \left| \frac{K}{s(s+2)} \right| = 1 \quad (7.6)$$

and

$$\angle KG(s) = \pm 180^\circ, \pm 540^\circ, \dots \quad (7.7)$$

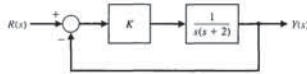
The gain K may be varied from zero to an infinitely large positive value. For a second-order system, the roots are

$$s_{1,2} = -\zeta\omega_n \pm \omega_n \sqrt{\zeta^2 - 1}, \quad (7.8)$$

and for $\zeta < 1$, we know that $\theta = \cos^{-1} \zeta$. Graphically, for two open-loop poles as shown in Figure 7.3, the locus of roots is a vertical line for $\zeta \leq 1$ in order to satisfy the angle requirement, Equation (7.7). For example, as shown in Figure 7.4, at a root s_1 , the angles are

$$\left. \frac{K}{s(s+2)} \right|_{s=s_1} = -\angle s_1 - \angle (s_1 + 2) = -[(180^\circ - \theta) + \theta] = -180^\circ. \quad (7.9)$$

FIGURE 7.2 Unity feedback control system. The gain K is a variable parameter.



where

$$A = \begin{bmatrix} 0 & 1 & 0 \\ 2 & 0 & 1 \\ -k & -3 & -2 \end{bmatrix}, B = \begin{bmatrix} -1 \\ 0 \\ 1 \end{bmatrix}, C = [1 \ 2 \ 0], D = [0].$$

- (a) For what values of k is the system stable?
- (b) Develop an m-file to plot the pole locations as a function of $0 < k < 10$ and comment on the results.



ANSWERS TO SKILLS CHECK

True or False: (1) False; (2) True; (3) False; (4) True; (5) True
 Word Match (in order, top to bottom): e, d, f, a, b, g, c
 Multiple Choice: (6) a; (7) c; (8) a; (9) b; (10) b; (11) a; (12) a; (13) b; (14) a; (15) b

TERMS AND CONCEPTS

- Absolute stability** A system description that reveals whether a system is stable or not stable without consideration of other system attributes such as degree of stability.
- Auxiliary polynomial** The equation that immediately precedes the zero entry in the Routh array.
- Marginally stable** A system is marginally stable if and only if the zero input response remains bounded as $t \rightarrow \infty$.
- Relative stability** The property that is measured by the relative real part of each root or pair of roots of the characteristic equation.
- Routh-Hurwitz criterion** A criterion for determining the stability of a system by examining the characteristic equation of the transfer function. The criterion states that the number of roots of the characteristic equation with positive real parts is equal to the number of changes of sign of the coefficients in the first column of the Routh array.
- Stability** A performance measure of a system. A system is stable if all the poles of the transfer function have negative real parts.
- Stable system** A dynamic system with a bounded system response to a bounded input.

7.1 INTRODUCTION

The relative stability and the transient performance of a closed-loop control system are directly related to the location of the closed-loop roots of the characteristic equation in the s -plane. It is frequently necessary to adjust one or more system parameters in order to obtain suitable root locations. Therefore, it is worthwhile to determine how the roots of the characteristic equation of a given system migrate about the s -plane as the parameters are varied; that is, it is useful to determine the locus of roots in the s -plane as a parameter is varied. The **root locus method** was introduced by Evans in 1948 and has been developed and utilized extensively in control engineering practice [1–3]. The root locus technique is a graphical method for sketching the locus of roots in the s -plane as a parameter is varied. In fact, the root locus method provides the engineer with a measure of the sensitivity of the roots of the system to a variation in the parameter being considered. The root locus technique may be used to great advantage in conjunction with the Routh–Hurwitz criterion.

The root locus method provides graphical information, and therefore an approximate sketch can be used to obtain qualitative information concerning the stability and performance of the system. Furthermore, the locus of roots of the characteristic equation of a multiloop system may be investigated as readily as for a single-loop system. If the root locations are not satisfactory, the necessary parameter adjustments often can be readily ascertained from the root locus [4].

7.2 THE ROOT LOCUS CONCEPT

The dynamic performance of a closed-loop control system is described by the closed-loop transfer function

$$T(s) = \frac{Y(s)}{R(s)} = \frac{p(s)}{q(s)}, \quad (7.1)$$

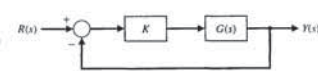
where $p(s)$ and $q(s)$ are polynomials in s . The roots of the characteristic equation $q(s)$ determine the modes of response of the system. In the case of the simple single-loop system shown in Figure 7.1, we have the characteristic equation

$$1 + KG(s) = 0, \quad (7.2)$$

where K is a variable parameter and $0 \leq K < \infty$. The characteristic roots of the system must satisfy Equation (7.2), where the roots lie in the s -plane. Because s is a complex variable, Equation (7.2) may be rewritten in polar form as

$$|KG(s)| / |KG(s)| = -1 + j0, \quad (7.3)$$

FIGURE 7.1 Closed-loop control system with a variable parameter K .



where L_n equals the value of the n th self-loop transmittance. Hence, we have a characteristic equation, which may be written as

$$q(s) = \Delta(s) = 1 + F(s). \quad (7.13)$$

To find the roots of the characteristic equation, we set Equation (7.13) equal to zero and obtain

$$1 + F(s) = 0. \quad (7.14)$$

Equation (7.14) may be rewritten as

$$F(s) = -1 + j0, \quad (7.15)$$

and the roots of the characteristic equation must also satisfy this relation.

In general, the function $F(s)$ may be written as

$$F(s) = \frac{K(s + z_1)(s + z_2)(s + z_3) \cdots (s + z_M)}{(s + p_1)(s + p_2)(s + p_3) \cdots (s + p_n)}$$

Then the magnitude and angle requirement for the root locus are

$$|F(s)| = \frac{K|s + z_1||s + z_2| \cdots}{|s + p_1||s + p_2| \cdots} = 1 \quad (7.16)$$

and

$$\angle F(s) = \angle s + z_1 + \angle s + z_2 + \cdots - (\angle s + p_1 + \angle s + p_2 + \cdots) = 180^\circ + k360^\circ, \quad (7.17)$$

where k is an integer. The magnitude requirement, Equation (7.16), enables us to determine the value of K for a given root location s_1 . A test point in the s -plane, s_1 , is verified as a root location when Equation (7.17) is satisfied. All angles are measured in a counterclockwise direction from a horizontal line.

To further illustrate the root locus procedure, let us consider again the second-order system of Figure 7.5(a). The effect of varying the parameter a can

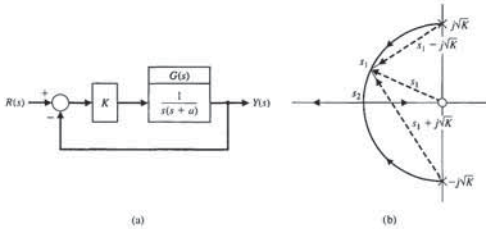


FIGURE 7.5 (a) Single-loop system. (b) Root locus as a function of the parameter a , where $a > 0$.

7.3 THE ROOT LOCUS PROCEDURE

The roots of the characteristic equation of a system provide a valuable insight concerning the response of the system. To locate the roots of the characteristic equation in a graphical manner on the s -plane, we will develop an orderly procedure of seven steps that facilitates the rapid sketching of the locus.

Step 1: Prepare the root locus sketch. Begin by writing the characteristic equation as

$$1 + F(s) = 0. \quad (7.22)$$

Rearrange the equation, if necessary, so that the parameter of interest, K , appears as the multiplying factor in the form,

$$1 + KP(s) = 0. \quad (7.23)$$

We are usually interested in determining the locus of roots as K varies as

$$0 \leq K \leq \infty.$$

In Section 7.7, we consider the case when K varies as $-\infty < K \leq 0$. Factor $P(s)$, and write the polynomial in the form of poles and zeros as follows:

$$1 + K \frac{\prod_{i=1}^M (s + z_i)}{\prod_{j=1}^n (s + p_j)} = 0. \quad (7.24)$$

Locate the poles $-p_j$ and zeros $-z_i$ on the s -plane with selected symbols. By convention, we use 'x' to denote poles and 'o' to denote zeros.

Rewriting Equation (7.24), we have

$$\prod_{j=1}^n (s + p_j) + K \prod_{i=1}^M (s + z_i) = 0. \quad (7.25)$$

Note that Equation (7.25) is another way to write the characteristic equation. When $K = 0$, the roots of the characteristic equation are the poles of $P(s)$. To see this, consider Equation (7.25) with $K = 0$. Then, we have

$$\prod_{j=1}^n (s + p_j) = 0.$$

When solved, this yields the values of s that coincide with the poles of $P(s)$. Conversely, as $K \rightarrow \infty$, the roots of the characteristic equation are the zeros of $P(s)$. To see this, first divide Equation (7.25) by K . Then, we have

$$\frac{1}{K} \prod_{j=1}^n (s + p_j) + \prod_{i=1}^M (s + z_i) = 0,$$

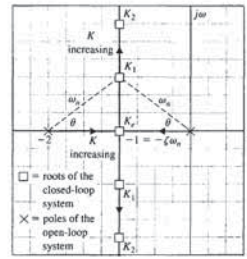


FIGURE 7.3 Root locus for a second-order system when $K_0 < K_1 < K_2$. The locus is shown as heavy lines, with arrows indicating the direction of increasing K . Note that roots of the characteristic equation are denoted by 'x' on the root locus.

This angle requirement is satisfied at any point on the vertical line that is a perpendicular bisector of the line 0 to -2 . Furthermore, the gain K at the particular points is found by using Equation (7.6) as

$$\left| \frac{K}{s(s+2)} \right|_{s=s_1} = \frac{K}{|s_1||s_1+2|} = 1, \quad (7.10)$$

and thus

$$K = |s_1||s_1+2|, \quad (7.11)$$

where $|s_1|$ is the magnitude of the vector from the origin to s_1 , and $|s_1+2|$ is the magnitude of the vector from -2 to s_1 .

For a multiloop closed-loop system, we found in Section 2.7 that by using Mason's signal-flow gain formula, we had

$$\Delta(s) = 1 - \sum_{n=1}^N L_n + \sum_{\substack{n,m \\ \text{non-touching}}} L_n L_m - \sum_{\substack{n,m,p \\ \text{non-touching}}} L_n L_m L_p + \cdots, \quad (7.12)$$

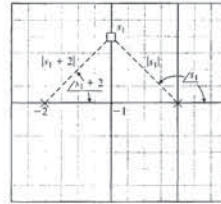


FIGURE 7.4 Evaluation of the angle and gain at s_1 for gain $K = K_1$.

be effectively portrayed by rewriting the characteristic equation for the root locus form with a as the multiplying factor in the numerator. Then the characteristic equation is

$$1 + KG(s) = 1 + \frac{K}{s(s+a)} = 0,$$

or, alternatively,

$$s^2 + as + K = 0.$$

Dividing by the factor $s^2 + K$, we obtain

$$1 + \frac{as}{s^2 + K} = 0. \quad (7.18)$$

Then the magnitude criterion is satisfied when

$$\frac{a|s_1|}{|s_1^2 + K|} = 1 \quad (7.19)$$

at the root s_1 . The angle criterion is

$$\angle s_1 - (\angle s_1 + j\sqrt{K} + \angle s_1 - j\sqrt{K}) = \pm 180^\circ, \pm 540^\circ, \dots$$

In principle, we could construct the root locus by determining the points in the s -plane that satisfy the angle criterion. In the next section, we will develop a multi-step procedure to sketch the root locus. The root locus for the characteristic equation in Equation (7.18) is shown in Figure 7.5(b). Specifically at the root s_1 , the magnitude of the parameter a is found from Equation (7.19) as

$$a = \frac{|s_1 - j\sqrt{K}||s_1 + j\sqrt{K}|}{|s_1|}. \quad (7.20)$$

The roots of the system merge on the real axis at the point s_2 and provide a critically damped response to a step input. The parameter a has a magnitude at the critically damped roots, $s_2 = \sigma_2$, equal to

$$a = \frac{|\sigma_2 - j\sqrt{K}||\sigma_2 + j\sqrt{K}|}{\sigma_2} = \frac{1}{\sigma_2}(\sigma_2^2 + K) = 2\sqrt{K}, \quad (7.21)$$

where σ_2 is evaluated from the s -plane vector lengths as $\sigma_2 = \sqrt{K}$. As a increases beyond the critical value, the roots are both real and distinct; one root is larger than σ_2 , and one is smaller.

In general, we desire an orderly process for locating the locus of roots as a parameter varies. In the next section, we will develop such an orderly approach to sketching a root locus diagram.

STEP 2: The angle criterion is satisfied on the real axis between the points 0 and -2, because the angle from pole p_1 at the origin is 180° , and the angle from the zero and pole p_2 at $s = -4$ is zero degrees. The locus begins at the pole and ends at the zero, and therefore the locus of roots appears as shown in Figure 7.6(b), where the direction of the locus as K is increasing ($K \uparrow$) is shown by an arrow. We note that because the system has two real poles and one real zero, the second locus segment ends at a zero at negative infinity. To evaluate the gain K at a specific root location on the locus, we use the magnitude criterion, Equation (7.16). For example, the gain K at the root $s = s_1 = -1$ is found from (7.16) as

$$\frac{(2K)|s_1 + 2|}{|s_1||s_1 + 4|} = 1$$

or

$$K = \frac{|-1||-1 + 4|}{2|-1 + 2|} = \frac{3}{2} \quad (7.28)$$

This magnitude can also be evaluated graphically, as shown in Figure 7.6(c). For the gain of $K = \frac{3}{2}$, one other root exists, located on the locus to the left of the pole at -4. The location of the second root is found graphically to be located at $s = -6$, as shown in Figure 7.6(c).

Now, we determine the number of separate loci, SL . Because the loci begin at the poles and end at the zeros, the **number of separate loci is equal to the number of poles** since the number of poles is greater than or equal to the number of zeros. Therefore, as we found in Figure 7.6, the number of separate loci is equal to two because there are two poles and one zero.

Note that the **root loci must be symmetrical with respect to the horizontal real axis** because the complex roots must appear as pairs of complex conjugate roots. ■

We now return to developing a general list of root locus steps.

STEP 3: The loci proceed to the zeros at infinity along asymptotes centered at σ_A and with angles ϕ_A . When the number of finite zeros of $P(s)$, M , is less than the number of poles n by the number $N = n - M$, then N sections of loci must end at zeros at infinity. These sections of loci proceed to the zeros at infinity along **asymptotes** as K approaches infinity. These linear asymptotes are centered at a point on the real axis given by

$$\sigma_A = \frac{\sum \text{poles of } P(s) - \sum \text{zeros of } P(s)}{n - M} = \frac{\sum_{i=1}^n (-p_i) - \sum_{i=1}^M (-z_i)}{n - M} \quad (7.29)$$

The **angle of the asymptotes** with respect to the real axis is

$$\phi_A = \frac{2k + 1}{n - M} 180^\circ, \quad k = 0, 1, 2, \dots, (n - M - 1) \quad (7.30)$$

The first two terms of

$$1 + \frac{K}{(s - \sigma_A)^{n-M}} = 0$$

are

$$1 + \frac{K}{s^{n-M} - (n - M)\sigma_A s^{n-M-1}} = 0.$$

Equating the term for s^{n-M-1} , we obtain

$$a_{n-1} - b_{M-1} = -(n - M)\sigma_A,$$

or

$$\sigma_A = \frac{\sum_{i=1}^n (-p_i) - \sum_{i=1}^M (-z_i)}{n - M}$$

which is Equation (7.29).

For example, reexamine the system shown in Figure 7.2 and discussed in Section 7.2. The characteristic equation is written as

$$1 + \frac{K}{s(s + 2)} = 0.$$

Because $n - M = 2$, we expect two loci to end at zeros at infinity. The asymptotes of the loci are located at a center

$$\sigma_A = \frac{-2}{2} = -1$$

and at angles of

$$\phi_A = 90^\circ \text{ (for } k = 0) \text{ and } \phi_A = 270^\circ \text{ (for } k = 1).$$

The root locus is readily sketched, and the locus shown in Figure 7.3 is obtained. An example will further illustrate the process of using the asymptotes.

EXAMPLE 7.2 Fourth-order system

A single-loop feedback control system has a characteristic equation as follows:

$$1 + GH(s) = 1 + \frac{K(s + 1)}{s(s + 2)(s + 4)^2} = 0 \quad (7.31)$$

We wish to sketch the root locus in order to determine the effect of the gain K . The poles and zeros are located in the s -plane, as shown in Figure 7.7(a). The root loci on the real axis must be located to the left of an odd number of poles and zeros; they are shown as heavy lines in Figure 7.7(a). The intersection of the asymptotes is

$$\sigma_A = \frac{(-2) + 2(-4) - (-1)}{4 - 1} = \frac{-9}{3} = -3. \quad (7.32)$$

which, as $K \rightarrow \infty$, reduces to

$$\prod_{i=1}^M (s + z_i) = 0.$$

When solved, this yields the values of s that coincide with the zeros of $P(s)$. Therefore, we note that the **locus of the roots of the characteristic equation $1 + KP(s) = 0$ begins at the poles of $P(s)$ and ends at the zeros of $P(s)$ as K increases from zero to infinity**. For most functions $P(s)$ that we will encounter, several of the zeros of $P(s)$ lie at infinity in the s -plane. This is because most of our functions have more poles than zeros. With n poles and M zeros and $n > M$, we have $n - M$ branches of the root locus approaching the $n - M$ zeros at infinity.

STEP 2: Locate the segments of the real axis that are root loci. **The root locus on the real axis always lies in a section of the real axis to the left of an odd number of poles and zeros.** This fact is ascertained by examining the angle criterion of Equation (7.17). These two useful steps in plotting a root locus will be illustrated by a suitable example.

EXAMPLE 7.1 Second-order system

A single-loop feedback control system possesses the characteristic equation

$$1 + GH(s) = 1 + \frac{K(\frac{1}{2}s + 1)}{\frac{1}{4}s^2 + s} = 0. \quad (7.26)$$

STEP 1: The characteristic equation can be written as

$$1 + K \frac{2(s + 2)}{s^2 + 4s} = 0,$$

where

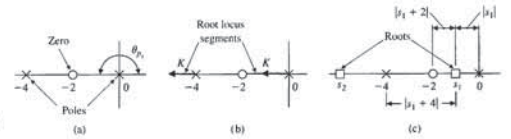
$$P(s) = \frac{2(s + 2)}{s^2 + 4s}.$$

The transfer function, $P(s)$, is rewritten in terms of poles and zeros as

$$1 + K \frac{2(s + 2)}{s(s + 4)} = 0, \quad (7.27)$$

and the multiplicative gain parameter is K . To determine the locus of roots for the gain $0 \leq K \leq \infty$, we locate the poles and zeros on the real axis as shown in Figure 7.6(a).

FIGURE 7.6 (a) The zero and poles of a second-order system, (b) the root locus segments, and (c) the magnitude of each vector at s_1 .



where k is an integer index [3]. The usefulness of this rule is obvious for sketching the approximate form of a root locus. Equation (7.30) can be readily derived by considering a point on a root locus segment at a remote distance from the finite poles and zeros in the s -plane. The net phase angle at this remote point is 180° , because it is a point on a root locus segment. The finite poles and zeros of $P(s)$ are a great distance from the remote point, and so the angles from each pole and zero, ϕ , are essentially equal, and therefore the net angle is simply $(n - M)\phi$, where n and M are the number of finite poles and zeros, respectively. Thus, we have

$$(n - M)\phi = 180^\circ,$$

or, alternatively,

$$\phi = \frac{180^\circ}{n - M}.$$

Accounting for all possible root locus segments at remote locations in the s -plane, we obtain Equation (7.30).

The center of the linear asymptotes, often called the **asymptote centroid**, is determined by considering the characteristic equation in Equation (7.24). For large values of s , only the higher-order terms need be considered, so that the characteristic equation reduces to

$$1 + \frac{Ks^M}{s^n} = 0.$$

However, this relation, which is an approximation, indicates that the centroid of $n - M$ asymptotes is at the origin, $s = 0$. A better approximation is obtained if we consider a characteristic equation of the form

$$1 + \frac{K}{(s - \sigma_A)^{n-M}} = 0$$

with a centroid at σ_A .

The centroid is determined by considering the first two terms of Equation (7.24), which may be found from the relation

$$1 + \frac{K \prod_{i=1}^M (s + z_i)}{\prod_{j=1}^n (s + p_j)} = 1 + K \frac{s^M + b_{M-1}s^{M-1} + \dots + b_0}{s^n + a_{n-1}s^{n-1} + \dots + a_0}.$$

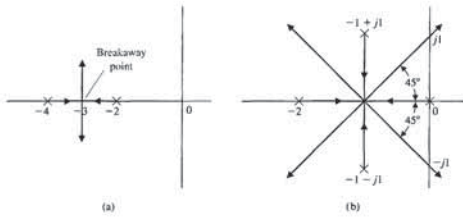
From Chapter 6, especially Equation (6.5), we note that

$$b_{M-1} = \sum_{i=1}^M z_i \text{ and } a_{n-1} = \sum_{j=1}^n p_j.$$

Considering only the first two terms of this expansion, we have

$$1 + \frac{K}{s^{n-M} + (a_{n-1} - b_{M-1})s^{n-M-1}} = 0.$$

FIGURE 7.8 Illustration of the breakaway point (a) for a simple second-order system and (b) for a fourth-order system.



the rearranging of the characteristic equation to isolate the multiplying factor K . Then the characteristic equation is written as

$$p(s) = K. \tag{7.33}$$

For example, consider a unity feedback closed-loop system with an open-loop transfer function

$$G(s) = \frac{K}{(s + 2)(s + 4)},$$

which has the characteristic equation

$$1 + G(s) = 1 + \frac{K}{(s + 2)(s + 4)} = 0. \tag{7.34}$$

Alternatively, the equation may be written as

$$K = p(s) = -(s + 2)(s + 4). \tag{7.35}$$

The root loci for this system are shown in Figure 7.8(a). We expect the breakaway point to be near $s = \sigma = -3$ and plot $p(s)|_{s=\sigma}$ near that point, as shown in Figure 7.9. In this case, $p(s)$ equals zero at the poles $s = -2$ and $s = -4$. The plot of $p(s)$ versus $s - \sigma$ is symmetrical, and the maximum point occurs at $s = \sigma = -3$, the breakaway point.

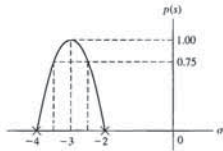


FIGURE 7.9 A graphical evaluation of the breakaway point.

Now, considering again the specific case where

$$G(s) = \frac{K}{(s + 2)(s + 4)},$$

we obtain

$$p(s) = K = -(s + 2)(s + 4) = -(s^2 + 6s + 8). \tag{7.43}$$

Then, when we differentiate, we have

$$\frac{dp(s)}{ds} = -(2s + 6) = 0, \tag{7.44}$$

or the breakaway point occurs at $s = -3$. A more complicated example will illustrate the approach and demonstrate the use of the graphical technique to determine the breakaway point.

EXAMPLE 7.3 Third-order system

A feedback control system is shown in Figure 7.10. The characteristic equation is

$$1 + G(s)H(s) = 1 + \frac{K(s + 1)}{s(s + 2)(s + 3)} = 0. \tag{7.45}$$

The number of poles n minus the number of zeros M is equal to 2, and so we have two asymptotes at $\pm 90^\circ$ with a center at $\sigma_A = -2$. The asymptotes and the sections of loci on the real axis are shown in Figure 7.11(a). A breakaway point occurs between $s = -2$ and $s = -3$. To evaluate the breakaway point, we rewrite the characteristic equation so that K is separated; thus,

$$s(s + 2)(s + 3) + K(s + 1) = 0,$$

or

$$p(s) = \frac{-s(s + 2)(s + 3)}{s + 1} = K. \tag{7.46}$$

Then, evaluating $p(s)$ at various values of s between $s = -2$ and $s = -3$, we obtain the results of Table 7.1, as shown in Figure 7.11(b). Alternatively, we differentiate

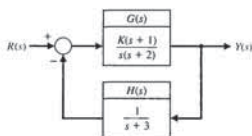


FIGURE 7.10 Closed-loop system.

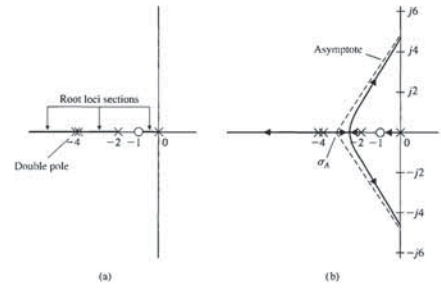


FIGURE 7.7 A fourth-order system with (a) a zero and (b) root locus.

The angles of the asymptotes are

$$\begin{aligned} \phi_A &= +60^\circ \quad (k = 0), \\ \phi_A &= 180^\circ \quad (k = 1), \text{ and} \\ \phi_A &= 300^\circ \quad (k = 2), \end{aligned}$$

where there are three asymptotes, since $n - M = 3$. Also, we note that the root loci must begin at the poles; therefore, two loci must leave the double pole at $s = -4$. Then with the asymptotes sketched in Figure 7.7(b), we may sketch the form of the root locus as shown in Figure 7.7(b). The actual shape of the locus in the area near σ_A would be graphically evaluated, if necessary. ■

We now proceed to develop more steps for the process of determining the root loci.

Step 4: Determine where the locus crosses the imaginary axis (if it does so), using the Routh–Hurwitz criterion. The actual point at which the root locus crosses the imaginary axis is readily evaluated by using the criterion.

Step 5: Determine the breakaway point on the real axis (if any). The root locus in Example 7.2 left the real axis at a breakaway point. The locus breakaway from the real axis occurs where the net change in angle caused by a small displacement is zero. The locus leaves the real axis where there is a multiplicity of roots (typically, two). The breakaway point for a simple second-order system is shown in Figure 7.8(a) and, for a special case of a fourth-order system, is shown in Figure 7.8(b). In general, due to the phase criterion, the tangents to the loci at the breakaway point are equally spaced over 360° . Therefore, in Figure 7.8(a), we find that the two loci at the breakaway point are spaced 180° apart, whereas in Figure 7.8(b), the four loci are spaced 90° apart.

The breakaway point on the real axis can be evaluated graphically or analytically. The most straightforward method of evaluating the breakaway point involves

Analytically, the very same result may be obtained by determining the maximum of $K = p(s)$. To find the maximum analytically, we differentiate, set the differentiated polynomial equal to zero, and determine the roots of the polynomial. Therefore, we may evaluate

$$\frac{dK}{ds} = \frac{dp(s)}{ds} = 0 \tag{7.36}$$

in order to find the breakaway point. Equation (7.36) is an analytical expression of the graphical procedure outlined in Figure 7.9 and will result in an equation of only one degree less than the total number of poles and zeros $n + M - 1$.

The proof of Equation (7.36) is obtained from a consideration of the characteristic equation

$$1 + F(s) = 1 + \frac{KY(s)}{X(s)} = 0,$$

which may be written as

$$X(s) + KY(s) = 0. \tag{7.37}$$

For a small increment in K , we have

$$X(s) + (K + \Delta K)Y(s) = 0.$$

Dividing by $X(s) + KY(s)$ yields

$$1 + \frac{\Delta KY(s)}{X(s) + KY(s)} = 0. \tag{7.38}$$

Because the denominator is the original characteristic equation, a multiplicity m of roots exists at a breakaway point, and

$$\frac{Y(s)}{X(s) + KY(s)} = \frac{C_i}{(s - s_i)^m} = \frac{C_i}{(\Delta s)^m}. \tag{7.39}$$

Then we may write Equation (7.38) as

$$1 + \frac{\Delta KC_i}{(\Delta s)^m} = 0, \tag{7.40}$$

or, alternatively,

$$\frac{\Delta K}{\Delta s} = \frac{-(\Delta s)^{m-1}}{C_i}. \tag{7.41}$$

Therefore, as we let Δs approach zero, we obtain

$$\frac{dK}{ds} = 0 \tag{7.42}$$

at the breakaway points.

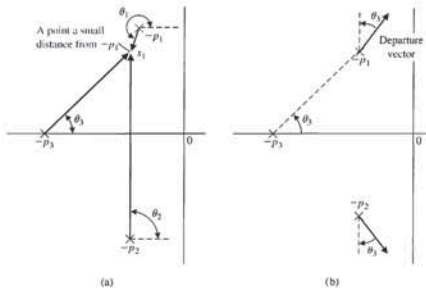


FIGURE 7.12 Illustration of the angle of departure. (a) Test point infinitesimal distance from $-p_1$. (b) Actual departure vector at $-p_1$.

meet the angle criterion. Therefore, since $\theta_2 = 90^\circ$, we have

$$\theta_1 + \theta_2 + \theta_3 = \theta_1 + 90^\circ + \theta_3 = +180^\circ,$$

or the angle of departure at pole p_1 is

$$\theta_1 = 90^\circ - \theta_3,$$

as shown in Figure 7.12(b). The departure at pole $-p_2$ is the negative of that at $-p_1$, because $-p_1$ and $-p_2$ are complex conjugates. Another example of a departure angle is shown in Figure 7.13. In this case, the departure angle is found from

$$\theta_2 - (\theta_1 + \theta_3 + 90^\circ) = 180^\circ + k360^\circ.$$

Since $\theta_2 - \theta_3 = \gamma$ in the diagram, we find that the departure angle is $\theta_1 = 90^\circ + \gamma$.

Step 7: The final step in the root locus sketching procedure is to complete the sketch. This entails sketching in all sections of the locus not covered in the previous

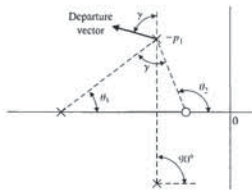


FIGURE 7.13 Evaluation of the angle of departure.

EXAMPLE 7.4 Fourth-order system

- (a) We desire to plot the root locus for the characteristic equation of a system as K varies for $K > 0$ when

$$1 + \frac{K}{s^4 + 12s^3 + 64s^2 + 128s} = 0.$$

- (b) Determining the poles, we have

$$1 + \frac{K}{s(s+4)(s+4+j4)(s+4-j4)} = 0 \quad (7.49)$$

as K varies from zero to infinity. This system has no finite zeros.

- (c) The poles are located on the s -plane as shown in Figure 7.14(a).
- (d) Because the number of poles n is equal to 4, we have four separate loci.
- (e) The root loci are symmetrical with respect to the real axis.

2. A segment of the root locus exists on the real axis between $s = 0$ and $s = -4$.
3. The angles of the asymptotes are

$$\phi_A = \frac{(2k+1)}{4} 180^\circ, \quad k = 0, 1, 2, 3;$$

$$\phi_A = +45^\circ, 135^\circ, 225^\circ, 315^\circ.$$

The center of the asymptotes is

$$\sigma_A = \frac{-4 - 4 - 4 - 4}{4} = -3.$$

Then the asymptotes are drawn as shown in Figure 7.14(a).

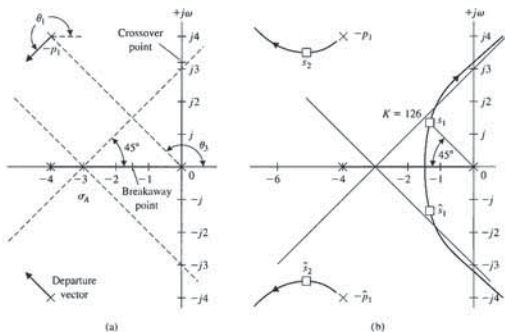


FIGURE 7.14 The root locus for Example 7.4. Locating (a) the poles and (b) the asymptotes.

Table 7.1

$p(s)$	0	0.411	0.419	0.417	+0.390	0
s	-2.00	-2.40	-2.46	-2.50	-2.60	-3.0

Equation (7.46) and set it equal to zero to obtain

$$\frac{d}{ds} \left(\frac{-s(s+2)(s+3)}{(s+1)} \right) = \frac{(s^3 + 5s^2 + 6s) - (s+1)(3s^2 + 10s + 6)}{(s+1)^2} = 0$$

$$2s^3 + 8s^2 + 10s + 6 = 0. \quad (7.47)$$

Now to locate the maximum of $p(s)$, we locate the roots of Equation (7.47) to obtain $s = -2.46, -0.77 \pm 0.79j$. The only value of s on the real axis in the interval $s = -2$ to $s = -3$ is $s = -2.46$; hence this must be the breakaway point. It is evident from this one example that the numerical evaluation of $p(s)$ near the expected breakaway point provides an effective method of evaluating the breakaway point. ■

Step 6: Determine the angle of departure of the locus from a pole and the angle of arrival of the locus at a zero, using the phase angle criterion. The angle of locus departure from a pole is the difference between the net angle due to all other poles and zeros and the criterion angle of $\pm 180^\circ (2k + 1)$, and similarly for the locus angle of arrival at a zero. The angle of departure (or arrival) is particularly of interest for complex poles (and zeros) because the information is helpful in completing the root locus. For example, consider the third-order open-loop transfer function

$$F(s) = G(s)H(s) = \frac{K}{(s + p_3)(s^2 + 2\zeta\omega_n s + \omega_n^2)}. \quad (7.48)$$

The pole locations and the vector angles at one complex pole $-p_1$ are shown in Figure 7.12(a). The angles at a test point s_1 , an infinitesimal distance from $-p_1$, must

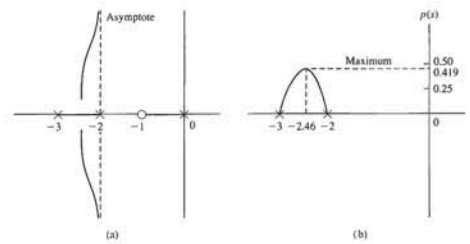


FIGURE 7.11 Evaluation of the (a) asymptotes and (b) breakaway point.

six steps. If a more detailed root locus is required, we recommend using a computer-aided tool. (See Section 7.8.)

In some situation, we may want to determine a root location s_x and the value of the parameter K_x at that root location. Determine the root locations that satisfy the phase criterion at the root $s_x, x = 1, 2, \dots, n$, using the phase criterion. The phase criterion, given in Equation (7.17), is

$$\angle P(s) = 180^\circ + k360^\circ, \quad \text{and } k = 0, \pm 1, \pm 2, \dots$$

To determine the parameter value K_x at a specific root s_x , we use the magnitude requirement (Equation 7.16). The magnitude requirement at s_x is

$$K_x = \left| \frac{\prod_{i=1}^n |s_x + p_i|}{\prod_{i=1}^M |s_x + z_i|} \right|.$$

It is worthwhile at this point to summarize the seven steps utilized in the root locus method (Table 7.2) and then illustrate their use in a complete example.

Table 7.2 Seven Steps for Sketching a Root Locus

Step	Related Equation or Rule
1. Prepare the root locus sketch.	
(a) Write the characteristic equation so that the parameter of interest, K , appears as a multiplier.	$1 + KP(s) = 0.$
(b) Factor $P(s)$ in terms of n poles and M zeros.	$1 + K \frac{\prod_{i=1}^M (s + z_i)}{\prod_{i=1}^n (s + p_i)} = 0.$
(c) Locate the open-loop poles and zeros of $P(s)$ in the s -plane with selected symbols.	$\times = \text{poles}, \circ = \text{zeros}$
(d) Determine the number of separate loci, SL .	Locus begins at a pole and ends at a zero.
(e) The root loci are symmetrical with respect to the horizontal real axis.	$SL = n$ when $n \geq M$; $n = \text{number of finite poles}, M = \text{number of finite zeros}.$
2. Locate the segments of the real axis that are root loci.	Locus lies to the left of an odd number of poles and zeros.
3. The loci proceed to the zeros at infinity along asymptotes centered at σ_A and with angles ϕ_A .	$\sigma_A = \frac{\sum (-p_i) - \sum (-z_i)}{n - M},$ $\phi_A = \frac{2k + 1}{n - M} 180^\circ, k = 0, 1, 2, \dots, (n - M - 1).$
4. Determine the points at which the locus crosses the imaginary axis (if it does so).	Use Routh-Hurwitz criterion (see Section 6.2).
5. Determine the breakaway point on the real axis (if any).	a) Set $K = p(s)$. b) Determine roots of $dp(s)/ds = 0$ or use graphical method to find maximum of $p(s)$. $\angle P(s) = 180^\circ + k360^\circ$ at $s = -p_i$ or $-z_i.$
6. Determine the angle of locus departure from complex poles and the angle of locus arrival at complex zeros, using the phase criterion.	
7. Complete the root locus sketch.	

Using the information derived from the seven steps of the root locus method, the complete root locus sketch is obtained by filling in the sketch as well as possible by visual inspection. The root locus for this system is shown in Figure 7.14(b). When the complex roots near the origin have a damping ratio of $\zeta = 0.707$, the gain K can be determined graphically as shown in Figure 7.14(b). The vector lengths to the root location s_1 from the open-loop poles are evaluated and result in a gain at s_1 of

$$K = |s_1||s_1 + 4||s_1 - p_1||s_1 - \bar{p}_1| = (1.9)(2.9)(3.8)(6.0) = 126. \quad (7.52)$$

The remaining pair of complex roots occurs at s_2 and \bar{s}_2 , when $K = 126$. The effect of the complex roots at s_2 and \bar{s}_2 on the transient response will be negligible compared to the roots s_1 and \bar{s}_1 . This fact can be ascertained by considering the damping of the response due to each pair of roots. The damping due to s_1 and \bar{s}_1 is

$$e^{-\sigma_1 \omega_0 t} = e^{-\sigma_1 t},$$

and the damping factor due to s_2 and \bar{s}_2 is

$$e^{-\zeta_2 \omega_0 t} = e^{-\sigma_2 t},$$

where σ_2 is approximately five times as large as σ_1 . Therefore, the transient response term due to s_2 will decay much more rapidly than the transient response term due to s_1 . Thus, the response to a unit step input may be written as

$$\begin{aligned} y(t) &= 1 + c_1 e^{-\sigma_1 t} \sin(\omega_1 t + \theta_1) + c_2 e^{-\sigma_2 t} \sin(\omega_2 t + \theta_2) \\ &\approx 1 + c_1 e^{-\sigma_1 t} \sin(\omega_1 t + \theta_1). \end{aligned} \quad (7.53)$$

The complex conjugate roots near the origin of the s -plane relative to the other roots of the closed-loop system are labeled the **dominant roots** of the system because they represent or dominate the transient response. The relative dominance of the complex roots, in a third-order system with a pair of complex conjugate roots, is determined by the ratio of the real root to the real part of the complex roots and will result in approximate dominance for ratios exceeding 5.

The dominance of the second term of Equation (7.53) also depends upon the relative magnitudes of the coefficients c_1 and c_2 . These coefficients, which are the residues evaluated at the complex roots, in turn depend upon the location of the zeros in the s -plane. Therefore, the concept of dominant roots is useful for estimating the response of a system, but must be used with caution and with a comprehension of the underlying assumptions. ■

EXAMPLE 7.5 Automatic self-balancing scale

The analysis and design of a control system can be accomplished by using the Laplace transform, a signal-flow diagram or block diagram, the s -plane, and the root locus method. At this point, it will be worthwhile to examine a control system and select suitable parameter values based on the root locus method.

Figure 7.15 shows an automatic self-balancing scale in which the weighing operation is controlled by the physical balance function through an electrical feedback loop [5]. The balance is shown in the equilibrium condition, and x is the travel of the counterweight W_c from an unloaded equilibrium condition. The weight W to be

Table 7.5 Specifications

Steady-state error	$K_p = \infty, e_{ss} = 0$ for a step input
Underdamped response	$\zeta = 0.5$
Settling time (2% criterion)	Less than 2 seconds

2 seconds in order to provide a rapid weight-measuring device. The settling time must be within 2% of the final value of the balance following the introduction of a weight to be measured. The specifications are summarized in Table 7.5.

The derivation of a model of the electromechanical system may be accomplished by obtaining the equations of motion of the balance. For small deviations from balance, the deviation angle is

$$\theta \approx \frac{y}{l_1}. \quad (7.54)$$

The motion of the beam about the pivot is represented by the torque equation

$$I \frac{d^2 \theta}{dt^2} = \sum \text{torques.}$$

Therefore, in terms of the deviation angle, the motion is represented by

$$I \frac{d^2 \theta}{dt^2} = l_1 W - x W_c - l_1^2 b \frac{d\theta}{dt} \quad (7.55)$$

The input voltage to the motor is

$$v_m(t) = K_v y - K_f x. \quad (7.56)$$

The lead screw motion and transfer function of the motor are described by

$$X(s) = K_s \theta_m(s) \quad \text{and} \quad \frac{\theta_m(s)}{V_m(s)} = \frac{K_m}{s(\tau s + 1)} \quad (7.57)$$

where τ will be negligible with respect to the time constants of the overall system, and θ_m is the output shaft rotation. A signal-flow graph and block diagram representing Equations (7.54) through (7.57) is shown in Figure 7.16. Examining the forward path from W to $X(s)$, we find that the system is a type one due to the integration preceding $Y(s)$. Therefore, the steady-state error of the system is zero.

The closed-loop transfer function of the system is obtained by utilizing Mason's signal-flow gain formula and is found to be

$$\frac{X(s)}{W(s)} = \frac{l_1 K_f K_m K_s / (l_1^2 s^2)}{1 + l_1^2 b / (l_1 s) + (K_m K_s K_f / s) + l_1 K_s K_m K_c W_c / (l_1 s^2) + l_1^2 b K_m K_s K_f / (l_1 s^2)} \quad (7.58)$$

where the numerator is the path factor from W to X , the second term in the denominator is the loop L_1 , the third term is the loop factor L_2 , the fourth term is the loop

4. The characteristic equation is rewritten as

$$s(s + 4)(s^2 + 8s + 32) + K = s^4 + 12s^3 + 64s^2 + 128s + K = 0. \quad (7.50)$$

Therefore, the Routh array is

$$\begin{array}{c|ccc} s^4 & 1 & 64 & K \\ s^3 & 12 & 128 & \\ s^2 & b_1 & K & \\ s^1 & c_1 & & \\ s^0 & K & & \end{array}$$

where

$$b_1 = \frac{12(64) - 128^2}{12} = 53.33 \quad \text{and} \quad c_1 = \frac{53.33(128) - 12K}{53.33}$$

Hence, the limiting value of gain for stability is $K = 568.89$, and the roots of the auxiliary equation are

$$53.33s^2 + 568.89 = 53.33(s^2 + 10.67) = 53.33(s + j3.266)(s - j3.266). \quad (7.51)$$

The points where the locus crosses the imaginary axis are shown in Figure 7.14(a). Therefore, when $K = 568.89$, the root locus crosses the $j\omega$ -axis at $s = \pm j3.266$.

5. The breakaway point is estimated by evaluating

$$K = p(s) = -s(s + 4)(s + 4 + j4)(s + 4 - j4)$$

between $s = -4$ and $s = 0$. We expect the breakaway point to lie between $s = -3$ and $s = -1$, so we search for a maximum value of $p(s)$ in that region. The resulting values of $p(s)$ for several values of s are given in Table 7.3. The maximum of $p(s)$ is found to lie at approximately $s = -1.577$, as indicated in the table. A more accurate estimate of the breakaway point is normally not necessary. The breakaway point is then indicated on Figure 7.14(a).

6. The angle of departure at the complex pole p_1 can be estimated by utilizing the angle criterion as follows:

$$\theta_1 + 90^\circ + 90^\circ + \theta_3 = 180^\circ + k360^\circ.$$

Here, θ_3 is the angle subtended by the vector from pole p_3 . The angles from the pole at $s = -4$ and $s = -4 - j4$ are each equal to 90° . Since $\theta_3 = 135^\circ$, we find that

$$\theta_1 = -135^\circ = +225^\circ,$$

as shown in Figure 7.14(a).

7. Complete the sketch as shown in Figure 7.14(b).

Table 7.3

$p(s)$	0	51.0	68.44	80.0	83.57	75.0	0
s	-4.0	-3.0	-2.5	-2.0	-1.577	-1.0	0

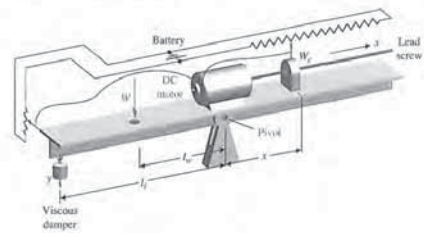


FIGURE 7.15 An automatic self-balancing scale. (Reprinted with permission from J. H. Goldberg, *Automatic Controls*, Allyn and Bacon, Boston, 1964.)

measured is applied 5 cm from the pivot, and the length l_1 of the beam to the viscous damper is 20 cm. We desire to accomplish the following:

1. Select the parameters and the specifications of the feedback system.
2. Obtain a model representing the system.
3. Select the gain K based on a root locus diagram.
4. Determine the dominant mode of response.

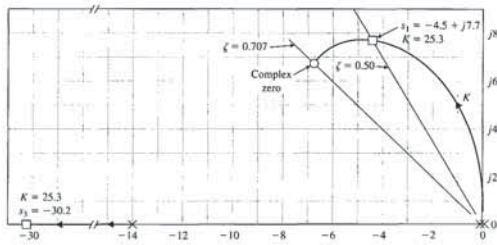
An inertia of the beam equal to 0.05 kg m^2 will be chosen. We must select a battery voltage that is large enough to provide a reasonable position sensor gain, so we will choose $E_b = 24$ volts. We will use a lead screw of 20 turns/cm and a potentiometer for x equal to 6 cm in length. Accurate balances are required; therefore, an input potentiometer 0.5 cm in length for y will be chosen. A reasonable viscous damper will be chosen with a damping constant $b = 10\sqrt{3} \text{ N/(m}\cdot\text{s)}$. Finally, a counterweight W_c is chosen so that the expected range of weights W can be balanced. The parameters of the system are selected as listed in Table 7.4.

Specifications. A rapid and accurate response resulting in a small steady-state weight measurement error is desired. Therefore, we will require that the system be at least a type one so that a zero measurement error is obtained. An underdamped response to a step change in the measured weight W is satisfactory, so a dominant response with $\zeta = 0.5$ will be specified. We want the settling time to be less than

Table 7.4 Self-Balancing Scale Parameters

$W_c = 2 \text{ N}$	Lead screw gain $K_s = \frac{1}{4000\text{m}}$ m/rad.
$I = 0.05 \text{ kg m}^2$	
$l_c = 5 \text{ cm}$	Input potentiometer gain $K_f = 4800 \text{ V/m}$.
$l_1 = 20 \text{ cm}$	
$b = 10\sqrt{3} \text{ N m/s}$	Feedback potentiometer gain $K_v = 400 \text{ V/m}$.

FIGURE 7.17 Root locus as K_m varies (only upper half-plane shown). One locus leaves the two poles at the origin and goes to the two complex zeros as K increases. The other locus is to the left of the pole at $s = -14$.



Then, rewriting Equation (7.62) in root locus form, we have

$$1 + KP(s) = 1 + \frac{K_m(10\pi)[s(s + 8\sqrt{3}) + 96]}{s^2(s + 8\sqrt{3})} = 0$$

$$= 1 + \frac{K_m(10\pi)(s + 6.93 + j6.93)(s + 6.93 - j6.93)}{s^2(s + 8\sqrt{3})} \quad (7.63)$$

The root locus as K_m varies is shown in Figure 7.17. The dominant roots can be placed at $\zeta = 0.5$ when $K = 25.3 = K_m/10\pi$. To achieve this gain,

$$K_m = 795 \frac{\text{rad/s}}{\text{volt}} = 7600 \frac{\text{rpm}}{\text{volt}} \quad (7.64)$$

an amplifier would be required to provide a portion of the required gain. The real part of the dominant roots is less than -4 ; therefore, the settling time, $4/\sigma$, is less than 1 second, and the settling time requirement is satisfied. The third root of the characteristic equation is a real root at $s = -30.2$, and the underdamped roots clearly dominate the response. Therefore, the system has been analyzed by the root locus method and a suitable design for the parameter K_m has been achieved. The efficiency of the s -plane and root locus methods is clearly demonstrated by this example. ■

7.4 PARAMETER DESIGN BY THE ROOT LOCUS METHOD

Originally, the root locus method was developed to determine the locus of roots of the characteristic equation as the system gain, K , is varied from zero to infinity. However, as we have seen, the effect of other system parameters may be readily

locus equation

$$1 + \frac{\beta s}{s^3 + s^2 + \alpha} = 0 \quad (7.74)$$

We note that the denominator of Equation (7.74) is the characteristic equation of the system with $\beta = 0$. Therefore, we must first evaluate the effect of varying α from zero to infinity by using the equation

$$s^3 + s^2 + \alpha = 0,$$

rewritten as

$$1 + \frac{\alpha}{s^2(s + 1)} = 0 \quad (7.75)$$

where β has been set equal to zero in Equation (7.73). Then, upon evaluating the effect of α , a value of α is selected and used with Equation (7.74) to evaluate the effect of β . This two-step method of evaluating the effect of α and then β may be carried out as two root locus procedures. First, we obtain a locus of roots as α varies, and we select a suitable value of α ; the results are satisfactory root locations. Then, we obtain the root locus for β by noting that the poles of Equation (7.74) are the roots evaluated by the root locus of Equation (7.75). A limitation of this approach is that we will not always be able to obtain a characteristic equation that is linear in the parameter under consideration (for example, α).

To illustrate this approach effectively, let us obtain the root locus for α and then β for Equation (7.73). A sketch of the root locus as α varies for Equation (7.75) is shown in Figure 7.18(a), where the roots for two values of gain α are shown. If the gain α is selected as α_1 , then the resultant roots of Equation (7.75) become the poles of Equation (7.74). The root locus of Equation (7.74) as β varies is shown in Figure 7.18(b), and a suitable β can be selected on the basis of the desired root locations.

Using the root locus method, we will further illustrate this parameter design approach by a specific design example.

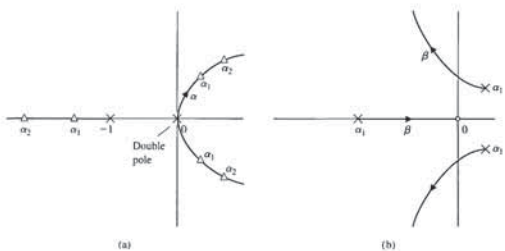


FIGURE 7.18 Root loci as a function of α and β . (a) Loci as α varies. (b) Loci as β varies for one value of $\alpha = \alpha_1$.

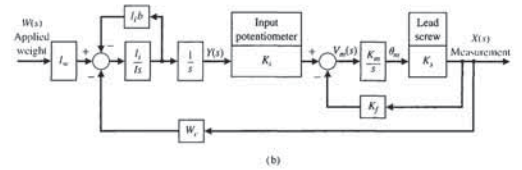
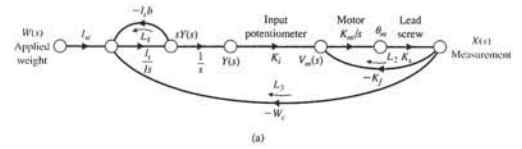


FIGURE 7.16 Model of the automatic self-balancing scale. (a) Signal-flow graph. (b) Block diagram.

L_3 , and the fifth term is the two nontouching loops L_1L_2 . Therefore, the closed-loop transfer function is

$$\frac{X(s)}{W(s)} = \frac{L_1L_2K_1K_mK_2}{s(Is + I^2b)(s + K_mK_1K_f) + W_1K_mK_1K_f} \quad (7.59)$$

The steady-state gain of the system is then

$$\lim_{t \rightarrow \infty} \frac{x(t)}{w} = \lim_{s \rightarrow 0} \frac{X(s)}{W(s)} = \frac{I_m}{W_c} = 2.5 \text{ cm/kg} \quad (7.60)$$

when $W(s) = |W|/s$. To obtain the root locus as a function of the motor constant K_m , we substitute the selected parameters into the characteristic equation, which is the denominator of Equation (7.59). Therefore, we obtain the following characteristic equation:

$$s(s + 8\sqrt{3}) \left(s + \frac{K_m}{10\pi} \right) + \frac{96K_m}{10\pi} = 0 \quad (7.61)$$

Rewriting the characteristic equation in root locus form, we first isolate K_m as follows:

$$s^2(s + 8\sqrt{3}) + s(s + 8\sqrt{3}) \frac{K_m}{10\pi} + \frac{96K_m}{10\pi} = 0 \quad (7.62)$$

investigated by using the root locus method. Fundamentally, the root locus method is concerned with a characteristic equation (Equation 7.22), which may be written as

$$1 + F(s) = 0 \quad (7.65)$$

Then the standard root locus method we have studied may be applied. The question arises: How do we investigate the effect of two parameters, α and β ? It appears that the root locus method is a single-parameter method; fortunately, it can be readily extended to the investigation of two or more parameters. This method of **parameter design** uses the root locus approach to select the values of the parameters.

The characteristic equation of a dynamic system may be written as

$$a_n s^n + a_{n-1} s^{n-1} + \dots + a_1 s + a_0 = 0 \quad (7.66)$$

Hence, the effect of the coefficient a_1 may be ascertained from the root locus equation

$$1 + \frac{a_1 s}{a_n s^n + a_{n-1} s^{n-1} + \dots + a_2 s^2 + a_0} = 0 \quad (7.67)$$

If the parameter of interest, α , does not appear solely as a coefficient, the parameter may be isolated as

$$a_n s^n + a_{n-1} s^{n-1} + \dots + (a_{n-q} - \alpha) s^{n-q} + \alpha s^{n-q} + \dots + a_1 s + a_0 = 0 \quad (7.68)$$

For example, a third-order equation of interest might be

$$s^3 + (3 + \alpha)s^2 + 3s + 6 = 0 \quad (7.69)$$

To ascertain the effect of the parameter α , we isolate the parameter and rewrite the equation in root locus form, as shown in the following steps:

$$s^3 + 3s^2 + \alpha s^2 + 3s + 6 = 0; \quad (7.70)$$

$$1 + \frac{\alpha s^2}{s^3 + 3s^2 + 3s + 6} = 0 \quad (7.71)$$

Then, to determine the effect of two parameters, we must repeat the root locus approach twice. Thus, for a characteristic equation with two variable parameters, α and β , we have

$$a_n s^n + a_{n-1} s^{n-1} + \dots + (a_{n-q} - \alpha) s^{n-q} + \alpha s^{n-q} + \dots + (a_{n-r} - \beta) s^{n-r} + \beta s^{n-r} + \dots + a_1 s + a_0 = 0 \quad (7.72)$$

The two variable parameters have been isolated, and the effect of α will be determined. Then, the effect of β will be determined. For example, for a certain third-order characteristic equation with α and β as parameters, we obtain

$$s^3 + s^2 + \beta s + \alpha = 0 \quad (7.73)$$

In this particular case, the parameters appear as the coefficients of the characteristic equation. The effect of varying β from zero to infinity is determined from the root

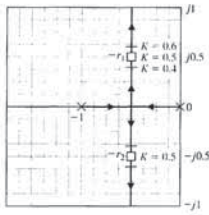


FIGURE 7.24 The root locus for K .

gain $\alpha = 0.4$ and $\alpha = 0.6$ are readily determined by root locus methods, and the root locations for $\Delta\alpha = \pm 0.1$ are shown in Figure 7.24. When $\alpha = K = 0.6$, the root in the second quadrant of the s -plane is

$$(-r_1) + \Delta r_1 = -0.5 + j0.59,$$

and the change in the root is $\Delta r_1 = +j0.09$. When $\alpha = K = 0.4$, the root in the second quadrant is

$$(-r_1) + \Delta r_1 = -0.5 + j0.387,$$

and the change in the root is $-\Delta r_1 = -j0.11$. Thus, the root sensitivity for r_1 is

$$S_{K^+}^r = \frac{\Delta r_1}{\Delta K/K} = \frac{+j0.09}{+0.2} = j0.45 = 0.45 \angle +90^\circ \quad (7.94)$$

for positive changes of gain. For negative increments of gain, the sensitivity is

$$S_{K^-}^r = \frac{\Delta r_1}{\Delta K/K} = \frac{-j0.11}{+0.2} = -j0.55 = 0.55 \angle -90^\circ.$$

For infinitesimally small changes in the parameter K , the sensitivity will be equal for negative or positive increments in K . The angle of the root sensitivity indicates the direction the root moves as the parameter varies. The angle of movement for $+\Delta\alpha$ is always 180° from the angle of movement for $-\Delta\alpha$ at the point $\alpha = \alpha_0$.

The pole β varies due to environmental changes, and it may be represented by $\beta = \beta_0 + \Delta\beta$, where $\beta_0 = 1$. Then the effect of variation of the poles is represented by the characteristic equation

$$s^2 + s + \Delta\beta s + K = 0,$$

or, in root locus form,

$$1 + \frac{\Delta\beta s}{s^2 + s + K} = 0. \quad (7.95)$$

where k is an integer. The locus of roots follows a zero-degree locus in contrast with the 180° locus considered previously. However, the root locus rules of Section 7.3 may be altered to account for the zero-degree phase angle requirement, and then the root locus may be obtained as in the preceding sections. Therefore, to obtain the effect of reducing β , we determine the zero-degree locus in contrast to the 180° locus, as shown by a dotted locus in Figure 7.25. To find the effect of a 20% change of the parameter β , we evaluate the new roots for $\Delta\beta = \pm 0.20$, as shown in Figure 7.25. The root sensitivity is readily evaluated graphically and, for a positive change in β , is

$$S_{\beta^+}^r = \frac{\Delta r_1}{\Delta\beta/\beta} = \frac{0.16 \angle -128^\circ}{0.20} = 0.80 \angle -128^\circ.$$

The root sensitivity for a negative change in β is

$$S_{\beta^-}^r = \frac{\Delta r_1}{\Delta\beta/\beta} = \frac{0.125 \angle 39^\circ}{0.20} = 0.625 \angle +39^\circ.$$

As the percentage change $\Delta\beta/\beta$ decreases, the sensitivity measures $S_{\beta^+}^r$ and $S_{\beta^-}^r$ will approach equality in magnitude and a difference in angle of 180° . Thus, for small changes when $\Delta\beta/\beta \approx 0.10$, the sensitivity measures are related as

$$|S_{\beta^+}^r| = |S_{\beta^-}^r|$$

and

$$\angle S_{\beta^+}^r = 180^\circ + \angle S_{\beta^-}^r.$$

Often, the desired root sensitivity measure is desired for small changes in the parameter. When the relative change in the parameter is of the order $\Delta\beta/\beta = 0.10$, we can estimate the increment in the root change by approximating the root locus with the line at the angle of departure θ_d . This approximation is shown in Figure 7.25 and is accurate for only relatively small changes in $\Delta\beta$. However, the use of this approximation allows the analyst to avoid sketching the complete root locus diagram. Therefore, for Figure 7.25, the root sensitivity may be evaluated for $\Delta\beta/\beta = 0.10$ along the departure line, and we obtain

$$S_{\beta^+}^r = \frac{0.075 \angle -132^\circ}{0.10} = 0.75 \angle -132^\circ. \quad (7.96)$$

The root sensitivity measure for a parameter variation is useful for comparing the sensitivity for various design parameters and at different root locations. Comparing Equation (7.96) for β with Equation (7.94) for α , we find (a) that the sensitivity for β is greater in magnitude by approximately 50% and (b) that the angle for $S_{\beta^+}^r$ indicates that the approach of the root toward the $j\omega$ axis is more sensitive for changes in β . Therefore, the tolerance requirements for β would be more stringent than for α . This information provides the designer with a comparative measure of the required tolerances for each parameter. ■

The evaluation of the root sensitivity for a control system can be readily accomplished by utilizing the root locus methods of the preceding section. The root sensitivity S_K^r may be evaluated at root $-r_1$ by examining the root contours for the parameter K . We can change K by a small finite amount ΔK and determine the modified root $-(r_1 + \Delta r_1)$ at $K + \Delta K$. Then, using Equation (7.86), we have

$$S_K^r \approx \frac{\Delta r_1}{\Delta K/K}. \quad (7.90)$$

Equation (7.90) is an approximation that approaches the actual value of the sensitivity as $\Delta K \rightarrow 0$. An example will illustrate the process of evaluating the root sensitivity.

EXAMPLE 7.7 Root sensitivity of a control system

The characteristic equation of the feedback control system shown in Figure 7.23 is

$$1 + \frac{K}{s(s + \beta)} = 0,$$

or, alternatively,

$$s^2 + \beta s + K = 0. \quad (7.91)$$

The gain K will be considered to be the parameter α . Then the effect of a change in each parameter can be determined by utilizing the relations

$$\alpha = \alpha_0 \pm \Delta\alpha \quad \text{and} \quad \beta = \beta_0 \pm \Delta\beta,$$

where α_0 and β_0 are the nominal or desired values for the parameters α and β , respectively. We shall consider the case when the nominal pole value is $\beta_0 = 1$ and the desired gain is $\alpha_0 = K = 0.5$. Then the root locus can be obtained as a function of $\alpha = K$ by utilizing the root locus equation

$$1 + \frac{K}{s(s + 1)} = 1 + \frac{K}{s(s + 1)} = 0, \quad (7.92)$$

as shown in Figure 7.24. The nominal value of gain $K = \alpha_0 = 0.5$ results in two complex roots, $-r_1 = -0.5 + j0.5$ and $-r_2 = -0.5 - j0.5$, as shown in Figure 7.24. To evaluate the effect of unavoidable changes in the gain, the characteristic equation with $\alpha = \alpha_0 \pm \Delta\alpha$ becomes

$$s^2 + s + \alpha_0 \pm \Delta\alpha = s^2 + s + 0.5 \pm \Delta\alpha. \quad (7.93)$$

Therefore, the effect of changes in the gain can be evaluated from the root locus of Figure 7.24. For a 20% change in α , we have $\Delta\alpha = \pm 0.1$. The root locations for a

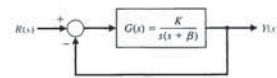


FIGURE 7.23 A feedback control system.

The denominator of the second term is the unchanged characteristic equation when $\Delta\beta = 0$. The root locus for the unchanged system ($\Delta\beta = 0$) is shown in Figure 7.24 as a function of K . For a design specification requiring $\zeta = 0.707$, the complex roots lie at

$$-r_1 = -0.5 + j0.5 \quad \text{and} \quad -r_2 = -0.5 - j0.5.$$

Then, because the roots are complex conjugates, the root sensitivity for r_1 is the conjugate of the root sensitivity for r_2 . Using the parameter root locus techniques discussed in the preceding section, we obtain the root locus for $\Delta\beta$ as shown in Figure 7.25. We are normally interested in the effect of a variation for the parameter so that $\beta = \beta_0 \pm \Delta\beta$, for which the locus as β decreases is obtained from the root locus equation

$$1 + \frac{-(\Delta\beta)s}{s^2 + s + K} = 0.$$

We note that the equation is of the form

$$1 - \Delta\beta P(s) = 0.$$

Comparing this equation with Equation (7.23) in Section 7.3, we find that the sign preceding the gain $\Delta\beta$ is negative in this case. In a manner similar to the development of the root locus method in Section 7.3, we require that the root locus satisfy the equations

$$|\Delta\beta P(s)| = 1 \quad \text{and} \quad \angle P(s) = 0^\circ \pm k360^\circ.$$

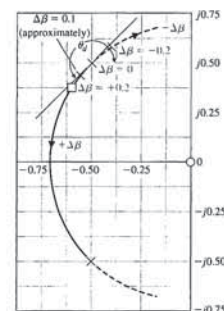


FIGURE 7.25 The root locus for the parameter β .

Therefore, the sensitivity at r_1 is

$$S_{\beta}^r = \frac{\Delta r_1}{\Delta \beta / \beta} = \frac{0.2 / -80^\circ}{0.48 / 8} = 3.34 / -80^\circ,$$

which indicates that the root is quite sensitive to this 6% change in the parameter β . For comparison, it is worthwhile to determine the sensitivity of the root $-r_1$ to a change in the zero $s = -3$. Then the characteristic equation is

$$s(s + 2)(s + 8) + 20.7(s + 3 + \Delta\gamma) = 0,$$

or

$$1 + \frac{20.7 \Delta\gamma}{(s + r_1)(s + \hat{r}_1)(s + r_3)} = 0. \quad (7.98)$$

The pole-zero diagram for Equation (7.98) is shown in Figure 7.27. The angle of departure at root $-r_1$ is $180^\circ = -(\theta_d + 90^\circ + 40^\circ)$, or

$$\theta_d = +50^\circ.$$

For a change of $\Delta r_1 = 0.2 / +50^\circ$, the $\Delta\gamma$ is positive. Obtaining the vector lengths, we find that

$$|\Delta\gamma| = \frac{5.22(4.18)(0.2)}{20.7} = 0.21.$$

Therefore, the sensitivity at r_1 for $+\Delta\gamma$ is

$$S_{\gamma}^r = \frac{\Delta r_1}{\Delta\gamma / \gamma} = \frac{0.2 / +50^\circ}{0.21 / 3} = 2.84 / +50^\circ.$$

Thus, we find that the magnitude of the root sensitivity for the pole β and the zero γ is approximately equal. However, the sensitivity of the system to the pole can be considered to be less than the sensitivity to the zero because the sensitivity, S_{γ}^r , is equal to $+50^\circ$ and the direction of the root change is toward the $j\omega$ -axis.

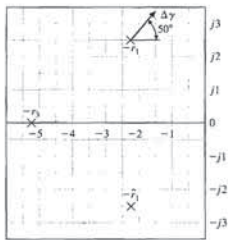


FIGURE 7.27 Pole-zero diagram for the parameter γ .

If we set $K_D = 0$, then we have the **proportional plus integral (PI) controller**

$$G_c(s) = K_p + \frac{K_I}{s}$$

When $K_I = 0$, we have

$$G_c(s) = K_p + K_D s,$$

which is called a **proportional plus derivative (PD) controller**.

The PID controller can also be viewed as a cascade of the PI and the PD controllers. Consider the PI controller

$$G_{PI}(s) = \hat{K}_p + \frac{\hat{K}_I}{s}$$

and the PD controller

$$G_{PD}(s) = \bar{K}_p + \bar{K}_D s,$$

where \hat{K}_p and \hat{K}_I are the PI controller gains and \bar{K}_p and \bar{K}_D are the PD controller gains. Cascading the two controllers (that is, placing them in series) yields

$$\begin{aligned} G_c(s) &= G_{PI}(s)G_{PD}(s) \\ &= \left(\hat{K}_p + \frac{\hat{K}_I}{s} \right) (\bar{K}_p + \bar{K}_D s) \\ &= (\bar{K}_p \hat{K}_p + \hat{K}_I \bar{K}_D) + \hat{K}_p \bar{K}_D s + \frac{\hat{K}_I \bar{K}_D}{s} \\ &= K_p + K_D s + \frac{K_I}{s}, \end{aligned}$$

where we have the following relationships between the PI and PD controller gains and the PID controller gains

$$\begin{aligned} K_p &= \bar{K}_p \hat{K}_p + \hat{K}_I \bar{K}_D \\ K_D &= \hat{K}_p \bar{K}_D \\ K_I &= \hat{K}_I \bar{K}_D. \end{aligned}$$

Consider the PID controller

$$\begin{aligned} G_c(s) &= K_p + \frac{K_I}{s} + K_D s = \frac{K_D s^2 + K_p s + K_I}{s} \\ &= \frac{K_D(s^2 + as + b)}{s} = \frac{K_D(s + z_1)(s + z_2)}{s}, \end{aligned}$$

where $a = K_p / K_D$ and $b = K_I / K_D$. Therefore, a PID controller introduces a transfer function with one pole at the origin and two zeros that can be located anywhere in the s -plane.

EXAMPLE 7.8 Root sensitivity to a parameter

A unity feedback control system has a forward transfer function

$$G(s) = \frac{20.7(s + 3)}{s(s + 2)(s + \beta)},$$

where $\beta = \beta_0 + \Delta\beta$ and $\beta_0 = 8$. The characteristic equation, as a function of $\Delta\beta$, is

$$s(s + 2)(s + 8 + \Delta\beta) + 20.7(s + 3) = 0,$$

or

$$s(s + 2)(s + 8) + \Delta\beta s(s + 2) + 20.7(s + 3) = 0.$$

When $\Delta\beta = 0$, the roots are

$$-r_1 = -2.36 + j2.48, \quad -r_2 = \hat{r}_1, \quad \text{and} \quad -r_3 = -5.27.$$

The root locus for $\Delta\beta$ is determined by using the root locus equation

$$1 + \frac{\Delta\beta s(s + 2)}{(s + r_1)(s + \hat{r}_1)(s + r_3)} = 0. \quad (7.97)$$

The roots and zeros of Equation (7.97) are shown in Figure 7.26. The angle of departure at r_1 is evaluated from the angles as follows:

$$\begin{aligned} 180^\circ &= -(\theta_d + 90^\circ + \theta_{p_2}) + (\theta_z + \theta_{z_2}) \\ &= -(\theta_d + 90^\circ + 40^\circ) + (133^\circ + 98^\circ). \end{aligned}$$

Therefore, $\theta_d = -80^\circ$ and the locus is approximated near $-r_1$ by the line at an angle of θ_d . For a change of $\Delta r_1 = 0.2 / -80^\circ$ along the departure line, the $+\Delta\beta$ is evaluated by determining the vector lengths from the poles and zeros. Then we have

$$+\Delta\beta = \frac{4.8(3.75)(0.2)}{(3.25)(2.3)} = 0.48.$$

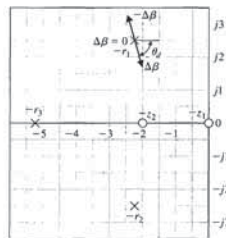


FIGURE 7.26 Pole and zero diagram for the parameter β .

Evaluating the root sensitivity in the manner of the preceding paragraphs, we find that the sensitivity for the pole $s = -\delta_0 = -2$ is

$$S_{\delta}^r = 2.1 / +27^\circ.$$

Thus, for the parameter δ , the magnitude of the sensitivity is less than for the other parameters, but the direction of the change of the root is more important than for β and γ .

To utilize the root sensitivity measure for the analysis and design of control systems, a series of calculations must be performed; they will determine the various selections of possible root configurations and the zeros and poles of the open-loop transfer function. Therefore, the root sensitivity measure as a design technique is somewhat limited by two things: the relatively large number of calculations required and the lack of an obvious direction for adjusting the parameters in order to provide a minimized or reduced sensitivity. However, the root sensitivity measure can be utilized as an analysis measure, which permits the designer to compare the sensitivity for several system designs based on a suitable method of design. The root sensitivity measure is a useful index of the system's sensitivity to parameter variations expressed in the s -plane. The weakness of the sensitivity measure is that it relies on the ability of the root locations to represent the performance of the system. As we have seen in the preceding chapters, the root locations represent the performance quite adequately for many systems, but due consideration must be given to the location of the zeros of the closed-loop transfer function and the dominance of the pertinent roots. The root sensitivity measure is a suitable measure of system performance sensitivity and can be used reliably for system analysis and design.

7.6 PID CONTROLLERS

One form of controller widely used in industrial process control is the three-term, **PID controller** [4, 10]. This controller has a transfer function

$$G_c(s) = K_p + \frac{K_I}{s} + K_D s.$$

The equation for the output in the time domain is

$$u(t) = K_p e(t) + K_I \int e(t) dt + K_D \frac{de(t)}{dt}.$$

The three-term controller is called a PID controller because it contains a proportional, an integral, and a derivative term represented by K_p , K_I , and K_D , respectively. The transfer function of the derivative term is actually

$$G_d(s) = \frac{K_D s}{\tau_d s + 1},$$

but τ_d is usually much smaller than the time constants of the process itself, so it is neglected.

Table 7.6 Effect of Increasing the PID Gains K_p , K_D , and K_I on the Step Response

PID Gain	Percent Overshoot	Settling Time	Steady-State Error
Increasing K_p	Increases	Minimal impact	Decreases
Increasing K_I	Increases	Increases	Zero steady-state error
Increasing K_D	Decreases	Decreases	No impact

engineers to operate them in a simple, straightforward manner. To implement the PID controller, three parameters must be determined, the proportional gain, denoted by K_p , integral gain, denoted by K_I , and derivative gain denoted by K_D [10].

There are many methods available to determine acceptable values of the PID gains. The process of determining the gains is often called **PID tuning**. A common approach to tuning is to use **manual PID tuning** methods, whereby the PID control gains are obtained by trial-and-error with minimal analytic analysis using step responses obtained via simulation, or in some cases, actual testing on the system and deciding on the gains based on observations and experience. A more analytic method is known as the **Ziegler-Nichols tuning** method. The Ziegler-Nichols tuning method actually has several variations. We discuss in this section a Ziegler-Nichols tuning method based on open-loop responses to a step input and a related Ziegler-Nichols tuning method based on closed-loop response to a step input.

One approach to manual tuning is to first set $K_I = 0$ and $K_D = 0$. This is followed by slowly increasing the gain K_p until the output of the closed-loop system oscillates just on the edge of instability. This can be done either in simulation or on the actual system if it cannot be taken off-line. Once the value of K_p (with $K_I = 0$ and $K_D = 0$) is found that brings the closed-loop system to the edge of stability, you reduce the value of gain K_p to achieve what is known as the **quarter amplitude decay**. That is, the amplitude of the closed-loop response is reduced approximately to one-fourth of the maximum value in one oscillatory period. A rule-of-thumb is to start by reducing the proportional gain K_p by one-half. The next step of the design process is to increase K_I and K_D manually to achieve a desired step response. Table 7.6 describes in general terms the effect of increasing K_I and K_D .

EXAMPLE 7.9 Manual PID tuning

Consider the closed-loop system in Figure 7.30 with

$$G(s) = \frac{1}{s(s+b)(s+2\zeta\omega_n)}$$

where $b = 10$, $\zeta = 0.707$, and $\omega_n = 4$.

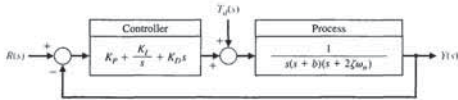


FIGURE 7.30 Unity feedback control system with PID controller.

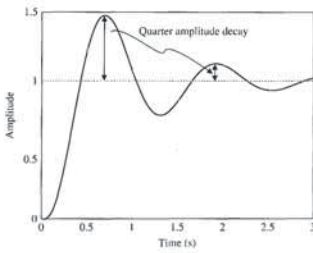


FIGURE 7.32 Step response with $K_p = 370$ showing the quarter amplitude decay.

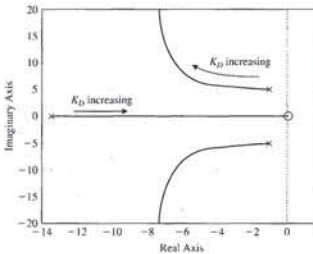


FIGURE 7.33 Root locus for $K_p = 370$, $K_I = 0$, and $0 \leq K_D < \infty$.

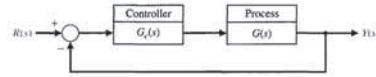
effects of varying K_D are consistent with information provided in Table 7.6. As K_D increases (when $K_D > 75$), the real root begins to dominate the response and the trends described in Table 7.6 become less accurate. The percent overshoot and settling time as a function of K_D are shown in Figure 7.34.

The root locus for $K_p = 370$, $K_D = 0$, and $0 \leq K_I < \infty$ is shown in Figure 7.35. The characteristic equation is

$$1 + K_I \left[\frac{1}{s(s+10)(s+5.66) + K_p} \right] = 0.$$

We see in Figure 7.35 that as K_I increases, the root locus shows that the closed-loop complex pair poles move right. This decreases the associated damping ratio and thereby increasing the percent overshoot. In fact, when $K_I = 778.2$, the system is marginally stable with closed-loop poles at $s = \pm 4.86j$. The movement of the

FIGURE 7.28 Closed-loop system with a controller.



Recall that a root locus begins at the poles and ends at the zeros. If we have a system, as shown in Figure 7.28, with

$$G(s) = \frac{1}{(s+2)(s+3)},$$

and we use a PID controller with complex zeros $-z_1$ and $-z_2$, where $-z_1 = -3 + j1$ and $-z_2 = -3 - j1$, we can plot the root locus as shown in Figure 7.29. As the gain, K_D , of the controller is increased, the complex roots approach the zeros. The closed-loop transfer function is

$$T(s) = \frac{G(s)G_c(s)}{1 + G(s)G_c(s)} = \frac{K_D(s+z_1)(s+\hat{z}_1)}{(s+r_2)(s+r_1)(s+\hat{r}_1)}$$

The response of this system will be attractive. The percent overshoot to a step will be less than 2%, and the steady-state error for a step input will be zero. The settling time will be approximately 1 second. If a shorter settling time is desired, then we select z_1 and z_2 to lie further left in the left-hand s -plane and set K_D to drive the roots near the complex zeros.

Many industrial processes are controlled using PID controllers. The popularity of PID controllers can be attributed partly to their good performance in a wide range of operating conditions and partly to their functional simplicity that allows

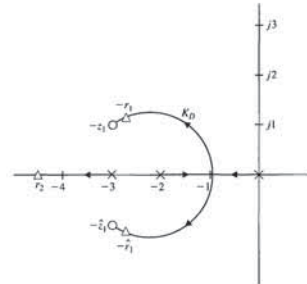


FIGURE 7.29 Root locus for plant with a PID controller with complex zeros.

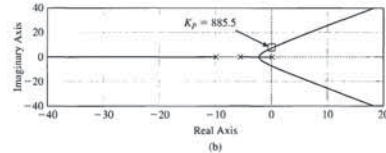
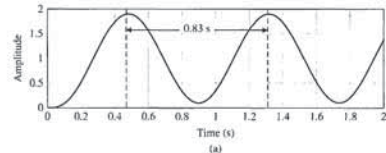


FIGURE 7.31 (a) Step response with $K_p = 885.5$, $K_D = 0$, and $K_I = 0$. (b) Root locus showing $K_p = 885.5$ results in marginal stability with $s = \pm 7.5j$.

To begin the manual tuning process, set $K_I = 0$ and $K_D = 0$ and increase K_p until the closed-loop system has sustained oscillations. As can be seen in Figure 7.31a, when $K_p = 885.5$, we have a sustained oscillation of magnitude $A = 1.9$ and period $P = 0.83$ s. The root locus shown in Figure 7.31b corresponds to the characteristic equation

$$1 + K_p \left[\frac{1}{s(s+10)(s+5.66)} \right] = 0.$$

The root locus shown in Figure 7.31b illustrates that when $K_p = 885.5$, we have closed-loop poles at $s = \pm 7.5j$ leading to the oscillatory behavior in the step response in Figure 7.31a.

Reduce $K_p = 885.5$ by half as a first step to achieving a step response with approximately a quarter amplitude decay. You may have to iterate on the value $K_p = 442.75$. The step response is shown in Figure 7.32 where we note that the peak amplitude is reduced to one-fourth of the maximum value in one period, as desired. To accomplish this reduction, we refined the value of K_p by slowly reducing the value from $K_p = 442.75$ to $K_p = 370$.

The root locus for $K_p = 370$, $K_I = 0$, and $0 \leq K_D < \infty$ is shown in Figure 7.33. In this case, the characteristic equation is

$$1 + K_D \left[\frac{s}{(s+10)(s+5.66) + K_p} \right] = 0.$$

We see in Figure 7.33 that as K_D increases, the root locus shows that the closed-loop complex poles move left, and in doing so, increases the associated damping ratio and thereby decreases the percent overshoot. The movement of the complex poles to the left also increases the associated $\zeta\omega_n$, thereby reducing the settling time. These

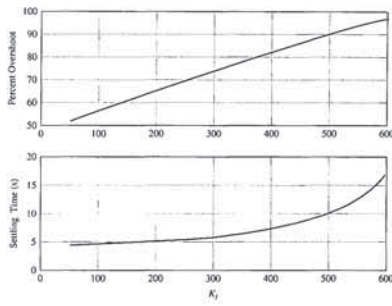


FIGURE 7.36 Percent overshoot and settling time with $K_p = 370$, $K_D = 0$, and $50 \leq K_I < 600$.

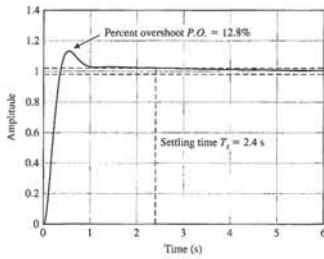


FIGURE 7.37 Percent overshoot and settling time with final design $K_p = 370$, $K_D = 60$, and $K_I = 100$.

Two important PID controller gain tuning methods were published in 1942 by John G. Ziegler and Nathaniel B. Nichols intended to achieve a fast closed-loop step response without excessive oscillations and excellent disturbance rejection. The two approaches are classified under the general heading of Ziegler-Nichols tuning methods. The first approach is based on closed-loop concepts requiring the computation of the **ultimate gain** and **ultimate period**. The second approach is based on open-loop concepts relying on **reaction curves**. The Ziegler-Nichols tuning methods are based on assumed forms of the models of the process, but the models do not have to be precisely known. This makes the tuning approach very practical in process

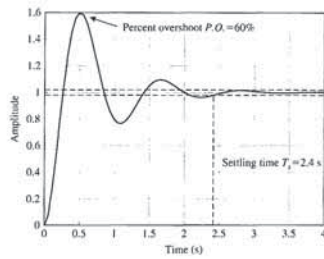


FIGURE 7.38 Time response for the Ziegler-Nichols PID tuning with $K_p = 531.3$, $K_I = 1280.2$, and $K_D = 55.1$.

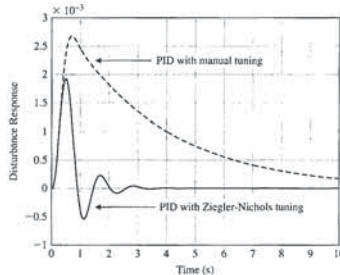


FIGURE 7.39 Disturbance response for the Ziegler-Nichols PID tuning versus the manual tuning in Example 7.9.

Ziegler-Nichols tuning is designed to provide the best disturbance rejection performance rather than the best input response performance.

In Figure 7.39, we see that the step disturbance performance of the Ziegler-Nichols PID controller is indeed better than the manually tuned controller. While Ziegler-Nichols approach provides a structured procedure for obtaining the PID controller gains, the appropriateness of the Ziegler-Nichols tuning depends on the requirements of the problem under investigation. ■

The open-loop Ziegler-Nichols tuning method utilizes a reaction curve obtained by taking the controller off-line (that is, out of the loop) and introducing a step input (or step disturbance). This approach is very commonly used in process control applications. The measured output is the reaction curve and is assumed to

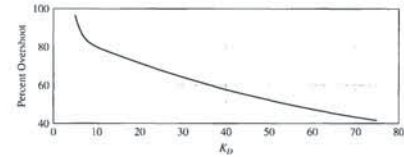


FIGURE 7.34 Percent overshoot and settling time with $K_p = 370$, $K_I = 0$, and $5 \leq K_D < 75$.

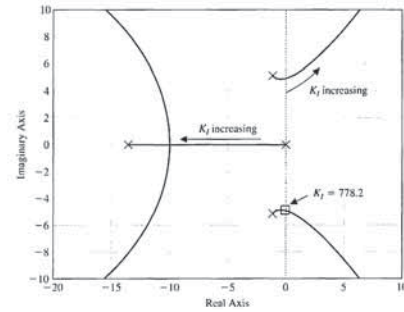
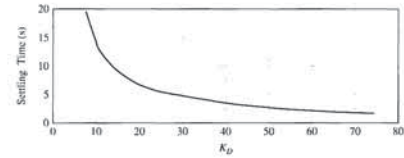


FIGURE 7.35 Root locus for $K_p = 370$, $K_D = 0$, and $0 \leq K_I < \infty$.

complex poles to the right also decreases the associated $\zeta\omega_n$, thereby increasing the settling time. The percent overshoot and settling time as a function of K_I are shown in Figure 7.36. The trends in Figure 7.36 are consistent with Table 7.6.

To meet the percent overshoot and settling time specifications, we can select $K_p = 370$, $K_D = 60$, and $K_I = 100$. The step response shown in Figure 7.37 indicates a $T_s = 2.4$ s and $P.O. = 12.8\%$ meeting the specifications. ■

Table 7.7 Ziegler-Nichols PID Tuning Using Ultimate Gain, K_U , and Oscillation Period, P_U

Ziegler-Nichols PID Controller Gain Tuning Using Closed-loop Concepts			
Controller Type	K_p	K_I	K_D
Proportional (P) $G_c(s) = K_p$	$0.5K_U$	—	—
Proportional-plus-integral (PI) $G_c(s) = K_p + \frac{K_I}{s}$	$0.45K_U$	$\frac{0.54K_U}{T_U}$	—
Proportional-plus-integral-plus-derivative (PID) $G_c(s) = K_p + \frac{K_I}{s} + K_D s$	$0.6K_U$	$\frac{1.2K_U}{T_U}$	$\frac{0.6K_U T_U}{8}$

control applications. Our suggestion is to consider the Ziegler-Nichols rules to obtain initial controller designs followed by design iteration and refinement. Remember that the Ziegler-Nichols rules will not work with all plants or processes.

The closed-loop Ziegler-Nichols tuning method considers the closed-loop system response to a step input (or step disturbance) with the PID controller in the loop. Initially the derivative and integral gains, K_D and K_I , respectively, are set to zero. The proportional gain K_p is increased (in simulation or on the actual system) until the closed-loop system reaches the boundary of instability. The gain on the border of instability, denoted by K_U , is called the ultimate gain. The period of the sustained oscillations, denoted by P_U , is called the ultimate period. Once K_U and P_U are determined, the PID gains are computed using the relationships in Table 7.7 according to the Ziegler-Nichols tuning method.

EXAMPLE 7.10 Closed-loop Ziegler-Nichols PID tuning

Re-consider the system in Example 7.9. The plant is

$$G(s) = \frac{1}{s(s+b)(s+2\zeta\omega_n)}$$

where $b = 10$, $\zeta = 0.707$, and $\omega_n = 4$. The controller is a PID controller

$$G_c(s) = K_p + \frac{K_I}{s} + K_D s,$$

where the gains K_p , K_D , and K_I are computed using the formulas in Table 7.7. We found in Example 7.9 that $K_U = 885.5$ and $T_U = 0.83$ s. By using the Ziegler-Nichols formulas we obtain

$$K_p = 0.6K_U = 531.3, \quad K_I = \frac{1.2K_U}{T_U} = 1280.2, \quad \text{and} \quad K_D = \frac{0.6K_U T_U}{8} = 55.1.$$

Comparing the step response in Figures 7.37 and 7.38 we note that the settling time is approximately the same for the manually tuned and the Ziegler-Nichols tuned PID controllers. However, the percent overshoot of the manually tuned controller is less than that of the Ziegler-Nichols tuning. This is due to the fact that the

where M is the magnitude of the response at steady-state, T_d is the transport delay, and p is related to the slope of the reaction curve. The parameters M , τ , and T_d can be estimated from the open-loop step response and then utilized to compute $R = M/\tau$. Once that is accomplished, the PID gains are computed as shown in Table 7.8. You can also use the Ziegler-Nichols open-loop tuning method to design a proportional controller or a proportional-plus-integral controller.

EXAMPLE 7.11 Open-loop Ziegler-Nichols PI controller tuning

Consider the reaction curve shown in Figure 7.41. We estimate the transport lag to be $T_d = 0.1$ s and the reaction rate $R = 0.8$.

Using the Ziegler-Nichols tuning for the PI controller gains we have

$$K_p = \frac{0.9}{RT_d} = 11.25 \quad \text{and} \quad K_I = \frac{0.27}{RT_d^2} = 33.75.$$

The closed-loop system step response (assuming unity feedback) is shown in Figure 7.42. The settling time is $T_s = 1.28$ s and the percent overshoot is $P.O. = 78\%$. Since we are using a PI controller, the steady-state is zero, as expected. ■

The manual tuning method and the two Ziegler-Nichols tuning approaches presented here will not always lead to the desired closed-loop performance. The three methods do provide structured design steps leading to candidate PID gains and should be viewed as first steps in the design iteration. Since the PID (and the related PD and PI) controllers are in wide use today in a variety of applications, it is important to become familiar with various design approaches. We will use the PD controller later in this chapter to control the hard disk drive sequential design problem (see Section 7.10).

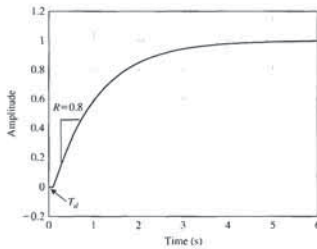


FIGURE 7.41 Reaction curve with $T_d = 0.1$ s and $R = 0.8$.

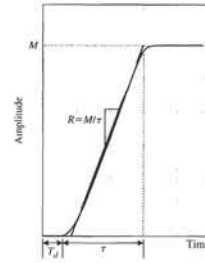


FIGURE 7.40 Reaction curve illustrating parameters R and T_d required for the Ziegler-Nichols open-loop tuning method.

have the general shape shown in Figure 7.40. The response in Figure 7.40 implies that the process is a first-order system with a transport delay. If the actual system does not match the assumed form, then another approach to PID tuning should be considered. However, if the underlying system is linear and lethargic (or sluggish and characterized by delay), the assumed model may suffice to obtain a reasonable PID gain selection using the open-loop Ziegler-Nichols tuning method.

The reaction curve is characterized by the transport delay, T_d , and the reaction rate, R . Generally, the reaction curve is recorded and numerical analysis is performed to obtain estimates of the parameters T_d and R . A system possessing the reaction curve shown in Figure 7.40 can be approximated by a first-order system with a transport delay as

$$G(s) = M \frac{p}{s+p} e^{-T_d s}$$

Table 7.8 Ziegler-Nichols PID Tuning Using Reaction Curve Characterized by Time Delay, T_d , and Reaction Rate, R

Ziegler-Nichols PID Controller Gain Tuning Using Open-loop Concepts			
Controller Type	K_p	K_I	K_D
Proportional (P)	$\frac{1}{RT_d}$	—	—
Proportional-plus-integral (PI)	$\frac{0.9}{RT_d}$	$\frac{0.27}{RT_d^2}$	—
Proportional-plus-integral-plus-derivative (PID)	$\frac{1.2}{RT_d}$	$\frac{0.6}{RT_d^2}$	$\frac{0.6}{R}$

that the phase condition in Equation (7.100) is different from the phase condition in Equation (7.4). As we will show, the new phase condition leads to several key modifications in the root locus sketching steps from those summarized in Table 7.2.

EXAMPLE 7.12 Negative gain root locus

Consider the system shown in Figure 7.43. The loop transfer function is

$$L(s) = KG(s) = K \frac{s-20}{s^2+5s-50}$$

and the characteristic equation is

$$1 + K \frac{s-20}{s^2+5s-50} = 0.$$

Sketching the root locus yields the plot shown in Figure 7.44a where it can be seen that the closed-loop system is not stable for any $0 \leq K < \infty$. The negative gain root locus is shown in Figure 7.44b. Using the negative gain root locus in Figure 7.44b we find that the stability is $-5.0 < K < -2.5$. The system in Figure 7.43 can thus be stabilized with only negative gain, K . ■

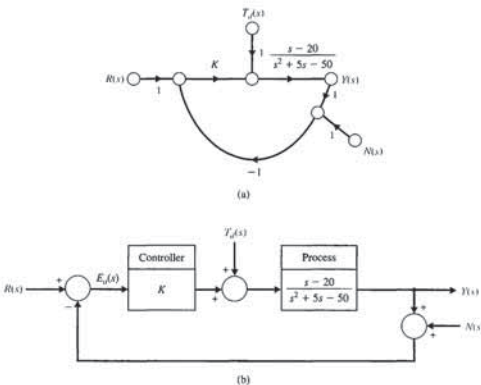


FIGURE 7.43 (a) Signal flow graph and (b) block diagram of unity feedback system with controller gain, K .

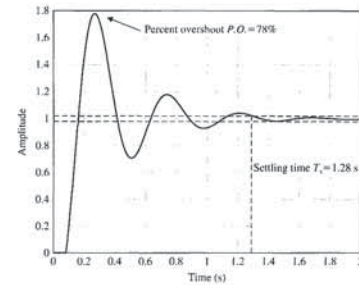


FIGURE 7.42 Time response for the Ziegler-Nichols PI tuning with $K_p = 11.25$ and $K_I = 33.75$.

7.7 NEGATIVE GAIN ROOT LOCUS

As discussed in Section 7.2, the dynamic performance of a closed-loop control system is described by the closed-loop transfer function, that is, by the poles and zeros of the closed-loop system. The root locus is a graphical illustration of the variation of the roots of the characteristic equation as a single parameter of interest varies. We know that the roots of the characteristic equation and the closed-loop poles are one in the same. In the case of the single-loop negative unity feedback system shown in Figure 7.1, the characteristic equation is

$$1 + KG(s) = 0, \tag{7.99}$$

where K is the parameter of interest. The orderly seven-step procedure for sketching the root locus described in Section 7.3 and summarized in Table 7.2 is valid for the case where $0 \leq K < \infty$. Sometimes the situation arises where we are interested in the root locus for negative values of the parameter of interest where $-\infty < K \leq 0$. We refer to this as the **negative gain root locus**. Our objective here is to develop an orderly procedure for sketching the negative gain root locus using familiar concepts from root locus sketching as described in Section 7.2.

Rearranging Equation (7.99) yields

$$G(s) = -\frac{1}{K}.$$

Since K is negative, it follows that

$$|KG(s)| = 1 \quad \text{and} \quad \angle KG(s) = 0^\circ + k360^\circ \tag{7.100}$$

where $k = 0, \pm 1, \pm 2, \pm 3, \dots$. The magnitude and phase conditions in Equation (7.100) must both be satisfied for all points on the negative gain root locus. Note

Step 3: When $n > M$, we have $n - M$ branches heading to the zeros at infinity as $K \rightarrow -\infty$ along asymptotes centered at σ_A and with angles ϕ_A . The linear asymptotes are centered at a point on the real axis given by

$$\sigma_A = \frac{\sum \text{poles of } P(s) - \sum \text{zeros of } P(s)}{n - M} = \frac{\sum_{i=1}^n (-p_i) - \sum_{i=1}^M (-z_i)}{n - M} \quad (7.102)$$

The angle of the asymptotes with respect to the real axis is

$$\phi_A = \frac{2k + 1}{n - M} 360^\circ, \quad k = 0, 1, 2, \dots, (n - M - 1), \quad (7.103)$$

where k is an integer index.

Step 4: Determine where the locus crosses the imaginary axis (if it does so), using the Routh-Hurwitz criterion.

Step 5: Determine the breakaway point on the real axis (if any). In general, due to the phase criterion, the tangents to the loci at the breakaway point are equally spaced over 360° . The breakaway point on the real axis can be evaluated graphically or analytically. The breakaway point can be computed by rearranging the characteristic equation

$$1 + K \frac{n(s)}{d(s)} = 0$$

as

$$p(s) = K,$$

where $p(s) = -d(s)/n(s)$ and finding the values of s that maximize $p(s)$. This is accomplished by solving the equation

$$n(s) \frac{d[d(s)]}{ds} - d(s) \frac{d[n(s)]}{ds} = 0. \quad (7.104)$$

Equation (7.104) yields a polynomial equation in s of degree $n + M - 1$, where n is the number of poles and M is the number of zeros. Hence the number of solutions is $n + M - 1$. The solutions that exist on the root locus are the breakaway points.

Step 6: Determine the angle of departure of the locus from a pole and the angle of arrival of the locus at a zero using the phase angle criterion. The angle of locus departure from a pole or angle of arrival at a zero is the difference between the net angle due to all other poles and zeros and the criterion angle of $\pm k360^\circ$.

Step 7: The final step is to complete the sketch by drawing in all sections of the locus not covered in the previous six steps.

The seven steps for sketching a negative gain root locus are summarized in Table 7.9.

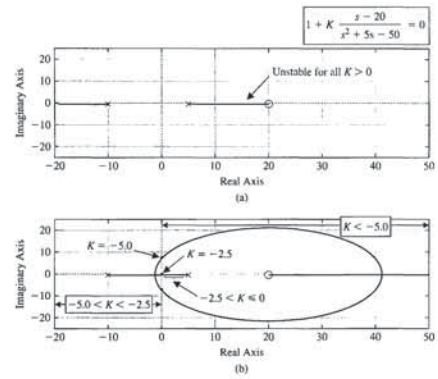


FIGURE 7.44 (a) Root locus for $0 \leq K < \infty$. (b) Negative gain root locus for $-\infty < K \leq 0$.

To locate the roots of the characteristic equation in a graphical manner on the s -plane for negative values of the parameter of interest, we will re-visit the seven steps summarized in Table 7.2 to obtain a similar orderly procedure to facilitate the rapid sketching of the locus.

Step 1: Prepare the root locus sketch. As before, you begin by writing the characteristic equation and rearranging, if necessary, so that the parameter of interest, K , appears as the multiplying factor in the form,

$$1 + KP(s) = 0. \quad (7.101)$$

For the negative gain root locus, we are interested in determining the locus of roots of the characteristic equation in Equation (7.101) for $-\infty < K \leq 0$. As in Equation (7.24), factor $P(s)$ in the form of poles and zeros and locate the poles and zeros on the s -plane with 'x' to denote poles and 'o' to denote zeros.

When $K = 0$, the roots of the characteristic equation are the poles of $P(s)$, and when $K \rightarrow -\infty$ the roots of the characteristic equation are the zeros of $P(s)$. Therefore, the locus of the roots of the characteristic equation begins at the poles of $P(s)$ when $K = 0$ and ends at the zeros of $P(s)$ as $K \rightarrow -\infty$. If $P(s)$ has n poles and M zeros and $n > M$, we have $n - M$ branches of the root locus approaching the zeros at infinity and the number of separate loci is equal to the number of poles. The root loci are symmetrical with respect to the horizontal real axis because the complex roots must appear as pairs of complex conjugate roots.

Step 2: Locate the segments of the real axis that are root loci. The root locus on the real axis always lies in a section of the real axis to the left of an even number of poles and zeros. This follows from the angle criterion of Equation (7.100).

automatic control of the velocity of an automobile is considered. In this example, the root locus method is extended from one parameter to three parameters as the three gains of a PID controller are determined. The design process is emphasized, including considering the control goals and associated variables to be controlled, the design specifications, and the PID controller design using root locus methods.

EXAMPLE 7.13 Wind turbine speed control

Wind energy conversion to electric power is achieved by wind energy turbines connected to electric generators. Of particular interest are wind turbines, as shown in Figure 7.45, that are located offshore [33]. The new concept is to allow the wind turbine to float rather than positioning the structure on a tower tied deep into the ocean floor. This allows the wind turbine structure to be placed in deeper waters up to 100 miles offshore far enough not to burden the landscape with unsightly structures [34]. Moreover, the wind is generally stronger on the open ocean potentially leading to the production of 5 MW versus the more typical 1.5 MW for wind turbines onshore. However, the irregular character of wind direction and power results in the need for reliable, steady electric energy by using control systems for the wind turbines. The goal of these control devices is to reduce the effects of wind intermittency and of wind direction change. The rotor and generator speed control can be achieved by adjusting the pitch angle of the blades.

A basic model of the generator speed control system is shown in Figure 7.46 [35]. A linearized model from the collective pitch to the generator speed is given by¹

$$G(s) = \frac{4.2158(s - 827.1)(s^2 - 5.489s + 194.4)}{(s + 0.195)(s^2 + 0.101s + 482.6)} \quad (7.105)$$

The model corresponds to a 600 kW turbine with hub height = 36.6 m, rotor diameter = 40 m, rated rotor speed = 41.7 rpm, rated generator speed = 1800 rpm,



FIGURE 7.45 Wind turbine placed offshore can help alleviate the energy needs. (Photo courtesy of Alamy Images.)

¹ Provided by Dr. Lucy Pao and Jason Laks in private correspondence.

Table 7.9 Seven Steps for Sketching a Negative Gain Root Locus (color text denotes changes from root locus steps in Table 7.2)

Step	Related Equation or Rule
1. Prepare the root locus sketch.	
(a) Write the characteristic equation so that the parameter of interest, K , appears as a multiplier.	(a) $1 + KP(s) = 0$
(b) Factor $P(s)$ in terms of n poles and M zeros	(b) $1 + K \frac{\prod_{i=1}^n (s + z_i)}{\prod_{j=1}^M (s + p_j)} = 0$
(c) Locate the open-loop poles and zeros of $P(s)$ in the s -plane with selected symbols.	(c) x = poles, o = zeros
(d) Determine the number of separate loci, SL .	(d) Locus begins at a pole and ends at a zero. $SL = n$ when $n \geq M$; $n =$ number of finite poles, $M =$ number of finite zeros.
(e) The root loci are symmetrical with respect to the horizontal real axis.	
2. Locate the segments of the real axis that are root loci.	Locus lies to the left of an even number of poles and zeros.
3. The loci proceed to the zeros at infinity along asymptotes centered at σ_A and with angles ϕ_A .	$\sigma_A = \frac{\sum_{i=1}^n (-p_i) - \sum_{i=1}^M (-z_i)}{n - M}$ $\phi_A = \frac{2k + 1}{n - M} 360^\circ, k = 0, 1, 2, \dots, (n - M - 1)$
4. Determine the points at which the locus crosses the imaginary axis (if it does so).	Use Routh-Hurwitz criterion (see Section 6.2).
5. Determine the breakaway point on the real axis (if any).	a) Set $K = p(s)$ b) Determine roots of $dp(s)/ds = 0$ or use graphical method to find maximum of $p(s)$. $\angle P(s) = \pm k360^\circ \text{ at } s = -p_i \text{ or } -z_j$
6. Determine the angle of locus departure from complex at or poles and the angle of locus arrival at complex zeros using the phase criterion.	
7. Complete the negative gain root locus sketch.	

7.8 DESIGN EXAMPLES

In this section we present four illustrative examples. The first example is a wind turbine control system. The feedback control system uses a PI controller to achieve a fast settling time and rise time while limiting the percent overshoot to a step input. The second example is a laser manipulator control system. Here the root locus method is used to show how the closed-loop system poles move in the s -plane as the proportional controller amplifier gain varies. The second example considers a simplified robotic replication facility. In the example, the system is represented by a fifth-order transfer function model. The feedback control strategy employs a velocity feedback coupled with a controller in the forward loop. Root locus design methods are used to select the two feedback controller gains. In the final example, the

The step response is shown in Figure 7.48 using the simplified first-order model in Equation (7.106). The step response has $T_r = 1.8$ seconds, $T_s = 0.34$ seconds, and $\zeta = 0.707$ which translates to $P.O. = 19\%$. The PI controller is able to meet all the control specifications. The step response using the third-order model in Equation (7.105) is shown in Figure 7.49 where we see the effect of the neglected components in the design as small oscillations in the speed response. The closed-loop impulse disturbance response in Figure 7.50 shows fast and accurate rejection of the disturbance in less than 3 seconds due to a 1° pitch angle change. ■

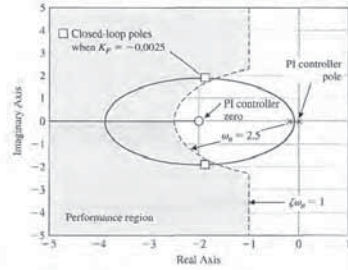


FIGURE 7.47 Wind turbine generator speed control root locus with a PI controller.

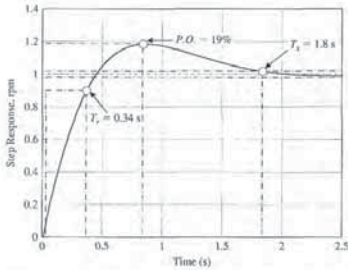


FIGURE 7.48 Step response of the wind turbine generator speed control system using the first-order model in Equation (7.106) with the designed PI controller showing all specifications are satisfied with $P.O. = 19\%$, $T_r = 1.8$ s, and $T_s = 0.34$ s.

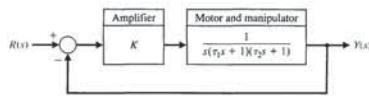


FIGURE 7.51 Laser manipulator control system.

To obtain the steady-state error required and a good response, we select a motor with a field time constant $\tau_1 = 0.1$ s and a motor-plus-load time constant $\tau_2 = 0.2$ s. We then have

$$T(s) = \frac{KG(s)}{1 + KG(s)} = \frac{K}{s(\tau_1 s + 1)(\tau_2 s + 1) + K} = \frac{50K}{0.02s^3 + 0.3s^2 + s + K} = \frac{50K}{s^3 + 15s^2 + 50s + 50K} \quad (7.107)$$

The steady-state error for a ramp, $R(s) = A/s^2$, from Equation (5.29), is

$$e_{ss} = \frac{A}{K_v} = \frac{A}{K}$$

Since we desire $e_{ss} = 0.1$ mm (or less) and $A = 1$ mm, we require $K = 10$ (or greater).

To ensure a stable system, we obtain the characteristic equation from Equation (7.107) as

$$s^3 + 15s^2 + 50s + 50K = 0.$$

Establishing the Routh array, we have

s^3	1	50
s^2	15	50K
s^1	b_1	0
s_0	50K	

where

$$b_1 = \frac{750 - 50K}{15}$$

Therefore, the system is stable for

$$0 \leq K \leq 15.$$

The characteristic equation can be written as

$$1 + K \frac{50}{s^3 + 15s^2 + 50s} = 0.$$

The root locus for $K > 0$ is shown in Figure 7.52. Using $K = 10$ results in a stable system that also satisfies the steady-state tracking error specification. The roots at $K = 10$ are $-r_2 = -13.98$, $-r_1 = -0.51 + j5.96$, and $-r_1$. The ζ of the complex

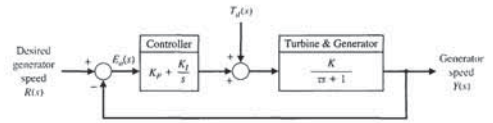


FIGURE 7.46 Wind turbine generator speed control system.

and maximum pitch rate = 18.7 deg/sec. Note that the linearized model in Equation (7.105) has zeros in the right half-plane at $s_1 = 827.1$ and $s_{2,3} = 0.0274 \pm 0.1367j$ making this a nonminimum phase system (see Chapter 8 for more information on nonminimum phase systems).

A simplified version of the model in Equation (7.105) is given by the transfer function

$$G(s) = \frac{K}{\tau s + 1} \quad (7.106)$$

where $\tau = 5$ seconds and $K = -7200$. We will design a PI controller to control the speed of the turbine generator using the simplified first-order model in Equation (7.106) and confirm that the design specifications are satisfied for both the first-order model and the third-order model in Equation (7.105). The PI controller, denoted by $G_c(s)$, is given by

$$G_c(s) = K_p + \frac{K_I}{s} = K_p \left[\frac{s + \tau_c}{s} \right],$$

where $\tau_c = K_I/K_p$ and the gains K_p and K_I are to be determined. A stability analysis indicates that negative gains $K_I < 0$ and $K_p < 0$ will stabilize the system. The main design specification is to have a settling time $T_s < 4$ seconds to a unit step input. We also desire a limited percent overshoot ($P.O. < 25\%$) and a short rise time ($T_r < 1$ s) while meeting the settling time specification. To this end, we will target the damping ratio of the dominant roots to be $\zeta > 0.4$ and the natural frequency $\omega_n > 2.5$ rad/s.

The root locus is shown in Figure 7.47 for the characteristic equation

$$1 + \hat{K}_p \left[\frac{s + \tau_c}{s} \frac{-7200}{5s + 1} \right] = 0,$$

where $\tau_c = 2$ and $\hat{K}_p = -K_p > 0$. The placement of the controller zero at $s = -\tau_c = -2$ is a design parameter. We select the value of \hat{K}_p such that the damping ratio of the closed-loop complex poles is $\zeta = 0.707$. Selecting $\hat{K}_p = 0.0025$ yields $K_p = -0.0025$ and $K_I = -0.005$. The PI controller is

$$G_c(s) = K_p + \frac{K_I}{s} = -0.0025 \left[\frac{s + 2}{s} \right].$$

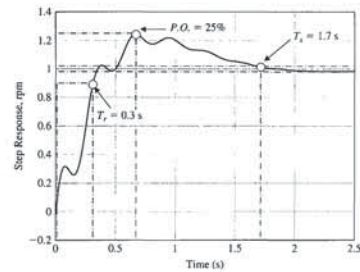


FIGURE 7.49 Step response of the third-order model in Equation (7.105) with the PI controller showing that all specifications are satisfied with $P.O. = 25\%$, $T_r = 1.7$ s, and $T_s = 0.3$ s.

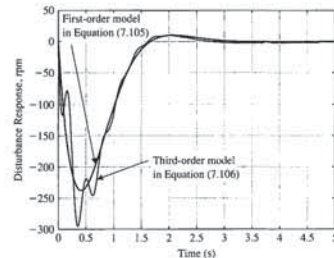


FIGURE 7.50 Disturbance response of the wind turbine generator speed control system with a PI controller shows excellent disturbance rejection characteristics.

EXAMPLE 7.14 Laser manipulator control system

Lasers can be used to drill the hip socket for the appropriate insertion of an artificial hip joint. The use of lasers for surgery requires high accuracy for position and velocity response. Let us consider the system shown in Figure 7.51, which uses a DC motor manipulator for the laser. The amplifier gain K must be adjusted so that the steady-state error for a ramp input, $r(t) = At$ (where $A = 1$ mm/s), is less than or equal to 0.1 mm, while a stable response is maintained.

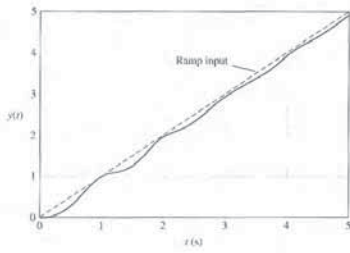


FIGURE 7.53 The response to a ramp input for a laser control system.

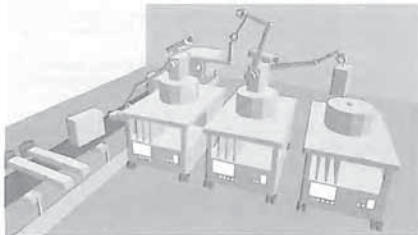


FIGURE 7.54 A robot replication facility.

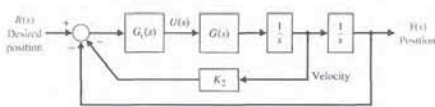


FIGURE 7.55 Proposed configuration for control of the lightweight robotic arm.

the use of a controller $G_c(s)$. The transfer function of the arm is

$$\frac{Y(s)}{U(s)} = \frac{1}{s^2} G(s)$$

where

$$G(s) = \frac{(s^2 + 4s + 10004)(s^2 + 12s + 90036)}{(s + 10)(s^2 + 2s + 2501)(s^2 + 6s + 22509)}$$

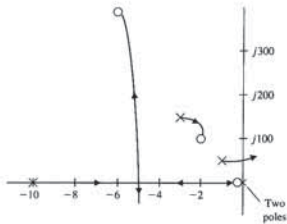


FIGURE 7.57 Root locus for the robot controller with a zero inserted at $s = -0.2$ with $G_c(s) = K_1$.

One possible selection of a controller is

$$G_c(s) = \frac{K_1(s + z)}{s + p}$$

If we select $z = 1$ and $p = 5$, then, when $K_1 = 5$, we obtain a step response with an overshoot of 8% and a settling time of 1.6 seconds. ■

EXAMPLE 7.16 Automobile velocity control

The automotive electronics market is expected to reach \$243 billion by 2015. It is predicted that there will be growth of about 6.4% up to the year 2015 in electronic braking, steering, and driver information. Much of the additional computing power will be used for new technology for smart cars and smart roads, such as IVHS (intelligent vehicle/highway systems) [14, 30, 31]. New systems on-board the automobile will support semi-autonomous automobiles, safety enhancements, emission reduction, and other features including intelligent cruise control, and brake by wire systems eliminating the hydraulics [32].

The term IVHS refers to a varied assortment of electronics that provides real-time information on accidents, congestion, and roadside services to drivers and traffic controllers. IVHS also encompasses devices that make vehicles more autonomous: collision-avoidance systems and lane-tracking technology that alert drivers to impending disasters and allow a car to drive itself.

An example of an automated highway system is shown in Figure 7.58. A velocity control system for maintaining the velocity between vehicles is shown in Figure 7.59. The output $Y(s)$ is the relative velocity of the two automobiles; the input $R(s)$ is the desired relative velocity between the two vehicles. Our design goal is to develop a controller that can maintain the prescribed velocity between the vehicles and maneuver the active vehicle (in this case the rearward automobile) as commanded. The elements of the design process emphasized in this example are depicted in Figure 7.60.

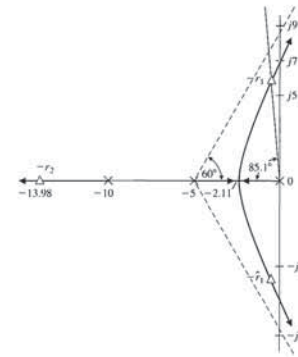


FIGURE 7.52 Root locus for a laser control system.

roots is 0.085 and $\zeta\omega_n = 0.51$. Thus, assuming that the complex roots are dominant, we expect (using Equation 5.16 and 5.13) a step input to have an overshoot of 76% and a settling time (to within 2% of the final value) of

$$T_s = \frac{4}{\zeta\omega_n} = \frac{4}{0.51} = 7.8 \text{ s.}$$

Plotting the actual system response, we find that the overshoot is 70% and the settling time is 7.5 seconds. Thus, the complex roots are essentially dominant. The system response to a step input is highly oscillatory and cannot be tolerated for laser surgery. The command signal must be limited to a low-velocity ramp signal. The response to a ramp signal is shown in Figure 7.53. ■

EXAMPLE 7.15 Robot control system

The concept of robot replication is relatively easy to grasp. The central idea is that robots replicate themselves and develop a factory that automatically produces robots. An example of a robot replication facility is shown in Figure 7.54. To achieve the rapid and accurate control of a robot, it is important to keep the robotic arm stiff and yet lightweight [6].

The specifications for controlling the motion of the arm are (1) a settling time to within 2% of the final value of less than 2 seconds, (2) a percent overshoot of less than 10% for a step input, and (3) a steady-state error of zero for a step input.

The block diagram of the proposed system with a controller is shown in Figure 7.55. The configuration proposes the use of velocity feedback as well as

The complex zeros are located at

$$s = -2 \pm j100 \quad \text{and} \quad s = -6 \pm j300.$$

The complex poles are located at

$$s = -1 \pm j50 \quad \text{and} \quad s = -3 \pm j150.$$

A sketch of the root locus when $K_2 = 0$ and the controller is an adjustable gain, $G_c(s) = K_1$, is shown in Figure 7.56. The system is unstable since two roots of the characteristic equation appear in the right-hand s -plane for $K_1 > 0$.

It is clear that we need to introduce the use of velocity feedback by setting K_2 to a positive magnitude. Then we have $H(s) = 1 + K_2s$; therefore, the loop transfer function is

$$\frac{1}{s^2} G_c(s) G(s) H(s) = \frac{K_1 K_2 \left(s + \frac{1}{K_2} \right) (s^2 + 4s + 10004)(s^2 + 12s + 90036)}{s^2 (s + 10)(s^2 + 2s + 2501)(s^2 + 6s + 22509)}$$

where K_1 is the gain of $G_c(s)$. We now have available two parameters, K_1 and K_2 , that we may adjust. We select $5 < K_2 < 10$ in order to place the adjustable zero near the origin.

When $K_2 = 5$ and K_1 is varied, we obtain the root locus sketched in Figure 7.57. When $K_1 = 0.8$ and $K_2 = 5$, we obtain a step response with a percent overshoot of 12% and a settling time of 1.8 seconds. This is the optimum achievable response. If we try $K_2 = 7$ or $K_2 = 4$, the overshoot will be larger than desired. Therefore, we have achieved the best performance with this system. If we desired to continue the design process, we would use a controller $G_c(s)$ with a pole and zero in addition to retaining the velocity feedback with $K_2 = 5$.

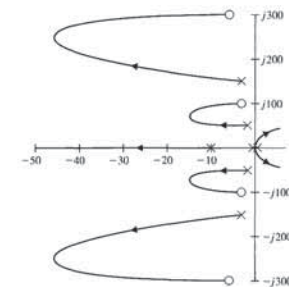


FIGURE 7.56 Root locus of the system if $K_2 = 0$, K_1 is varied from $K_1 = 0$ to $K_1 = \infty$, and $G_c(s) = K_1$.

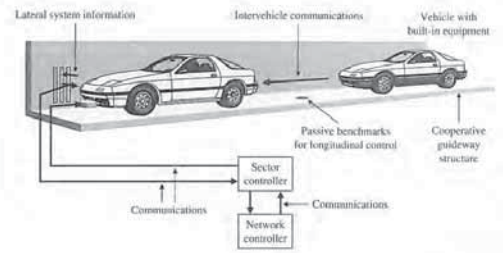


FIGURE 7.58 Automated Highway system.

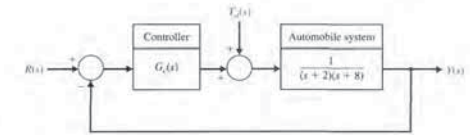


FIGURE 7.59 Vehicle velocity control system.

The control goal is

Control Goal

Maintain the prescribed velocity between the two vehicles, and maneuver the active vehicle as commanded.

The variable to be controlled is the relative velocity between the two vehicles:

Variable to Be Controlled

The relative velocity between vehicles, denoted by $y(t)$.

The design specifications are

Design Specifications

- DS1 Zero steady-state error to a step input.
- DS2 Steady-state error due to a ramp input of less than 25% of the input magnitude.
- DS3 Percent overshoot less than 5% to a step input.
- DS4 Settling time less than 1.5 seconds to a step input (using a 2% criterion to establish settling time).

From the design specifications and knowledge of the open-loop system, we find that we need a type 1 system to guarantee a zero steady-state error to a step input. The open-loop system transfer function is a type 0 system; therefore, the controller

Section 7.8 Design Examples

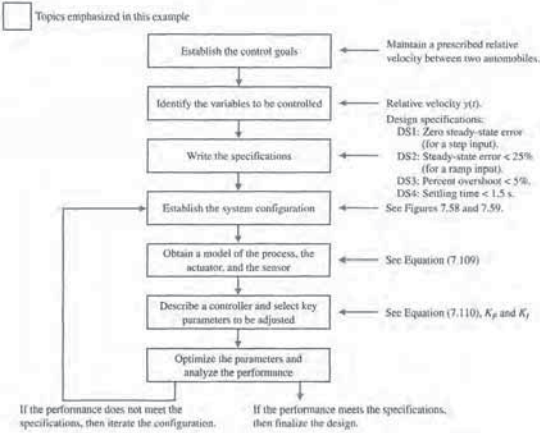


FIGURE 7.60 Elements of the control system design process emphasized in the automobile velocity control example.

needs to increase the system type by at least 1. A type 1 controller (that is, a controller with one integrator) satisfies DS1. To meet DS2 we need to have the velocity error constant (see Equation (5.29))

$$K_v = \lim_{s \rightarrow 0} sG_c(s)G(s) \approx \frac{1}{0.25} = 4, \quad (7.108)$$

where

$$G(s) = \frac{1}{(s+2)(s+8)}, \quad (7.109)$$

and $G_c(s)$ is the controller (yet to be specified).

The percent overshoot specification DS3 allows us to define a target damping ratio (see Figure 5.8):

$$P.O. \leq 5\% \text{ implies } \zeta \geq 0.69.$$

Section 7.8 Design Examples

From the first column, third row, we have the inequality

$$K_p > \frac{K_I}{10} - 16. \quad (7.112)$$

It follows from DS2 that

$$K_v = \lim_{s \rightarrow 0} sG_c(s)G(s) = \lim_{s \rightarrow 0} s \frac{K_p \left(s + \frac{K_I}{K_p} \right)}{s} \frac{1}{(s+2)(s+8)} = \frac{K_I}{16} > 4.$$

Therefore, the integral gain must satisfy

$$K_I > 64. \quad (7.113)$$

If we select $K_I > 64$, then the inequality in Equation (7.103) is satisfied. The valid region for K_p is then given by Equation (7.112), where $K_I > 64$.

We need to consider DS4. Here we want to have the dominant poles to the left of the $\sigma = -2.6$ line. We know from our experience sketching the root locus that since we have three poles (at $s = 0, -2,$ and -8) and one zero (at $s = -K_I/K_p$), we expect two branches of the loci to go to infinity along two asymptotes at $\phi = -90^\circ$ and $+90^\circ$ centered at

$$\sigma_A = \frac{\sum(-p_i) - \sum(-z_i)}{n_p - n_z},$$

where $n_p = 3$ and $n_z = 1$. In our case

$$\sigma_A = \frac{-2 - 8 - \left(-\frac{K_I}{K_p} \right)}{2} = -5 + \frac{1}{2} \frac{K_I}{K_p}.$$

We want to have $\sigma_A < -2.6$ so that the two branches will bend into the desired regions. Therefore,

$$-5 + \frac{1}{2} \frac{K_I}{K_p} < -2.6,$$

or

$$\frac{K_I}{K_p} < 4.7. \quad (7.114)$$

So as a first design, we can select K_p and K_I such that

$$K_I > 64, K_p > \frac{K_I}{10} - 16, \text{ and } \frac{K_I}{K_p} < 4.7.$$

Suppose we choose $K_I/K_p = 2.5$. Then the closed-loop characteristic equation is

$$1 + K_p \frac{s + 2.5}{s(s+2)(s+8)} = 0.$$

Similarly from the settling time specification DS4 we have (see Equation (5.13))

$$T_s \approx \frac{4}{\zeta\omega_n} \leq 1.5.$$

Solving for $\zeta\omega_n$ yields $\zeta\omega_n \geq 2.6$.

The desired region for the poles of the closed-loop transfer function is shown in Figure 7.61. Using a proportional controller $G_c(s) = K_p$ is not reasonable, because DS2 cannot be satisfied. We need at least one pole at the origin to track a ramp input. Consider the PI controller

$$G_c(s) = \frac{K_p s + K_I}{s} = K_p \frac{s + \frac{K_I}{K_p}}{s}. \quad (7.110)$$

The question is where to place the zero at $s = -K_I/K_p$.

We ask for what values of K_p and K_I is the system stable. The closed-loop transfer function is

$$T(s) = \frac{K_p s + K_I}{s^3 + 10s^2 + (16 + K_p)s + K_I}.$$

The corresponding Routh array is

$$\begin{array}{c|cc} s^3 & 1 & 16 + K_p \\ s^2 & 10 & K_I \\ s & 10(K_p + 16) - K_I & 0 \\ 1 & K_p & \end{array}$$

The first requirement for stability (from column one, row four) is

$$K_I > 0. \quad (7.111)$$

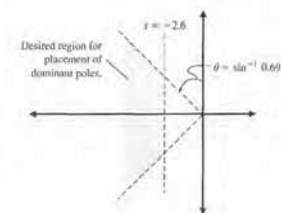


FIGURE 7.61 Desired region in the complex plane for locating the dominant system poles.

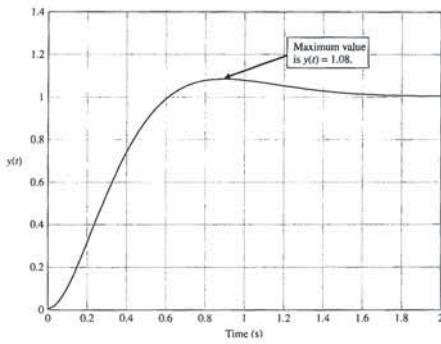


FIGURE 7.63 Automobile velocity control using the PI controller in Equation (7.107).

approximate root locus. The fundamental concepts behind the root locus method are embedded in the manual steps, and it is essential to understand their application fully.

The section begins with a discussion on obtaining a computer-generated root locus plot. This is followed by a discussion of the connections between the partial fraction expansion, dominant poles, and the closed-loop system response. Root sensitivity is covered in the final paragraphs.

The functions covered in this section are `rlocus`, `rlocfind`, and `residue`. The functions `rlocus` and `rlocfind` are used to obtain root locus plots, and the `residue` function is utilized for partial fraction expansions of rational functions.

Obtaining a Root Locus Plot. Consider the closed-loop control system in Figure 7.10. The closed-loop transfer function is

$$T(s) = \frac{Y(s)}{R(s)} = \frac{K(s+1)(s+3)}{s(s+2)(s+3) + K(s+1)}$$

The characteristic equation can be written as

$$1 + K \frac{s+1}{s(s+2)(s+3)} = 0. \quad (7.116)$$

The form of the characteristic equation in Equation (7.116) is necessary to use the `rlocus` function for generating root locus plots. The general form of the characteristic equation necessary for application of the `rlocus` function is

$$1 + KG(s) = 1 + K \frac{p(s)}{q(s)} = 0, \quad (7.117)$$

the `rlocfind` function to do this, but only after a root locus has been obtained with the `rlocus` function. Executing the `rlocfind` function will result in a cross-hair marker appearing on the root locus plot. We move the cross-hair marker to the location on the locus of interest and hit the enter key. The value of the parameter K and the value of the selected point will then be displayed in the command display. The use of the `rlocfind` function is illustrated in Figure 7.66.



Control design software packages may respond differently when interacting with plots, such as with the `rlocfind` function on the root locus. The response of `rlocfind` in Figure 7.66 corresponds to MATLAB. Refer to the companion website for more information on other control design software applications.

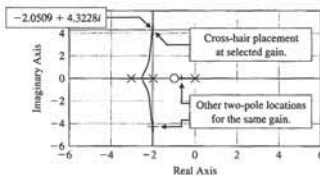
Continuing our third-order root locus example, we find that when $K = 20.5775$, the closed-loop transfer function has three poles and two zeros, at

$$\text{poles: } s = \begin{pmatrix} -2.0505 + j4.3227 \\ -2.0505 - j4.3227 \\ -0.8989 \end{pmatrix}; \quad \text{zeros: } s = \begin{pmatrix} -1 \\ -3 \end{pmatrix}$$

Considering the closed-loop pole locations only, we would expect that the real pole at $s = -0.8989$ would be the dominant pole. To verify this, we can study the closed-loop system response to a step input, $R(s) = 1/s$. For a step input, we have

$$Y(s) = \frac{20.5775(s+1)(s+3)}{s(s+2)(s+3) + 20.5775(s+1)} \cdot \frac{1}{s} \quad (7.118)$$

Generally, the first step in computing $y(t)$ is to expand Equation (7.118) in a partial fraction expansion. The residue function can be used to expand Equation (7.118), as shown in Figure 7.67. The residue function is described in Figure 7.68.



```
>>p=[1 1]; q=[1 5 6 0]; sys=tf(p,q); rlocus(sys)
>>rlcfind(sys)
rlcfind follows the rlocus function.
Select a point in the graphics window
selected_point =
-2.0509 + 4.3228i
ans =
20.5775
Value of K at selected point
```

FIGURE 7.66 Using the `rlcfind` function.

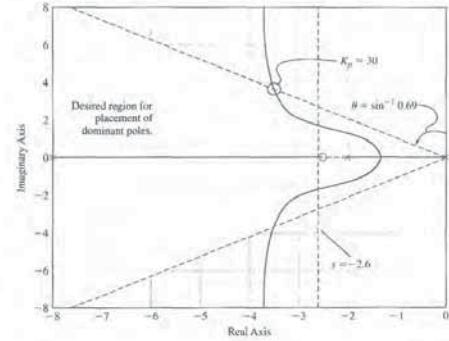


FIGURE 7.62 Root locus for $K_f/K_p = 2.5$.

The root locus is shown in Figure 7.62. To meet the $\zeta = 0.69$ (which evolved from DS3), we need to select $K_p < 30$. We selected the value at the boundary of the performance region (see Figure 7.62) as carefully as possible.

Selecting $K_p = 26$, we have $K_f/K_p = 2.5$ which implies $K_f = 65$. This satisfies the steady-state tracking error specification (DS2) since $K_f > 64$.

The resulting PI controller is

$$G_c(s) = 26 + \frac{65}{s} \quad (7.115)$$

The step response is shown in Figure 7.63.

The percent overshoot is $P.O. = 8\%$, and the settling time is $T_s = 1.45$ s. The percent overshoot specification is not precisely satisfied, but the controller in Equation (7.115) represents a very good first design. We can iteratively refine it. Even though the closed-loop poles lie in the desired region, the response does not exactly meet the specifications because the controller zero influences the response. The closed-loop system is a third-order system and does not have the performance of a second-order system. We might consider moving the zero to $s = -2$ (by choosing $K_f/K_p = 2$) so that the pole at $s = -2$ is cancelled and the resulting system is a second-order system. ■

7.9 THE ROOT LOCUS USING CONTROL DESIGN SOFTWARE

An approximate root locus sketch can be obtained by applying the orderly procedure summarized in Table 7.2. Alternatively, we can use control design software to obtain an accurate root locus plot. However, we should not be tempted to rely solely on the computer for obtaining root locus plots while neglecting the manual steps in developing an

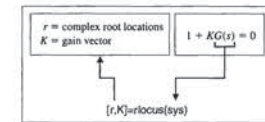


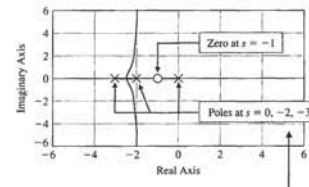
FIGURE 7.64 The `rlocus` function.

where K is the parameter of interest to be varied from $0 < K < \infty$. The root locus is shown in Figure 7.64, where we define the transfer function object $sys = G(s)$. The steps to obtaining the root locus plot associated with Equation (7.116), along with the associated root locus plot, are shown in Figure 7.65. Invoking the `rlocus` function without left-hand arguments results in an automatic generation of the root locus plot. When invoked with left-hand arguments, the `rlocus` function returns a matrix of root locations and the associated gain vector.

The steps to obtain a computer-generated root locus plot are as follows:

1. Obtain the characteristic equation in the form given in Equation (7.117), where K is the parameter of interest.
2. Use the `rlocus` function to generate the plots.

Referring to Figure 7.65, we can see that as K increases, two branches of the root locus break away from the real axis. This means that, for some values of K , the closed-loop system characteristic equation will have two complex roots. Suppose we want to find the value of K corresponding to a pair of complex roots. We can use



```
>>p=[1 1]; q=[1 5 6 0]; sys=tf(p,q); rlocus(sys)
Generating a root locus plot.

>>p=[1 1]; q=[1 5 6 0]; sys=tf(p,q); [r,K]=rlocus(sys);
Obtaining root locations r associated with various values of the gain K.
```

FIGURE 7.65 The root locus for the characteristic equation, Equation (7.116).

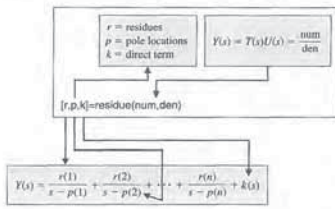


FIGURE 7.68 The residue function.

When using the step function, we can right-click on the figure to access the pull-down menu, which allows us to determine the step response settling time and peak response, as illustrated in Figure 7.69. On the pull-down menu select "Characteristics" and select "Settling Time." A dot will appear on the figure at the settling point. Place the cursor over the dot to determine the settling time.

In this example, the role of the system zeros on the transient response is illustrated. The proximity of the zero at $s = -1$ to the pole at $s = -0.8989$ reduces the impact of that pole on the transient response. The main contributors to the transient response are the complex-conjugate poles at $s = -2.0505 \pm j4.3228$ and the zero at $s = -3$. There is one final point regarding the residue function: We can convert the partial fraction expansion back to the polynomials num/den, given the residues r , the pole locations p , and the direct terms k , with the command shown in Figure 7.70.

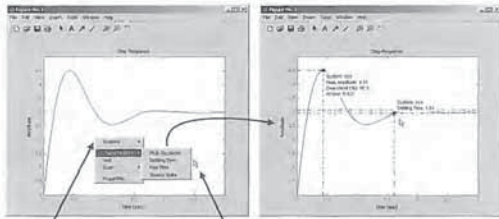


FIGURE 7.69 Step response for the closed-loop system in Figure 7.10 with $K = 20.5775$.

```
>>K=20.5775;num=k*[1 4 3]; den=[1 5 6+K K];
>>step(sys)
```

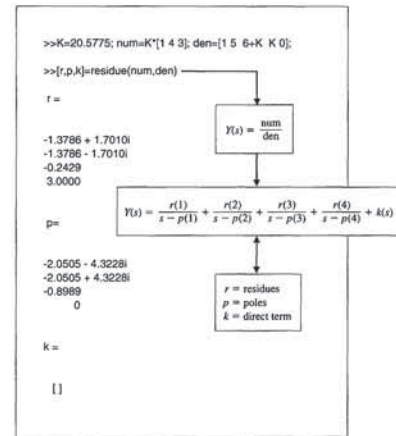


FIGURE 7.67 Partial fraction expansion of Equation (7.118).

The partial fraction expansion of Equation (7.118) is

$$Y(s) = \frac{-1.3786 + j1.7010}{s + 2.0505 + j4.3228} + \frac{-1.3786 - j1.7010}{s + 2.0505 - j4.3228} + \frac{-0.2429}{s + 0.8989} + \frac{3}{s}$$

Comparing the residues, we see that the coefficient of the term corresponding to the pole at $s = -0.8989$ is considerably smaller than the coefficient of the terms corresponding to the complex-conjugate poles at $s = -2.0505 \pm j4.3227$. From this, we expect that the influence of the pole at $s = -0.8989$ on the output response $y(t)$ is not dominant. The settling time (to within 2% of the final value) is then predicted by considering the complex-conjugate poles. The poles at $s = -2.0505 \pm j4.3227$ correspond to a damping of $\zeta = 0.4286$ and a natural frequency of $\omega_n = 4.7844$. Thus, the settling time is predicted to be

$$T_s \approx \frac{4}{\zeta \omega_n} = 1.95 \text{ s.}$$

Using the step function, as shown in Figure 7.69, we find that $T_s = 1.6$ s. Hence, our approximation of settling time $T_s \approx 1.95$ is a fairly good approximation. The percent overshoot can be predicted using Figure 5.13 since the zero of $T(s)$ at $s = -3$ will impact the system response. Using Figure 5.13, we predict an overshoot of 60%. As can be seen in Figure 7.48, the actual overshoot is 50%.

```
% Compute the system sensitivity to a parameter
% variation
K=20.5775; den=[1 5 6+K K]; r1=roots(den);
%
dk=1.0289; % 5% change in K
%
Km=K+dK; denm=[1 5+Km Km]; r2=roots(denm);
drr=1-r2; %
%
S=dr1/(dk/K); % Sensitivity formula
```

FIGURE 7.71 Sensitivity calculations for the root locus for a 5% change in $K = 20.5775$.

We use the root locus to select the controller gains. The PID controller introduced in this chapter is

$$G_c(s) = K_p + \frac{K_I}{s} + K_D s.$$

Since the process model $G_1(s)$ already possesses an integration, we set $K_I = 0$. Then we have the PD controller

$$G_c(s) = K_p + K_D s,$$

and our goal is to select K_p and K_D in order to meet the specifications. The system is shown in Figure 7.72. The closed-loop transfer function of the system is

$$\frac{Y(s)}{R(s)} = T(s) = \frac{G_c(s)G_1(s)G_2(s)}{1 + G_c(s)G_1(s)G_2(s)H(s)}$$

where $H(s) = 1$.

In order to obtain the root locus as a function of a parameter, we write $G_c(s)G_1(s)G_2(s)H(s)$ as

$$G_c(s)G_1(s)G_2(s)H(s) = \frac{5000(K_p + K_D s)}{s(s + 20)(s + 1000)} = \frac{5000K_D s + z}{s(s + 20)(s + 1000)},$$

where $z = K_p/K_D$. We use K_p to select the location of the zero z and then sketch the locus as a function of K_D . Based on the insight developed in Section 6.7, we select $z = 1$ so that

$$G_c(s)G_1(s)G_2(s)H(s) = \frac{5000K_D s + 1}{s(s + 20)(s + 1000)}.$$

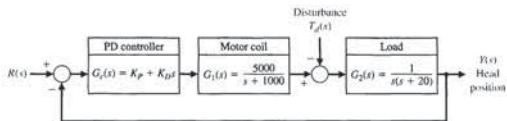


FIGURE 7.72 Disk drive control system with a PD controller.

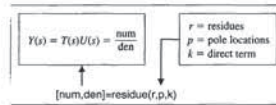


FIGURE 7.70 Converting a partial fraction expansion back to a rational function.

Sensitivity and the Root Locus. The roots of the characteristic equation play an important role in defining the closed-loop system transient response. The effect of parameter variations on the roots of the characteristic equation is a useful measure of sensitivity. The root sensitivity is defined to be

$$\frac{\partial r_i}{\partial K/K} \quad (7.119)$$

We can use Equation (7.119) to investigate the sensitivity of the roots of the characteristic equation to variations in the parameter K . If we change K by a small finite amount ΔK , and evaluate the modified root $r_i + \Delta r_i$, it follows that

$$S_K^r \approx \frac{\Delta r_i}{\Delta K/K} \quad (7.120)$$

The quantity S_K^r is a complex number. Referring back to the third-order example of Figure 7.10 (Equation 7.116), if we change K by a factor of 5%, we find that the dominant complex-conjugate pole at $s = -2.0505 \pm j4.3228$ changes by

$$\Delta r_i = -0.0025 - j0.1168$$

when K changes from $K = 20.5775$ to $K = 21.6064$. From Equation (7.120), it follows that

$$S_K^r = \frac{-0.0025 - j0.1168}{1.0289/20.5775} = -0.0494 - j2.3355.$$

The sensitivity S_K^r can also be written in the form

$$S_K^r = 2.34 / 268.79^\circ.$$

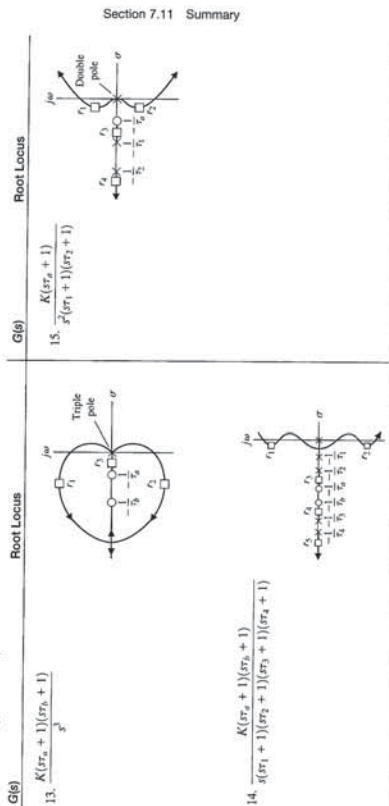
The magnitude and direction of S_K^r provides a measure of the root sensitivity. The script used to perform these sensitivity calculations is shown in Figure 7.71.

The root sensitivity measure may be useful for comparing the sensitivity for various system parameters at different root locations.

7.10 SEQUENTIAL DESIGN EXAMPLE: DISK DRIVE READ SYSTEM

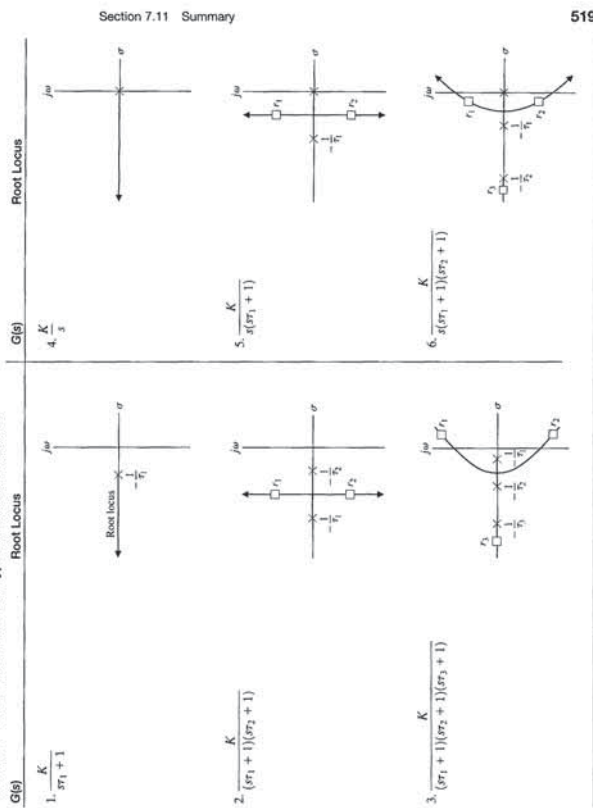
In Chapter 6, we introduced a new configuration for the control system using velocity feedback. In this chapter, we will use the PID controller to obtain a desirable response. We will proceed with our model and then select a controller. Finally, we will optimize the parameters and analyze the performance. In this chapter, we will use the root locus method in the selection of the controller parameters.

Table 7.11 (continued)



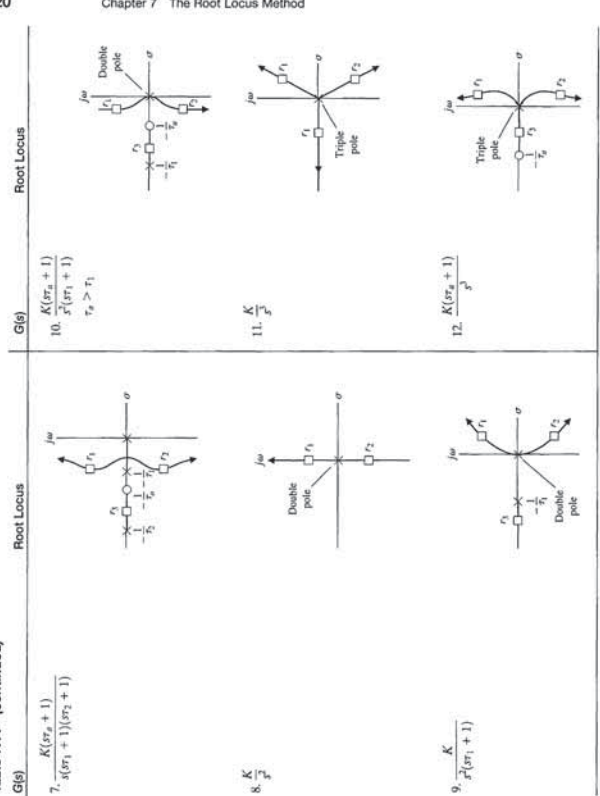
Section 7.11 Summary

Table 7.11 Root Locus Plots for Typical Transfer Functions



Section 7.11 Summary

Table 7.11 (continued)



Chapter 7 The Root Locus Method

FIGURE 7.73 Sketch of the root locus.

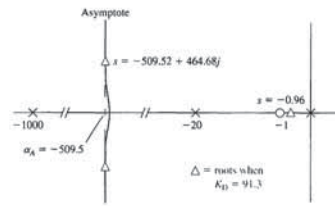


Table 7.10 Disk Drive Control System Specifications and Actual Design Performance

Performance Measure	Desired Value	Actual Response
Percent overshoot	Less than 5%	0%
Settling time	Less than 250 ms	20 ms
Maximum response to a unit disturbance	Less than 5×10^{-3}	2×10^{-3}

The number of poles minus the number of zeros is 2, and we expect asymptotes at $\phi_A = \pm 90^\circ$ with a centroid

$$\sigma_A = \frac{-1020 + 1}{2} = -509.5,$$

as shown in Figure 7.73. We can quickly sketch the root locus, as shown in Figure 7.73. We use the computer-generated root locus to determine the root values for various values of K_D . When $K_D = 91.3$, we obtain the roots shown in Figure 7.73. Then, obtaining the system response, we achieve the actual response measures as listed in Table 7.10. As designed, the system meets all the specifications. It takes the system a settling time of 20 ms to "practically" reach the final value. In reality, the system drifts very slowly toward the final value after quickly achieving 97% of the final value.

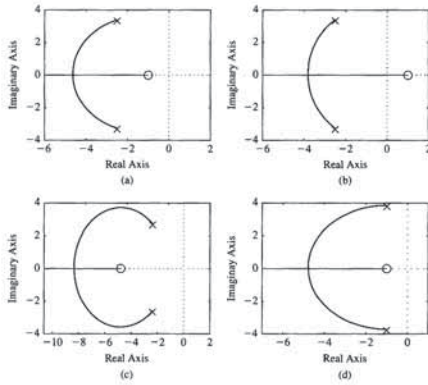
7.11 SUMMARY

The relative stability and the transient response performance of a closed-loop control system are directly related to the location of the closed-loop roots of the characteristic equation. We investigated the movement of the characteristic roots on the s -plane as key system parameters (such as controller gains) are varied. The root locus and the negative gain root locus are graphical representations of the variation of the system closed-loop poles as one parameter varies. The plots can be sketched by hand using a given set of rules in order to analyze the initial design of a system and determine suitable alterations of the system structure and the parameter values. A computer is then commonly used to obtain the accurate root locus for use in the final design and analysis. A summary of fifteen typical root locus diagrams is shown in Table 7.11.

In Problems 7 and 8, consider the unity feedback system in Figure 7.74 with

$$L(s) = G_c(s)G(s) = \frac{K(s+1)}{s^2 + 5s + 17.33}$$

7. The approximate angles of departure of the root locus from the complex poles are
 - a. $\phi_d = \pm 180^\circ$
 - b. $\phi_d = \pm 115^\circ$
 - c. $\phi_d = \pm 205^\circ$
 - d. None of the above
8. The root locus of this system is given by which of the following



9. A unity feedback system has the closed-loop transfer function given by

$$T(s) = \frac{K}{(s+45)^2 + K}$$

Using the root locus method, determine the value of the gain K so that the closed-loop system has a damping ratio $\zeta = \sqrt{2}/2$.

- a. $K = 25$
- b. $K = 1250$
- c. $K = 2025$
- d. $K = 10500$

Furthermore, we extended the root locus method for the design of several parameters for a closed-loop control system. Then the sensitivity of the characteristic roots was investigated for undesired parameter variations by defining a root sensitivity measure. It is clear that the root locus method is a powerful and useful approach for the analysis and design of modern control systems and will continue to be one of the most important procedures of control engineering.



SKILLS CHECK

In this section, we provide three sets of problems to test your knowledge: True or False, Multiple Choice, and Word Match. To obtain direct feedback, check your answers with the answer key provided at the conclusion of the end-of-chapter problems. Use the block diagram in Figure 7.74 as specified in the various problem statements.

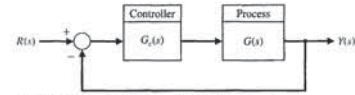


FIGURE 7.74 Block diagram for the Skills Check.

In the following True or False and Multiple Choice problems, circle the correct answer.

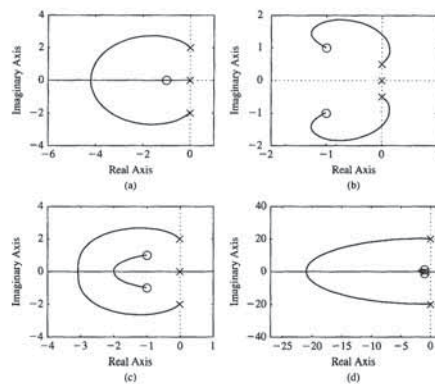
1. The root locus is the path the roots of the characteristic equation (given by $1 + KG(s) = 0$) trace out on the s -plane as the system parameter $0 \leq K < \infty$ varies. True or False
2. On the root locus plot, the number of separate loci is equal to the number of poles of $G(s)$. True or False
3. The root locus always starts at the zeros and ends at the poles of $G(s)$. True or False
4. The root locus provides the control system designer with a measure of the sensitivity of the poles of the system to variations of a parameter of interest. True or False
5. The root locus provides valuable insight into the response of a system to various test inputs. True or False
6. Consider the control system in Figure 7.74, where the loop transfer function is

$$L(s) = G_c(s)G(s) = \frac{K(s^2 + 5s + 9)}{s^2(s + 3)}$$

Using the root locus method, determine the value of K such that the dominant roots have a damping ratio $\zeta = 0.5$.

- a. $K = 1.2$
- b. $K = 4.5$
- c. $K = 9.7$
- d. $K = 37.4$

14. Which of the following is the associated root locus?



15. The departure angles from the complex poles and the arrival angles at the complex zeros are:
 - a. $\phi_D = \pm 180^\circ$, $\phi_A = 0^\circ$
 - b. $\phi_D = \pm 116.6^\circ$, $\phi_A = \pm 198.4^\circ$
 - c. $\phi_D = \pm 45.8^\circ$, $\phi_A = \pm 116.6^\circ$
 - d. None of the above

In the following Word Match problems, match the term with the definition by writing the correct letter in the space provided.

- | | | |
|---|--|-------|
| a. Parameter design | The amplitude of the closed-loop response is reduced approximately to one-fourth of the maximum value in one oscillatory period. | _____ |
| b. Root sensitivity | The path the root locus follows as the parameter becomes very large and approaches ∞ . | _____ |
| c. Root locus | The center of the linear asymptotes, σ_s . | _____ |
| d. Root locus segments on the real axis | The process of determining the PID controller gains using one of several analytic methods based on open-loop and closed-loop responses to step inputs. | _____ |
| e. Root locus method | A method of selecting one or two parameters using the root locus method. | _____ |

10. Consider the unity feedback control system in Figure 7.74 where

$$L(s) = G_c(s)G(s) = \frac{10(s+z)}{s(s^2 + 4s + 8)}$$

Using the root locus method, determine that maximum value of z for closed-loop stability.

- a. $z = 7.2$
- b. $z = 12.8$
- c. Unstable for all $z > 0$
- d. Stable for all $z > 0$

In Problems 11 and 12, consider the control system in Figure 7.74 where the model of the process is

$$G(s) = \frac{7500}{(s+1)(s+10)(s+50)}$$

11. Suppose that the controller is

$$G_c(s) = \frac{K(1 + 0.2s)}{1 + 0.025s}$$

Using the root locus method, determine the maximum value of the gain K for closed-loop stability.

- a. $K = 2.13$
- b. $K = 3.88$
- c. $K = 14.49$
- d. Stable for all $K > 0$

12. Suppose that a simple proportional controller is utilized, that is, $G_c(s) = K$. Using the root locus method, determine the maximum controller gain K for closed-loop stability.
 - a. $K = 0.50$
 - b. $K = 1.49$
 - c. $K = 4.49$
 - d. Unstable for $K > 0$
13. Consider the unity feedback system in Figure 7.74 where

$$L(s) = G_c(s)G(s) = \frac{K}{s(s+5)(s^2 + 6s + 17.76)}$$

Determine the breakaway point on the real axis and the respective gain, K .

- a. $s = -1.8$, $K = 58.75$
- b. $s = -2.5$, $K = 4.59$
- c. $s = 1.4$, $K = 58.75$
- d. None of the above

In Problems 14 and 15, consider the feedback system in Figure 7.74, where

$$L(s) = G_c(s)G(s) = \frac{K(s+1+j)(s+1-j)}{s(s+2)(s-2)}$$

(a) Find the angle of departure of the root locus from the complex poles. (b) Find the entry point for the root locus as it enters the real axis.

Answers: $\pm 225^\circ; -2.4$

E7.5 Consider a unity feedback system with a loop transfer function

$$G_c(s)G(s) = \frac{s^2 + 2s + 10}{s^4 + 38s^3 + 515s^2 + 2950s + 6000}$$

(a) Find the breakaway points on the real axis (b) Find the asymptote centroid. (c) Find the values of K at the breakaway points.

E7.6 One version of a space station is shown in Figure E7.6 [28]. It is critical to keep this station in the proper orientation toward the Sun and the Earth for generating power and communications. The orientation controller may be represented by a unity feedback system with an actuator and controller, such as

$$G_c(s)G(s) = \frac{15K}{s(s^2 + 15s + 75)}$$

Sketch the root locus of the system as K increases. Find the value of K that results in an unstable system.

Answers: $K = 75$

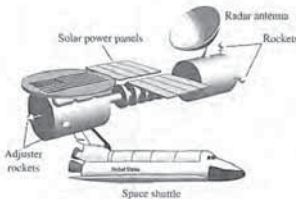


FIGURE E7.6 Space station.

E7.7 The elevator in a modern office building travels at a top speed of 25 feet per second and is still able to stop within one-eighth of an inch of the floor outside. The loop transfer function of the unity feedback elevator position control is

$$L(s) = G_c(s)G(s) = \frac{K(s + 8)}{s(s + 4)(s + 6)(s + 9)}$$

Determine the gain K when the complex roots have a ζ equal to 0.8.

E7.8 Sketch the root locus for a unity feedback system with

$$L(s) = G_c(s)G(s) = \frac{K(s + 1)}{s^2(s + 9)}$$

(a) Find the gain when all three roots are real and equal. (b) Find the roots when all the roots are equal in part (a).

Answers: $K = 27; s = -3$

E7.9 The world's largest telescope is located in Hawaii. The primary mirror has a diameter of 10 m and consists of a mosaic of 36 hexagonal segments with the orientation of each segment actively controlled. This unity feedback system for the mirror segments has the loop transfer function

$$L(s) = G_c(s)G(s) = \frac{K}{s(s^2 + 2s + 5)}$$

(a) Find the asymptotes and draw them in the s -plane. (b) Find the angle of departure from the complex poles. (c) Determine the gain when two roots lie on the imaginary axis. (d) Sketch the root locus.

E7.10 A unity feedback system has the loop transfer function

$$L(s) = KG(s) = \frac{K(s + 2)}{s(s + 1)}$$

(a) Find the breakaway and entry points on the real axis. (b) Find the gain and the roots when the real part of the complex roots is located at -2 . (c) Sketch the locus.

Answers: (a) $-0.59, -3.41$; (b) $K = 3, s = -2 \pm j\sqrt{2}$

E7.11 A robot force control system with unity feedback has a loop transfer function [6]

$$L(s) = KG(s) = \frac{K(s + 2.5)}{(s^2 + 2s + 2)(s^2 + 4s + 5)}$$

(a) Find the gain K that results in dominant roots with a damping ratio of 0.707. Sketch the root locus. (b) Find the actual percent overshoot and peak time for the gain K of part (a).

E7.12 A unity feedback system has a loop transfer function

$$L(s) = KG(s) = \frac{K(s + 1)}{s(s^2 + 6s + 18)}$$

(a) Sketch the root locus for $K > 0$. (b) Find the roots when $K = 10$ and 20. (c) Compute the rise time, percent overshoot, and settling time (with a 2% criterion) of the system for a unit step input when $K = 10$ and 20.

E7.22 A high-performance missile for launching a satellite has a unity feedback system with a loop transfer function

$$G_c(s)G(s) = \frac{K(s^2 + 18)(s + 2)}{(s^2 - 2)(s + 12)}$$

Sketch the root locus as K varies from $0 < K < \infty$.

E7.23 A unity feedback system has a loop transfer function

$$L(s) = G_c(s)G(s) = \frac{4(s^2 + 1)}{s(s + a)}$$

Sketch the root locus for $0 \leq a < \infty$.

E7.24 Consider the system represented in state variable form

$$\dot{\mathbf{x}} = \mathbf{A}\mathbf{x} + \mathbf{B}u$$

$$y = \mathbf{C}\mathbf{x} + \mathbf{D}u,$$

where

$$\mathbf{A} = \begin{bmatrix} 0 & 1 \\ -4 & -k \end{bmatrix}, \mathbf{B} = \begin{bmatrix} 0 \\ 1 \end{bmatrix}$$

$$\mathbf{C} = [1 \ 0], \text{ and } \mathbf{D} = [0].$$

Determine the characteristic equation and then sketch the root locus as $0 < k < \infty$.

E7.25 A closed-loop feedback system is shown in Figure E7.25. For what range of values of the parameters K is the system stable? Sketch the root locus as $0 < K < \infty$.

E7.26 Consider the single-input, single-output system is described by

$$\dot{\mathbf{x}}(t) = \mathbf{A}\mathbf{x}(t) + \mathbf{B}u(t)$$

$$y(t) = \mathbf{C}\mathbf{x}(t)$$

where

$$\mathbf{A} = \begin{bmatrix} 0 & 1 \\ 3 - K & -2 - K \end{bmatrix}, \mathbf{B} = \begin{bmatrix} 0 \\ 1 \end{bmatrix}, \mathbf{C} = [1 \ -1].$$

Compute the characteristic polynomial and plot the root locus as $0 \leq K < \infty$. For what values of K is the system stable?

E7.27 Consider the unity feedback system in Figure E7.27. Sketch the root locus as $0 \leq p < \infty$.

E7.28 Consider the feedback system in Figure E7.28. Obtain the negative gain root locus as $-\infty < K \leq 0$. For what values of K is the system stable?

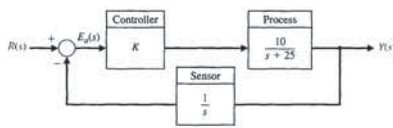


FIGURE E7.25 Nonunity feedback system with parameter K .

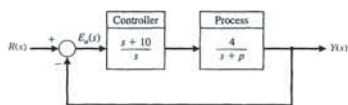


FIGURE E7.27 Unity feedback system with parameter p .

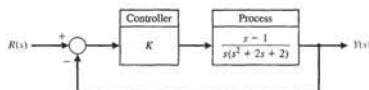


FIGURE E7.28 Feedback system for negative gain root locus.

f. Asymptote centroid	The root locus lying in a section of the real axis to the left of an odd number of poles and zeros.
g. Breakaway point	The root locus for negative values of the parameter of interest where $-\infty < K \leq 0$.
h. Locus	The angle at which a locus leaves a complex pole in the s -plane.
i. Angle of departure	A path or trajectory that is traced out as a parameter is changed.
j. Number of separate loci	The locus or path of the roots traced out on the s -plane as a parameter is changed.
k. Asymptote	The sensitivity of the roots as a parameter changes from its normal value.
l. Negative gain root locus	The method for determining the locus of roots of the characteristic equation $1 + KG(s) = 0$ as $0 \leq K < \infty$.
m. PID tuning	The process of determining the PID controller gains.
n. Quarter amplitude decay	The point on the real axis where the locus departs from the real axis of the s -plane.
o. Ziegler-Nichols PID tuning method	Equal to the number of poles of the transfer function, assuming that the number of poles is greater than or equal to the number of zeros of the transfer function.

EXERCISES

E7.1 Let us consider a device that consists of a ball rolling on the inside rim of a hoop [11]. This model is similar to the problem of liquid fuel sloshing in a rocket. The hoop is free to rotate about its horizontal principal axis as shown in Figure E7.1. The angular position of the hoop may be controlled via the torque T applied to the hoop from a torque motor attached to the hoop drive shaft. If negative feedback is used, the system characteristic equation is

$$1 + \frac{Ks(s + 4)}{s^2 + 2s + 2} = 0.$$

(a) Sketch the root locus. (b) Find the gain when the roots are both equal. (c) Find these two equal roots.

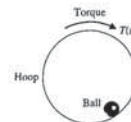


FIGURE E7.1 Hoop rotated by motor.

(d) Find the settling time of the system when the roots are equal.

E7.2 A tape recorder has a speed control system so that $H(s) = 1$ with negative feedback and

$$L(s) = G_c(s)G(s) = \frac{K}{s(s + 2)(s^2 + 4s + 5)}$$

(a) Sketch a root locus for K , and show that the dominant roots are $s = -0.35 \pm j0.80$ when $K = 6.5$. (b) For the dominant roots of part (a), calculate the settling time and overshoot for a step input.

E7.3 A control system for an automobile suspension tester has negative unity feedback and a process [12]

$$L(s) = G_c(s)G(s) = \frac{K(s^2 + 4s + 8)}{s^2(s + 4)}$$

We desire the dominant roots to have a ζ equal to 0.5. Using the root locus, show that $K = 7.35$ is required and the dominant roots are $s = -1.3 \pm j2.2$.

E7.4 Consider a unity feedback system with

$$L(s) = G_c(s)G(s) = \frac{K(s + 1)}{s^2 + 4s + 5}$$

E7.13 A unity feedback system has a loop transfer function

$$L(s) = G_c(s)G(s) = \frac{4(s + z)}{s(s + 1)(s + 3)}$$

(a) Draw the root locus as z varies from 0 to 100. (b) Using the root locus, estimate the percent overshoot and settling time (with a 2% criterion) of the system at $z = 0.6, 2,$ and 4 for a step input. (c) Determine the actual overshoot and settling time at $z = 0.6, 2,$ and 4.

E7.14 A unity feedback system has the loop transfer function

$$L(s) = G_c(s)G(s) = \frac{K(s + 10)}{s(s + 5)}$$

(a) Determine the breakaway and entry points of the root locus and sketch the root locus for $K > 0$. (b) Determine the gain K when the two characteristic roots have a ζ of $1/\sqrt{2}$. (c) Calculate the roots.

E7.15 (a) Plot the root locus for a unity feedback system with loop transfer function

$$L(s) = G_c(s)G(s) = \frac{K(s + 10)(s + 2)}{s^3}$$

(b) Calculate the range of K for which the system is stable. (c) Predict the steady-state error of the system for a ramp input.

Answers: (a) $K > 1.67$; (b) $e_{ss} = 0$

E7.16 A negative unity feedback system has a loop transfer function

$$L(s) = G_c(s)G(s) = \frac{Ke^{-sT}}{s + 1}$$

where $T = 0.1$ s. Show that an approximation to the time delay is

$$e^{-sT} \approx \frac{2 - sT}{2 + sT}$$

Using

$$e^{-0.1s} \approx \frac{20 - s}{20 + s}$$

obtain the root locus for the system for $K > 0$. Determine the range of K for which the system is stable.

E7.17 A control system, as shown in Figure E7.17, has a process

$$G(s) = \frac{1}{s(s - 1)}$$



FIGURE E7.17 Feedback system.

(a) When $G_c(s) = K$, show that the system is always unstable by sketching the root locus. (b) When

$$G_c(s) = \frac{K(s + 2)}{s + 20}$$

sketch the root locus and determine the range of K for which the system is stable. Determine the value of K and the complex roots when two roots lie on the $j\omega$ -axis.

E7.18 A closed-loop negative unity feedback system is used to control the yaw of the A-6 Intruder attack jet. When the loop transfer function is

$$L(s) = G_c(s)G(s) = \frac{K}{s(s + 3)(s^2 + 2s + 2)}$$

determine (a) the root locus breakaway point and (b) the value of the roots on the $j\omega$ -axis and the gain required for those roots. Sketch the root locus.

Answers: (a) Breakaway: $s = -2.29$ (b) $j\omega$ -axis: $s = \pm j1.09, K = 8$

E7.19 A unity feedback system has a loop transfer function

$$L(s) = G_c(s)G(s) = \frac{K}{s(s + 3)(s^2 + 6s + 64)}$$

(a) Determine the angle of departure of the root locus at the complex poles. (b) Sketch the root locus. (c) Determine the gain K when the roots are on the $j\omega$ -axis and determine the location of these roots.

E7.20 A unity feedback system has a loop transfer function

$$L(s) = G_c(s)G(s) = \frac{K(s + 1)}{s(s - 2)(s + 6)}$$

(a) Determine the range of K for stability. (b) Sketch the root locus. (c) Determine the maximum ζ of the stable complex roots.

Answers: (a) $K > 16$; (b) $\zeta = 0.25$

E7.21 A unity feedback system has a loop transfer function

$$L(s) = G_c(s)G(s) = \frac{Ks}{s^2 + 5s^2 + 10}$$

Sketch the root locus. Determine the gain K when the complex roots of the characteristic equation have a ζ approximately equal to 0.66.

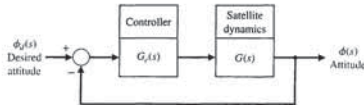


FIGURE P7.6 Satellite attitude control.

$$G_c(s) = \frac{(s + 2 + j1.5)(s + 2 - j1.5)}{s + 4.0}$$

(a) Draw the root locus of the system as K varies from 0 to ∞ . (b) Determine the gain K that results in a system with a settling time (with a 2% criterion) less than 12 seconds and a damping ratio for the complex roots greater than 0.50.

P7.7 The speed control system for an isolated power system is shown in Figure P7.7. The valve controls the steam flow input to the turbine in order to account for load changes $\Delta L(s)$ within the power distribution network. The equilibrium speed desired results in a generator frequency equal to 60 cps. The effective rotary inertia J is equal to 4000 and the friction constant b is equal to 0.75. The steady-state speed regulation factor R is represented by the equation $R \approx (\omega_0 - \omega_s)/\Delta L$, where ω_0 equals the speed at rated load and ω_s equals the speed at no load. We want to obtain a very small R , usually less than 0.10. (a) Using root locus techniques, determine the regulation R attainable when the damping ratio of the roots of the system must be greater than 0.60. (b) Verify that the steady-state speed deviation for a load torque change $\Delta L(s) = \Delta L/s$ is, in fact, approximately equal to $R\Delta L$ when $R \approx 0.1$.

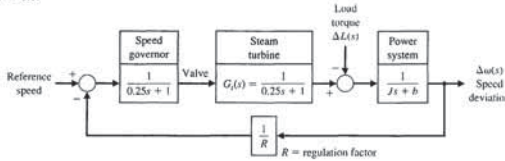


FIGURE P7.7 Power system control.

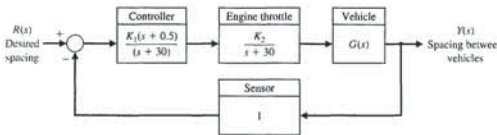


FIGURE P7.9 Guided vehicle control.

P7.8 Consider again the power control system of Problem P7.7 when the steam turbine is replaced by a hydroturbine. For hydroturbines, the large inertia of the water used as a source of energy causes a considerably larger time constant. The transfer function of a hydroturbine may be approximated by

$$G_t(s) = \frac{-\tau s + 1}{(\tau/2)s + 1}$$

where $\tau = 1$ second. With the rest of the system remaining as given in Problem P7.7, repeat parts (a) and (b) of Problem P7.7.

P7.9 The achievement of safe, efficient control of the spacing of automatically controlled guided vehicles is an important part of the future use of the vehicles in a manufacturing plant [14, 15]. It is important that the system eliminate the effects of disturbances (such as oil on the floor) as well as maintain accurate spacing between vehicles on a guideway. The system can be represented by the block diagram of Figure P7.9. The vehicle dynamics can be represented by

$$G(s) = \frac{(s + 0.1)(s^2 + 2s + 289)}{s(s - 0.4)(s + 0.8)(s^2 + 1.45s + 361)}$$

PROBLEMS

P7.1 Sketch the root locus for the following loop transfer functions of the system shown in Figure P7.1 when $0 < K < \infty$:

(a) $G_c(s)G(s) = \frac{K}{s(s + 10)(s + 8)}$

(b) $G_c(s)G(s) = \frac{K}{(s^2 + 2s + 2)(s + 2)}$

(c) $G_c(s)G(s) = \frac{K(s + 5)}{s(s + 1)(s + 10)}$

(d) $G_c(s)G(s) = \frac{K(s^2 + 4s + 8)}{s^2(s + 1)}$

P7.2 The linear model of a phase detector was presented in Problem P6.7. Sketch the root locus as a function of the gain $K_p = K_p K$. Determine the value of K_p attained if the complex roots have a damping ratio equal to 0.60 [13].

P7.3 A unity feedback system has the loop transfer function

$$G_c(s)G(s) = \frac{K}{s(s + 2)(s + 5)}$$

Find (a) the breakaway point on the real axis and the gain K for this point, (b) the gain and the roots when two roots lie on the imaginary axis, and (c) the roots when $K = 6$. (d) Sketch the root locus.

P7.4 The analysis of a large antenna was presented in Problem P4.5. Sketch the root locus of the system as

$0 < k_a < \infty$. Determine the maximum allowable gain of the amplifier for a stable system.

P7.5 Automatic control of helicopters is necessary because, unlike fixed-wing aircraft which possess a fair degree of inherent stability, the helicopter is quite unstable. A helicopter control system that utilizes an automatic control loop plus a pilot stick control is shown in Figure P7.5. When the pilot is not using the control stick, the switch may be considered to be open. The dynamics of the helicopter are represented by the transfer function

$$G(s) = \frac{25(s + 0.03)}{(s + 0.4)(s^2 - 0.36s + 0.16)}$$

(a) With the pilot control loop open (hands-off control), sketch the root locus for the automatic stabilization loop. Determine the gain K_2 that results in a damping for the complex roots equal to $\zeta = 0.707$. (b) For the gain K_2 obtained in part (a), determine the steady-state error due to a wind gust $T_d(s) = 1/s$. (c) With the pilot loop added, draw the root locus as K_1 varies from zero to ∞ when K_2 is set at the value calculated in part (a). (d) Recalculate the steady-state error of part (b) when K_1 is equal to a suitable value based on the root locus.

P7.6 An attitude control system for a satellite vehicle within the earth's atmosphere is shown in Figure P7.6. The transfer functions of the system are

$$G(s) = \frac{K(s + 0.20)}{(s + 0.90)(s - 0.60)(s - 0.10)}$$

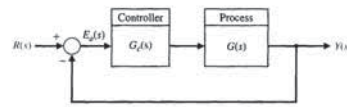


FIGURE P7.1

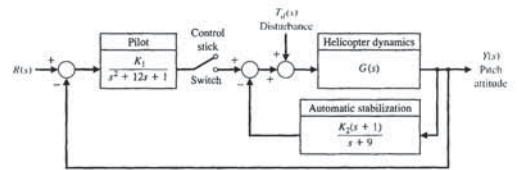
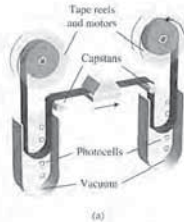
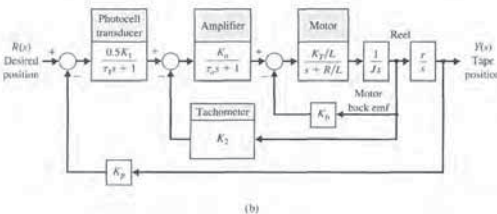


FIGURE P7.5 Helicopter control.



(a)



(b)

FIGURE P7.11 (a) Tape control system. (b) Block diagram.

100 in/s. The motor and components selected for this system possess the following characteristics:

$$\begin{aligned} K_1 &= 0.40 & r &= 0.2 \\ K_2 &= 1 & K_3 &= 2.0 \\ \tau_1 &= \tau_2 = 1 \text{ ms} & K_4 &= 2.0 \\ K_5 &= \text{adjustable} & K_5 &= \text{adjustable} \\ K_5 &= 1/L & & \end{aligned}$$

The inertia of the reel and motor rotor is 2.5×10^{-3} when the reel is empty, and 5.0×10^{-3} when the reel is full. A series of photocells is used as an error-sensing device. The time constant of the motor is $L/R = 0.5$ ms. (a) Sketch the root locus for the system when $K_2 = 10$ and $J = 5.0 \times 10^{-3}$, $0 < K_1 < \infty$. (b) Determine the gain K_1 that results in a well-damped system so that the ζ of all the roots is greater than or equal to 0.60. (c) With the K_1 determined from part (b), sketch a root locus for $0 < K_2 < \infty$.

P7.12 A precision speed control system (Figure P7.12) is required for a platform used in gyroscope and inertial system testing where a variety of closely controlled

speeds is necessary. A direct-drive DC torque motor system was utilized to provide (1) a speed range of 0.01% to 600%, and (2) 0.1% steady-state error maximum for a step input. The direct-drive DC torque motor avoids the use of a gear train with its attendant backlash and friction. Also, the direct-drive motor has a high-torque capability, high efficiency, and low motor time constants. The motor gain constant is nominally $K_m = 1.3$, but is subject to variations up to 50%. The amplifier gain K_a is normally greater than 10 and subject to a variation of 10%. (a) Determine the minimum loop gain necessary to satisfy the steady-state error requirement. (b) Determine the limiting value of gain for stability. (c) Sketch the root locus as K_m varies from 0 to ∞ . (d) Determine the roots when $K_m = 40$, and estimate the response to a step input.

P7.13 A unity feedback system has the loop transfer function

$$L(s) = G_c(s)G(s) = \frac{K}{s(s + 3)(s^2 + 4s + 7.84)}$$

(a) Sketch the root locus of the system. (b) Determine all the roots when the loop gain $K = K_1 K_2$ is equal to 4000.

P7.10 New concepts in passenger airliner design will have the range to cross the Pacific in a single flight and the efficiency to make it economical [16, 29]. These new designs will require the use of temperature-resistant, lightweight materials and advanced control systems. Noise control is an important issue in modern aircraft designs since most airports have strict noise level requirements. One interesting concept is the Boeing Sonic Cruiser depicted in Figure P7.10(a). It would seat 200 to 250 passengers and cruise at just below the speed of sound.

The flight control system must provide good handling characteristics and comfortable flying conditions. An automatic control system can be designed for the next generation passenger aircraft.

The desired characteristics of the dominant roots of the control system shown in Figure P7.10(b) have a

$\zeta = 0.707$. The characteristics of the aircraft are $\omega_n = 2.5$, $\zeta = 0.30$, and $\tau = 0.1$. The gain factor K_1 , however, will vary over the range 0.02 to medium-weight cruise conditions to 0.20 at lightweight descent conditions. (a) Sketch the root locus as a function of the loop gain $K_1 K_2$. (b) Determine the gain K_2 necessary to yield roots with $\zeta = 0.707$ when the aircraft is in the medium-cruise condition. (c) With the gain K_2 as found in part (b), determine the ζ of the roots when the gain K_1 results from the condition of light descent.

P7.11 A computer system requires a high-performance magnetic tape transport system [17]. The environmental conditions imposed on the system result in a severe test of control engineering design. A direct-drive DC motor system for the magnetic tape reel system is shown in Figure P7.11, where r equals the reel radius, and J equals the reel and rotor inertia. A complete reversal of the tape reel direction is required in 6 ms, and the tape reel must follow a step command in 3 ms or less. The tape is normally operating at a speed of



(a)

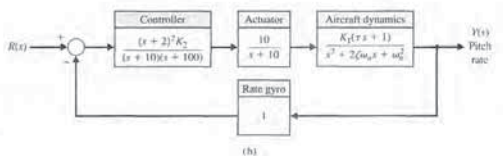


FIGURE P7.10 (a) A passenger jet aircraft of the future. (™ and © Boeing. Used under license.) (b) Control system.

(b)

position is compared with a reference voltage and integrated where it is assumed that a change in looper position is proportional to a change in the steel strip tension. The time constant τ of the filter is negligible relative to the other time constants in the system. (a) Sketch the root locus of the control system for $0 < K_c < \infty$. (b) Determine the gain K_c that results in a system whose roots have a damping ratio of $\zeta = 0.707$ or greater. (c) Determine the effect of τ as τ increases from a negligible quantity.

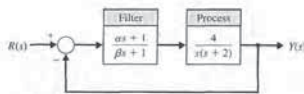


FIGURE P7.18 Filter design.

P7.17 Consider again the vibration absorber discussed in Problems 2.2 and 2.10 as a design problem. Using the root locus method, determine the effect of the parameters M_2 and k_{12} . Determine the specific values of the parameters M_2 and k_{12} so that the mass M_1 does not vibrate when $F(t) = a \sin(\omega_0 t)$. Assume that $M_1 = 1$, $k_1 = 1$, and $b = 1$. Also assume that $k_{12} < 1$ and that the term $k_2 l^2$ may be neglected.

P7.19 In recent years, many automatic control systems for guided vehicles in factories have been installed. One system uses a magnetic tape applied to the floor to guide the vehicle along the desired lane [10, 15]. Using transponder tags on the floor, the automatically guided vehicle can be tasked (for example, to speed up or slow down) at key locations. An example of a guided vehicle in a factory is shown in Figure P7.19(a). We have

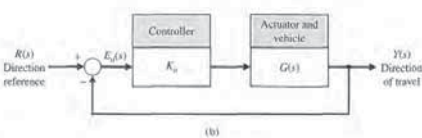
$$G(s) = \frac{s^2 + 4s + 100}{s(s+2)(s+6)}$$

and K_a is the amplifier gain. Sketch a root locus and determine a suitable gain K_a so that the damping ratio of the complex roots is 0.707.

P7.18 A feedback control system is shown in Figure P7.18. The filter $G_f(s)$ is often called a compensator, and the design problem involves selecting the parameters α and β . Using the root locus method, determine the effect of varying the parameters. Select a suitable filter so that the time to settle (to within 2% of the final value) is less than 4 seconds and the damping ratio of the dominant roots is greater than 0.60.



(a)



(b)

FIGURE P7.19 (a) An automatically guided vehicle. (Photo courtesy of the Jervis B. Webb Company) (b) Block diagram.

reexamine this problem after studying Chapter 8.) An interesting case arises when the distributed RC network occurs in a series-to-shunt feedback path of a transistor amplifier. Then the loop transfer function may be written as

$$L(s) = G_c(s)G(s) = \frac{K(s-1)(s+3)^{1/2}}{(s+1)(s+2)^{1/2}}$$

(a) Using the root locus method, determine the locus of roots as K varies from zero to infinity. (b) Calculate the gain at borderline stability and the frequency of oscillation for this gain.

P7.26 A single-loop negative feedback system has a loop transfer function

$$L(s) = G_c(s)G(s) = \frac{K(s+2)^2}{s(s^2+1)(s+8)}$$

(a) Sketch the root locus for $0 \leq K \leq \infty$ to indicate the significant features of the locus. (b) Determine the range of the gain K for which the system is stable. (c) For what value of K in the range $K \geq 0$ do purely imaginary roots exist? What are the values of these roots? (d) Would the use of the dominant roots approximation for an estimate of settling time be justified in this case for a large magnitude of gain ($K > 50$)?

P7.27 A unity negative feedback system has a loop transfer function

$$L(s) = G_c(s)G(s) = \frac{K(s^2 + 0.1)}{s(s^2 + 2)} = \frac{K(s + j0.3162)(s - j0.3162)}{s(s^2 + 1)}$$

Sketch the root locus as a function of K . Carefully calculate where the segments of the locus enter and leave the real axis.

P7.28 To meet current U.S. emissions standards for automobiles, hydrocarbon (HC) and carbon monoxide (CO) emissions are usually controlled by a catalytic converter in the automobile exhaust. Federal standards for nitrogen oxides (NO_x) emissions are met mainly by exhaust-gas recirculation (EGR) techniques. However, as NO_x emissions standards were tightened from the

current limit of 2.0 grams per mile to 1.0 gram per mile, these techniques alone were no longer sufficient.

Although many schemes are under investigation for meeting the emissions standards for all three emissions, one of the most promising employs a three-way catalytic—for HC, CO, and NO_x emissions—in conjunction with a closed-loop engine-control system. The approach is to use a closed-loop engine control, as shown in Figure P7.28 [19, 23]. The exhaust-gas sensor gives an indication of a rich or lean exhaust and compares it to a reference. The difference signal is processed by the controller, and the output of the controller modulates the vacuum level in the carburetor to achieve the best air-fuel ratio for proper operation of the catalytic converter. The loop transfer function is represented by

$$L(s) = \frac{Ks^2 + 12s + 20}{s^3 + 10s^2 + 25s}$$

Calculate the root locus as a function of K . Carefully calculate where the segments of the locus enter and leave the real axis. Determine the roots when $K = 2$. Predict the step response of the system when $K = 2$.

P7.29 A unity feedback control system has a transfer function

$$L(s) = G_c(s)G(s) = \frac{K(s^2 + 10s + 30)}{s^2(s + 10)}$$

We desire the dominant roots to have a damping ratio equal to 0.707. Find the gain K when this condition is satisfied. Show that the complex roots are $s = -3.56 \pm j3.56$ at this gain.

P7.30 An RLC network is shown in Figure P7.30. The nominal values (normalized) of the network elements are $L = C = 1$ and $R = 2.5$. Show that the root sensitivity of the two roots of the input impedance $Z(s)$ to a change in R is different by a factor of 4.

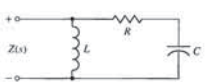


FIGURE P7.30 RLC network.

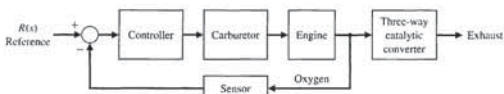


FIGURE P7.28 Auto engine control.

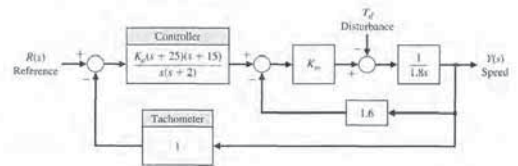


FIGURE P7.12 Speed control.

(a) Find the breakaway point on the real axis and the gain for this point. (b) Find the gain to provide two complex roots nearest the $j\omega$ -axis with a damping ratio of 0.707. (c) Are the two roots of part (b) dominant? (d) Determine the settling time (with a 2% criterion) of the system when the gain of part (b) is used.

P7.14 The loop transfer function of a single-loop negative feedback system is

$$L(s) = G_c(s)G(s) = \frac{K(\tau + 2.5)(s + 3.2)}{s^2(s + 1)(s + 10)(s + 30)}$$

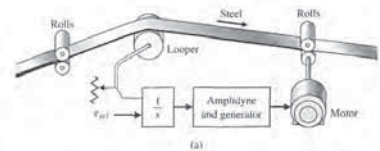
This system is called conditionally stable because it is stable only for a range of the gain K such that $k_1 < K < k_2$. Using the Routh-Hurwitz criteria and the root locus method, determine the range of the gain for which the system is stable. Sketch the root locus for $0 < K < \infty$.

P7.15 Let us again consider the stability and ride of a rider and high performance motorcycle as outlined in Problem P6.13. The dynamics of the motorcycle and rider can be represented by the loop transfer function

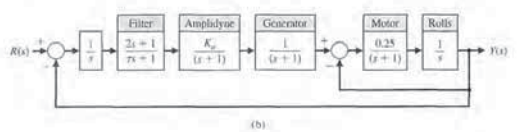
$$G_c(s)G(s) = \frac{K(s^2 + 30s + 625)}{s(s + 20)(s^2 + 20s + 200)(s^2 + 60s + 3400)}$$

Sketch the root locus for the system. Determine the ζ of the dominant roots when $K = 3 \times 10^4$.

P7.16 Control systems for maintaining constant tension on strip steel in a hot strip finishing mill are called "loopers." A typical system is shown in Figure P7.16. The looper is an arm 2 to 3 feet long with a roller on the end; it is raised and pressed against the strip by a motor [18]. The typical speed of the strip passing the looper is 2000 ft/min. A voltage proportional to the looper



(a)



(b)

FIGURE P7.16 Steel mill control system.

P7.20 Determine the root sensitivity for the dominant roots of the design for Problem P7.18 for the gain $K = 4\alpha/\beta$ and the pole $s = -2$.

P7.21 Determine the root sensitivity of the dominant roots of the power system of Problem P7.7. Evaluate the sensitivity for variations of (a) the poles at $s = -4$, and (b) the feedback gain, $1/R$.

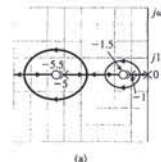
P7.22 Determine the root sensitivity of the dominant roots of Problem P7.1(a) when K is set so that the damping ratio of the unperturbed roots is 0.707. Evaluate and compare the sensitivity as a function of the poles and zeros of $G_c(s)G(s)$.

P7.23 Repeat Problem P7.22 for the loop transfer function $G_c(s)G(s)$ of Problem P7.1(c).

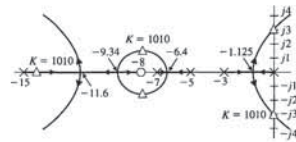
P7.24 For systems of relatively high degree, the form of the root locus can often assume an unexpected pattern.

The root loci of four different feedback systems of third order or higher are shown in Figure P7.24. The open-loop poles and zeros of $KG(s)$ are shown, and the form of the root loci as K varies from zero to infinity is presented. Verify the diagrams of Figure P7.24 by constructing the root locus.

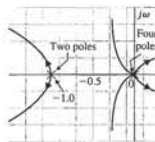
P7.25 Solid-state integrated electronic circuits are composed of distributed R and C elements. Therefore, feedback electronic circuits in integrated circuit form must be investigated by obtaining the transfer function of the distributed RC networks. It has been shown that the slope of the attenuation curve of a distributed RC network is $10n$ dB/decade, where n is the order of the RC filter [13]. This attenuation is in contrast with the normal 20n dB/decade for the lumped parameter circuits. (The concept of the slope of an attenuation curve is considered in Chapter 8. If it is unfamiliar,



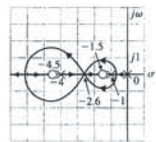
(a)



(b)



(c)



(d)

FIGURE P7.24 Root loci of four systems.

P7.35 A powerful electrohydraulic forklift can be used to lift pallets weighing several tons on top of 35-foot scaffolds at a construction site. The negative unity feedback system has a loop transfer function

$$L(s) = G_c(s)G(s) = \frac{K(s+1)^2}{s(s^2+1)}$$

(a) Sketch the root locus for $K > 0$. (b) Find the gain K when two complex roots have a ζ of 0.707, and calculate all three roots. (c) Find the entry point of the root locus at the real axis. (d) Estimate the expected overshoot to a step input, and compare it with the actual overshoot determined from a computer program.

P7.36 A microrobot with a high-performance manipulator has been designed for testing very small particles, such as simple living cells [6]. The single-loop unity negative feedback system has a loop transfer function

$$L(s) = G_c(s)G(s) = \frac{K(s+1)(s+2)(s+3)}{s^3(s-1)}$$

(a) Sketch the root locus for $K > 0$. (b) Find the gain and roots when the characteristic equation has two imaginary roots. (c) Determine the characteristic roots when $K = 20$ and $K = 100$. (d) For $K = 20$, estimate the percent overshoot to a step input, and compare the estimate to the actual overshoot determined from a computer program.

P7.37 Identify the parameters K , a , and b of the system shown in Figure P7.37. The system is subject to a unit step input, and the output response has an overshoot but ultimately attains the final value of 1. When the closed-loop system is subjected to a ramp input, the output response follows the ramp input with a finite steady-state error. When the gain is doubled to $2K$, the output response to an impulse input is a pure sinusoid with a period of 0.314 second. Determine K , a , and b .

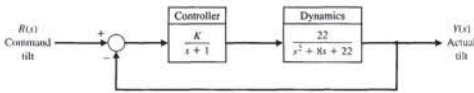


FIGURE P7.39 Tilt control for a high-speed train.

ADVANCED PROBLEMS

AP7.1 The top view of a high-performance jet aircraft is shown in Figure AP7.1(a) [20]. Sketch the root locus and determine the gain K so that the ζ of the complex poles near the $j\omega$ -axis is the maximum achievable.

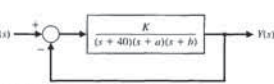


FIGURE P7.37 Feedback system.

P7.38 A unity feedback system has the loop transfer function

$$L(s) = G_c(s)G(s) = \frac{K(s+1)}{s(s-3)}$$

This system is open-loop unstable. (a) Determine the range of K so that the closed-loop system is stable. (b) Sketch the root locus. (c) Determine the roots for $K = 10$. (d) For $K = 10$, predict the percent overshoot for a step input using Figure 5.13. (e) Determine the actual overshoot by plotting the response.

P7.39 High-speed trains for U.S. railroad tracks must traverse twists and turns. In conventional trains, the axes are fixed in steel frames called trucks. The trucks pivot as the train goes into a curve, but the fixed axles stay parallel to each other, even though the front axle tends to go in a different direction from the rear axle [24]. If the train is going fast, it may jump the tracks. One solution uses axes that pivot independently. To counterbalance the strong centrifugal forces in a curve, the train also has a computerized hydraulic system that tilts each car as it rounds a turn. On-board sensors calculate the train's speed and the sharpness of the curve and feed this information to hydraulic pumps under the floor of each car. The pumps tilt the car up to eight degrees, causing it to lean into the curve like a race car on a banked track.

The tilt control system is shown in Figure P7.39. Sketch the root locus, and determine the value of K when the complex roots have maximum damping. Predict the response of this system to a step input $R(s)$.

P7.31 The development of high-speed aircraft and missiles requires information about aerodynamic parameters prevailing at very high speeds. Wind tunnels are used to test these parameters. These wind tunnels are constructed by compressing air to very high pressures and releasing it through a valve to create a wind. Since the air pressure drops as the air escapes it is necessary to open the valve wider to maintain a constant wind speed. Thus, a control system is needed to adjust the valve to maintain a constant wind speed. The loop transfer function for a unity feedback system is

$$L(s) = G_c(s)G(s) = \frac{K(s+4)}{s(s+0.16)(s+p)(s-p)}$$

where $p = 7.3 + j9.7831j$. Sketch the root locus and show the location of the roots for $K = 326$ and $K = 1350$.

P7.32 A mobile robot suitable for nighttime guard duty is available. This guard never sleeps and can tirelessly patrol large warehouses and outdoor yards. The steering control system for the mobile robot has a unity feedback with the loop transfer function

$$L(s) = G_c(s)G(s) = \frac{K(s+1)(s+5)}{s(s+1.5)(s+2)}$$

(a) Find K for all breakaway and entry points on the real axis. (b) Find K when the damping ratio of the complex roots is 0.707. (c) Find the minimum value of the damping ratio for the complex roots and the associated gain K . (d) Find the overshoot and the time to settle (to within 2% of the final value) for a unit step input for the gain K , determined in parts (b) and (c).

P7.33 The Bell-Boeing V-22 Osprey Tiltrotor is both an airplane and a helicopter. Its advantage is the ability to rotate its engines to 90° from a vertical position for takeoffs and landings as shown in Figure P7.33(a), and then to switch the engines to a horizontal position for cruising as an airplane [20]. The altitude control system in the helicopter mode is shown in Figure P7.33(b). (a) Determine the root locus as K varies and determine the range of K for a stable system. (b) For $K = 280$, find the actual $y(t)$ for a unit step input $r(t)$ and the percentage overshoot and settling time (with a 2% criterion). (c) When $K = 280$ and $r(t) = 0$, find $y(t)$ for a unit step disturbance. $T_d(s) = 1/s$. (d) Add a prefilter between $R(s)$ and the summing node so that

$$G_p(s) = \frac{0.5}{s^2 + 1.5s + 0.5}$$

and repeat part (b).

P7.34 The fuel control for an automobile uses a diesel pump that is subject to parameter variations. A unity negative feedback has a loop transfer function

$$G_c(s)G(s) = \frac{K(s-2)}{(s+1)(s+2.5)(s+4)(s+10)}$$

(a) Sketch the root locus as K varies from 0 to 2000. (b) Find the roots for K equal to 400, 500, and 600. (c) Predict how the percent overshoot to a step will vary for the gain K , assuming dominant roots. (d) Find the actual time response for a step input for all three gains and compare the actual overshoot with the predicted overshoot.



(a)

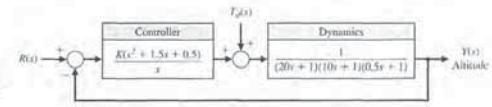


FIGURE P7.33 (a) Osprey Tiltrotor aircraft. (b) Its control system.

AP7.3 A compact disc player for portable use requires a good rejection of disturbances and an accurate position of the optical reader sensor. The position control system uses unity feedback and a loop transfer function

$$L(s) = G_c(s)G(s) = \frac{10}{s(s+1)(s+p)}$$

The parameter p can be chosen by selecting the appropriate DC motor. Sketch the root locus as a function of p . Select p so that the ζ of the complex roots of the characteristic equation is approximately $1/\sqrt{2}$.

AP7.4 A remote manipulator control system has unity feedback and a loop transfer function

$$G_c(s)G(s) = \frac{(s+a)}{s^3 + (1+a)s^2 + (a-1)s + 1 - a}$$

We want the steady-state position error for a step input to be less than or equal to 10% of the magnitude of the input. Sketch the root locus as a function of the parameter a . Determine the range of a required for the desired steady-state error. Locate the roots for the allowable value of a to achieve the required steady-state error, and estimate the step response of the system.

AP7.5 A unity feedback system has a loop transfer function

$$L(s) = G_c(s)G(s) = \frac{K}{s^3 + 10s^2 + 7s - 18}$$

(a) Sketch the root locus and determine K for a stable system with complex roots with ζ equal to $1/\sqrt{2}$. (b) Determine the root sensitivity of the complex roots of part (a). (c) Determine the percent change in K (increase or decrease) so that the roots lie on the $j\omega$ -axis.

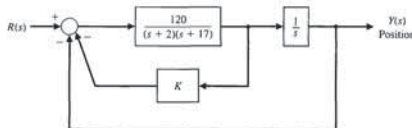


FIGURE AP7.8 A position control system with velocity feedback.

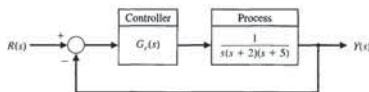


FIGURE AP7.9 A unity feedback control system.

AP7.6 A unity feedback system has a loop transfer function

$$L(s) = G_c(s)G(s) = \frac{K(s^2 + 3s + 6)}{s^3 + 2s^2 + 3s + 1}$$

Sketch the root locus for $K > 0$, and select a value for K that will provide a closed step response with settling time less than 1 second.

AP7.7 A feedback system with positive feedback is shown in Figure AP7.7. The root locus for $K > 0$ must meet the condition

$$KG(s) = 1/\pm k360^\circ$$

$$\text{for } k = 0, 1, 2, \dots$$

Sketch the root locus for $0 < K < \infty$.

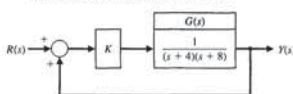


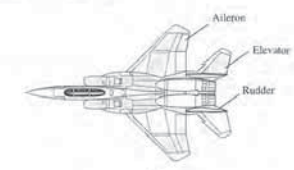
FIGURE AP7.7 A closed-loop system with positive feedback.

AP7.8 A position control system for a DC motor is shown in Figure AP7.8. Obtain the root locus for the velocity feedback constant K , and select K so that all the roots of the characteristic equation are real (two are equal and real). Estimate the step response of the system for the K selected. Compare the estimate with the actual response.

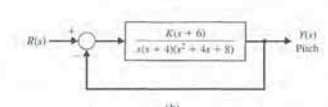
AP7.9 A control system is shown in Figure AP7.9. Sketch the root loci for the following transfer functions $G_c(s)$:

- (a) $G_c(s) = K$
- (b) $G_c(s) = K(s+3)$

Evaluate the roots at this K and predict the response to a step input. Determine the actual response and compare it to the predicted response.



(a)



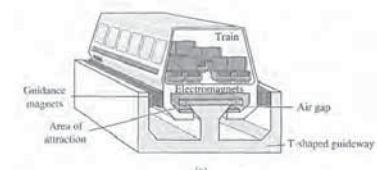
(b)

FIGURE AP7.1 (a) High-performance aircraft. (b) Pitch control system.

AP7.2 A magnetically levitated high-speed train "flies" on an air gap above its rail system, as shown in Figure AP7.2(a) [24]. The air gap control system has a unity feedback system with a loop transfer function

$$G_c(s)G(s) = \frac{K(s+1)(s+3)}{s(s-1)(s+4)(s+8)}$$

The feedback control system is illustrated in Figure AP7.2(b). The goal is to select K so that the response for a unit step input is reasonably damped and the settling time is less than 3 seconds. Sketch the root locus, and select K so that all of the complex roots have a ζ greater than 0.6. Determine the actual response for the selected K and the percent overshoot.



(a)

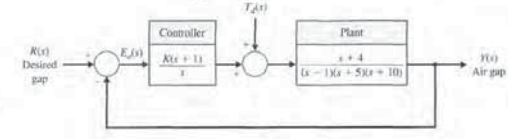


FIGURE AP7.2 (a) Magnetically levitated high-speed train. (b) Feedback control system.

AP7.14 A unity feedback control system shown in Figure AP7.14 has the process

$$G(s) = \frac{10}{s(s+10)(s+7.5)}$$

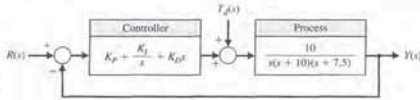


FIGURE AP7.14 Unity feedback loop with PID controller.

Design a PID controller using Ziegler-Nichols method. Determine the unit step response and the unit disturbance response. What is the maximum percent overshoot and settling time for the unit step input?

DESIGN PROBLEMS

CDP7.1 The drive motor and slide system uses the output of a tachometer mounted on the shaft of the motor as shown in Figure CDP4.1 (switch-closed option). The output voltage of the tachometer is $v_T = K_t \theta$. Use the velocity feedback with the adjustable gain K_1 . Select the best values for the gain K_1 and the amplifier gain K_2 so that the transient response to a step input has an overshoot less than 5% and a settling time (to within 2% of the final value) less than 300 ms.

DP7.1 A high-performance aircraft, shown in Figure DP7.1(a), uses the ailerons, rudder, and elevator to steer through a three-dimensional flight path [20]. The pitch rate control system for a fighter aircraft at 10,000 m and Mach 0.9 can be represented by the system in Figure DP7.1(b), where

$$G(s) = \frac{-18(s + 0.015)(s + 0.45)}{(s^2 + 1.2s + 12)(s^2 + 0.01s + 0.0025)}$$

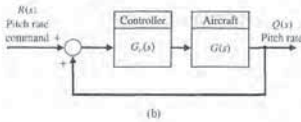


FIGURE DP7.1 (a) High-performance aircraft. (b) Pitch rate control system.

(a) Sketch the root locus when the controller is a gain, so that $G_c(s) = K$, and determine K when ζ for the roots with $\omega_n > 2$ is larger than 0.15 (seek a maximum ζ). (b) Plot the response $q(t)$ for a step input $r(t)$ with K as in (a). (c) A designer suggests an anticipatory controller with $G_c(s) = K_1 + K_2s = K(s+2)$. Sketch the root locus for this system as K varies and determine a K so that the ζ of all the closed-loop roots is > 0.8 . (d) Plot the response $q(t)$ for a step input $r(t)$ with K as in (c).

DP7.2 A large helicopter uses two tandem rotors rotating in opposite directions, as shown in Figure P7.33(a). The controller adjusts the tilt angle of the main rotor and thus the forward motion as shown in Figure DP7.2. The helicopter dynamics are represented by

$$G(s) = \frac{10}{s^2 + 4.5s + 9}$$

(c) $G_c(s) = \frac{K(s+1)}{s+20}$
 (d) $G_c(s) = \frac{K(s+1)(s+4)}{s+10}$

AP7.10 A feedback system is shown in Figure AP7.10. Sketch the root locus as K varies when $K \geq 0$. Determine a value for K that will provide a step response with an overshoot less than 5% and a settling time (with a 2% criterion) less than 2.5 seconds.

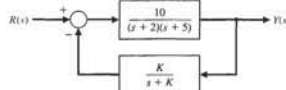


FIGURE AP7.10 A nonunity feedback control system.

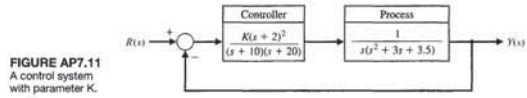


FIGURE AP7.11 A control system with parameter K.

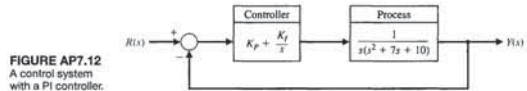


FIGURE AP7.12 A control system with a PI controller.

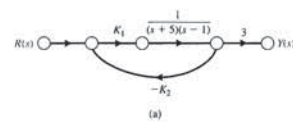


FIGURE AP7.13 An unstable plant with two parameters K_1 and K_2 .

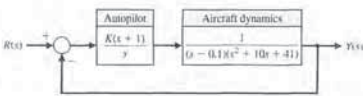
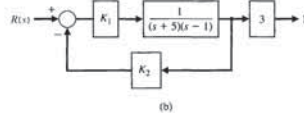


FIGURE DP7.5 High-performance jet aircraft.

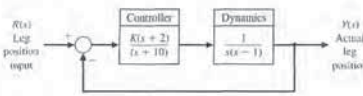


FIGURE DP7.6 Automatic control of walking motion.

DP7.6 A system to aid and control the walk of a partially disabled person could use automatic control of the walking motion [25]. One model of a system that is open-loop unstable is shown in Figure DP7.6. Using the root locus, select K for the maximum achievable ζ of the complex roots. Predict the step response of the system, and compare it with the actual step response.

DP7.7 A mobile robot using a vision system as the measurement device is shown in Figure DP7.7(a) [36]. The control system is shown in Figure DP7.7(b) where

$$G(s) = \frac{1}{(s+1)(0.5s+1)}$$

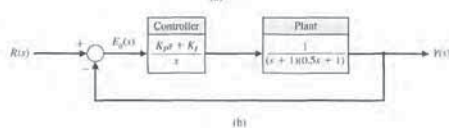
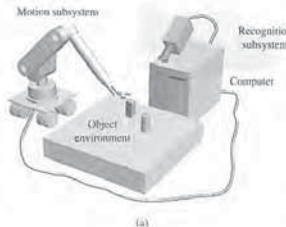


FIGURE DP7.7 (a) A robot and vision system. (b) Feedback control system.

and $G_c(s)$ is selected as a PI controller so that the steady-state error for a step input is equal to zero. We then have

$$G_c(s) = K_p + \frac{K_f}{s}$$

Design the PI controller so that (a) the percent overshoot for a step input is $P.O. = 5\%$; (b) the settling time (with a 2% criterion) is $T_s = 6$ seconds; (c) the system velocity error constant $K_v > 0.9$; and (d) the peak time, T_p , for a step input is minimized.

DP7.8 Most commercial op-amps are designed to be unity-gain stable [26]. That is, they are stable when

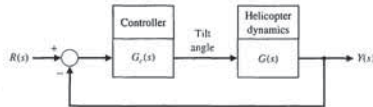


FIGURE DP7.2 Two-rotor helicopter velocity control.

and the controller is selected as

$$G_c(s) = K_1 + \frac{K_2}{s} = \frac{K(s+1)}{s}$$

(a) Sketch the root locus of the system and determine K when ζ of the complex roots is equal to 0.6. (b) Plot the response of the system to a step input $r(t)$ and find the settling time (with a 2% criterion) and overshoot for the system of part (a). What is the steady-state error for a step input? (c) Repeat parts (a) and (b) when the ζ of the complex roots is 0.41. Compare the results with those obtained in parts (a) and (b).

DP7.3 The vehicle Rover has been designed for maneuvering at 0.25 mph over Martian terrain. Because Mars is 189 million miles from Earth and it would take up to 40 minutes each way to communicate with Earth [22, 27], Rover must act independently and reliably. Resembling a cross between a small flatbed truck and an elevated jeep, Rover is constructed of three articulated sections, each with its own two independent, axle-bearing, one-meter conical wheels. A pair of sampling arms—one for chipping and drilling, the other for manipulating fine objects—extend from its front end like pincers. The control of the arms can

be represented by the system shown in Figure DP7.3. (a) Sketch the root locus for K and identify the roots for $K = 4.1$ and 41. (b) Determine the gain K that results in an overshoot to a step of approximately 1%. (c) Determine the gain that minimizes the settling time (with a 2% criterion) while maintaining an overshoot of less than 1%.

DP7.4 A welding torch is remotely controlled to achieve high accuracy while operating in changing and hazardous environments [21]. A model of the welding arm position control is shown in Figure DP7.4, with the disturbance representing the environmental changes. (a) With $T_d(s) = 0$, select K_1 and K to provide high-quality performance of the position control system. Select a set of performance criteria, and examine the results of your design. (b) For the system in part (a), let $R(s) = 0$ and determine the effect of a unit step $T_d(s) = 1/s$ by obtaining $y(t)$.

DP7.5 A high-performance jet aircraft with an autopilot control system has a unity feedback and control system, as shown in Figure DP7.5. Sketch the root locus and select a gain K that leads to dominant poles. With this gain K , predict the step response of the system, and compare it to the predicted response.

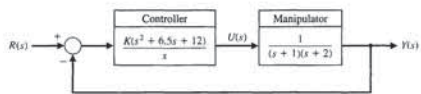


FIGURE DP7.3 Mars vehicle robot control system.

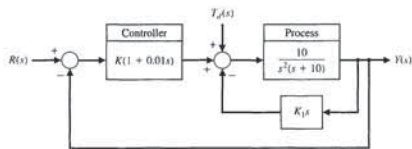


FIGURE DP7.4 Remotely controlled welder.

an m-file using root locus methods find the values of K_D/J and K_P/J so that the settling time T_s is less than or equal to 4 seconds, and the peak overshoot PO is less than or equal to 10% for a unit step input. Use a 2% criterion in determining the settling time.

CP7.9 Consider the feedback control system in Figure CP7.9. Develop an m-file to plot the root locus for $0 < K < \infty$. Find the value of K resulting in a damping ratio of the closed-loop poles equal to 0.707.

CP7.10 Consider the system represented in state variable form

$$\dot{\mathbf{x}} = \mathbf{A}\mathbf{x} + \mathbf{B}u$$

$$y = \mathbf{C}\mathbf{x} + \mathbf{D}u$$

where

$$\mathbf{A} = \begin{bmatrix} 0 & 1 & 0 \\ 0 & 0 & 1 \\ -1 & -5 & -2-k \end{bmatrix}, \mathbf{B} = \begin{bmatrix} 1 \\ 0 \\ 4 \end{bmatrix}$$

$$\mathbf{C} = [1 \quad -9 \quad 12], \text{ and } \mathbf{D} = [0].$$

(a) Determine the characteristic equation. (b) Using the Routh-Hurwitz criterion, determine the values of k for which the system is stable. (c) Develop an m-file to plot the root locus and compare the results to those obtained in (b).

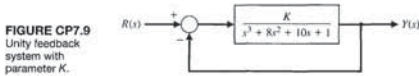


FIGURE CP7.9 Unity feedback system with parameter K .

ANSWERS TO SKILLS CHECK

- True or False: (1) True; (2) True; (3) False; (4) True; (5) True
 Multiple Choice: (6) b; (7) c; (8) a; (9) c; (10) a; (11) b; (12) c; (13) a; (14) c; (15) b
- Word Match (in order, top to bottom): k, f, a, d, i, h, c, b, e, g, j

TERMS AND CONCEPTS

- Angle of departure** The angle at which a locus leaves a complex pole in the s -plane.
- Angle of the asymptotes** The angle ϕ_A that the asymptote makes with respect to the real axis.
- Asymptote** The path the root locus follows as the parameter becomes very large and approaches infinity. The number of asymptotes is equal to the number of poles minus the number of zeros.
- Asymptote centroid** The center σ_A of the linear asymptotes.
- Breakaway point** The point on the real axis where the locus departs from the real axis of the s -plane.
- Dominant roots** The roots of the characteristic equation that represent or dominate the closed-loop transient response.
- Locus** A path or trajectory that is traced out as a parameter is changed.
- Logarithmic sensitivity** A measure of the sensitivity of the system performance to specific parameter changes, given by $S_K^T(s) = -\frac{\partial T(s)/T(s)}{\partial K/K}$, where $T(s)$ is the system transfer function and K is the parameter of interest.
- Manual PID tuning methods** The process of determining the PID controller gains by trial-and-error with minimal analytic analysis.
- Negative gain root locus** The root locus for negative values of the parameter of interest, where $-\infty < K \leq 0$.
- Number of separate loci** Equal to the number of poles of the transfer function, assuming that the number of poles is greater than or equal to the number of zeros of the transfer function.
- Parameter design** A method of selecting one or two parameters using the root locus method.

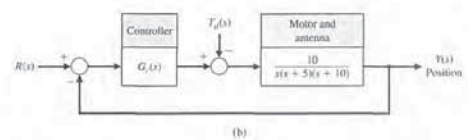


FIGURE CP7.6 Antenna position control.

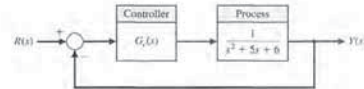


FIGURE CP7.7 A single-loop feedback control system with controller $G_c(s)$.

- determine the value of K so that the design specifications are satisfied.
 (b) Repeat part (a) for the integral controller.
 (c) Repeat part (a) for the PI controller.
 (d) Co-plot the unit step responses for the closed-loop systems with each controller designed in parts (a)–(c).
- (e) Compare and contrast the three controllers obtained in parts (a)–(c), concentrating on the steady-state errors and transient performance.

CP7.8 Consider the spacecraft single-axis attitude control system shown in Figure CP7.8. The controller is known as a proportional-derivative (PD) controller. Suppose that we require the ratio of $K_P/K_D = 5$. Then, develop

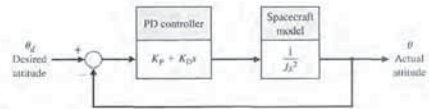


FIGURE CP7.8 A spacecraft attitude control system with a proportional-derivative controller.

CHAPTER 8

Frequency Response Methods

8.1	Introduction	554
8.2	Frequency Response Plots	556
8.3	Frequency Response Measurements	557
8.4	Performance Specifications in the Frequency Domain	579
8.5	Log Magnitude and Phase Diagrams	582
8.6	Design Examples	583
8.7	Frequency Response Methods Using Control Design Software	596
8.8	Sequential Design Example: Disk Drive Read System	602
8.9	Summary	603

P R E V I E W

In previous chapters, we examined the use of test signals such as a step and a ramp signal. In this chapter, we consider the steady-state response of a system to a sinusoidal input test signal. We will see that the response of a linear constant coefficient system to a sinusoidal input signal is an output sinusoidal signal at the same frequency as the input. However, the magnitude and phase of the output signal differ from those of the input sinusoidal signal, and the amount of difference is a function of the input frequency. Thus, we will be investigating the steady-state response of the system to a sinusoidal input as the frequency varies.

We will examine the transfer function $G(s)$ when $s = j\omega$ and develop methods for graphically displaying the complex number $G(j\omega)$ as ω varies. The Bode plot is one of the most powerful graphical tools for analyzing and designing control systems, and we will cover that subject in this chapter. We will also consider polar plots and log magnitude and phase diagrams. We will develop several time-domain performance measures in terms of the frequency response of the system, as well as introduce the concept of system bandwidth. The chapter concludes with a frequency response analysis of the Sequential Design Example: Disk Drive Read System.

DESIRED OUTCOMES

Upon completion of Chapter 8, students should:

- Understand the powerful concept of frequency response and its role in control system design.
- Know how to sketch a Bode plot and also how to obtain a computer-generated Bode plot.
- Be familiar with log magnitude and phase diagrams.
- Understand performance specifications in the frequency domain and relative stability based on gain and phase margins.
- Be capable of designing a controller to meet desired specifications using frequency response methods.

PD controller A widely used controller used in industry of the form $G_c(s) = K_P + \frac{K_I}{s} + K_D s$, where K_P is the proportional gain, K_I is the integral gain, and K_D is the derivative gain.

PD tuning The process of determining the PID controller gains.

Proportional plus derivative (PD) controller A two-term controller of the form $G_c(s) = K_P + K_D s$, where K_P is the proportional gain and K_D is the derivative gain.

Proportional plus integral (PI) controller A two-term controller of the form $G_c(s) = K_P + \frac{K_I}{s}$, where K_P is the proportional gain and K_I is the integral gain.

Quarter amplitude decay The amplitude of the closed-loop response is reduced approximately to one-fourth of the maximum value in one oscillatory period.

Reaction curve The response obtained by taking the controller off-line and introducing a step input. The underlying process is assumed to be a first-order system with a transport delay.

Root contours The family of loci that depict the effect of varying two parameters on the roots of the characteristic equation.

Root locus The locus or path of the roots traced out on the s -plane as a parameter is changed.

Root locus method The method for determining the locus of roots of the characteristic equation $1 + KP(s) = 0$ as K varies from 0 to infinity.

Root locus segments on the real axis The root locus lying in a section of the real axis to the left of an odd number of poles and zeros.

Root sensitivity The sensitivity of the roots as a parameter changes from its normal value. The root sensitivity is given by $S_K^r = \frac{\partial r}{\partial K/K}$, the incremental change in the root divided by the proportional change of the parameter.

Ultimate gain The PD controller proportional gain, K_P , on the border of instability when $K_D = 0$ and $K_I = 0$.

Ultimate period The period of the sustained oscillations when K_P is the ultimate gain and $K_D = 0$ and $K_I = 0$.

Ziegler-Nichols PID tuning method The process of determining the PID controller gains using one of several analytic methods based on open-loop and closed-loop responses to step inputs.

Thus, the steady-state output signal depends only on the magnitude and phase of $T(j\omega)$ at a specific frequency ω . Notice that the steady-state response, as described in Equation (8.1), is true only for stable systems, $T(s)$.

One advantage of the frequency response method is the ready availability of sinusoid test signals for various ranges of frequencies and amplitudes. Thus, the experimental determination of the system's frequency response is easily accomplished; it is the most reliable and uncomplicated method for the experimental analysis of a system. Often, as we shall find in Section 8.4, the unknown transfer function of a system can be deduced from the experimentally determined frequency response of a system [1, 2]. Furthermore, the design of a system in the frequency domain provides the designer with control of the bandwidth of a system, as well as some measure of the response of the system to undesired noise and disturbances.

A second advantage of the frequency response method is that the transfer function describing the sinusoidal steady-state behavior of a system can be obtained by replacing s with $j\omega$ in the system transfer function $T(s)$. The transfer function representing the sinusoidal steady-state behavior of a system is then a function of the complex variable $j\omega$ and is itself a complex function $T(j\omega)$ that possesses a magnitude and phase angle. The magnitude and phase angle of $T(j\omega)$ are readily represented by graphical plots that provide significant insight into the analysis and design of control systems.

The basic disadvantage of the frequency response method for analysis and design is the indirect link between the frequency and the time domain. Direct correlations between the frequency response and the corresponding transient response characteristics are somewhat tenuous, and in practice the frequency response characteristic is adjusted by using various design criteria that will normally result in a satisfactory transient response.

The Laplace transform pair was given in Section 2.4; it is written as

$$F(s) = \mathcal{L}\{f(t)\} = \int_0^{\infty} f(t)e^{-st} dt \quad (8.2)$$

and

$$f(t) = \mathcal{L}^{-1}\{F(s)\} = \frac{1}{2\pi j} \int_{\sigma-j\infty}^{\sigma+j\infty} F(s)e^{st} ds, \quad (8.3)$$

where the complex variable $s = \sigma + j\omega$. Similarly, the Fourier transform pair is written as

$$F(\omega) = \mathcal{F}\{f(t)\} = \int_{-\infty}^{\infty} f(t)e^{-j\omega t} dt \quad (8.4)$$

and

$$f(t) = \mathcal{F}^{-1}\{F(\omega)\} = \frac{1}{2\pi} \int_{-\infty}^{\infty} F(\omega)e^{j\omega t} d\omega. \quad (8.5)$$

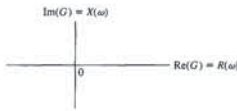


FIGURE 8.1 The polar plane.



See the MCS website for a review of complex numbers.

Alternatively, the transfer function can be represented by a magnitude $|G(j\omega)|$ and a phase $\phi(j\omega)$ as

$$G(j\omega) = |G(j\omega)|e^{j\phi(\omega)} = |G(j\omega)|\angle\phi(\omega), \quad (8.9)$$

where

$$\phi(\omega) = \tan^{-1} \frac{X(\omega)}{R(\omega)} \quad \text{and} \quad |G(j\omega)|^2 = [R(\omega)]^2 + [X(\omega)]^2.$$

The graphical representation of the frequency response of the system $G(j\omega)$ can utilize either Equation (8.8) or Equation (8.9). The polar plot representation of the frequency response is obtained by using Equation (8.8). The coordinates of the polar plot are the real and imaginary parts of $G(j\omega)$, as shown in Figure 8.1. An example of a polar plot will illustrate this approach.

EXAMPLE 8.1 Frequency response of an RC filter

A simple RC filter is shown in Figure 8.2. The transfer function of this filter is

$$G(s) = \frac{V_2(s)}{V_1(s)} = \frac{1}{RCs + 1}, \quad (8.10)$$

and the sinusoidal steady-state transfer function is

$$G(j\omega) = \frac{1}{j\omega(RC) + 1} = \frac{1}{j(\omega/\omega_1) + 1}, \quad (8.11)$$

where

$$\omega_1 = \frac{1}{RC}.$$

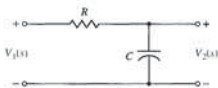


FIGURE 8.2 An RC filter.

8.1 INTRODUCTION

In preceding chapters, the response and performance of a system have been described in terms of the complex frequency variable s and the location of the poles and zeros on the s -plane. A very practical and important alternative approach to the analysis and design of a system is the frequency response method.

The frequency response of a system is defined as the steady-state response of the system to a sinusoidal input signal. The sinusoid is a unique input signal, and the resulting output signal for a linear system, as well as signals throughout the system, is sinusoidal in the steady state; it differs from the input waveform only in amplitude and phase angle.

For example, consider the system $Y(s) = T(s)R(s)$ with $r(t) = A \sin \omega t$. We have

$$R(s) = \frac{A\omega}{s^2 + \omega^2}$$

and

$$T(s) = \frac{m(s)}{q(s)} = \frac{m(s)}{\prod_{i=1}^n (s + p_i)},$$

where $-p_i$ are assumed to be distinct poles. Then, in partial fraction form, we have

$$Y(s) = \frac{k_1}{s + p_1} + \dots + \frac{k_n}{s + p_n} + \frac{\alpha s + \beta}{s^2 + \omega^2}.$$

Taking the inverse Laplace transform yields

$$y(t) = k_1 e^{-p_1 t} + \dots + k_n e^{-p_n t} + \mathcal{L}^{-1} \left\{ \frac{\alpha s + \beta}{s^2 + \omega^2} \right\},$$

where α and β are constants which are problem dependent. If the system is stable, then all p_i have positive real parts and

$$\lim_{t \rightarrow \infty} y(t) = \lim_{t \rightarrow \infty} \mathcal{L}^{-1} \left\{ \frac{\alpha s + \beta}{s^2 + \omega^2} \right\},$$

since each exponential term $k_i e^{-p_i t}$ decays to zero as $t \rightarrow \infty$.

In the limit for $y(t)$, it can be shown, for $t \rightarrow \infty$ (the steady state),

$$\begin{aligned} y(t) &= \mathcal{L}^{-1} \left[\frac{\alpha s + \beta}{s^2 + \omega^2} \right] \\ &= \frac{1}{\omega} A \omega T(j\omega) \sin(\omega t + \phi) \\ &= A |T(j\omega)| \sin(\omega t + \phi), \end{aligned} \quad (8.1)$$

where $\phi = \angle T(j\omega)$.

The Fourier transform exists for $f(t)$ when

$$\int_{-\infty}^{\infty} |f(t)| dt < \infty.$$

The Fourier and Laplace transforms are closely related, as we can see by examining Equations (8.2) and (8.4). When the function $f(t)$ is defined only for $t \geq 0$, as is often the case, the lower limits on the integrals are the same. Then we note that the two equations differ only in the complex variable. Thus, if the Laplace transform of a function $f_1(t)$ is known to be $F_1(s)$, we can obtain the Fourier transform of this same time function by setting $s = j\omega$ in $F_1(s)$ [3].

Again we might ask, Since the Fourier and Laplace transforms are so closely related, why can't we always use the Laplace transform? Why use the Fourier transform at all? The Laplace transform permits us to investigate the s -plane location of the poles and zeros of a transfer function $T(s)$, as in Chapter 7. However, the frequency response method allows us to consider the transfer function $T(j\omega)$ and to concern ourselves with the amplitude and phase characteristics of the system. This ability to investigate and represent the character of a system by amplitude, phase equations, and curves is an advantage for the analysis and design of control systems.

If we consider the frequency response of the closed-loop system, we might have an input $r(t)$ that has a Fourier transform in the frequency domain as follows:

$$R(j\omega) = \int_{-\infty}^{\infty} r(t)e^{-j\omega t} dt.$$

Then the output frequency response of a single-loop control system can be obtained by substituting $s = j\omega$ in the closed-loop system relationship, $Y(s) = T(s)R(s)$, so that we have

$$Y(j\omega) = T(j\omega)R(j\omega) = \frac{G(j\omega)}{1 + G(j\omega)H(j\omega)} R(j\omega). \quad (8.6)$$

Using the inverse Fourier transform, the output transient response would be

$$y(t) = \mathcal{F}^{-1}\{Y(j\omega)\} = \frac{1}{2\pi} \int_{-\infty}^{\infty} Y(j\omega)e^{j\omega t} d\omega. \quad (8.7)$$

However, it is usually quite difficult to evaluate this inverse transform integral for all but the simplest systems, and a graphical integration may be used. Alternatively, as we will note in succeeding sections, several measures of the transient response can be related to the frequency characteristics and utilized for design purposes.

8.2 FREQUENCY RESPONSE PLOTS

The transfer function of a system $G(s)$ can be described in the frequency domain by the relation

$$G(j\omega) = G(s)|_{s=j\omega} = R(\omega) + jX(\omega), \quad (8.8)$$

where

$$R(\omega) = \text{Re}\{G(j\omega)\} \quad \text{and} \quad X(\omega) = \text{Im}\{G(j\omega)\}.$$

Table 8.1

ω	0	$1/2\tau$	$1/\tau$	∞
$ G(j\omega) $	∞	$4K\tau/\sqrt{5}$	$K\tau/\sqrt{2}$	0
$\phi(\omega)$	-90°	-117°	-135°	-180°

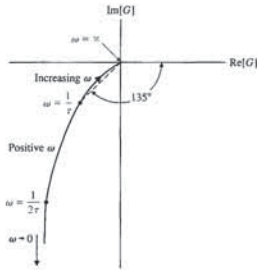


FIGURE 8.4 Polar plot for $G(j\omega) = K/(j\omega(j\omega\tau + 1))$. Note that $\omega = \infty$ is at the origin.

Then the magnitude and phase angle are written as

$$|G(j\omega)| = \frac{K}{(\omega^2 + \omega^2\tau^2)^{1/2}} \quad \text{and} \quad \phi(\omega) = -\tan^{-1} \frac{1}{\omega\tau}$$

The phase angle and the magnitude are readily calculated at the frequencies $\omega = 0$, $\omega = 1/\tau$, and $\omega = \infty$. The values of $|G(j\omega)|$ and $\phi(\omega)$ are given in Table 8.1, and the polar plot of $G(j\omega)$ is shown in Figure 8.4.

An alternative solution uses the real and imaginary parts of $G(j\omega)$ as

$$G(j\omega) = \frac{K}{j\omega - \omega^2\tau} = \frac{K(-j\omega - \omega^2\tau)}{\omega^2 + \omega^4\tau^2} = R(\omega) + jX(\omega), \quad (8.15)$$

where $R(\omega) = -K\omega^2\tau/M(\omega)$ and $X(\omega) = -\omega K/M(\omega)$, and where $M(\omega) = \omega^2 + \omega^4\tau^2$. Then when $\omega = \infty$, we have $R(\omega) = 0$ and $X(\omega) = 0$. When $\omega = 0$, we have $R(\omega) = -K\tau$ and $X(\omega) = -\infty$. When $\omega = 1/\tau$, we have $R(\omega) = -K\tau/2$ and $X(\omega) = -K\tau/2$, as shown in Figure 8.4.

Another method of obtaining the polar plot is to evaluate the vector $G(j\omega)$ graphically at specific frequencies, ω , along the $s = j\omega$ axis on the s -plane. We consider

$$G(s) = \frac{K/\tau}{s(s + 1/\tau)}$$

with the two poles shown on the s -plane in Figure 8.5.

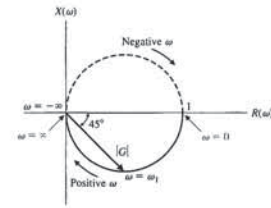


FIGURE 8.3 Polar plot for RC filter.

Then the polar plot is obtained from the relation

$$\begin{aligned} G(j\omega) &= R(\omega) + jX(\omega) \\ &= \frac{1 - j(\omega/\omega_1)}{(\omega/\omega_1)^2 + 1} \\ &= \frac{1}{1 + (\omega/\omega_1)^2} - \frac{j(\omega/\omega_1)}{1 + (\omega/\omega_1)^2}. \end{aligned} \quad (8.12)$$

The first step is to determine $R(\omega)$ and $X(\omega)$ at the two frequencies, $\omega = 0$ and $\omega = \infty$. At $\omega = 0$, we have $R(\omega) = 1$ and $X(\omega) = 0$. At $\omega = \infty$, we have $R(\omega) = 0$ and $X(\omega) = 0$. These two points are shown in Figure 8.3. The locus of the real and imaginary parts is also shown in Figure 8.3 and is easily shown to be a circle with the center at $(\frac{1}{2}, 0)$. When $\omega = \omega_1$, the real and imaginary parts are equal in magnitude, and the angle $\phi(\omega) = -45^\circ$. The polar plot can also be readily obtained from Equation (8.9) as

$$G(j\omega) = |G(j\omega)|/\phi(\omega), \quad (8.13)$$

where

$$|G(j\omega)| = \frac{1}{[1 + (\omega/\omega_1)^2]^{1/2}} \quad \text{and} \quad \phi(\omega) = -\tan^{-1}(\omega/\omega_1).$$

Hence, when $\omega = \omega_1$, the magnitude is $|G(j\omega_1)| = 1/\sqrt{2}$ and the phase $\phi(\omega_1) = -45^\circ$. Also, when ω approaches ∞ , we have $|G(j\omega)| \rightarrow 0$ and $\phi(\omega) = -90^\circ$. Similarly, when $\omega = 0$, we have $|G(j\omega)| = 1$ and $\phi(\omega) = 0$.

EXAMPLE 8.2 Polar plot of a transfer function

The polar plot of a transfer function is useful for investigating system stability and will be utilized in Chapter 9. Therefore, it is worthwhile to complete another example at this point. Consider a transfer function

$$G(s)_{s=j\omega} = G(j\omega) = \frac{K}{j\omega(j\omega\tau + 1)} = \frac{K}{j\omega - \omega^2\tau}. \quad (8.14)$$

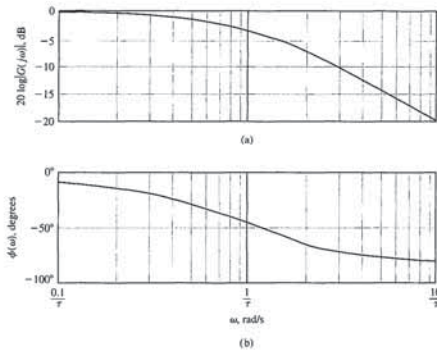


FIGURE 8.6 Bode diagram for $G(j\omega) = 1/(j\omega\tau + 1)$: (a) magnitude plot and (b) phase plot.

where the units are **decibels (dB)**. A decibel conversion table is given on the MCS website. The logarithmic gain in dB and the angle $\phi(\omega)$ can be plotted versus the frequency ω by utilizing several different arrangements. For a Bode diagram, the plot of logarithmic gain in dB versus ω is normally plotted on one set of axes, and the phase $\phi(\omega)$ versus ω on another set of axes, as shown in Figure 8.6. For example, the Bode diagram of the transfer function of Example 8.1 can be readily obtained, as we will find in the following example.

EXAMPLE 8.3 Bode diagram of an RC filter

The transfer function of Example 8.1 is

$$G(j\omega) = \frac{1}{j\omega(RC) + 1} = \frac{1}{j\omega\tau + 1}, \quad (8.18)$$

where

$$\tau = RC,$$

the time constant of the network. The logarithmic gain is

$$20 \log|G(j\omega)| = 20 \log \left(\frac{1}{1 + (\omega\tau)^2} \right)^{1/2} = -10 \log(1 + (\omega\tau)^2). \quad (8.19)$$

For small frequencies—that is, $\omega \ll 1/\tau$ —the logarithmic gain is

$$20 \log|G(j\omega)| = -10 \log(1) = 0 \text{ dB}, \quad \omega \ll 1/\tau. \quad (8.20)$$

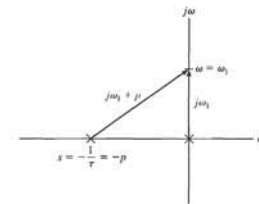


FIGURE 8.5 Two vectors on the s -plane to evaluate $G(j\omega_1)$.

When $s = j\omega$, we have

$$G(j\omega) = \frac{K/\tau}{j\omega(j\omega + p)},$$

where $p = 1/\tau$. The magnitude and phase of $G(j\omega)$ can be evaluated at a specific frequency, ω_1 , on the $j\omega$ -axis, as shown in Figure 8.5. The magnitude and the phase are, respectively,

$$|G(j\omega_1)| = \frac{K/\tau}{|j\omega_1||j\omega_1 + p|}$$

and

$$\phi(\omega) = -\angle(j\omega_1) - \angle(j\omega_1 + p) = -90^\circ - \tan^{-1}(\omega_1/p). \blacksquare$$

There are several possibilities for coordinates of a graph portraying the frequency response of a system. As we have seen, we may use a polar plot to represent the frequency response (Equation 8.8) of a system. However, the limitations of polar plots are readily apparent. The addition of poles or zeros to an existing system requires the recalculation of the frequency response, as outlined in Examples 8.1 and 8.2. (See Table 8.1.) Furthermore, calculating the frequency response in this manner is tedious and does not indicate the effect of the individual poles or zeros.

The introduction of **logarithmic plots**, often called **Bode plots**, simplifies the determination of the graphical portrayal of the frequency response. The logarithmic plots are called Bode plots in honor of H. W. Bode, who used them extensively in his studies of feedback amplifiers [4, 5]. The **transfer function in the frequency domain** is

$$G(j\omega) = |G(j\omega)|e^{j\phi(\omega)}. \quad (8.16)$$

The logarithm of the magnitude is normally expressed in terms of the logarithm to the base 10, so we use

$$\boxed{\text{Logarithmic gain} = 20 \log_{10}|G(j\omega)|}. \quad (8.17)$$

The frequency interval $\omega_2 = 2\omega_1$ is often used and is called an **octave** of frequencies. The difference between the logarithmic gains for $\omega \gg 1/\tau$, for an octave, is

$$20 \log |G(j\omega_1)| - 20 \log |G(j\omega_2)| = -20 \log \frac{\omega_1 \tau}{\omega_2 \tau} = -20 \log \frac{1}{2} = 6.02 \text{ dB.} \quad (8.25)$$

Therefore, the slope of the asymptotic line is -6 dB/octave .

The primary advantage of the logarithmic plot is the conversion of multiplicative factors, such as $(j\omega\tau + 1)$, into additive factors, $20 \log |j\omega\tau + 1|$, by virtue of the definition of logarithmic gain. This can be readily ascertained by considering the generalized transfer function

$$G(j\omega) = \frac{K_b \prod_{i=1}^Q (1 + j\omega\tau_i)}{(j\omega)^N \prod_{m=1}^M (1 + j\omega\tau_m) \prod_{k=1}^R [(1 + 2\zeta_k/\omega_{nk})j\omega + (j\omega/\omega_{nk})^2]} \quad (8.26)$$

This transfer function includes Q zeros, N poles at the origin, M poles on the real axis, and R pairs of complex conjugate poles. Obtaining the polar plot of such a function would be a formidable task indeed. However, the logarithmic magnitude of $G(j\omega)$ is

$$20 \log |G(j\omega)| = 20 \log K_b + 20 \sum_{i=1}^Q \log |1 + j\omega\tau_i| - 20 \log |(j\omega)^N| - 20 \sum_{m=1}^M \log |1 + j\omega\tau_m| - 20 \sum_{k=1}^R \log \left| 1 + \frac{2\zeta_k}{\omega_{nk}} j\omega + \left(\frac{j\omega}{\omega_{nk}}\right)^2 \right| \quad (8.27)$$

and the Bode diagram can be obtained by adding the plot due to each individual factor. Furthermore, the separate phase angle plot is obtained as

$$\phi(\omega) = + \sum_{i=1}^Q \tan^{-1}(\omega\tau_i) - N(90^\circ) - \sum_{m=1}^M \tan^{-1}(\omega\tau_m) - \sum_{k=1}^R \tan^{-1} \frac{2\zeta_k \omega_{nk} \omega}{\omega_{nk}^2 - \omega^2} \quad (8.28)$$

which is simply the summation of the phase angles due to each individual factor of the transfer function.

Therefore, the four different kinds of factors that may occur in a transfer function are as follows:

1. Constant gain K_b
2. Poles (or zeros) at the origin $(j\omega)^N$
3. Poles (or zeros) on the real axis $(j\omega\tau + 1)$
4. Complex conjugate poles (or zeros) $[1 + (2\zeta/\omega_n)j\omega + (j\omega/\omega_n)^2]$

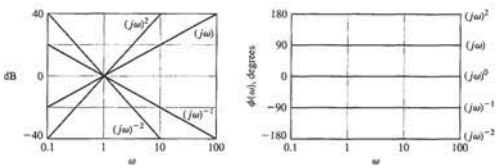


FIGURE 8.8 Bode diagram for $(j\omega)^N$.

$$20 \log \left| \frac{1}{1 + j\omega\tau} \right| = -10 \log |1 + \omega^2\tau^2| \quad (8.32)$$

The asymptotic curve for $\omega \ll 1/\tau$ is $20 \log 1 = 0 \text{ dB}$, and the asymptotic curve for $\omega \gg 1/\tau$ is $-20 \log(\omega\tau)$, which has a slope of -20 dB/decade . The intersection of the two asymptotes occurs when

$$20 \log 1 = 0 \text{ dB} = -20 \log(\omega\tau),$$

or when $\omega = 1/\tau$, the **break frequency**. The actual logarithmic gain when $\omega = 1/\tau$ is -3 dB for this factor. The phase angle is $\phi(\omega) = -\tan^{-1}(\omega\tau)$ for the denominator factor. The Bode diagram of a pole factor $(1 + j\omega\tau)^{-1}$ is shown in Figure 8.9.

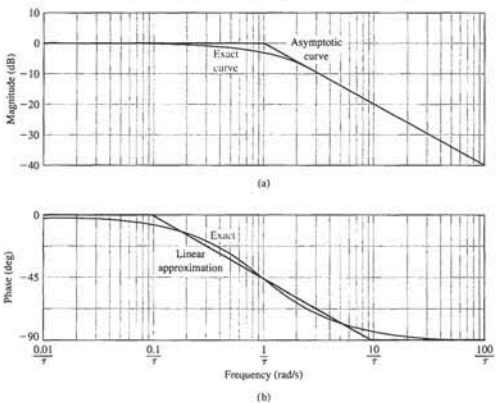


FIGURE 8.9 Bode diagram for $(1 + j\omega\tau)^{-1}$.

For large frequencies—that is, $\omega \gg 1/\tau$ —the logarithmic gain is

$$20 \log G(j\omega) = -20 \log(\omega\tau) \quad \omega \gg 1/\tau, \quad (8.21)$$

and at $\omega = 1/\tau$, we have

$$20 \log |G(j\omega)| = -10 \log 2 = -3.01 \text{ dB.}$$

The magnitude plot for this network is shown in Figure 8.6(a). The phase angle of the network is

$$\phi(\omega) = -\tan^{-1}(\omega\tau). \quad (8.22)$$

The phase plot is shown in Figure 8.6(b). The frequency $\omega = 1/\tau$ is often called the **break frequency** or **corner frequency**. ■

A linear scale of frequency is not the most convenient or judicious choice, and we consider the use of a logarithmic scale of frequency. The convenience of a logarithmic scale of frequency can be seen by considering Equation (8.21) for large frequencies $\omega \gg 1/\tau$, as follows:

$$20 \log |G(j\omega)| = -20 \log(\omega\tau) = -20 \log \tau - 20 \log \omega. \quad (8.23)$$

Then, on a set of axes where the horizontal axis is $\log \omega$, the asymptotic curve for $\omega \gg 1/\tau$ is a straight line, as shown in Figure 8.7. The slope of the straight line can be ascertained from Equation (8.21). An interval of two frequencies with a ratio equal to 10 is called a **decade**, so that the range of frequencies from ω_1 to ω_2 , where $\omega_2 = 10\omega_1$, is called a decade. The difference between the logarithmic gains, for $\omega \gg 1/\tau$, over a decade of frequency is

$$20 \log |G(j\omega_1)| - 20 \log |G(j\omega_2)| = -20 \log(\omega_1\tau) - (-20 \log(\omega_2\tau)) = -20 \log \frac{\omega_1\tau}{\omega_2\tau} = -20 \log \frac{1}{10} = +20 \text{ dB;} \quad (8.24)$$

that is, the slope of the asymptotic line for this first-order transfer function is -20 dB/decade , and the slope is shown for this transfer function in Figure 8.7. Instead of using a horizontal axis of $\log \omega$ and linear rectangular coordinates, it is easier to use semilog paper with a linear rectangular coordinate for dB and a logarithmic coordinate for ω . Alternatively, we could use a logarithmic coordinate for the magnitude as well as for frequency and avoid the necessity of calculating the logarithm of the magnitude.

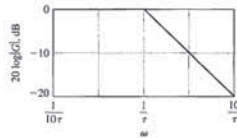


FIGURE 8.7 Asymptotic curve for $(j\omega\tau + 1)^{-1}$.

We can determine the logarithmic magnitude plot and phase angle for these four factors and then use them to obtain a Bode diagram for any general form of a transfer function. Typically, the curves for each factor are obtained and then added together graphically to obtain the curves for the complete transfer function. Furthermore, this procedure can be simplified by using the asymptotic approximations to these curves and obtaining the actual curves only at specific important frequencies.

Constant Gain K_b . The logarithmic gain for the constant K_b is

$$20 \log K_b = \text{constant in dB,}$$

and the phase angle is

$$\phi(\omega) = 0.$$

The gain curve is a horizontal line on the Bode diagram.

If the gain is a negative value, $-K_b$, the logarithmic gain remains $20 \log K_b$. The negative sign is accounted for by the phase angle, -180° .

Poles (or Zeros) at the Origin, $(j\omega)^N$. A pole at the origin has a logarithmic magnitude

$$20 \log \left| \frac{1}{j\omega} \right| = -20 \log \omega \text{ dB} \quad (8.29)$$

and a phase angle

$$\phi(\omega) = -90^\circ.$$

The slope of the magnitude curve is -20 dB/decade for a pole. Similarly, for a multiple pole at the origin, we have

$$20 \log \left| \frac{1}{(j\omega)^N} \right| = -20N \log \omega, \quad (8.30)$$

and the phase is

$$\phi(\omega) = -90^\circ N.$$

In this case, the slope due to the multiple pole is $-20N \text{ dB/decade}$. For a zero at the origin, we have a logarithmic magnitude

$$20 \log |j\omega| = +20 \log \omega, \quad (8.31)$$

where the slope is $+20 \text{ dB/decade}$ and the phase angle is

$$\phi(\omega) = +90^\circ.$$

The Bode diagram of the magnitude and phase angle of $(j\omega)^{kN}$ is shown in Figure 8.8 for $N = 1$ and $N = 2$.

Poles or Zeros on the Real Axis. The pole factor $(1 + j\omega\tau)^{-1}$ has been considered previously, and we found that, for a pole on the real axis,

pair of complex conjugate poles is shown in Figure 8.10. The maximum value M_{pw} of the frequency response occurs at the resonant frequency ω_r . When the damping ratio approaches zero, then ω_r approaches ω_n , the natural frequency. The resonant frequency is determined by taking the derivative of the magnitude of Equation (8.33) with respect to the normalized frequency, u , and setting it equal to zero. The resonant frequency is given by the relation

$$\omega_r = \omega_n \sqrt{1 - 2\zeta^2}, \quad \zeta < 0.707. \quad (8.36)$$

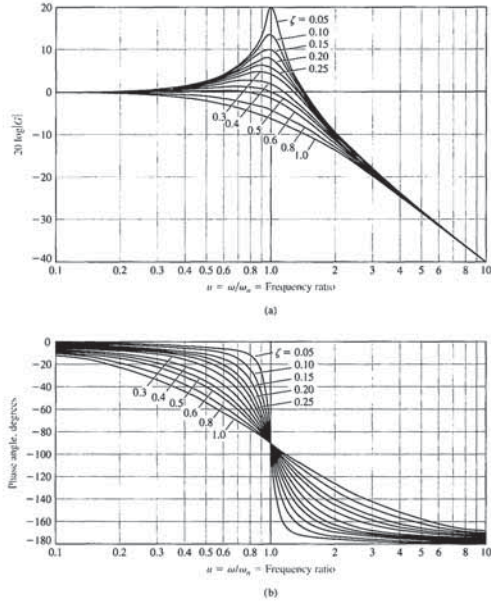


FIGURE 8.10 Bode diagram for $G(j\omega) = [1 + (2\zeta/\omega_n)j\omega + (j\omega/\omega_n)^2]^{-1}$.

The poles for varying ζ lie on a circle of radius ω_n and are shown for a particular ζ in Figure 8.12(a). The transfer function evaluated for real frequency $s = j\omega$ is written as

$$G(j\omega) = \frac{\omega_n^2}{(s - s_1)(s - \hat{s}_1)} \Big|_{s=j\omega} = \frac{\omega_n^2}{(j\omega - s_1)(j\omega - \hat{s}_1)} \quad (8.39)$$

where s_1 and \hat{s}_1 are the complex conjugate poles. The vectors $j\omega - s_1$ and $j\omega - \hat{s}_1$ are the vectors from the poles to the frequency $j\omega$, as shown in Figure 8.12(a). Then the magnitude and phase may be evaluated for various specific frequencies. The magnitude is

$$|G(j\omega)| = \frac{\omega_n^2}{|j\omega - s_1||j\omega - \hat{s}_1|} \quad (8.40)$$

and the phase is

$$\phi(\omega) = -\angle(j\omega - s_1) - \angle(j\omega - \hat{s}_1).$$

The magnitude and phase may be evaluated for three specific frequencies, namely,

$$\omega = 0, \quad \omega = \omega_r, \quad \text{and} \quad \omega = \omega_d,$$

as shown in Figure 8.12 in parts (b), (c), and (d), respectively. The magnitude and phase corresponding to these frequencies are shown in Figure 8.13.

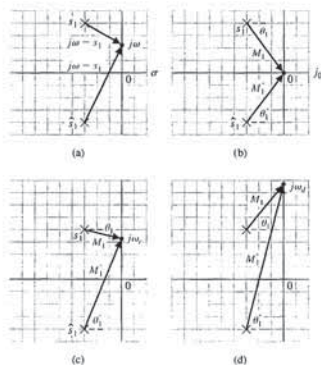


FIGURE 8.12 Vector evaluation of the frequency response for selected values of ω .

The Bode diagram of a zero factor $1 + j\omega\tau$ is obtained in the same manner as that of the pole. However, the slope is positive at +20 dB/decade, and the phase angle is $\phi(\omega) = +\tan^{-1}(\omega\tau)$.

A piecewise linear approximation to the phase angle curve can be obtained as shown in Figure 8.9. This linear approximation, which passes through the correct phase at the break frequency, is within 6° of the actual phase curve for all frequencies. This approximation will provide a useful means for readily determining the form of the phase angle curves of a transfer function $G(s)$. However, often the accurate phase angle curves are required, and the actual phase curve for the first-order factor must be obtained via a computer program. The exact values of the frequency response for the pole $(1 + j\omega\tau)^{-1}$, as well as the values obtained by using the approximation for comparison, are given in Table 8.2.

Complex Conjugate Poles or Zeros $[1 + (2\zeta/\omega_n)j\omega + (j\omega/\omega_n)^2]$. The quadratic factor for a pair of complex conjugate poles can be written in normalized form as

$$[1 + j2\zeta u - u^2]^{-1}, \quad (8.33)$$

where $u = \omega/\omega_n$. Then the logarithmic magnitude for a pair of complex conjugate poles is

$$20 \log|G(j\omega)| = -10 \log[(1 - u^2)^2 + 4\zeta^2 u^2], \quad (8.34)$$

and the phase angle is

$$\phi(\omega) = -\tan^{-1} \frac{2\zeta u}{1 - u^2}. \quad (8.35)$$

When $u \ll 1$, the magnitude is

$$20 \log|G(j\omega)| = -10 \log 1 = 0 \text{ dB},$$

and the phase angle approaches 0° . When $u \gg 1$, the logarithmic magnitude approaches

$$20 \log|G(j\omega)| = -10 \log u^4 = -40 \log u,$$

which results in a curve with a slope of -40 dB/decade. The phase angle, when $u \gg 1$, approaches -180° . The magnitude asymptotes meet at the 0 dB line when $u = \omega/\omega_n = 1$. However, the difference between the actual magnitude curve and the asymptotic approximation is a function of the damping ratio and must be accounted for when $\zeta < 0.707$. The Bode diagram of a quadratic factor due to a

Table 8.2

$\omega\tau$	0.10	0.50	0.76	1	1.31	2	5	10
$20 \log (1 + j\omega\tau)^{-1} $, dB	-0.04	-1.0	-2.0	-3.0	-4.3	-7.0	-14.2	-20.04
Asymptotic approximation, dB	0	0	0	0	-2.3	-6.0	-14.0	-20.0
$\phi(\omega)$, degrees	-5.7	-26.6	-37.4	-45.0	-52.7	-63.4	-78.7	-84.3
Linear approximation, degrees	0	-31.50	-39.5	-45.0	-50.3	-58.5	-76.5	-90.0

and the maximum value of the magnitude $|G(j\omega)|$ is

$$M_{pw} = |G(j\omega_r)| = (2\zeta\sqrt{1 - \zeta^2})^{-1}, \quad \zeta < 0.707, \quad (8.37)$$

for a pair of complex poles. The maximum value of the frequency response, M_{pw} , and the resonant frequency ω_r are shown as a function of the damping ratio ζ for a pair of complex poles in Figure 8.11. Assuming the dominance of a pair of complex conjugate closed-loop poles, we find that these curves are useful for estimating the damping ratio of a system from an experimentally determined frequency response.

The frequency response curves can be evaluated on the s -plane by determining the vector lengths and angles at various frequencies ω along the $(s = +j\omega)$ -axis. For example, considering the second-order factor with complex conjugate poles, we have

$$G(s) = \frac{1}{(s/\omega_n)^2 + 2\zeta s/\omega_n + 1} = \frac{\omega_n^2}{s^2 + 2\zeta\omega_n s + \omega_n^2}. \quad (8.38)$$

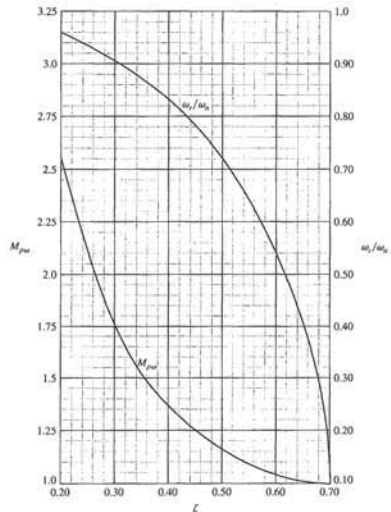


FIGURE 8.11 The maximum M_{pw} of the frequency response and the resonant frequency ω_r versus ζ for a pair of complex conjugate poles.

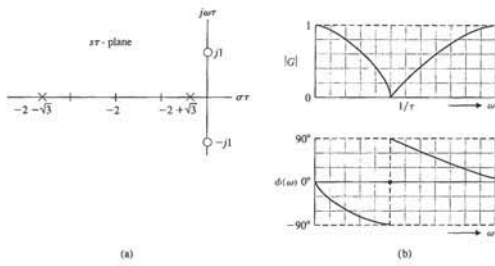


FIGURE 8.15 Twin-T network. (a) Pole-zero pattern. (b) Frequency response.

shown that the net phase shift over the frequency range from zero to infinity is less for the system with all its zeros in the left-hand s -plane. Thus, the transfer function $G_1(s)$, with all its zeros in the left-hand s -plane, is called a **minimum phase transfer function**. The transfer function $G_2(s)$, with $|G_2(j\omega)| = |G_1(j\omega)|$ and all the zeros of $G_1(s)$ reflected about the $j\omega$ -axis into the right-hand s -plane, is called a nonminimum phase transfer function. Reflection of any zero or pair of zeros into the right half-plane results in a nonminimum phase transfer function.

A transfer function is called a minimum phase transfer function if all its zeros lie in the left-hand s -plane. It is called a nonminimum phase transfer function if it has zeros in the right-hand s -plane.

The two pole-zero patterns shown in Figures 8.16(a) and (b) have the same amplitude characteristics as can be deduced from the vector lengths. However, the phase characteristics are different for Figures 8.16(a) and (b). The minimum phase characteristic of Figure 8.16(a) and the nonminimum phase characteristic of Figure 8.16(b) are shown in Figure 8.17. Clearly, the phase shift of

$$G_1(s) = \frac{s+z}{s+p}$$

ranges over less than 80° , whereas the phase shift of

$$G_2(s) = \frac{s-z}{s+p}$$

ranges over 180° . The meaning of the term **minimum phase** is illustrated by Figure 8.17. The range of phase shift of a minimum phase transfer function is the least possible or minimum corresponding to a given amplitude curve, whereas the range of the nonminimum phase curve is the greatest possible for the given amplitude curve.

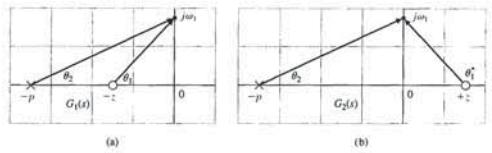


FIGURE 8.16 Pole-zero patterns giving the same amplitude response and different phase characteristics.

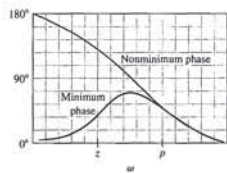


FIGURE 8.17 The phase characteristics for the minimum phase and nonminimum phase transfer function.

A particularly interesting nonminimum phase network is the **all-pass network**, which can be realized with a symmetrical lattice network [8]. A symmetrical pattern of poles and zeros is obtained as shown in Figure 8.18(a). Again, the magnitude $|G(j\omega)|$ remains constant; in this case, it is equal to unity. However, the angle varies

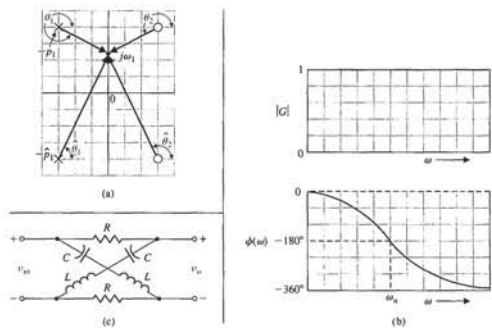


FIGURE 8.18 The all-pass network (a) pole-zero pattern, (b) frequency response, and (c) a lattice network.

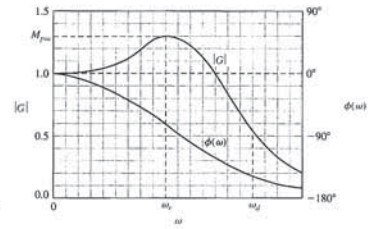


FIGURE 8.13 Bode diagram for complex conjugate poles.

EXAMPLE 8.4 Bode diagram of a twin-T network

As an example of the determination of the frequency response using the pole-zero diagram and the vectors to $j\omega$, consider the twin-T network shown in Figure 8.14 [6]. The transfer function of this network is

$$G(s) = \frac{V_o(s)}{V_{in}(s)} = \frac{(s\tau)^2 + 1}{(s\tau)^2 + 4s\tau + 1} \quad (8.41)$$

where $\tau = RC$. The zeros are at $\pm j1$, and the poles are at $-2 \pm \sqrt{3}$ in the $s\tau$ -plane, as shown in Figure 8.15(a). At $\omega = 0$, we have $|G(j\omega)| = 1$ and $\phi(\omega) = 0^\circ$. At $\omega = 1/\tau$, $|G(j\omega)| = 0$ and the phase angle of the vector from the zero at $s\tau = j1$ passes through a transition of 180° . When ω approaches ∞ , $|G(j\omega)| = 1$ and $\phi(\omega) = 0$ again. Evaluating several intermediate frequencies, we can readily obtain the frequency response, as shown in Figure 8.15(b). ■

A summary of the asymptotic curves for basic terms of a transfer function is provided in Table 8.3.

In the previous examples, the poles and zeros of $G(s)$ have been restricted to the left-hand plane. However, a system may have zeros located in the right-hand s -plane and may still be stable. Transfer functions with zeros in the right-hand s -plane are classified as **nonminimum phase transfer functions**. If the zeros of a transfer function are all reflected about the $j\omega$ -axis, there is no change in the magnitude of the transfer function, and the only difference is in the phase-shift characteristics. If the phase characteristics of the two system functions are compared, it can be readily

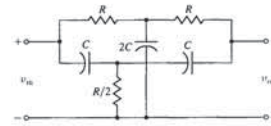


FIGURE 8.14 Twin-T network.

Table 8.3 Asymptotic Curves for Basic Terms of a Transfer Function

Term	Magnitude $20 \log G $	Phase $\phi(\omega)$
1. Gain, $G(j\omega) = K$		
2. Zero, $G(j\omega) = 1 + j\omega/\omega_1$		
3. Pole, $G(j\omega) = (1 + j\omega/\omega_1)^{-1}$		
4. Pole at the origin, $G(j\omega) = 1/j\omega$		
5. Two complex poles, $0.1 < \zeta < 1$, $G(j\omega) = (1 + j2\zeta u - u^2)^{-1}$, $u = \omega/\omega_n$		

- The magnitude for the complex poles is -40 dB/decade. The break frequency is $\omega = \omega_n = 50$, as shown in Figure 8.19. This approximation must be corrected to the actual magnitude because the damping ratio is $\zeta = 0.3$, and the magnitude differs appreciably from the approximation, as shown in Figure 8.20.

Therefore, the total asymptotic magnitude can be plotted by adding the asymptotes due to each factor, as shown by the solid line in Figure 8.20. Examining the asymptotic curve of Figure 8.20, we note that the curve can be obtained directly by plotting each asymptote in order as frequency increases. Thus, the slope is -20 dB/decade due to $K(j\omega)^{-1}$ intersecting 14 dB at $\omega = 1$. Then, at $\omega = 2$, the slope becomes -40 dB/decade due to the pole at $\omega = 2$. The slope changes to -20 dB/decade due to the zero at $\omega = 10$. Finally, the slope becomes -60 dB/decade at $\omega = 50$ due to the pair of complex poles at $\omega_n = 50$.

The exact magnitude curve is then obtained by using Table 8.2, which provides the difference between the actual and asymptotic curves for a single pole or zero. The exact magnitude curve for the pair of complex poles is obtained by utilizing Figure 8.10(a) for the quadratic factor. The exact magnitude curve for $G(j\omega)$ is shown by a dashed line in Figure 8.20.

The phase characteristic can be obtained by adding the phase due to each individual factor. Usually, the linear approximation of the phase characteristic for a single pole or zero is suitable for the initial analysis or design attempt. Thus, the individual phase characteristics for the poles and zeros are shown in Figure 8.21 and are as follows:

- The phase of the constant gain is 0° .
- The phase of the pole at the origin is a constant -90° .
- The linear approximation of the phase characteristic for the pole at $\omega = 2$ is shown in Figure 8.21, where the phase shift is -45° at $\omega = 2$.
- The linear approximation of the phase characteristic for the zero at $\omega = 10$ is also shown in Figure 8.21, where the phase shift is $+45^\circ$ at $\omega = 10$.

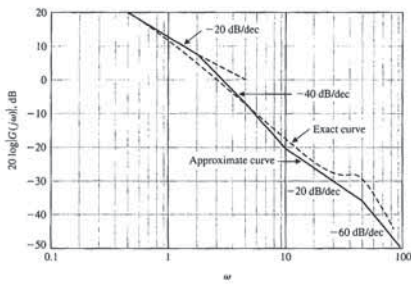


FIGURE 8.20 Magnitude characteristic.

Section 8.3 Frequency Response Measurements

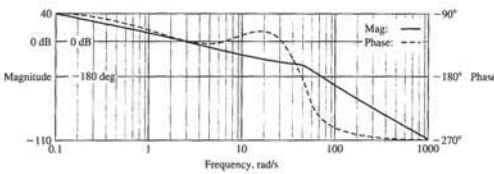


FIGURE 8.22 The Bode plot of the $G(j\omega)$ of Equation (8.42).

exact magnitude and phase shift can be readily evaluated by using the exact equations, such as Equation (8.43).

The frequency response of $G(j\omega)$ can be calculated and plotted using a computer program. The Bode plot for the example in this section (Equation 8.42) can be readily obtained, as shown in Figure 8.22. The plot is generated for four decades, and the 0-dB line is indicated, as well as the -180° line. The data above the plot indicate that the magnitude is 34 dB and that the phase is -92.36° at $\omega = 0.1$. Similarly, the data indicate that the magnitude is -43 dB and that the phase is -243° at $\omega = 100$. Using the tabular data provided, we find that the magnitude is 0 dB at $\omega = 3.0$, and the phase is -180° at $\omega = 50$.

8.3 FREQUENCY RESPONSE MEASUREMENTS

A sine wave can be used to measure the open-loop frequency response of a control system. In practice, a plot of amplitude versus frequency and phase versus frequency will be obtained [1, 3, 6]. From these two plots, the open-loop transfer function $GH(j\omega)$ can be deduced. Similarly, the closed-loop frequency response of a control system, $T(j\omega)$, may be obtained and the actual transfer function deduced.

A device called a wave analyzer can be used to measure the amplitude and phase variations as the frequency of the input sine wave is altered. Also, a device called a transfer function analyzer can be used to measure the open-loop and closed-loop transfer functions [6].

A typical signal analyzer instrument can perform frequency response measurements from DC to 100 kHz. Built-in analysis and modeling capabilities can derive poles and zeros from measured frequency responses or construct phase and magnitude responses from user-supplied models. This device can also synthesize the frequency response of a model of a system, allowing a comparison with an actual response.

As an example of determining the transfer function from the Bode plot, let us consider the plot shown in Figure 8.23. The system is a stable circuit consisting of resistors and capacitors. Because the magnitude declines at about -20 dB/decade as ω increases between 100 and 1000, and because the phase is -45° and the magnitude is -3 dB at 300 rad/s, we can deduce that one factor is a pole at $p_1 = 300$. Next, we deduce that a pair of quadratic zeros exist at $\omega_n = 2450$. This is inferred by noting

from 0° to -360° . Because $\theta_2 = 180^\circ - \theta_1$ and $\theta_2^* = 180^\circ - \theta_1^*$, the phase is given by $\phi(\omega) = -2(\theta_1 + \theta_1^*)$. The magnitude and phase characteristic of the all-pass network is shown in Figure 8.18(b). A nonminimum phase lattice network is shown in Figure 8.18(c).

EXAMPLE 8.5 Sketching a Bode plot

The Bode diagram of a transfer function $G(s)$, which contains several zeros and poles, is obtained by adding the plot due to each individual pole and zero. The simplicity of this method will be illustrated by considering a transfer function that possesses all the factors considered in the preceding section. The transfer function of interest is

$$G(j\omega) = \frac{5(1 + j0.1\omega)}{j\omega(1 + j0.5\omega)(1 + j0.6(\omega/50) + (j\omega/50)^2)} \quad (8.42)$$

The factors, in order of their occurrence as frequency increases, are as follows:

- A constant gain $K = 5$
- A pole at the origin
- A pole at $\omega = 2$
- A zero at $\omega = 10$
- A pair of complex poles at $\omega = \omega_n = 50$

First, we plot the magnitude characteristic for each individual pole and zero factor and the constant gain:

- The constant gain is $20 \log 5 = 14$ dB, as shown in Figure 8.19.
- The magnitude of the pole at the origin extends from zero frequency to infinite frequencies and has a slope of -20 dB/decade intersecting the 0-dB line at $\omega = 1$, as shown in Figure 8.19.
- The asymptotic approximation of the magnitude of the pole at $\omega = 2$ has a slope of -20 dB/decade beyond the break frequency at $\omega = 2$. The asymptotic magnitude below the break frequency is 0 dB, as shown in Figure 8.19.
- The asymptotic magnitude for the zero at $\omega = 10$ has a slope of +20 dB/decade beyond the break frequency at $\omega = 10$, as shown in Figure 8.19.

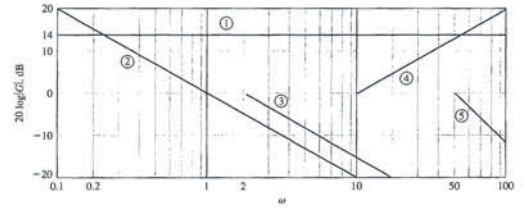


FIGURE 8.19 Magnitude asymptotes of poles and zeros used in the example.

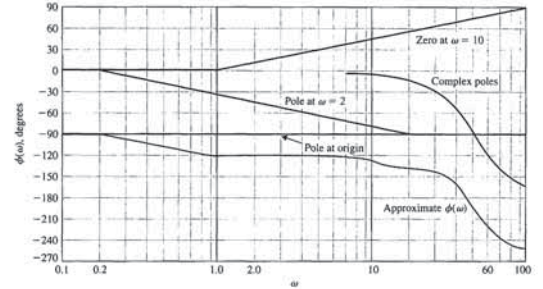


FIGURE 8.21 Phase characteristic.

- The actual phase characteristic for the pair of complex poles is obtained from Figure 8.10 and is shown in Figure 8.21.

Therefore, the total phase characteristic, $\phi(\omega)$, is obtained by adding the phase due to each factor as shown in Figure 8.21. While this curve is an approximation, its usefulness merits consideration as a first attempt to determine the phase characteristic. Thus, a frequency of interest, as we shall note in the following section, is the frequency for which $\phi(\omega) = -180^\circ$. The approximate curve indicates that a phase shift of -180° occurs at $\omega = 46$. The actual phase shift at $\omega = 46$ can be readily calculated as

$$\phi(\omega) = -90^\circ - \tan^{-1} \omega\tau_1 + \tan^{-1} \omega\tau_2 - \tan^{-1} \frac{2\zeta u}{1 - u^2} \quad (8.43)$$

where

$$\tau_1 = 0.5, \quad \tau_2 = 0.1, \quad 2\zeta = 0.6, \quad \text{and} \quad u = \omega/\omega_n = \omega/50.$$

Then we find that

$$\phi(46) = -90^\circ - \tan^{-1} 23 + \tan^{-1} 4.6 - \tan^{-1} 3.55 = -175^\circ, \quad (8.44)$$

and the approximate curve has an error of 5° at $\omega = 46$. However, once the approximate frequency of interest is ascertained from the approximate phase curve, the accurate phase shift for the neighboring frequencies is readily determined by using the exact phase shift relation (Equation 8.43). This approach is usually preferable to the calculation of the exact phase shift for all frequencies over several decades. In summary, we may obtain approximate curves for the magnitude and phase shift of a transfer function $G(j\omega)$ in order to determine the important frequency ranges. Then, within the relatively small important frequency ranges, the

The difference in magnitude from the corner frequency ($\omega_n = 2450$) of the asymptotes to the minimum response is 10 dB, which, from Equation (8.37), indicates that $\zeta = 0.16$. (Compare the plot of the quadratic zeros to the plot of the quadratic poles in Figure 8.10. Note that the plots need to be turned "upside down" for the quadratic zeros and that the phase goes from 0° to $+180^\circ$ instead of -180° .) Therefore, the transfer function is

$$T(s) = \frac{(s/2450)^2 + (0.32/2450)s + 1}{(s/300 + 1)(s/20000 + 1)}$$

This frequency response is actually obtained from a bridged-T network (see Problems P2.8 and P8.3 and Figure 8.14).

8.4 PERFORMANCE SPECIFICATIONS IN THE FREQUENCY DOMAIN

We must continually ask the question: how does the frequency response of a system relate to the expected transient response of the system? In other words, given a set of time-domain (transient performance) specifications, how do we specify the frequency response? For a simple second-order system, we have already answered this question by considering the time-domain performance in terms of overshoot, settling time, and other performance criteria, such as integral squared error. For the second-order system shown in Figure 8.24, the closed-loop transfer function is

$$T(s) = \frac{\omega_n^2}{s^2 + 2\zeta\omega_n s + \omega_n^2} \tag{8.46}$$

The frequency response of this feedback system will appear as shown in Figure 8.25. Because this is a second-order system, the damping ratio of the system is related to the maximum magnitude M_{pw} , which occurs at the frequency ω_r , as shown in Figure 8.25.

At the resonant frequency ω_r , a maximum value M_{pw} of the frequency response is attained.

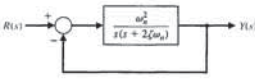


FIGURE 8.24 A second-order closed-loop system.

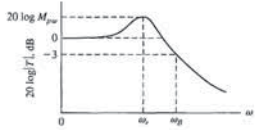


FIGURE 8.25 Magnitude characteristic of the second-order system.

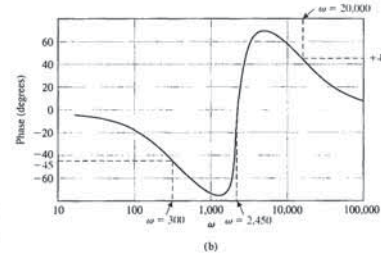
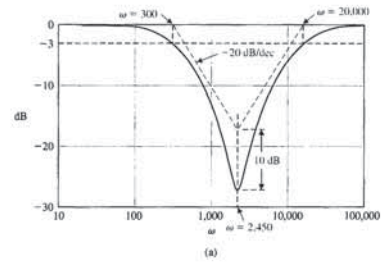


FIGURE 8.23 A Bode diagram for a system with an unidentified transfer function.

that the phase changes abruptly by nearly $+180^\circ$, passing through 0° at $\omega_n = 2450$. Also, the slope of the magnitude changes from -20 dB/decade to $+20$ dB/decade at $\omega_n = 2450$. Because the slope of the magnitude returns to 0 dB/decade as ω exceeds $50,000$, we determine that there is a second pole as well as two zeros. This second pole is at $p_2 = 20,000$, because the magnitude is -3 dB from the asymptote and the phase is $+45^\circ$ at this point (-90° for the first pole, $+180^\circ$ for the pair of quadratic zeros, and -45° for the second pole). We sketch the asymptotes for the poles and the numerator of the proposed transfer function $T(s)$ of Equation (8.45), as shown in Figure 8.23(a). The equation is

$$T(s) = \frac{(s/\omega_n)^2 + (2\zeta/\omega_n)s + 1}{(s/p_1 + 1)(s/p_2 + 1)} \tag{8.45}$$

The usefulness of these frequency response specifications and their relation to the actual transient performance depend upon the approximation of the system by a second-order pair of complex poles. This approximation was discussed in Section 7.3, and the second-order poles of $T(s)$ are called the **dominant roots**. If the frequency response is dominated by a pair of complex poles, the relationships between the frequency response and the time response discussed in this section will be valid. Fortunately, a large proportion of control systems satisfy this dominant second-order approximation in practice.

The steady-state error specification can also be related to the frequency response of a closed-loop system. As we found in Section 5.6, the steady-state error for a specific test input signal can be related to the gain and number of integrations (poles at the origin) of the loop transfer function. Therefore, for the system shown in Figure 8.24, the steady-state error for a ramp input is specified in terms of K_v , the velocity constant. The steady-state error for the system is

$$\lim_{t \rightarrow \infty} e(t) = \frac{A}{K_v}$$

where A = magnitude of the ramp input. The velocity constant for the system of Figure 8.24 without feedback is

$$K_v = \lim_{s \rightarrow 0} sG(s) = \lim_{s \rightarrow 0} s \left(\frac{\omega_n^2}{s(s + 2\zeta\omega_n)} \right) = \frac{\omega_n}{2\zeta} \tag{8.48}$$

In Bode diagram form (in terms of time constants), the transfer function is written as

$$G(s) = \frac{\omega_n/(2\zeta)}{s(s/(2\zeta\omega_n) + 1)} = \frac{K_v}{s(\tau s + 1)} \tag{8.49}$$

and the gain constant is K_v for this type-one system. For example, reexamining Example 8.5, we had a type-one system with a loop transfer function

$$G(j\omega) = \frac{5(1 + j\omega\tau_2)}{j\omega(1 + j\omega\tau_1)(1 + j\omega\tau_2 - \omega^2)} \tag{8.50}$$

where $\omega = \omega/\omega_n$. Therefore, in this case, we have $K_v = 5$. In general, if the loop transfer function of a feedback system is written as

$$G(j\omega) = \frac{K \prod_{i=1}^M (1 + j\omega\tau_i)}{(j\omega)^N \prod_{k=1}^Q (1 + j\omega\tau_k)} \tag{8.51}$$

then the system is type N and the gain K is the gain constant for the steady-state error. Thus, for a type-zero system that has two poles, we have

$$G(j\omega) = \frac{K}{(1 + j\omega\tau_1)(1 + j\omega\tau_2)} \tag{8.52}$$

In this equation, $K = K_p$ (the position error constant) that appears as the low-frequency gain on the Bode diagram.

The bandwidth, ω_B , is a measure of an ability of the system to faithfully reproduce an input signal.

The bandwidth is the frequency ω_B at which the frequency response has declined 3 dB from its low-frequency value. This corresponds to approximately half an octave, or about $1/\sqrt{2}$ of the low-frequency value.

The resonant frequency ω_r and the -3 -dB bandwidth can be related to the speed of the transient response. Thus, as the bandwidth ω_B increases, the rise time of the step response of the system will decrease. Furthermore, the overshoot to a step input can be related to M_{pw} through the damping ratio ζ . The curves of Figure 8.11 relate the resonance magnitude and frequency to the damping ratio of the second-order system. Then the step response overshoot may be estimated from Figure 5.8 or may be calculated by utilizing Equation (5.15). Thus, we find as the resonant peak M_{pw} increases in magnitude, the overshoot to a step input increases. In general, the magnitude M_{pw} indicates the relative stability of a system.

The bandwidth of a system ω_B , as indicated on the frequency response, can be approximately related to the natural frequency of the system. Figure 8.26 shows the normalized bandwidth ω_B/ω_n versus ζ for the second-order system of Equation (8.46). The response of the second-order system to a unit step input is of the form (see Equation (5.9))

$$y(t) = 1 + B e^{-\zeta\omega_n t} \cos(\omega_d t + \theta) \tag{8.47}$$

The greater the magnitude of ω_n when ζ is constant, the more rapidly the response approaches the desired steady-state value. Thus, desirable frequency-domain specifications are as follows:

1. Relatively small resonant magnitudes: $M_{pw} < 1.5$, for example.
2. Relatively large bandwidths so that the system time constant $\tau = 1/(\zeta\omega_n)$ is sufficiently small.

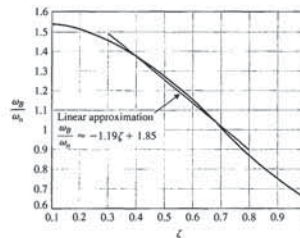


FIGURE 8.26 Normalized bandwidth, ω_B/ω_n , versus ζ for a second-order system (Equation 8.46). The linear approximation $\omega_B/\omega_n = -1.19\zeta + 1.85$ is accurate for $0.3 \leq \zeta \leq 0.8$.

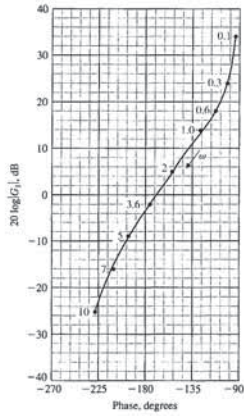


FIGURE 8.27 Log-magnitude-phase curve for $G_1(j\omega)$.

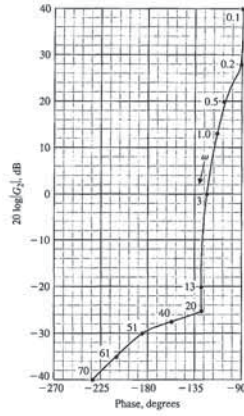


FIGURE 8.28 Log-magnitude-phase curve for $G_2(j\omega)$.

8.6 DESIGN EXAMPLES

In this section, we present three illustrative examples using frequency response methods to design controllers. The first example describes the control of a photovoltaic generator to achieve maximum power delivery as the sunlight varies over time. The second example illustrates the use of log-magnitude-phase plots, as well as open- and closed-loop Bode plots. The specific problem is to design a proportional controller gain for an engraving machine control feedback control system. The second example considers the control of one leg of a six-legged robotic device. In this example, the specifications that must be satisfied include a mix of time-domain specifications (percent overshoot and settling time) and frequency-domain specifications (bandwidth). The design process leads to a viable PID controller meeting all the specifications.

EXAMPLE 8.6 Maximum power pointing tracking for photovoltaic generators

As discussed in Chapter 1, the goal of green engineering is to design products that will minimize pollution and improve the environment. Using solar energy is one

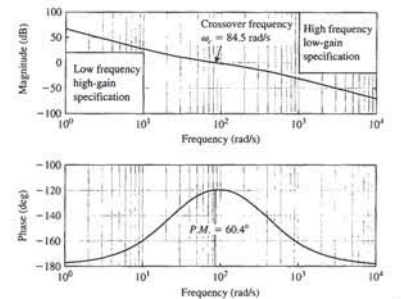


FIGURE 8.30 Bode plot of compensated system with $G_c(s) = 250 \frac{0.04s + 1}{100s + 1}$.

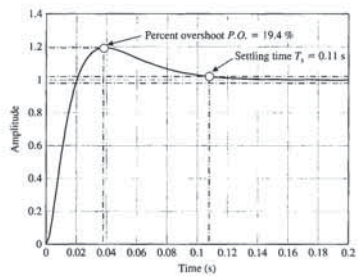


FIGURE 8.31 Step response of the closed-loop system.

settling time is $T_s = 0.11$ s and the percent overshoot is $P.O. = 19.4\%$, both very acceptable for the control of the photovoltaic generator voltage. ■

EXAMPLE 8.7 Engraving machine control system

The engraving machine shown in Figure 8.32(a) uses two drive motors and associated lead screws to position the engraving scribe in the x direction [7]. A separate motor is used for both the y - and z -axes, as shown. The block diagram model for the

Furthermore, the gain constant $K = K_v$ for the type-one system appears as the gain of the low-frequency section of the magnitude characteristic. Considering only the pole and gain of the type-one system of Equation (8.50), we have

$$G(j\omega) = \frac{5}{j\omega} = \frac{K_v}{j\omega}, \quad \omega < 1/\tau_1, \quad (8.53)$$

and the K_v is equal to the magnitude when this portion of the magnitude characteristic intersects the 0-dB line. For example, the low-frequency intersection of $K_v/j\omega$ in Figure 8.20 is equal to $\omega = 5$, as we expect.

Therefore, the frequency response characteristics represent the performance of a system quite adequately, and with some experience, they are quite useful for the analysis and design of feedback control systems.

8.5 LOG MAGNITUDE AND PHASE DIAGRAMS

There are several alternative methods for presenting the frequency response of a function $G(j\omega)$. We have seen that suitable graphical presentations of the frequency response are (1) the polar plot and (2) the Bode diagram. An alternative approach to portraying the frequency response graphically is to plot the logarithmic magnitude in dB versus the phase angle for a range of frequencies. Because this information is equivalent to that portrayed by the Bode diagram, it is normally easier to obtain the Bode diagram and transfer the information to the coordinates of the log magnitude versus phase diagram.

An illustration will best portray the use of the log-magnitude-phase diagram. This diagram for a transfer function

$$G_1(j\omega) = \frac{5}{j\omega(0.5j\omega + 1)(j\omega/6 + 1)} \quad (8.54)$$

is shown in Figure 8.27. The numbers indicated along the curve are for values of frequency ω .

The log-magnitude-phase curve for the transfer function

$$G_2(j\omega) = \frac{5(0.1j\omega + 1)}{j\omega(0.5j\omega + 1)(1 + j0.6(\omega/50) + (j\omega/50)^2)} \quad (8.55)$$

considered in Section 8.2 is shown in Figure 8.28. This curve is obtained most readily by utilizing the Bode diagrams of Figures 8.20 and 8.21 to transfer the frequency response information to the log magnitude and phase coordinates. The shape of the locus of the frequency response on a log-magnitude-phase diagram is particularly important as the phase approaches -180° and the magnitude approaches 0 dB. The locus of Equation (8.54) and Figure 8.27 differs substantially from the locus of Equation (8.55) and Figure 8.28. Therefore, as the correlation between the shape of the locus and the transient response of a system is established, we will obtain another useful portrayal of the frequency response of a system. In Chapter 9, we will establish a stability criterion in the frequency domain for which it will be useful to utilize the log-magnitude-phase diagram to investigate the relative stability of closed-loop feedback control systems.

way to provide clean energy using photovoltaic generators converting sunlight to electricity directly. However, the output of a photovoltaic generator is variable and depends on the available sunlight, the temperature, and the attached loads. In this example, we provide a discussion on regulating the voltage provided by a photovoltaic generator system using feedback control [24]. In Chapter 2, we discussed the modeling of the plant and closed-loop system. In this example, we design a controller to achieve the desired specifications.

Consider the feedback control system in Figure 8.29. The plant transfer function is

$$G(s) = \frac{K}{s(s + p)}$$

where $K = 300,000$ and $p = 360$. This model is consistent with a photovoltaic generator with 182 cells generating over 1100 W [24]. Assume a controller of the form

$$G_c(s) = K_c \frac{\tau_1 s + 1}{\tau_2 s + 1}, \quad (8.56)$$

where K_c , τ_1 , and τ_2 are to be determined. The controller in Equation (8.56) is a lead or lag compensator depending on τ_1 and τ_2 and is discussed in more detail in Chapter 10. The controller should minimize the effects of disturbances and plant changes by providing a high gain at low frequencies while minimizing the measurement noise by providing a low gain at high frequencies [24]. To accomplish these goals, the design specifications are:

1. $|G_c(j\omega)G(j\omega)| \geq 20$ dB at $\omega \leq 10$ rad/s
2. $|G_c(j\omega)G(j\omega)| \leq -20$ dB at $\omega \geq 1000$ rad/s
3. Phase margin $P.M. \geq 60^\circ$

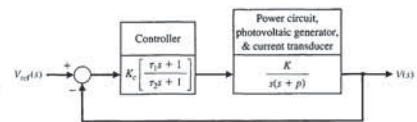
The phase margin of the uncompensated system is $P.M. = 36.3^\circ$ implying that the compensated system needs to add approximately $P.M. = 25^\circ$, hence the use of the compensator to add the required phase lead. Also, the magnitude of the uncompensated frequency response at $\omega = 1000$ rad/s is -11 dB indicating that the gain needs to be further reduced at high frequencies to meet the specifications.

One possible controller is

$$G_c(s) = 250 \frac{0.04s + 1}{100s + 1}$$

The compensated phase margin is $P.M. = 60.4^\circ$. As can be seen in Figure 8.30, the low-frequency, high-gain specification is satisfied, as well as the high-frequency, low-gain specification. The closed-loop step response is shown in Figure 8.31. The

FIGURE 8.29 Photovoltaic generator feedback control system to a track reference input voltage.



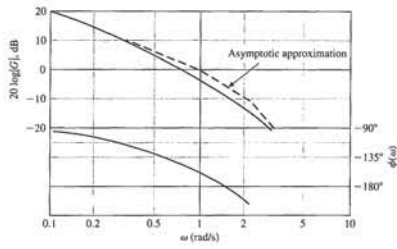


FIGURE 8.33 Bode diagram for $G(j\omega)$.

Therefore, we let $s = j\omega$, obtaining

$$T(j\omega) = \frac{2}{(2 - 3\omega^2) + j\omega(2 - \omega^2)} \quad (8.58)$$

The Bode diagram of the closed-loop system is shown in Figure 8.34, where $20 \log|T(j\omega)| = 5 \text{ dB}$ at $\omega_c = 0.8$. Hence,

$$20 \log M_{pw} = 5 \text{ or } M_{pw} = 1.78.$$

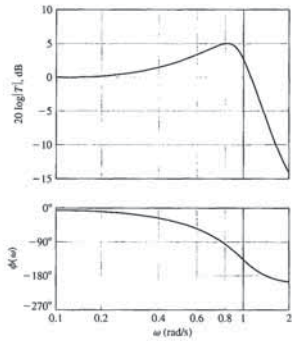


FIGURE 8.34 Bode diagram for closed-loop system.

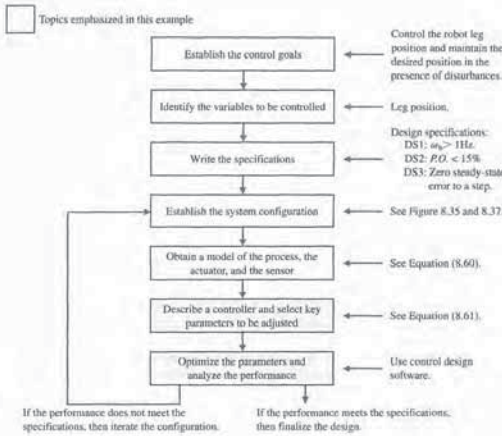


FIGURE 8.36 Elements of the control system design process emphasized in this six-legged robot example.

The input is a voltage command to the actuator, and the output is the leg position (vertical position only). A block diagram of the control system is shown in Figure 8.37. The control goal is

Control Goal
Control the robot leg position and maintain the position in the presence of unwanted measurement noise.

The variable to be controlled is

Variable to Be Controlled
Leg position, $Y(s)$.

We want the leg to move to the commanded position as fast as possible but with minimal overshoot. As a practical first step, the design goal will be to produce a system that moves, albeit slowly. In other words, the control system bandwidth will initially be low.

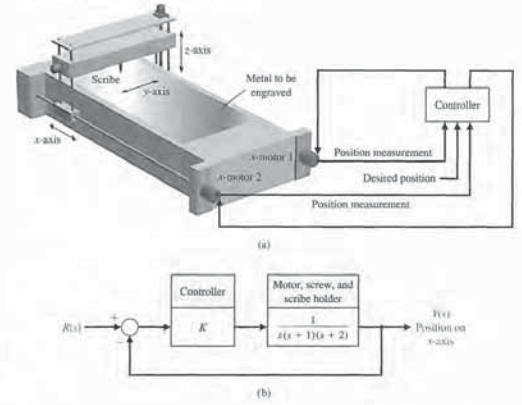


FIGURE 8.32 (a) Engraving machine control system. (b) Block diagram model.

x -axis position control system is shown in Figure 8.32(b). The goal is to select an appropriate gain K , using frequency response methods, so that the time response to step commands is acceptable.

To represent the frequency response of the system, we will first obtain the open-loop and closed-loop Bode diagrams. Then we will use the closed-loop Bode diagram to predict the time response of the system and check the predicted results with the actual results.

To plot the frequency response, we arbitrarily select $K = 2$ and proceed with obtaining the Bode diagram. If the resulting system is not acceptable, we will later adjust the gain.

The frequency response of $G(j\omega)$ is partially listed in Table 8.4 and is plotted in Figure 8.33. We need the frequency response of the closed-loop transfer function

$$T(s) = \frac{2}{s^2 + 3s^2 + 2s + 2} \quad (8.57)$$

Table 8.4 Frequency Response for $G(j\omega)$

ω	0.2	0.4	0.8	1.0	1.4	1.8
$20 \log G $	14	7	-1	-4	-9	-13
ϕ	-107°	-123°	-150.5°	-162°	-179.5°	-193°

If we assume that the system has dominant second-order roots, we can approximate the system with a second-order frequency response of the form shown in Figure 8.10. Since $M_{pw} = 1.78$, we use Figure 8.11 to estimate ζ to be 0.29. Using this ζ and $\omega_c = 0.8$, we can use Figure 8.11 to estimate $\omega_n/\omega_c = 0.91$. Therefore,

$$\omega_n = \frac{0.8}{0.91} = 0.88.$$

Since we are now approximating $T(s)$ as a second-order system, we have

$$T(s) \approx \frac{\omega_n^2}{s^2 + 2\zeta\omega_n s + \omega_n^2} = \frac{0.774}{s^2 + 0.51s + 0.774} \quad (8.59)$$

We use Figure 5.8 to predict the overshoot to a step input as 37% for $\zeta = 0.29$. The settling time (to within 2% of the final value) is estimated as

$$T_s = \frac{4}{\zeta\omega_n} = \frac{4}{(0.29)(0.88)} = 15.7s.$$

The actual overshoot for a step input is 34%, and the actual settling time is 17 seconds. We see that the second-order approximation is reasonable in this case and can be used to determine suitable parameters on a system. If we require a system with lower overshoot, we would reduce K to 1 and repeat the procedure. ■

EXAMPLE 8.8 Control of one leg of a six-legged robot

The Ambler is a six-legged walking machine being developed at Carnegie-Mellon University [23]. An artist's conception of the Ambler is shown in Figure 8.35.

In this example we consider the control system design for position control of one leg. The elements of the design process emphasized in this example are highlighted in Figure 8.36. The mathematical model of the actuator and leg is provided. The transfer function is

$$G(s) = \frac{1}{s(s^2 + 2s + 10)} \quad (8.60)$$

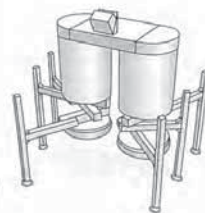


FIGURE 8.35 An artist's conception of the six-legged Ambler.

The bandwidth ω_B is approximately related to the natural frequency ω_n by

$$\frac{\omega_B}{\omega_n} \approx -1.1961\zeta + 1.8508 \quad (0.3 \leq \zeta \leq 0.8). \quad (8.63)$$

This approximation applies to second-order systems. Per specification DS1, we want

$$\omega_B = 1 \text{ Hz} = 6.28 \text{ rad/s}. \quad (8.64)$$

From the percent overshoot specification, we can determine the minimum value of ζ . Thus for $P.O. \leq 15\%$, we require

$$\zeta \geq 0.52. \quad (8.65)$$

where we have used Equation (5.16) (valid for second-order systems) that

$$P.O. = 100e^{-\zeta\pi/\sqrt{1-\zeta^2}}.$$

Another useful design formula (Equation (8.37)) relates $M_{pw} = |T(\omega_r)|$ to the damping ratio:

$$M_{pw} = |T(\omega_r)| = \frac{1}{2\zeta\sqrt{1-\zeta^2}} \quad (\zeta < 0.707). \quad (8.66)$$

The relationship between the resonant frequency ω_r , the natural frequency ω_n , and the damping ratio ζ is given by (Equation (8.36))

$$\omega_r = \omega_n\sqrt{1-2\zeta^2} \quad (\zeta < 0.707). \quad (8.67)$$

We require $\zeta \geq 0.52$; therefore, we will design with $\zeta = 0.52$. Even though settling time is not a design specification for this problem, we usually attempt to make the system response as fast as possible while still meeting all the design specifications. From Equations (8.63) and (8.64) it follows that

$$\omega_n = \frac{\omega_B}{-1.1961\zeta + 1.8508} = 5.11 \text{ rad/s}. \quad (8.68)$$

Then with $\omega_n = 5.11$ rad/s and $\zeta = 0.52$ and using Equation (8.67) we compute

$$\omega_r = 3.46 \text{ rad/s}. \quad (8.69)$$

So if we had a second-order system, we would want to determine values of the control gains such that

$$\omega_n = 5.11 \text{ rad/s} \quad \text{and} \quad \zeta = 0.52,$$

which give

$$M_{pw} = 1.125 \quad \text{and} \quad \omega_r = 3.46 \text{ rad/s}.$$

Our closed-loop system is a fourth-order system and not a second-order system. So, a valid design approach would be to select K , a , b , and c so that two poles are dominant and located appropriately to meet the design specifications. This will be the approach followed here.

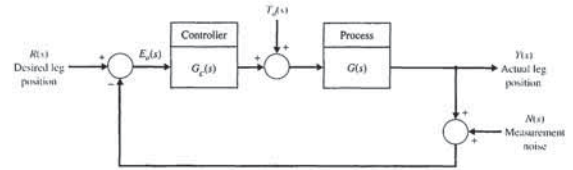


FIGURE 8.37 Control system for one leg.

The control design specifications are

Control Design Specifications

DS1 Closed-loop bandwidth greater than 1 Hz.

DS2 Percent overshoot less than 15% to a step input.

DS3 Zero steady-state tracking error to a step input.

Specifications DS1 and DS2 are intended to ensure acceptable tracking performance. Design specification DS3 is actually a nonissue in our design: the actuator/leg transfer function is a type-one system so a zero steady-state tracking error to a step input is guaranteed. We simply need to ensure that $G_c(s)G(s)$ remains at least a type-one system.

Consider the controller

$$G_c(s) = \frac{K(s^2 + as + b)}{s + c}. \quad (8.61)$$

As $c \rightarrow 0$, a PID controller is obtained with $K_P = K$, $K_D = K$, and $K_I = Kb$. We can let c be a parameter at this point and see if the additional freedom in selecting $c \neq 0$ is useful. It may be that we can simply set $c = 0$ and use the PID form. The key tuning parameters are

Select Key Tuning Parameters

K , a , b , and c .

The controller in Equation (8.61) is not the only controller that we can consider. For example, we might consider

$$G_c(s) = K \frac{s + z}{s + p}, \quad (8.62)$$

where K , z , and p are the key tuning parameters. The design of the type of controller given in Equation (8.62) will be left as a design problem at the end of the chapter.

The response of a closed-loop control system is determined predominantly by the location of the dominant poles. Our approach to the design is to determine appropriate locations for the dominant poles of the closed-loop system. We can determine the locations from the performance specifications by using second-order system approximation formulas. Once the controller parameters are obtained so that the closed-loop system has the desired dominant poles, the remaining poles are located so that their contribution to the overall response is negligible.

Choosing $d_0 = \alpha^2 \zeta^2 \omega_n^2$ is not required, but this seems to be a reasonable choice since we would like the contribution of the nondominant roots to the overall response to be quickly fading and nonoscillatory.

The desired characteristic polynomial is then

$$s^4 + [2\zeta\omega_n(1 + \alpha)]s^3 + [\omega_n^2(1 + \alpha\zeta^2(\alpha + 4))]s^2 + [2\alpha\zeta\omega_n^3(1 + \zeta^2\alpha)]s + \alpha^2\zeta^2\omega_n^4 = 0. \quad (8.72)$$

Equating the coefficients of Equations (8.70) and (8.71) yields four relationships involving K , a , b , c , and α :

$$\begin{aligned} 2\zeta\omega_n(1 + \alpha) &= 2 + c, \\ \omega_n^2(1 + \alpha\zeta^2(\alpha + 4)) &= 10 + 2c + K, \\ 2\alpha\zeta\omega_n^3(1 + \zeta^2\alpha) &= 10c + Ka, \\ \alpha^2\zeta^2\omega_n^4 &= Kb. \end{aligned}$$

In our case $\zeta = 0.52$, $\omega_n = 5.11$, and $\alpha = 12$. Thus we obtain

$$\begin{aligned} c &= 67.13 \\ K &= 1239.2 \\ a &= 5.17 \\ b &= 21.48 \end{aligned}$$

and the resulting controller is

$$G_c(s) = 1239 \frac{s^2 + 5.17s + 21.48}{s + 67.13}. \quad (8.73)$$

The step response of the closed-loop system using the controller in Equation (8.73) is shown in Figure 8.38. The percent overshoot is $P.O. = 14\%$, and the settling time is $T_s = 0.96$ second.

The magnitude plot of the closed-loop system is shown in Figure 8.39. The bandwidth is $\omega_B = 27.2$ rad/s = 4.33 Hz. This satisfies DS1 but is larger than the $\omega_B = 1$ Hz used in the design (due to the fact that our system is not a second-order system). The higher bandwidth leads us to expect a faster settling time. The peak magnitude is $M_{pw} = 1.21$. We were expecting $M_{pw} = 1.125$.

What is the steady-state response of the closed-loop system if the input is a sinusoidal input? From our previous discussions we expect that as the input frequency increases, the magnitude of the output will decrease. Two cases are presented here. In Figure 8.40 the input frequency is $\omega = 1$ rad/s. The output magnitude is approximately equal to 1 in the steady-state. In Figure 8.41 the input frequency is $\omega = 500$ rad/s. The output magnitude is less than 0.005 in the steady-state. This verifies our intuition that the system response decreases as the input sinusoidal frequency increases.

Using simple analytic methods, we obtained an initial set of controller parameters for the mobile robot. The controller thus designed proved to satisfy the design requirements. Some fine-tuning would be necessary to meet the design specifications exactly. ■

Another valid approach is to develop a second-order approximation of the fourth-order system. In the approximate transfer function, the parameters K , a , b , and c are left as variables. Following the approach discussed in Chapter 5, we can obtain an approximate transfer function $T_L(s)$ in such a way that the frequency response of $T_L(s)$ is very close to that of the original system.

The loop transfer function is

$$G_c(s)G(s) = \frac{K(s^2 + as + b)}{s(s^2 + 2s + 10)(s + c)},$$

and the closed-loop transfer function is

$$T(s) = \frac{G_c(s)G(s)}{1 + G_c(s)G(s)} \quad (8.70)$$

$$= \frac{K(s^2 + as + b)}{s^4 + (2 + c)s^3 + (10 + 2c + K)s^2 + (10c + Ka)s + Kb}.$$

The associated characteristic equation is

$$s^4 + (2 + c)s^3 + (10 + 2c + K)s^2 + (10c + Ka)s + Kb = 0. \quad (8.71)$$

The desired characteristic polynomial must also be fourth-order, but we want it to be composed of multiple factors, as follows:

$$P_d(s) = (s^2 + 2\zeta\omega_n s + \omega_n^2)(s^2 + d_1 s + d_0),$$

where ζ and ω_n are selected to meet the design specifications, and the roots of $s^2 + 2\zeta\omega_n s + \omega_n^2 = 0$ are the dominant roots. Conversely we want the roots of $s^2 + d_1 s + d_0 = 0$ to be the nondominant roots. The dominant roots should lie on a vertical line in the complex plane defined by the distance $s = -\zeta\omega_n$ away from the imaginary axis. Let

$$d_1 = 2\alpha\zeta\omega_n.$$

Then the roots of $s^2 + d_1 s + d_0 = 0$, when complex, lie on a vertical line in the complex plane defined by $s = -\alpha\zeta\omega_n$. By choosing $\alpha > 1$, we effectively move the roots to the left of the dominant roots. The larger we select α , the further the nondominant roots lie to the left of the dominant roots. A reasonable value of α is

$$\alpha = 12.$$

Also, if we select

$$d_0 = \alpha^2 \zeta^2 \omega_n^2,$$

then we obtain two real roots

$$s^2 + d_1 s + d_0 = (s + \alpha\zeta\omega_n)^2 = 0.$$

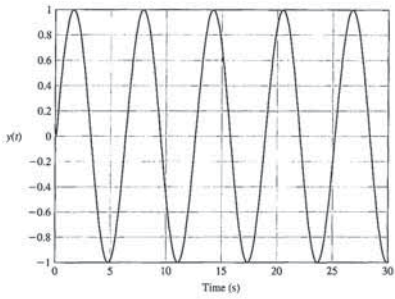


FIGURE 8.40
Output response of the closed-loop system when the input is a sinusoidal signal of frequency $\omega = 1$ rad/s.

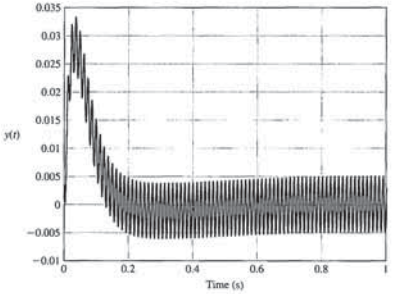


FIGURE 8.41
Output response of the closed-loop system when the input is a sinusoidal signal of frequency $\omega = 500$ rad/s.

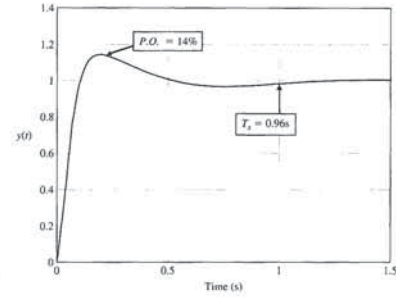


FIGURE 8.38
Step response using the controller in Equation (8.73).

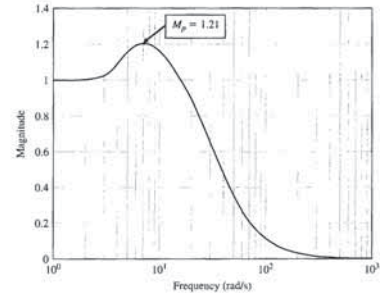


FIGURE 8.39
Magnitude plot of the closed-loop system with the controller in Equation (8.73).

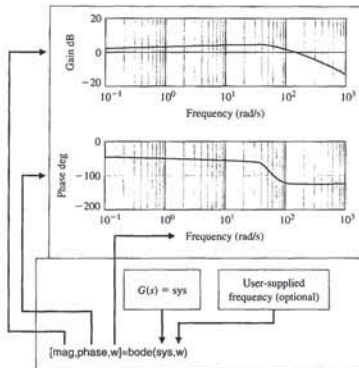


FIGURE 8.43
The bode function, given $G(s)$.

If ω is not specified, the `bode` function will automatically choose the frequency values by placing more points in regions where the frequency response is changing quickly. If the frequencies are specified explicitly, it is desirable to generate the vector ω using the `logspace` function. The `logspace` function is shown in Figure 8.44.

The Bode diagram in Figure 8.42 is generated using the script shown in Figure 8.45. The `bode` function automatically selected the frequency range. This range is user selectable using the `logspace` function. The `bode` function can be used with a state variable model, as shown in Figure 8.46. The use of the `bode` function is exactly the same as with transfer functions, except that the input is a state-space object instead of a transfer function object.

Keep in mind that our goal is to design control systems that satisfy certain performance specifications given in the time domain. Thus, we must establish a connection between the frequency response and the transient time response of a system. The relationship between specifications given in the time domain to those given in the frequency domain depends upon approximation of the system by a second-order system with the poles being the system dominant roots.

Consider the second-order system shown in Figure 8.24. The closed-loop transfer function is

$$T(s) = \frac{\omega_n^2}{s^2 + 2\zeta\omega_n s + \omega_n^2} \quad (8.74)$$

The Bode diagram magnitude characteristic associated with the closed-loop transfer function in Equation (8.75) is shown in Figure 8.25. The relationship

8.7 FREQUENCY RESPONSE METHODS USING CONTROL DESIGN SOFTWARE

This section begins with an introduction to the Bode diagram and then discusses the connection between the frequency response and performance specifications in the time domain. The section concludes with an illustrative example of designing a control system in the frequency domain.

We will cover the functions `bode` and `logspace`. The `bode` function is used to generate a Bode diagram, and the `logspace` function generates a logarithmically spaced vector of frequencies utilized by the `bode` function.

Bode Diagram. Consider the transfer function

$$G(s) = \frac{S(1 + 0.1s)}{s(1 + 0.5s)(1 + (0.6/50)s + (1/50^2)s^2)} \quad (8.74)$$

The Bode diagram corresponding to Equation (8.74) is shown in Figure 8.42. The diagram consists of the logarithmic gain in dB versus ω in one plot and the phase $\phi(\omega)$ versus ω in a second plot. As with the root locus plots, it will be tempting to rely exclusively on control design software to obtain the Bode diagrams. The software should be treated as one tool in a tool kit that can be used to design and analyze control systems. It is essential to develop the capability to obtain approximate Bode diagrams manually. There is no substitute for a clear understanding of the underlying theory.

A Bode diagram is obtained with the `bode` function, shown in Figure 8.43. The Bode diagram is automatically generated if the `bode` function is invoked without left-hand arguments. Otherwise, the magnitude and phase characteristics are placed in the workspace through the variables `mag` and `phase`. A Bode diagram is obtained with the `plot` or `semilogx` function using `mag`, `phase`, and `w`. The vector `w` contains the values of the frequency in rad/s at which the Bode diagram will be calculated.

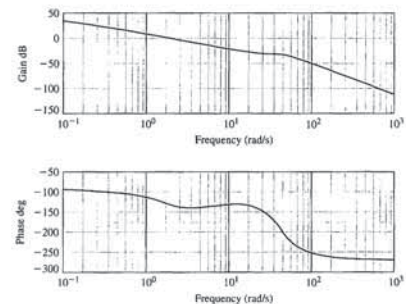


FIGURE 8.42
The Bode plot associated with Equation (8.74).

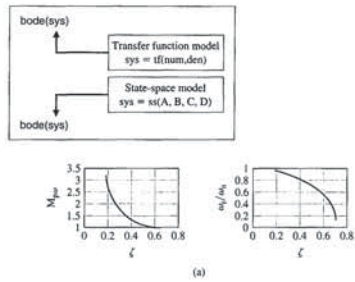


FIGURE 8.46 The Bode function with a state variable model.

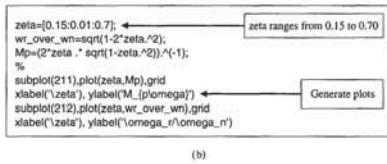


FIGURE 8.47 (a) The relationship between M_p , ω_n and ζ , ω_n for a second-order system. (b) m-file script.

EXAMPLE 8.9 Engraving machine system

Consider the block diagram model in Figure 8.32. Our objective is to select K so that the closed-loop system has an acceptable time response to a step command. A functional block diagram describing the frequency-domain design process is shown in Figure 8.48. First, we choose $K = 2$ and then iterate K if the performance is unacceptable. The script shown in Figure 8.49 is used in the design. The value of K is defined at the command level. Then the script is executed and the closed-loop Bode diagram is generated. The values of M_p and ω_n are determined by inspection from the Bode diagram. Those values are used in conjunction with Figure 8.47 to determine the corresponding values of ζ and ω_n .

Given the damping ratio, ζ , and the natural frequency, ω_n , the settling time and percent overshoot are estimated using the formulas

$$T_s \approx \frac{4}{\zeta \omega_n}, \quad P.O. \approx 100 \exp\left(-\frac{\zeta \pi}{\sqrt{1-\zeta^2}}\right)$$

If the time-domain specifications are not satisfied, then we adjust K and iterate.

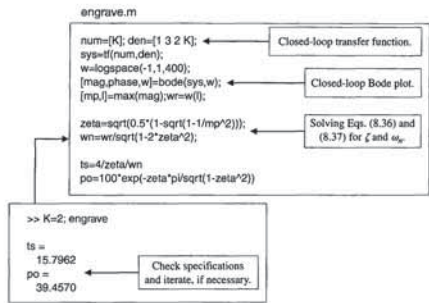


FIGURE 8.49 Script for the design of an engraving machine.

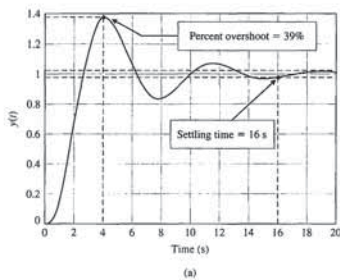


FIGURE 8.50 (a) Engraving machine step response for $K = 2$. (b) m-file script.

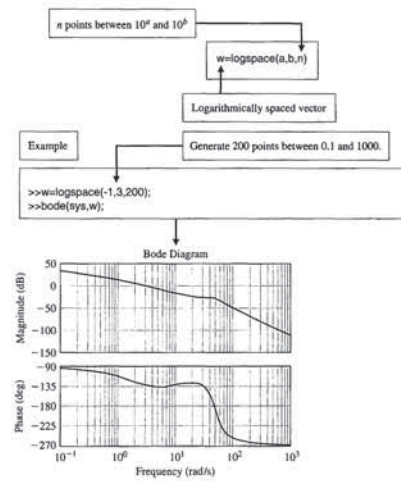


FIGURE 8.44 The logspace function.

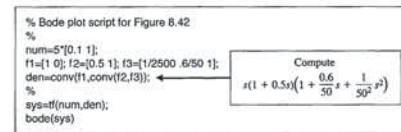


FIGURE 8.45 The script for the Bode diagram in Figure 8.42.

between the resonant frequency, ω_r , the maximum of the frequency response, M_p , and the damping ratio, ζ , and the natural frequency, ω_n , is shown in Figure 8.47 (and in Figure 8.11). The information in Figure 8.47 will be quite helpful in designing control systems in the frequency domain while satisfying time-domain specifications.

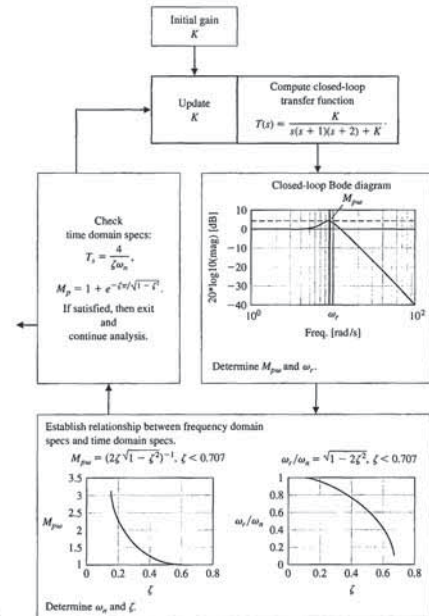


FIGURE 8.48 Frequency design functional block diagram for the engraving machine.

The values for ζ and ω_n corresponding to $K = 2$ are $\zeta = 0.29$ and $\omega_n = 0.88$. This leads to a prediction of $P.O. = 37\%$ and $T_s = 15.7$ seconds. The step response, shown in Figure 8.50, is a verification that the performance predictions are quite accurate and that the closed-loop system performs adequately.

In this example, the second-order system approximation is reasonable and leads to an acceptable design. However, the second-order approximation may not always lead directly to a good design. Fortunately, the control design software allows us to construct an interactive design facility to assist in the design process by reducing the manual computational loads while providing easy access to a host of classical and modern control tools. ■

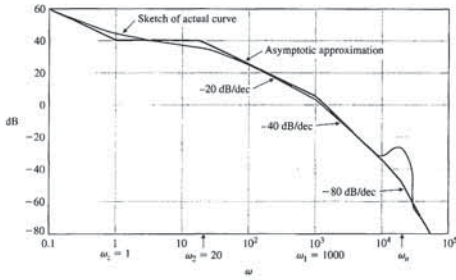


FIGURE 8.53 Sketch of the Bode diagram magnitude for the system of Figure 8.52.

Plots of the magnitude of the open-loop Bode diagram and the closed-loop Bode diagram are shown in Figure 8.54. The bandwidth of the closed-loop system is $\omega_B = 2000$ rad/s. We can estimate the settling time (with a 2% criterion) of this system using

$$T_s = \frac{4}{\zeta\omega_n}$$

where $\zeta \approx 0.8$ and $\omega_n \approx \omega_B = 2000$ rad/s. Therefore, we expect $T_s = 2.5$ ms for the system of Figure 8.52. As long as $K \leq 400$, the resonance is outside the bandwidth of the system.

8.9 SUMMARY

In this chapter, we have considered the representation of a feedback control system by its frequency response characteristics. The frequency response of a system was defined as the steady-state response of the system to a sinusoidal input signal. Several alternative forms of frequency response plots were considered. They included the polar plot of the frequency response of a system $G(j\omega)$ and logarithmic plots, often called Bode plots. The value of the logarithmic measure was also illustrated. The ease of obtaining a Bode plot for the various factors of $G(j\omega)$ was noted, and an example was considered in detail. The asymptotic approximation for

8.8 SEQUENTIAL DESIGN EXAMPLE: DISK DRIVE READ SYSTEM



The disk drive uses a flexure suspension to hold the reader head mount, as shown in Figure 2.75. As noted in Section 3.10, this flexure may be modeled by a spring and mass, as shown in Figure 3.40. In this chapter, we will include the effect of the flexure within the model of the motor-load system [22].

We model the flexure with the mounted head as a mass M , a spring k , and a sliding friction b , as shown in Figure 8.51. Here, we assume that the force $u(t)$ is exerted on the flexure by the arm, where the transfer function of a spring-mass-damper was developed in Chapter 2, where

$$\frac{Y(s)}{U(s)} = G_3(s) = \frac{\omega_n^2}{s^2 + 2\zeta\omega_n s + \omega_n^2} = \frac{1}{1 + (2\zeta s/\omega_n) + (s/\omega_n)^2}$$

A typical flexure and head has $\zeta = 0.3$ and a natural resonance at $f_n = 3000$ Hz. Therefore, $\omega_n = 18.85 \times 10^3$ as shown in the model of the system (see Figure 8.52).

First, we sketch the magnitude characteristics for the open-loop Bode diagram. The Bode diagram sketch is shown in Figure 8.53. Note that the actual plot has a 10-dB gain (over the asymptotic plot) at the resonance $\omega = \omega_n$, as shown in the sketch. The sketch is a plot of

$$20 \log |K(j\omega + 1)G_1(j\omega)G_2(j\omega)G_3(j\omega)|,$$

for the system of Figure 8.52 when $K = 400$. Note the resonance at ω_n . Clearly, we wish to avoid exciting this resonance.

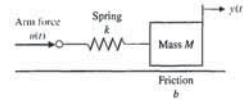


FIGURE 8.51 Spring, mass, friction model of flexure and head.

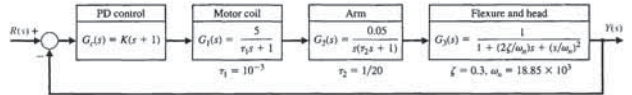


FIGURE 8.52 Disk drive head position control, including effect of flexure head mount.

sketching the Bode diagram simplifies the computation considerably. A summary of fifteen typical Bode plots is shown in Table 8.5. Several performance specifications in the frequency domain were discussed; among them were the maximum magnitude M_{pw} and the resonant frequency ω_r . The relationship between the Bode diagram plot and the system error constants (K_p and K_v) was noted. Finally, the log-magnitude versus phase diagram was considered for graphically representing the frequency response of a system.

Table 8.5 Bode Diagram Plots for Typical Transfer Functions

$G(s)$	Bode Diagram	$G(s)$	Bode Diagram
1. $\frac{K}{s\tau_1 + 1}$		7. $\frac{K(s\tau_1 + 1)}{s(s\tau_1 + 1)(s\tau_2 + 1)}$	
2. $\frac{K}{(s\tau_1 + 1)(s\tau_2 + 1)}$		8. $\frac{K}{s^2}$	
3. $\frac{K}{(s\tau_1 + 1)(s\tau_2 + 1)(s\tau_3 + 1)}$		9. $\frac{K}{s^2(s\tau_1 + 1)}$	

Section 8.9 Summary

605

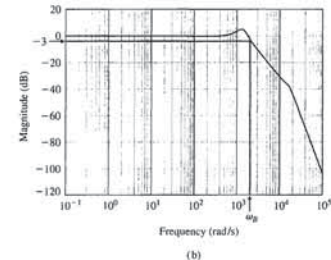
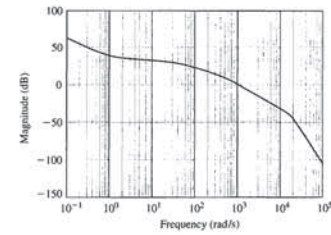
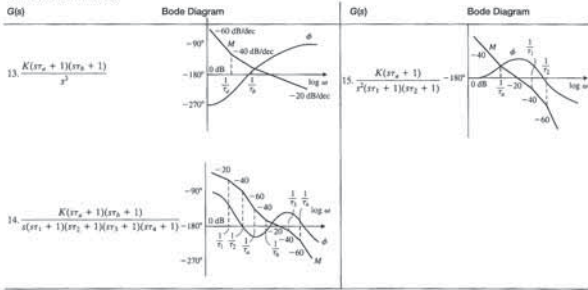


FIGURE 8.54 The magnitude Bode plot for (a) the open-loop transfer function and (b) the closed-loop system.

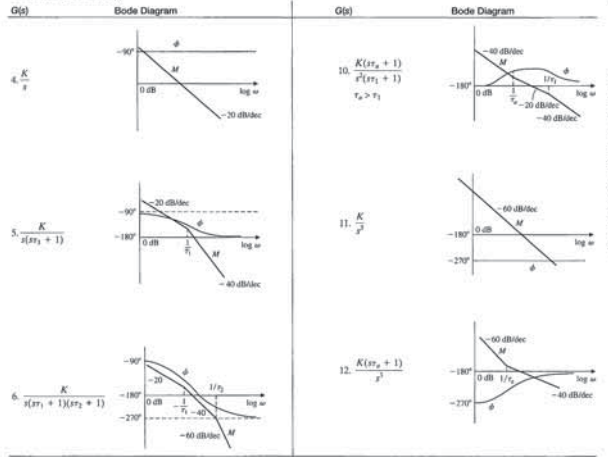
Table 8.5 (continued)



Section 8.9 Summary

607

Table 8.5 (continued)



Skills Check

609

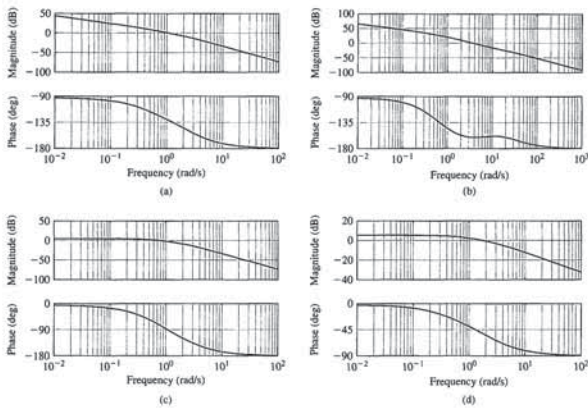


FIGURE 8.56 Bode plot selections.

In Problems 9 and 10, consider the feedback system in Figure 8.55 with the loop transfer function

$$L(s) = G(s)G_c(s) = \frac{50}{s^2 + 12s + 20}$$

- The break frequencies on the Bode plot are
 - $\omega = 1$ and $\omega = 12$ rad/s
 - $\omega = 2$ and $\omega = 10$ rad/s
 - $\omega = 20$ and $\omega = 1$ rad/s
 - $\omega = 12$ and $\omega = 20$ rad/s
- The slope of the asymptotic plot at very low ($\omega \ll 1$) and high ($\omega \gg 10$) frequencies are, respectively:
 - At low frequency: slope = 20 dB/decade and at high frequency: slope = 20 dB/decade
 - At low frequency: slope = 0 dB/decade and at high frequency: slope = -20 dB/decade
 - At low frequency: slope = 0 dB/decade and at high frequency: slope = -40 dB/decade
 - At low frequency: slope = -20 dB/decade and at high frequency: slope = -20 dB/decade

608

Chapter 8 Frequency Response Methods

SKILLS CHECK

In this section, we provide three sets of problems to test your knowledge: True or False, Multiple Choice, and Word Match. To obtain direct feedback, check your answers with the answer key provided at the conclusion of the end-of-chapter problems. Use the block diagram in Figure 8.55 as specified in the various problem statements.

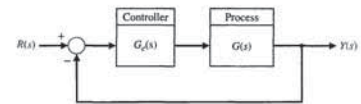


FIGURE 8.55 Block diagram for the Skills Check.

In the following **True or False** and **Multiple Choice** problems, circle the correct answer.

- The frequency response represents the steady-state response of a stable system to a sinusoidal input signal at various frequencies. True or False
- A plot of the real part of $G(j\omega)$ versus the imaginary part of $G(j\omega)$ is called a Bode plot. True or False
- A transfer function is termed minimum phase if all its zeros lie in the right-hand s -plane. True or False
- The resonant frequency and bandwidth can be related to the speed of the transient response. True or False
- One advantage of frequency response methods is the ready availability of sinusoidal test signals for various ranges of frequencies and amplitudes. True or False
- Consider the stable system represented by the differential equation $\ddot{x}(t) + 3\dot{x}(t) = u(t)$, where $u(t) = \sin 3t$. Determine the phase lag for this system.
 - $\phi = 0^\circ$
 - $\phi = -45^\circ$
 - $\phi = -60^\circ$
 - $\phi = -180^\circ$

In Problems 7 and 8, consider the feedback system in Figure 8.55 with the loop transfer function

$$L(s) = G(s)G_c(s) = \frac{8(s + 1)}{s(2 + s)(2 + 3s)}$$

- The Bode diagram of this system corresponds to which plot in Figure 8.56?
- Determine the frequency at which the gain has unit magnitude and compute the phase angle at that frequency.
 - $\omega = 1$ rad/s, $\phi = -82^\circ$
 - $\omega = 1.26$ rad/s, $\phi = -133^\circ$
 - $\omega = 1.26$ rad/s, $\phi = 133^\circ$
 - $\omega = 4.2$ rad/s, $\phi = -160^\circ$

- The resonant frequency, ω_r , and the bandwidth, ω_b , are:
- $\omega_r = 1.59 \text{ rad/s}$, $\omega_b = 1.86 \text{ rad/s}$
 - $\omega_r = 3.26 \text{ rad/s}$, $\omega_b = 16.64 \text{ rad/s}$
 - $\omega_r = 12.52 \text{ rad/s}$, $\omega_b = 3.25 \text{ rad/s}$
 - $\omega_r = 5.49 \text{ rad/s}$, $\omega_b = 11.6 \text{ rad/s}$

For Problems 14 and 15, consider the frequency response of a process $G(j\omega)$ depicted in Figure 8.58.

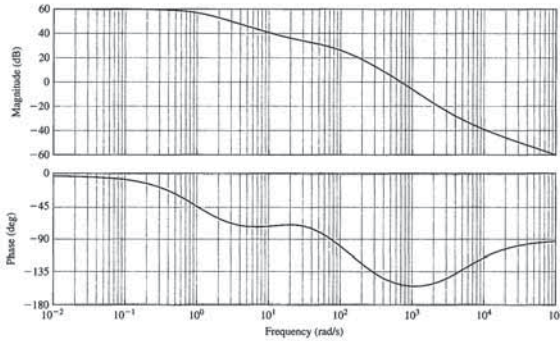


FIGURE 8.58 Bode plot for $G(j\omega)$.

14. Determine the system type (that is, the number of integrators, N):

- $N = 0$
- $N = 1$
- $N = 2$
- $N > 2$

15. The transfer function corresponding to the Bode plot in Figure 8.58 is:

- $G(s) = \frac{100(s + 10)(s + 5000)}{s(s + 5)(s + 6)}$
- $G(s) = \frac{100}{(s + 1)(s + 20)}$
- $G(s) = \frac{100}{(s + 1)(s + 50)(s + 200)}$
- $G(s) = \frac{100(s + 20)(s + 5000)}{(s + 1)(s + 50)(s + 200)}$

Exercises

EXERCISES

E8.1 Increased track densities for computer disk drives necessitate careful design of the head positioning control [1]. The loop transfer function is

$$L(s) = G_c(s)G(s) = \frac{K}{(s + 2)^2}$$

Plot the frequency response for this system when $K = 4$. Calculate the phase and magnitude at $\omega = 0.5, 1, 2, 4$, and ∞ .

Answer: $|L(j0.5)| = 0.94$ and $\angle L(j0.5) = -28.1^\circ$.

E8.2 A tendon-operated robotic hand can be implemented using a pneumatic actuator [8]. The actuator can be represented by

$$G(s) = \frac{5000}{(s + 70)(s + 500)}$$

Plot the frequency response of $G(j\omega)$. Show that the magnitude of $G(j\omega)$ is -17 dB at $\omega = 10$ and -27.1 dB at $\omega = 200$. Show also that the phase is -138.7° at $\omega = 700$.

E8.3 A robotic arm has a joint-control loop transfer function

$$L(s) = G_c(s)G(s) = \frac{300(s + 100)}{s(s + 10)(s + 40)}$$

Show that the frequency equals 28.3 rad/s when the phase angle of $L(j\omega)$ is -180° . Find the magnitude of $L(j\omega)$ at that frequency.

Answer: $|L(j28.3)| = -2.5 \text{ dB}$

E8.4 The frequency response for a process of the form

$$G(s) = \frac{Ks}{(s + a)(s^2 + 20s + 100)}$$

is shown in Figure E8.4. Determine K and a by examining the frequency response curves.

E8.5 The magnitude plot of a transfer function

$$G(s) = \frac{K(1 + 0.5s)(1 + as)}{s(1 + s/8)(1 + bs)(1 + s/36)}$$

is shown in Figure E8.5. Determine K , a , and b from the plot.

Answer: $K = 8$, $a = 1/4$, $b = 1/24$

E8.6 Several studies have proposed an extravehicular robot that could move around in a NASA space station and perform physical tasks at various worksites [9]. The arm is controlled by a unity feedback control with loop transfer function

$$L(s) = G_c(s)G(s) = \frac{K}{s(s/5 + 1)(s/100 + 1)}$$

Draw the Bode diagram for $K = 20$, and determine the frequency when $20 \log |L(j\omega)|$ is 0 dB .

E8.7 Consider a system with a closed-loop transfer function

$$T(s) = \frac{Y(s)}{R(s)} = \frac{4}{(s^2 + s + 1)(s^2 + 0.4s + 4)}$$

This system will have no steady-state error for a step input. (a) Plot the frequency response, noting the two peaks in the magnitude response. (b) Predict the time response to a step input, noting that the system has four poles and cannot be represented as a dominant second-order system. (c) Plot the step response.

E8.8 A feedback system has a loop transfer function

$$L(s) = G_c(s)G(s) = \frac{100(s - 1)}{s^2 + 25s + 100}$$

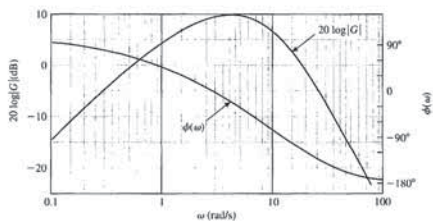


FIGURE E8.4 Bode diagram.

11. Consider the Bode plot in Figure 8.57.

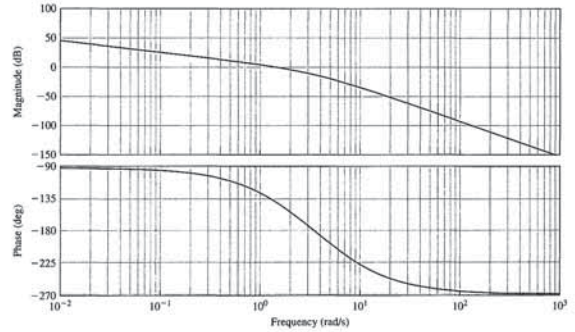


FIGURE 8.57 Bode plot for unknown system.

Which loop transfer function $L(s) = G_c(s)G(s)$ corresponds to the Bode plot in Figure 8.57?

- $L(s) = G_c(s)G(s) = \frac{100}{s(s + 5)(s + 6)}$
- $L(s) = G_c(s)G(s) = \frac{24}{s(s + 2)(s + 6)}$
- $L(s) = G_c(s)G(s) = \frac{24}{s^2(s + 6)}$
- $L(s) = G_c(s)G(s) = \frac{10}{s^2 + 0.5s + 10}$

12. Suppose that one design specification for a feedback control system requires that the percent overshoot to a step input be less than 10%. The corresponding specification in the frequency domain is

- $M_{pw} \leq 0.55$
- $M_{pw} \leq 0.59$
- $M_{pw} \leq 1.05$
- $M_{pw} \leq 1.27$

13. Consider the feedback control system in Figure 8.55 with

$$G_c(s)G(s) = \frac{100}{s(s + 11.8)}$$

In the following Word Match problems, match the term with the definition by writing the correct letter in the space provided.

- | | | |
|--|---|-------|
| a. Laplace transform pair | The logarithm of the magnitude of the transfer function and the phase are plotted versus the logarithm of ω , the frequency. | _____ |
| b. Decibel (dB) | The logarithm of the magnitude of the transfer function, $20 \log_{10} G(j\omega) $. | _____ |
| c. Fourier transform | A plot of the real part of $G(j\omega)$ versus the imaginary part of $G(j\omega)$. | _____ |
| d. Bode plot | The steady-state response of a system to a sinusoidal input signal. | _____ |
| e. Transfer function in the frequency domain | All the zeros of a transfer function lie in the left-hand side of the s -plane. | _____ |
| f. Decade | The frequency at which the frequency response has declined 3 dB from its low frequency value. | _____ |
| g. Dominant roots | The frequency at which the maximum value of the frequency response of a complex pair of poles is attained. | _____ |
| h. All-pass network | The frequency of natural oscillation that would occur for two complex poles if the damping were equal to zero. | _____ |
| i. Logarithmic magnitude | Transfer functions with zeros in the right-hand s -plane. | _____ |
| j. Natural frequency | The frequency at which the asymptotic approximation of the frequency response for a pole (or zero) changes slope. | _____ |
| k. Fourier transform pair | The transformation of a function of time into the frequency domain. | _____ |
| l. Minimum phase | The ratio of the output to the input signal where the input is a sinusoid. | _____ |
| m. Bandwidth | The units of the logarithmic gain. | _____ |
| n. Frequency response | A pair of complex poles will result in a maximum value for the frequency response occurring at the resonant frequency. | _____ |
| o. Resonant frequency | A nonminimum phase system that passes all frequencies with equal gain. | _____ |
| p. Break frequency | A factor of ten in frequency. | _____ |
| q. Polar plot | The roots of the characteristic equation that represent or dominate the closed-loop transient response. | _____ |
| r. Maximum value of the frequency response | A pair of functions, one in the time domain, and the other in the frequency domain, and both related by the Fourier transform. | _____ |
| s. Nonminimum phase | A pair of functions, one in the time domain, and the other in the frequency domain, and both related by the Laplace transform. | _____ |

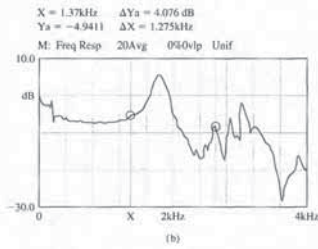


FIGURE E8.10 (a) Photo showing the Signal Analyzer 35670A used to analyze mechanical vibration in the cockpit of an automobile. (b) Frequency response. (Courtesy of the Agilent Technologies Foundation.)

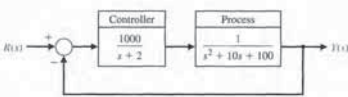


FIGURE E8.11 Unity feedback system.

Problems

- response. (b) Compare the frequency response of the twin-T and bridged-T networks when $Q = 10$.
- P8.4** A control system for controlling the pressure in a closed chamber is shown in Figure P8.4. The transfer function for the measuring element is
- $$H(s) = \frac{150}{s^2 + 15s + 150}$$
- and the transfer function for the valve is
- $$G_v(s) = \frac{1}{(0.1s + 1)(s/20 + 1)}$$
- The controller transfer function is
- $$G_c(s) = 2s + 1.$$
- Obtain the frequency response characteristics for the loop transfer function
- $$G_c(s)G_v(s)H(s) \cdot [1/s].$$
- P8.5** The robot industry in the United States is growing at a rate of 30% a year [8]. A typical industrial robot has degrees of freedom. A unity feedback position control system for a force-sensing joint has a loop transfer function

- $$G_c(s)G(s) = \frac{K}{(1 + s/4)(1 + s)(1 + s/20)(1 + s/80)}$$
- where $K = 10$. Sketch the Bode diagram of this system.
- P8.6** The asymptotic log-magnitude curves for two transfer functions are given in Figure P8.6. Sketch the corresponding asymptotic phase shift curves for each system. Determine the transfer function for each system. Assume that the systems have minimum phase transfer functions.
- P8.7** Driverless vehicles can be used in warehouses, airports, and many other applications. These vehicles follow a wire embedded in the floor and adjust the steerable front wheels in order to maintain proper direction, as shown in Figure P8.7(a) [10]. The sensing coils, mounted on the front wheel assembly, detect an error in the direction of travel and adjust the steering. The overall control system is shown in Figure P8.7(b). The loop transfer function is
- $$L(s) = \frac{K}{s(s + \pi)^2} = \frac{K_v}{s(s/\pi + 1)^2}$$
- We want the bandwidth of the closed-loop system to exceed 2π rad/s. (a) Set $K_v = 2\pi$ and sketch the Bode diagram. (b) Using the Bode diagram, obtain the logarithmic-magnitude versus phase angle curve.

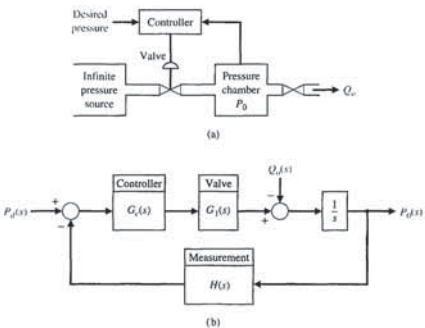


FIGURE P8.4 (a) Pressure controller. (b) Block diagram model.

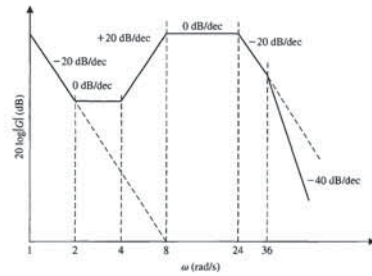


FIGURE E8.5 Bode diagram.

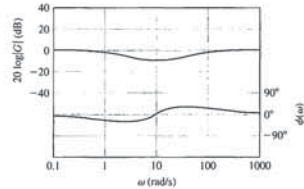


FIGURE E8.9 Bode diagram.

- (a) Determine the corner frequencies (break frequencies) for the Bode plot. (b) Determine the slope of the asymptotic plot at very low frequencies and at high frequencies. (c) Sketch the Bode magnitude plot.
- E8.9** The Bode diagram of a system is shown in Figure E8.9. Determine the transfer function $G(s)$.
- E8.10** The dynamic analyzer shown in Figure E8.10(a) can be used to display the frequency response of a system. Also shown is the signal analyzer used to measure the mechanical vibration in the cockpit of an automobile. Figure E8.10(b) shows the actual frequency response of a system. Estimate the poles and zeros of the device. Note $X = 1.37$ kHz at the first cursor, and $\Delta X = 1.257$ kHz at the second cursor.
- E8.11** Consider the feedback control system in Figure E8.11. Sketch the Bode plot of $G(s)$ and determine the crossover frequency, that is, the frequency when $20 \log_{10}|G(j\omega)| = 0$ dB.
- E8.12** Consider the system represented in state variable form
- $$\dot{\mathbf{x}} = \begin{bmatrix} 0 & 1 \\ -2 & -3 \end{bmatrix} \mathbf{x} + \begin{bmatrix} 0 \\ 5 \end{bmatrix} u$$
- $$y = [1 \ -1] \mathbf{x} + [0]u$$
- (a) Determine the transfer function representation of the system. (b) Sketch the Bode plot.
- E8.13** Determine the bandwidth of the feedback control system in Figure E8.13.
- E8.14** Consider the nonunity feedback system in Figure E8.14, where the controller gain is $K = 2$. Sketch the Bode plot of the loop transfer function. Determine the

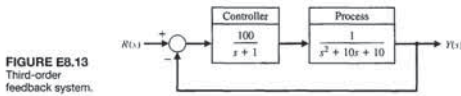


FIGURE E8.13 Third-order feedback system.

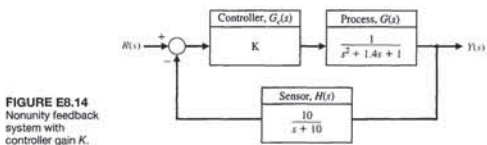


FIGURE E8.14 Nonunity feedback system with controller gain K .

- phase of the loop transfer function when the magnitude $20 \log_{10}|L(j\omega)| = 0$ dB. Recall that the loop transfer function is $L(s) = G_c(s)G(s)H(s)$.
- E8.15** Consider the single-input, single-output system described by
- $$\dot{\mathbf{x}}(t) = \mathbf{A}\mathbf{x}(t) + \mathbf{B}u(t)$$
- $$y(t) = \mathbf{C}\mathbf{x}(t)$$
- where
- $$\mathbf{A} = \begin{bmatrix} 0 & 1 \\ -6 - K & -1 \end{bmatrix}, \mathbf{B} = \begin{bmatrix} 0 \\ 1 \end{bmatrix}, \mathbf{C} = [5 \ 3].$$
- Compute the bandwidth of the system for $K = 1, 2$, and 10. As K increases, does the bandwidth increase or decrease?

PROBLEMS

- P8.1** Sketch the polar plot of the frequency response for the following loop transfer functions:
- (a) $G_c(s)G(s) = \frac{1}{(1 + 0.25s)(1 + 3s)}$
- (b) $G_c(s)G(s) = \frac{5(s^2 + 1.4s + 1)}{(s - 1)^2}$
- (c) $G_c(s)G(s) = \frac{s - 8}{s^2 + 6s + 8}$
- (d) $G_c(s)G(s) = \frac{20(s + 8)}{s(s + 2)(s + 4)}$
- P8.2** Sketch the Bode diagram representation of the frequency response for the transfer functions given in Problem P8.1.
- P8.3** A rejection network that can be used instead of the twin-T network of Example 8.4 is the bridged-T network shown in Figure P8.3. The transfer function of this network is

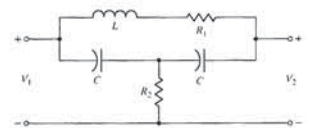


FIGURE P8.3 Bridged-T network.

$$G(s) = \frac{s^2 + \omega_n^2}{s^2 + 2(\omega_n/Q)s + \omega_n^2}$$

(can you show this?), where $\omega_n^2 = 2/LC$, $Q = \omega_n L/R_1$, and R_2 is adjusted so that $R_2 = (\omega_n L)^2/4R_1$ [3]. (a) Determine the pole-zero pattern and, using the vector approach, evaluate the approximate frequency

FIGURE P8.8
Second-order unity feedback system.

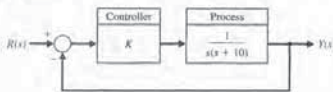
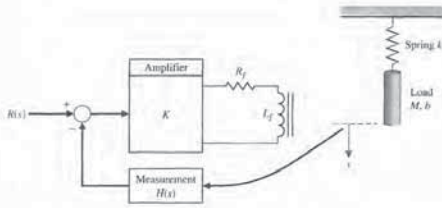


FIGURE P8.10
Linear actuator control.



and $L_f = 0.2$ H. The mass of the load is 0.1 kg, and the friction is 0.2 N·s/m. The spring constant is equal to 0.4 N/m. (a) Determine the gain K necessary to maintain a steady-state error for a step input less than 1%. That is, K_s must be greater than 99. (b) Sketch the Bode diagram of the loop transfer function, $L(s) = G(s)H(s)$. (c) Sketch the logarithmic magnitude versus phase angle curve for $L(j\omega)$. (d) Sketch the Bode diagram for the closed-loop transfer function, $Y(j\omega)/R(j\omega)$. Determine M_{pw} , ω_p , and the bandwidth.

P8.11 Automatic steering of a ship would be a particularly useful application of feedback control theory [20]. In the case of heavily traveled seas, it is important to maintain the motion of the ship along an accurate track. An automatic system would be more likely to maintain a smaller error from the desired heading than a helmsman who recorrects at infrequent intervals. A mathematical model of the steering system has been developed for a ship moving at a constant velocity and for small deviations from the desired track. For a large tanker, the transfer function of the ship is

$$G(s) = \frac{E(s)}{\delta(s)} = \frac{0.164(s + 0.2)(-s + 0.32)}{s^2(s + 0.25)(s - 0.009)}$$

where $E(s)$ is the Laplace transform of the deviation of the ship from the desired heading and $\delta(s)$ is the Laplace transform of the angle of deflection of the steering rudder. Verify that the frequency response of the ship, $E(j\omega)/\delta(j\omega)$, is that shown in Figure P8.11.

P8.12 The block diagram of a feedback control system is shown in Figure P8.12(a). The transfer functions of the blocks are represented by the frequency response curves shown in Figure P8.12(b). (a) When G_1 is disconnected from the system, determine the damping ratio ζ of the system. (b) Connect G_1 and determine the damping ratio ζ . Assume that the systems have minimum phase transfer functions.

P8.13 A position control system may be constructed by using an AC motor and AC components, as shown in Figure P8.13. The synchro and control transformer may be considered to be a transformer with a rotating winding. The synchro position detector rotor turns with the load through an angle θ_p . The synchro motor is energized with an AC reference voltage, for example, 115 volts, 60 Hz. The input signal or command is $R(s) = \theta_m(s)$ and is applied by turning the rotor of the control transformer. The AC two-phase motor operates as a result of the amplified error signal. The advantages of an AC control system are (1) freedom from DC drift effects and (2) the simplicity and accuracy of AC components. To measure the open-loop frequency response, we simply disconnect X from Y and X' from Y' and then apply a sinusoidal modulation signal generator to the $Y - Y'$ terminals and measure the response at $X - X'$. (The error $(\theta_p - \theta_i)$ will be adjusted to zero before applying the AC generator.) The resulting frequency response of the loop transfer function $L(j\omega) = G_c(j\omega)G(j\omega)H(j\omega)$ is

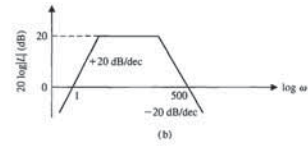
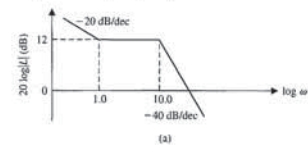


FIGURE P8.6
Log-magnitude curves.

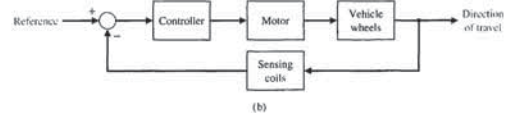
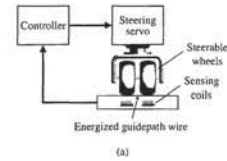


FIGURE P8.7
Steerable wheel control.

P8.8 A feedback control system is shown in Figure P8.8. The specification for the closed-loop system requires that the overshoot to a step input be less than 15%. (a) Determine the corresponding specification M_{pw} in the frequency domain for the closed-loop transfer function

$$\frac{Y(j\omega)}{R(j\omega)} = T(j\omega)$$

(b) Determine the resonant frequency ω_p . (c) Determine the bandwidth of the closed-loop system.

P8.9 Sketch the logarithmic-magnitude versus phase angle curves for the transfer functions (a) and (b) of Problem P8.1.

P8.10 A linear actuator is used in the system shown in Figure P8.10 to position a mass M . The actual position of the mass is measured by a slide wire resistor, and thus $H(s) = 1.0$. The amplifier gain is selected so that the steady-state error of the system is less than 1% of the magnitude of the position reference $R(s)$. The actuator has a field coil with a resistance $R_f = 0.1 \Omega$

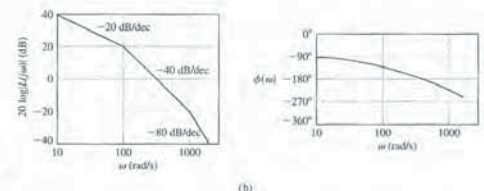
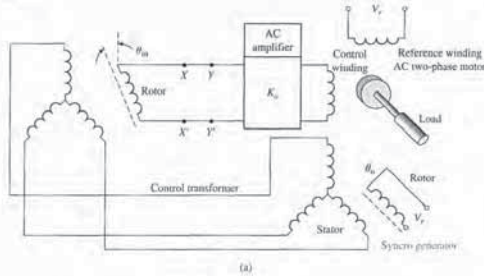


FIGURE P8.13
(a) AC motor control.
(b) Frequency response.

shown in Figure P8.13(b). Determine the transfer function $L(j\omega)$. Assume that the system has a minimum phase transfer function.

P8.14 A bandpass amplifier may be represented by the circuit model shown in Figure P8.14 [3]. When $R_1 = R_2 = 1 \text{ k}\Omega$, $C_1 = 100 \text{ pF}$, $C_2 = 1 \mu\text{F}$, and $K = 100$, show that

$$G(s) = \frac{10^3}{(s + 1000)(s + 10^5)}$$

(a) Sketch the Bode diagram of $G(j\omega)$. (b) Find the midband gain (in dB). (c) Find the high and low frequency -3 dB points.

P8.15 To determine the transfer function of a process $G(s)$, the frequency response may be measured using a sinusoidal input. One system yields the data in the following table:

ω , rad/s	$ G(j\omega) $	Phase, degrees
0.1	50	-90
1	5.02	-92.4
2	2.57	-96.2
4	1.36	-100
5	1.17	-104
6.3	1.03	-110
8	0.97	-120
10	0.97	-143
12.5	0.74	-169
20	0.13	-245
31	0.026	-258

Determine the transfer function $G(s)$.
P8.16 The space shuttle has been used to repair satellites and the Hubble telescope. Figure P8.16 illustrates how

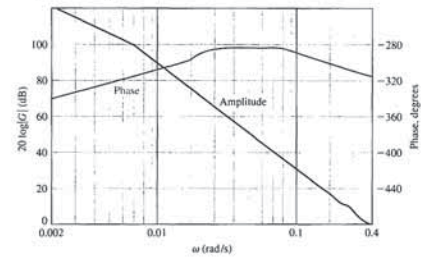


FIGURE P8.11
Frequency response of ship control system.

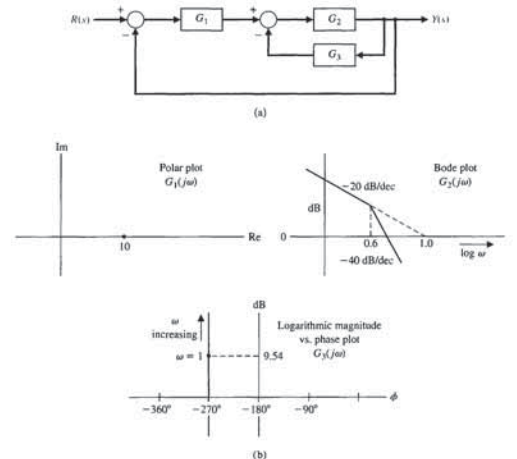


FIGURE P8.12
Feedback system.

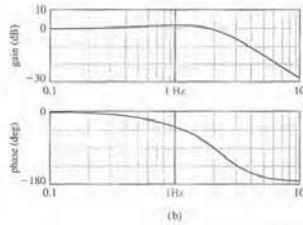
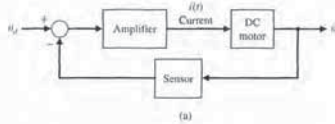


FIGURE P8.19 (a) Motor controller. (b) Measured plot.

P8.20 For the successful development of space projects, robotics and automation will be a key technology. Autonomous and dexterous space robots can reduce the workload of astronauts and increase operational efficiency in many missions. Figure P8.20 shows a concept called a free-flying robot [9, 13]. A major characteristic of space robots, which clearly distinguishes them from robots operated on earth, is the lack of a fixed base. Any motion of the manipulator arm will induce reaction forces and moments in the base, which disturb its position and attitude.



FIGURE P8.20 A space robot with three arms, shown capturing a satellite.

The control of one of the joints of the robot can be represented by the loop transfer function

$$L(s) = G_c(s)G(s) = \frac{823(s + 9.8)}{s^2 + 22s + 471}$$

(a) Sketch the Bode diagram of $L(j\omega)$. (b) Determine the maximum value of $L(j\omega)$, the frequency at which it occurs, and the phase at that frequency.

P8.21 Low-altitude wind shear is a major cause of air carrier accidents in the United States. Most of these accidents have been caused by either microbursts (small-scale, low-altitude, intense thunderstorm downdrafts that impact the surface and cause strong divergent outflows of wind) or by the gust front at the leading edge of expanding thunderstorm outflows. A microburst encounter is a serious problem for either landing or departing aircraft, because the aircraft is at low altitudes and is traveling at just over 25% above its stall speed [12].

The design of the control of an aircraft encountering wind shear after takeoff may be treated as a problem of stabilizing the climb rate about a desired value of the climb rate. The resulting controller uses only climb rate information.

The standard negative unity feedback system of Figure 8.24 has a loop transfer function

$$G_c(s)G(s) = \frac{-200s^2}{s^4 + 14s^2 + 44s + 40}$$

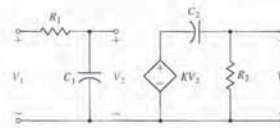


FIGURE P8.14 Bandpass amplifier.

a crew member, with his feet strapped to the platform on the end of the shuttle's robotic arm, used his arms to stop the satellite's spin. The control system of the robotic arm has a closed-loop transfer function

$$\frac{Y(s)}{R(s)} = \frac{60.2}{s^2 + 12.1s + 60.2}$$

(a) Determine the response $y(t)$ to a unit step input, $R(s) = 1/s$. (b) Determine the bandwidth of the system.

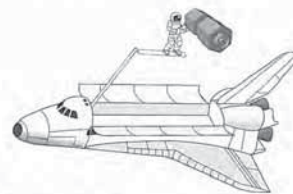


FIGURE P8.16 Satellite repair.

P8.17 The experimental Oblique Wing Aircraft (OWA) has a wing that pivots, as shown in Figure P8.17. The wing is in the normal unskewed position for low speeds and can move to a skewed position for improved supersonic flight [1]. The aircraft control system loop transfer function is

$$G_c(s)G(s) = \frac{4(0.5s + 1)}{s(2s + 1) \left[\left(\frac{s}{8} \right)^2 + \left(\frac{s}{20} \right) + 1 \right]}$$

(a) Sketch the Bode diagram. (b) Find the frequency ω_0 when the magnitude is 0 dB, and find the frequency ω_1 when the phase is -180° .

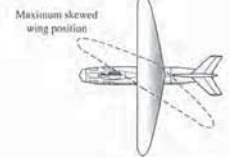


FIGURE P8.17 The Oblique Wing Aircraft, top and side views.

P8.18 Remote operation plays an important role in hostile environments, such as those in nuclear or high-temperature environments and in deep space. In spite of the efforts of many researchers, a teleoperation system that is comparable to the human's direct operation has not been developed. Research engineers have been trying to improve teleoperations by feeding back rich sensory information acquired by the robot to the operator with a sensation of presence. This concept is called tele-existence or telepresence [9].

The tele-existence master-slave system consists of a master system with a visual and auditory sensation of presence, a computer control system, and an anthropomorphic slave robot mechanism with an arm having seven degrees of freedom and a locomotion mechanism. The operator's head movement, right arm movement, right hand movement, and other auxiliary motion are measured by the master system. A specially designed stereo visual and auditory input system mounted on the neck mechanism of the slave robot gathers visual and auditory information from the remote environment. These pieces of information are sent back to the master system and are applied to the specially designed stereo display system to evoke the sensation of presence of the operator. The locomotion control system has the loop transfer function

$$G_c(s)G(s) = \frac{12(s + 0.5)}{s^2 + 13s + 30}$$

Obtain the Bode diagram for $G_c(j\omega)G(j\omega)$ and determine the frequency when $20 \log |G_c(j\omega)G(j\omega)|$ is very close to 0 dB.

P8.19 A DC motor controller used extensively in automobiles is shown in Figure P8.19(a). The measured plot of $\Theta(s)/I(s)$ is shown in Figure P8.19(b). Determine the transfer function of $\Theta(s)/I(s)$.

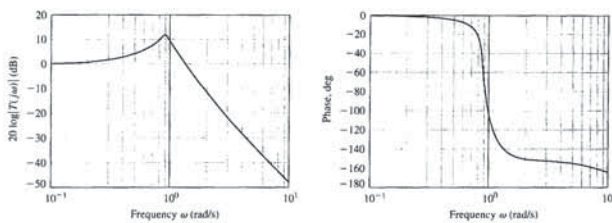


FIGURE P8.24 Bode plot of a closed-film transport system.

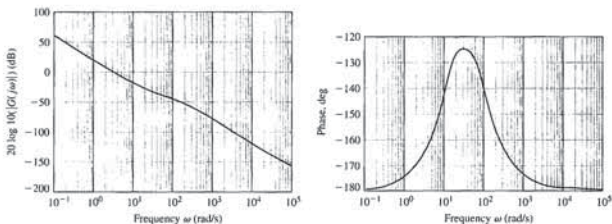


FIGURE P8.25 Bode plot of a unity feedback system.

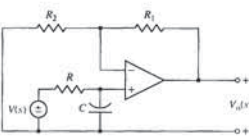


FIGURE P8.26 An op-amp circuit.

Note the negative gain in $G_c(s)G(s)$. This system represents the control system for the climb rate. Sketch the Bode diagram and determine gain (in dB) when the phase is -180° .

P8.22 The frequency response of a process $G(j\omega)$ is shown in Figure P8.22. Determine $G(s)$.

P8.23 The frequency response of a process $G(j\omega)$ is shown in Figure P8.23. Deduce the type number (number of integrations) for the system. Determine the transfer function of the system, $G(s)$. Calculate the error to a unit step input.

P8.24 The Bode diagram of a closed-loop film transport system is shown in Figure P8.24 [17]. Assume that the system transfer function $T(s)$ has two dominant complex conjugate poles. (a) Determine the best second-order model for the system. (b) Determine the system bandwidth. (c) Predict the percent overshoot and settling time (with a 2% criterion) for a step input.

P8.25 A unity feedback closed-loop system has a steady-state error equal to $A/10$, where the input is

$r(t) = A t^2/2$. The Bode plot of the magnitude and phase angle versus ω is shown in Figure P8.25 for $G(j\omega)$. Determine the transfer function $G(s)$.

P8.26 Determine the transfer function of the op-amp circuit shown in Figure P8.26. Assume an ideal op-amp. Plot the frequency response when $R = 10 \text{ k}\Omega$, $R_1 = 9 \text{ k}\Omega$, $R_2 = 1 \text{ k}\Omega$, and $C = 1 \mu\text{F}$.

P8.27 A unity feedback system has the loop transfer function

$$L(s) = G_c(s)G(s) = \frac{K(s + 50)}{s^2 + 10s + 25}$$

Sketch the Bode plot of the loop transfer function and indicate how the magnitude $20 \log |L(j\omega)|$ plot varies as K varies. Develop a table for $K = 0.75, 2, \text{ and } 10$, and for each K determine the crossover frequency (ω_c for $20 \log |L(j\omega_c)| = 0 \text{ dB}$), the magnitude at low frequency ($20 \log |L(j\omega)|$ for $\omega \ll 1$), and for the closed-loop system determine the bandwidth for each K .

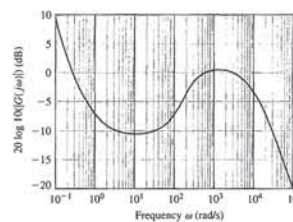


FIGURE P8.22 Bode plot of $G(s)$.

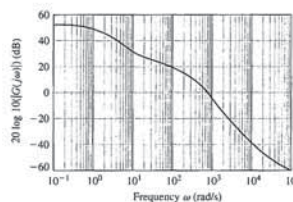


FIGURE P8.23 Frequency response of $G(j\omega)$.

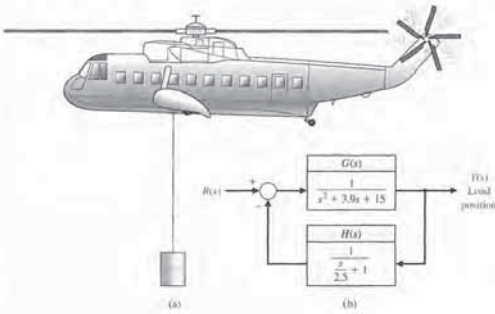


FIGURE AP8.4 A helicopter feedback control system.

1, 10, 50, 110, and 500. (c) Is the open-loop system stable? Is the closed-loop system stable?

AP8.6 Consider the spring-mass system depicted in Figure AP8.6. Develop a transfer function model to describe the motion of the mass $M = 2$ kg, when the input is $u(t)$ and the output is $x(t)$. Assume that the initial conditions are $x(0) = 0$ and $\dot{x}(0) = 0$. Determine values of k and b such that the maximum steady-state response of the system to a sinusoidal input $u(t) = \sin(\omega t)$ is less than 1 for all ω . For the values

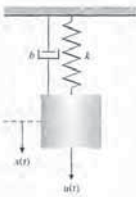


FIGURE AP8.6 Suspended spring-mass system with parameters k and b .

you selected for k and b , what is the frequency at which the peak response occurs?

AP8.7 An op-amp circuit is shown in Figure AP8.7. The circuit represents a lead compensator discussed in more detail in Chapter 10.

(a) Determine the transfer function of this circuit.
 (b) Sketch the frequency response of the circuit when $R_1 = 10$ k Ω , $R_2 = 10$ Ω , $C_1 = 0.1$ μ F, and $C_2 = 1$ mF.

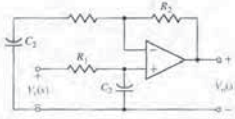


FIGURE AP8.7 Op-amp lead circuit.

ADVANCED PROBLEMS

AP8.1 A spring-mass-damper system is shown in Figure AP8.1(a). The Bode diagram obtained by experimental means using a sinusoidal forcing function is shown

in Figure AP8.1(b). Determine the numerical values of m , b , and k .

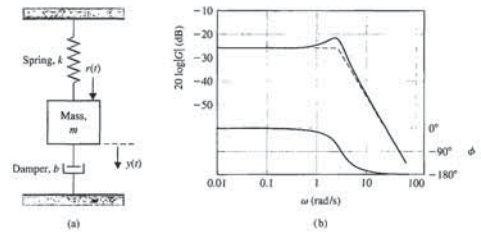


FIGURE AP8.1 A spring-mass-damper system.

AP8.2 A system is shown in Figure AP8.2. The nominal value of the parameter b is 4.0. Determine the sensi-

tivity S_b^y and plot $20 \log |S_b^y|$, the Bode magnitude diagram for $K = 5$.

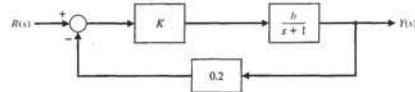


FIGURE AP8.2 System with parameter b .

AP8.3 As an automobile moves along the road, the vertical displacements at the tires act as the motion excitation to the automobile suspension system [16]. Figure

AP8.3 is a schematic diagram of a simplified automobile suspension system, for which we assume the input is sinusoidal. Determine the transfer function $X(s)/R(s)$, and sketch the Bode diagram when $M = 1$ kg, $b = 4$ N s/m, and $k = 18$ N/m.

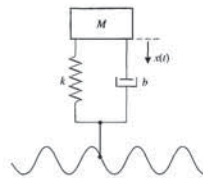


FIGURE AP8.3 Auto suspension system model.

AP8.4 A helicopter with a load on the end of a cable is shown in Figure AP8.4(a). The position control system is shown in Figure AP8.4(b), where the visual feedback is represented by $H(s)$. Sketch the Bode diagram of the loop transfer function $L(j\omega) = G(j\omega)H(j\omega)$.

AP8.5 A closed-loop system with unity feedback has a transfer function

$$T(s) = \frac{10(s+1)}{s^2 + 9s + 10}$$

(a) Determine the loop transfer function $G_c(s)G(s)$. (b) Plot the log-magnitude-phase (similar to Figure 8.27), and identify the frequency points for ω equal to



FIGURE DP8.2 (a) The Mars-bound Spider-bot. (Photo courtesy of NASA.) (b) Block diagram of the control system for one leg.

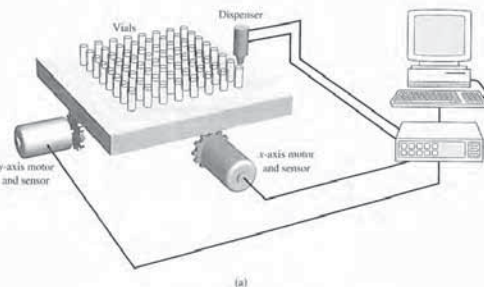
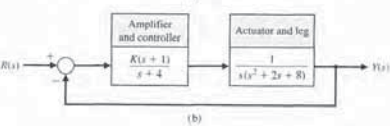
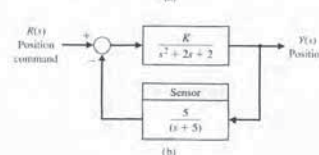


FIGURE DP8.3 Automatic table and dispenser.



DESIGN PROBLEMS

CDP8.1 In this chapter, we wish to use a PD controller such that

$$G_c(s) = K(s + 2).$$

The tachometer is not used (see Figure CDP4.1). Plot the Bode diagram for the system when $K = 40$. Determine the step response of this system and estimate the overshoot and settling time (with a 2% criterion).

DP8.1 Understanding the behavior of a human steering an automobile remains an interesting subject [14, 15, 16, 21]. The design and development of systems for four-wheel steering, active suspensions, active, independent braking, and "drive-by-wire" steering provide the engineer with considerably more freedom in altering vehicle-handling qualities than existed in the past.

The vehicle and the driver are represented by the model in Figure DP8.1, where the driver develops anticipation of the vehicle deviation from the center line. For $K = 1$, plot the Bode diagram of (a) the loop transfer function $G_c(s)G(s)$ and (b) the closed-loop transfer function $T(s)$. (c) Repeat parts (a) and (b) when $K = 50$. (d) A driver can select the gain K . Determine the appropriate gain so that $M_{pw} \leq 2$, and the bandwidth is the maximum attainable for the closed-loop system. (e) Determine the steady-state error of the system for a ramp input $r(t) = t$.

DP8.2 The unmanned exploration of planets such as Mars requires a high level of autonomy because of the communication delays between robots in space and their Earth-based stations. This affects all the components of the system: planning, sensing, and mechanism. In particular, such a level of autonomy can be achieved only if each robot has a perception system that can reliably build and maintain models of the environment. The perception system is a major part of the development of a complete system that includes planning and mechanism design. The target vehicle is the Spider-bot, a four-legged walking robot shown in Figure DP8.2(a), being developed at NASA Jet Propulsion Laboratory [18]. The control system of one leg is shown in Figure DP8.2(b).

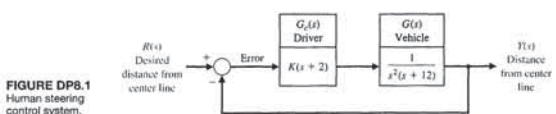


FIGURE DP8.1 Human steering control system.

(a) Sketch the Bode diagram for $G_c(s)G(s)$ when $K = 20$. Determine (1) the frequency when the phase is -180° and (2) the frequency when $20 \log |G_c G| = 0$ dB. (b) Plot the Bode diagram for the closed-loop transfer function $T(s)$ when $K = 20$. (c) Determine M_{pw} , ω_n , and ω_d for the closed-loop system when $K = 22$ and $K = 25$. (d) Select the best gain of the two specified in part (c) when it is desired that the overshoot of the system to a step input $r(t)$ be less than 5% and the settling time be as short as possible.

DP8.3 A table is used to position vials under a dispenser head, as shown in Figure DP8.3(a). The objective is speed, accuracy, and smooth motion in order to eliminate spilling. The position control system is shown in Figure DP8.3(b). Since we want small overshoot for a step input and yet desire a short settling time, we will limit $20 \log M_{pw}$ to 3 dB for $T(j\omega)$. Plot the Bode diagram for a gain K that will result in a stable system. Then adjust K until $20 \log M_{pw} = 3$ dB, and determine the closed-loop system bandwidth. Determine the steady-state error for the system for the gain K selected to meet the requirement for M_{pw} .

DP8.4 Anesthesia can be administered automatically by a control system. For certain operations, such as brain and eye surgery, involuntary muscle movements can be disastrous. To ensure adequate operating conditions for the surgeon, muscle relaxant drugs, which block involuntary muscle movements, are administered.

A conventional method used by anesthesiologists for muscle relaxant administration is to inject a bolus dose whose size is determined by experience and to inject supplements as required. However, an anesthesiologist may sometimes fail to maintain a steady level of relaxation, resulting in a large drug consumption by the patient. Significant improvements may be achieved by introducing the concept of automatic control, which results in a considerable reduction in the total relaxant drug consumed [19].

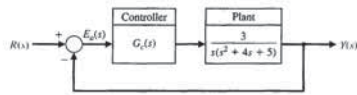
A model of the anesthesia process is shown in Figure DP8.4. Select a gain K so that the bandwidth of the closed-loop system is maximized while $M_{pw} \leq 1.5$. Determine the bandwidth attained for your design.

DP8.7 Consider the system of Figure DP8.7. Consider the controller to be a proportional plus integral plus derivative (PID) given by

$$G_c(s) = K_p + K_D s + \frac{K_I}{s}$$

Design the PID controller gains to achieve (a) an acceleration constant $K_a = 2$, (b) a phase margin of $P.M. \approx 45^\circ$, and (c) a bandwidth $\omega_b \approx 3.0$. Plot the response of the closed-loop system to a unit step input.

FIGURE DP8.7 Closed-loop feedback system.



COMPUTER PROBLEMS

CP8.1 Consider the closed-loop transfer function

$$T(s) = \frac{25}{s^2 + s + 25}$$

Develop an m-file to obtain the Bode plot and verify that the resonant frequency is 5 rad/s and that the peak magnitude M_{p_m} is 14 dB.

CP8.2 For the following transfer functions, sketch the Bode plots, then verify with the bode function:

(a) $G(s) = \frac{1000}{(s+10)(s+100)}$

(b) $G(s) = \frac{s+100}{(s+2)(s+25)}$

(c) $G(s) = \frac{100}{s^2 + 2s + 50}$

(d) $G(s) = \frac{100}{(s+3)(s^2 + 12s + 50)}$

CP8.3 For each of the following transfer functions, sketch the Bode plot and determine the crossover frequency (that is, the frequency at which $20 \log_{10}|G(j\omega)| = 0$ dB):

(a) $G(s) = \frac{2000}{(s+10)(s+100)}$

(b) $G(s) = \frac{100}{(s+1)(s^2 + 10s + 2)}$

(c) $G(s) = \frac{50(s+100)}{(s+1)(s+50)}$

(d) $G(s) = \frac{100(s^2 + 14s + 50)}{(s+1)(s+2)(s+500)}$

CP8.4 A unity negative feedback system has the loop transfer function

$$G_c(s)G(s) = \frac{54}{s(s+6)}$$

Determine the closed-loop system bandwidth. Using the bode function obtain the Bode plot and label the plot with the bandwidth.

CP8.5 A block diagram of a second-order system is shown in Figure CP8.5.

(a) Determine the resonant peak M_{p_m} , the resonant frequency ω_n , and the bandwidth ω_b of the system from the closed-loop Bode plot. Generate the Bode plot with an m-file for $\omega = 0.1$ to $\omega = 1000$ rad/s using the logspace function. (b) Estimate the system damping ratio, ζ , and natural frequency ω_n using Equations (8.36) and (8.37) in Section 8.2. (c) From the closed-loop transfer function, compute the actual ζ and ω_n and compare with your results in part (b).

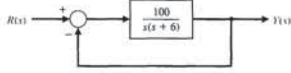


FIGURE CP8.5 A second-order feedback control system.

CP8.6 Consider the feedback system in Figure CP8.6. Obtain the Bode plots of the loop and closed-loop transfer functions using an m-file.

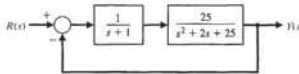


FIGURE CP8.6 Closed-loop feedback system.

Terms and Concepts

CP8.9 Design a filter, $G(s)$, with the following frequency response:

- For $\omega < 1$ rad/s, the magnitude $20 \log_{10}|G(j\omega)| < 0$ dB
- For $1 < \omega < 1000$ rad/s, the magnitude $20 \log_{10}|G(j\omega)| \approx 0$ dB

3. For $\omega > 1000$ rad/s, the magnitude $20 \log_{10}|G(j\omega)| < 0$ dB

Try to maximize the peak magnitude as close to $\omega = 40$ rad/s as possible.

ANSWERS TO SKILLS CHECK

True or False: (1) True; (2) False; (3) False; (4) True; (5) True
 Multiple Choice: (6) a; (7) a; (8) b; (9) b; (10) c; (11) b; (12) c; (13) d; (14) a; (15) d

Word Match (in order, top to bottom): d, i, q, n, l, m, o, j, s, p, c, e, b, r, h, f, g, k, a

TERMS AND CONCEPTS

All-pass network A nonminimum phase system that passes all frequencies with equal gain.

Bandwidth The frequency at which the frequency response has declined 3 dB from its low-frequency value.

Bode plot The logarithm of the magnitude of the transfer function is plotted versus the logarithm of ω , the frequency. The phase ϕ of the transfer function is separately plotted versus the logarithm of the frequency.

Break frequency The frequency at which the asymptotic approximation of the frequency response for a pole (or zero) changes slope.

Corner frequency See Break frequency.

Decade A factor of 10 in frequency (e.g., the range of frequencies from 1 rad/s to 10 rad/s is one decade).

Decibel (dB) The units of the logarithmic gain.

Dominant roots The roots of the characteristic equation that represent or dominate the closed-loop transient response.

Fourier transform The transformation of a function of time $f(t)$ into the frequency domain.

Fourier transform pair A pair of functions, one in the time domain, denoted by $f(t)$, and the other in the frequency domain, denoted by $F(\omega)$, related by the Fourier transform as $F(\omega) = \mathcal{F}\{f(t)\}$, where \mathcal{F} denotes the Fourier transform.

Frequency response The steady-state response of a system to a sinusoidal input signal.

Laplace transform pair A pair of functions, one in the time domain, denoted by $f(t)$, and the other in the

frequency domain, denoted by $F(s)$, related by the Laplace transform as $F(s) = \mathcal{L}\{f(t)\}$, where \mathcal{L} denotes the Laplace transform.

Logarithmic magnitude The logarithm of the magnitude of the transfer function, usually expressed in units of 20 dB, thus $20 \log_{10}|G|$.

Logarithmic plot See Bode plot.

Maximum value of the frequency response A pair of complex poles will result in a maximum value for the frequency response occurring at the resonant frequency.

Minimum phase transfer function All the zeros of a transfer function lie in the left-hand side of the s -plane.

Natural frequency The frequency of natural oscillation that would occur for two complex poles if the damping were equal to zero.

Nonminimum phase transfer function Transfer functions with zeros in the right-hand s -plane.

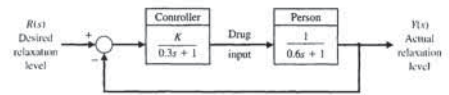
Octave The frequency interval $\omega_2 = 2\omega_1$ is an octave of frequencies (e.g., the range of frequencies from $\omega_1 = 100$ rad/s to $\omega_2 = 200$ rad/s is one octave).

Polar plot A plot of the real part of $G(j\omega)$ versus the imaginary part of $G(j\omega)$.

Resonant frequency The frequency ω_r at which the maximum value of the frequency response of a complex pair of poles is attained.

Transfer function in the frequency domain The ratio of the output to the input signal where the input is a sinusoid. It is expressed as $G(j\omega)$.

FIGURE DP8.4 Model of an anesthesia control system.



DP8.5 Consider the control system depicted in Figure DP8.5(a) where the plant is a "black box" for which little is known in the way of mathematical models. The only information available on the plant is the frequency response shown in Figure DP8.5(b). Design a controller $G_c(s)$ to meet the following specifications: (i) The crossover frequency is between 10 rad/s and 50 rad/s; (ii) The magnitude of $G_c(s)G(s)$ is greater than 20 dB for $\omega < 0.1$ rad/s.

- Determine p and K such that the unit step response exhibits a zero steady-state error and the percent overshoot meets the requirement $P.O. \leq 5\%$.
- For the values of p and K determined in part (a), determine the system damping ratio ζ and the natural frequency ω_n .
- For the values of p and K determined in part (a), obtain the Bode plot of the system and determine the bandwidth ω_b .

DP8.6 A single-input, single-output system is described by

$$\dot{\mathbf{x}}(t) = \begin{bmatrix} 0 & 1 \\ -1 & -p \end{bmatrix} \mathbf{x}(t) + \begin{bmatrix} K \\ 0 \end{bmatrix} u(t)$$

$$y(t) = [0 \ 1] \mathbf{x}(t)$$

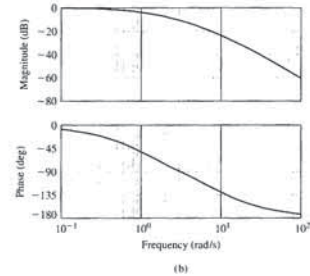
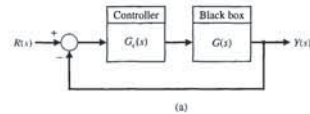


FIGURE DP8.5 (a) Feedback system with "black box" plant. (b) Frequency response plot of the "black box" represented by $G(s)$.

CP8.7 A unity feedback system has the loop transfer function

$$L(s) = G_c(s)G(s) = \frac{1}{s(s+2p)}$$

Generate a plot of the bandwidth versus the parameter p as $0 < p < 1$.

CP8.8 Consider the problem of controlling an inverted pendulum on a moving base, as shown in Figure CP8.8(a). The transfer function of the system is

$$G(s) = \frac{-1/(M_p L)}{s^2 - (M_p + M_b)g/(M_b L)}$$

The design objective is to balance the pendulum (i.e., $\theta(t) \approx 0$) in the presence of disturbance inputs. A block diagram representation of the system is depicted in Figure CP8.8(b). Let $M_p = 10$ kg, $M_b = 100$ kg, $L = 1$ m, $g = 9.81$ m/s², $a = 5$, and $b = 10$. The design specifications, based on a unit step disturbance, are as follows:

- settling time (with a 2% criterion) less than 10 seconds,
- percent overshoot less than 40%, and
- steady-state tracking error less than 0.1% in the presence of the disturbance.

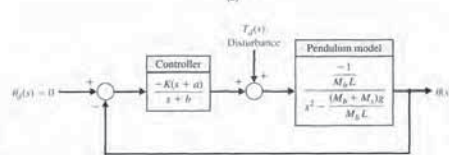
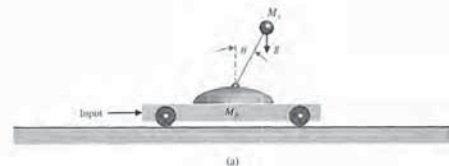


FIGURE CP8.8 (a) An inverted pendulum on a moving base. (b) A block diagram representation.

Develop a set of interactive m-file scripts to aid in the control system design. The first script should accomplish at least the following:

- Compute the closed-loop transfer function from the disturbance to the output with K as an adjustable parameter.
 - Draw the Bode plot of the closed-loop system.
 - Automatically compute and output M_{p_m} and ω_b .
- As an intermediate step, use M_{p_m} and ω_b and Equations (8.36) and (8.37) in Section 8.2 to estimate ζ and ω_n . The second script should at least estimate the settling time and percent overshoot using ζ and ω_n as input variables.

If the performance specifications are not satisfied, change K and iterate on the design using the first two scripts. After completion of the first two steps, the final step is to test the design by simulation. The functions of the third script are as follows:

- plot the response, $\theta(t)$, to a unit step disturbance with K as an adjustable parameter, and
 - label the plot appropriately.
- Utilizing the interactive scripts, design the controller to meet the specifications using frequency response Bode methods. To start the design process, use analytic methods to compute the minimum value of K to meet the steady-state tracking error specification. Use the minimum K as the first guess in the design iteration.

9.1 INTRODUCTION

For a control system, it is necessary to determine whether the system is stable. Furthermore, if the system is stable, it is often necessary to investigate the relative stability. In Chapter 6, we discussed the concept of stability and several methods of determining the absolute and relative stability of a system. The Routh-Hurwitz method, discussed in Chapter 6, is useful for investigating the characteristic equation expressed in terms of the complex variable $s = \sigma + j\omega$. Then, in Chapter 7, we investigated the relative stability of a system utilizing the root locus method, which is also expressed in terms of the complex variable s . In this chapter, we are concerned with investigating the stability of a system in the real frequency domain, that is, in terms of the frequency response discussed in Chapter 8.

The frequency response of a system represents the sinusoidal steady-state response of a system and provides sufficient information for the determination of the relative stability of the system. The frequency response of a system can readily be obtained experimentally by exciting the system with sinusoidal input signals; therefore, it can be utilized to investigate the relative stability of a system when the system parameter values have not been determined. Furthermore, a frequency-domain stability criterion would be useful for determining suitable approaches to adjusting the parameters of a system in order to increase its relative stability.

A frequency domain stability criterion was developed by H. Nyquist in 1932, and it remains a fundamental approach to the investigation of the stability of linear control systems [1, 2]. The **Nyquist stability criterion** is based on a theorem in the theory of the function of a complex variable due to Cauchy. Cauchy's theorem is concerned with mapping contours in the complex s -plane, and fortunately the theorem can be understood without a formal proof requiring complex variable theory.

To determine the relative stability of a closed-loop system, we must investigate the characteristic equation of the system:

$$F(s) = 1 + L(s) = 0. \tag{9.1}$$

For the single-loop control system of Figure 9.1, $L(s) = G_c(s)G(s)H(s)$. For a multiloop system, we found in Section 2.7 that, in terms of signal-flow graphs, the characteristic equation is

$$F(s) = \Delta(s) = 1 - \Sigma L_{\alpha} + \Sigma L_{\alpha}L_{\beta} \dots = 0,$$

where $\Delta(s)$ is the graph determinant. Therefore, we can represent the characteristic equation of single-loop or multiple-loop systems by Equation (9.1), where $L(s)$ is a rational function of s . To ensure stability, we must ascertain that all the zeros of $F(s)$ lie in the left-hand s -plane. Nyquist thus proposed a mapping of the right-hand s -plane into the $F(s)$ -plane. Nyquist's criterion, we shall first consider briefly the mapping of contours in the complex plane.

Section 9.2 Mapping Contours in the s -Plane

of the s -plane unit square contour to the $F(s)$ -plane is accomplished through the relation $F(s)$, and so

$$u + jv = F(s) = 2s + 1 = 2(\sigma + j\omega) + 1. \tag{9.2}$$

Therefore, in this case, we have

$$u = 2\sigma + 1 \tag{9.3}$$

and

$$v = 2\omega. \tag{9.4}$$

Thus, the contour has been mapped by $F(s)$ into a contour of an identical form, a square, with the center shifted by one unit and the magnitude of a side multiplied by two. This type of mapping, which retains the angles of the s -plane contour on the $F(s)$ -plane, is called a **conformal mapping**. We also note that a closed contour in the s -plane results in a closed contour in the $F(s)$ -plane.

The points $A, B, C,$ and D , as shown in the s -plane contour, map into the points $A, B, C,$ and D shown in the $F(s)$ -plane. Furthermore, a direction of traversal of the s -plane contour can be indicated by the direction $ABCD$ and the arrows shown on the contour. Then a similar traversal occurs on the $F(s)$ -plane contour as we pass $ABCD$ in order, as shown by the arrows. By convention, the area within a contour to the right of the traversal of the contour is considered to be the area enclosed by the contour. Therefore, we will assume clockwise traversal of a contour to be positive and the area enclosed within the contour to be on the right. This convention is opposite to that usually employed in complex variable theory, but is equally applicable and is generally used in control system theory. We might consider the area on the right as we walk along the contour in a clockwise direction and call this rule "clockwise and eyes right."

Typically, we are concerned with an $F(s)$ that is a rational function of s . Therefore, it will be worthwhile to consider another example of a mapping of a contour. Let us again consider the unit square contour for the function

$$F(s) = \frac{s}{s+2}. \tag{9.5}$$

Several values of $F(s)$ as s traverses the square contour are given in Table 9.1, and the resulting contour in the $F(s)$ -plane is shown in Figure 9.3(b). The contour in the $F(s)$ -plane encloses the origin of the $F(s)$ -plane because the origin lies within the enclosed area of the contour in the $F(s)$ -plane.

Table 9.1 Values of $F(s)$

	Point A	Point B	Point C	Point D
$s = \sigma + j\omega$	$1 + j1$	$1 - j1$	$-1 - j1$	$-1 + j1$
$F(s) = u + jv$	$\frac{4 + 2j}{10}$	$\frac{4 - 2j}{10}$	$\frac{1 - 2j}{5}$	$\frac{1 + 2j}{5}$

9.1 Introduction 635
 9.2 Mapping Contours in the s -Plane 636
 9.3 The Nyquist Criterion 642
 9.4 Relative Stability and the Nyquist Criterion 653
 9.5 Time-Domain Performance Criteria in the Frequency Domain 661
 9.6 System Bandwidth 668
 9.7 The Stability of Control Systems with Time Delays 666
 9.8 Design Examples 673
 9.9 PID Controllers in the Frequency Domain 691
 9.10 Stability in the Frequency Domain Using Control Design Software 692
 9.11 Sequential Design Example: Disk Drive Read System 700
 9.12 Summary 703

PREVIEW

In previous chapters, we discussed stability and developed various tools to determine stability and to assess relative stability. We continue that discussion in this chapter by showing how frequency response methods can be used to investigate stability. The important concepts of gain margin, phase margin, and bandwidth are developed in the context of Bode plots and Nyquist diagrams. A frequency response stability result—known as the Nyquist stability criterion—is presented and its use illustrated through several interesting examples. The implications of having pure time delays in the system on both stability and performance are discussed. We will see that the phase lag introduced by the time delay can destabilize an otherwise stable system. The chapter concludes with a frequency response analysis of the Sequential Design Example: Disk Drive Read System.

DESIRED OUTCOMES

Upon completion of Chapter 9, students should:

- Understand the Nyquist stability criterion and the role of the Nyquist plot.
- Be familiar with time-domain performance specifications in the frequency domain.
- Appreciate the importance of considering time delays in feedback control systems.
- Be capable of analyzing the relative stability and performance of feedback control systems using frequency response methods considering phase and gain margin, and system bandwidth.

Chapter 9 Stability in the Frequency Domain

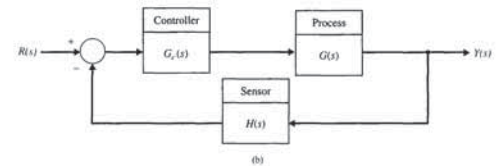
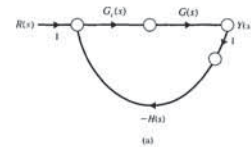


FIGURE 9.1 Single-loop feedback control system.

9.2 MAPPING CONTOURS IN THE s -PLANE

We are concerned with the mapping of contours in the s -plane by a function $F(s)$. A **contour map** is a contour or trajectory in one plane mapped or translated into another plane by a relation $F(s)$. Since s is a complex variable, $s = \sigma + j\omega$, the function $F(s)$ is itself complex; it can be defined as $F(s) = u + jv$ and can be represented on a complex $F(s)$ -plane with coordinates u and v . As an example, let us consider a function $F(s) = 2s + 1$ and a contour in the s -plane, as shown in Figure 9.2(a). The mapping

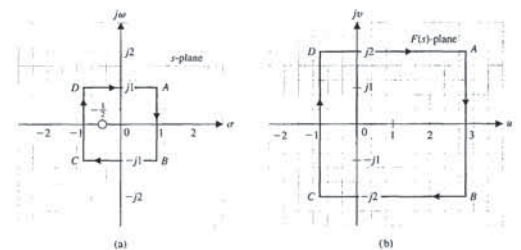


FIGURE 9.2 Mapping a square contour by $F(s) = 2s + 1 = 2(\sigma + j\omega)$.

Reexamining the example when $F(s) = 2(s + 1/2)$, we have one zero of $F(s)$ at $s = -1/2$, as shown in Figure 9.2. The contour that we chose (that is, the unit square) enclosed and encircled the zero once within the area of the contour. Similarly, for the function $F(s) = s/(s + 2)$, the unit square encircled the zero at the origin but did not encircle the pole at $s = -2$. The encirclement of the poles and zeros of $F(s)$ can be related to the encirclement of the origin in the $F(s)$ -plane by **Cauchy's theorem**, commonly known as the **principle of the argument**, which states [3, 4]:

If a contour Γ_s in the s -plane encircles Z zeros and P poles of $F(s)$ and does not pass through any poles or zeros of $F(s)$ and the traversal is in the clockwise direction along the contour, the corresponding contour Γ_F in the $F(s)$ -plane encircles the origin of the $F(s)$ -plane $N = Z - P$ times in the clockwise direction.

Thus, for the examples shown in Figures 9.2 and 9.3, the contour in the $F(s)$ -plane encircles the origin once, because $N = Z - P = 1$, as we expect. As another example, consider the function $F(s) = s/(s + 1/2)$. For the unit square contour shown in Figure 9.4(a), the resulting contour in the $F(s)$ plane is shown in Figure 9.4(b). In this case, $N = Z - P = 0$, as is the case in Figure 9.4(b), since the contour Γ_F does not encircle the origin.

Cauchy's theorem can be best comprehended by considering $F(s)$ in terms of the angle due to each pole and zero as the contour Γ_s is traversed in a clockwise direction. Thus, let us consider the function

$$F(s) = \frac{(s + z_1)(s + z_2)}{(s + p_1)(s + p_2)} \quad (9.10)$$

where $-z_k$ is a zero of $F(s)$, and $-p_k$ is a pole of $F(s)$. Equation (9.10) can be written as

$$\begin{aligned} F(s) &= |F(s)| \angle F(s) \\ &= \frac{|s + z_1| |s + z_2|}{|s + p_1| |s + p_2|} \left(\angle s + z_1 + \angle s + z_2 - \angle s + p_1 - \angle s + p_2 \right) \\ &= |F(s)| (\phi_{z_1} + \phi_{z_2} - \phi_{p_1} - \phi_{p_2}). \end{aligned} \quad (9.11)$$

Now, considering the vectors as shown for a specific contour Γ_s (Figure 9.5a), we can determine the angles as s traverses the contour. Clearly, the net angle change as s traverses along Γ_s (a full rotation of 360° for ϕ_{z_1} , ϕ_{z_2} , and ϕ_{p_1}) is zero degrees. However, for ϕ_{p_2} as s traverses 360° around Γ_s , the angle ϕ_{p_2} traverses a full 360° clockwise. Thus, as Γ_s is completely traversed, the net angle increase of $F(s)$ is equal to 360° , since only one zero is enclosed. If Z zeros were enclosed within Γ_s , then the net angle increase would be equal to $\phi_z = 2\pi Z$ rad. Following this reasoning, if Z zeros and P poles are encircled as Γ_s is traversed, then $2\pi Z - 2\pi P$ is the net resultant angle increase of $F(s)$. Thus, the net angle increase of Γ_F of the contour in the

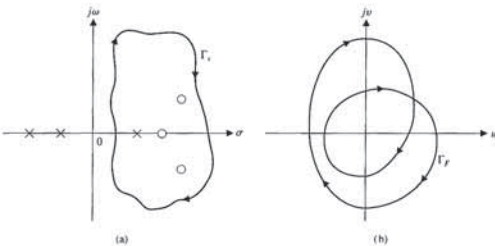


FIGURE 9.6 Example of Cauchy's theorem with three zeros and one pole within Γ_s .

As an example of the use of Cauchy's theorem, consider the pole-zero pattern shown in Figure 9.6(a) with the contour Γ_s to be considered. The contour encloses and encircles three zeros and one pole. Therefore, we obtain

$$N = 3 - 1 = +2,$$

and Γ_F completes two clockwise encirclements of the origin in the $F(s)$ -plane, as shown in Figure 9.6(b).

For the pole and zero pattern shown and the contour Γ_s as shown in Figure 9.7(a), one pole is encircled and no zeros are encircled. Therefore, we have

$$N = Z - P = -1,$$

and we expect one encirclement of the origin by the contour Γ_F in the $F(s)$ -plane. However, since the sign of N is negative, we find that the encirclement moves in the counterclockwise direction, as shown in Figure 9.7(b).

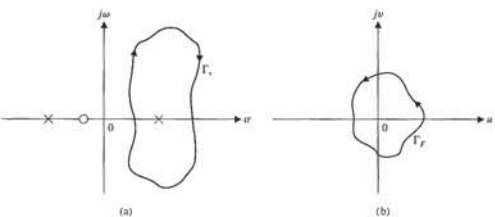


FIGURE 9.7 Example of Cauchy's theorem with one pole within Γ_s .

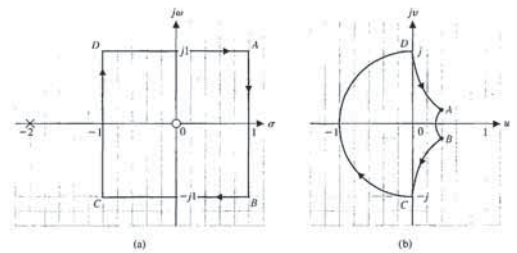


FIGURE 9.3 Mapping for $F(s) = s/(s + 2)$.

Cauchy's theorem is concerned with mapping a function $F(s)$ that has a finite number of poles and zeros within the contour, so that we may express $F(s)$ as

$$F(s) = \frac{K \prod_{k=1}^n (s + z_k)}{\prod_{l=1}^m (s + p_l)} \quad (9.6)$$

where $-z_k$ are the zeros of the function $F(s)$ and $-p_k$ are the poles of $F(s)$. The function $F(s)$ is the characteristic equation, and so

$$F(s) = 1 + L(s), \quad (9.7)$$

where

$$L(s) = \frac{N(s)}{D(s)}$$

Therefore, we have

$$F(s) = 1 + L(s) = 1 + \frac{N(s)}{D(s)} = \frac{D(s) + N(s)}{D(s)} = \frac{K \prod_{k=1}^n (s + z_k)}{\prod_{l=1}^m (s + p_l)} \quad (9.8)$$

and the poles of $L(s)$ are the poles of $F(s)$. However, it is the zeros of $F(s)$ that are the characteristic roots of the system and that indicate its response. This is clear if we recall that the output of the system is

$$Y(s) = T(s)R(s) = \frac{\sum P_k \Delta_k}{\Delta(s)} R(s) = \frac{\sum P_k \Delta_k}{F(s)} R(s), \quad (9.9)$$

where P_k and Δ_k are the path factors and cofactors as defined in Section 2.7.

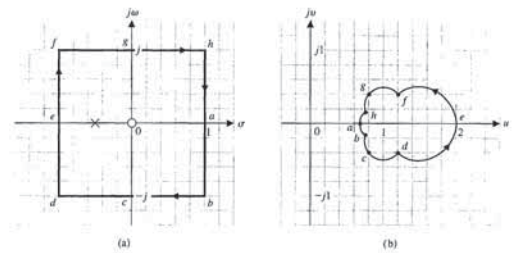


FIGURE 9.4 Mapping for $F(s) = s/(s + 1/2)$.

$F(s)$ -plane is simply

$$\phi_F = \phi_z - \phi_p,$$

or

$$2\pi N = 2\pi Z - 2\pi P, \quad (9.12)$$

and the net number of encirclements of the origin of the $F(s)$ -plane is $N = Z - P$. Thus, for the contour shown in Figure 9.5(a), which encircles one zero, the contour Γ_F shown in Figure 9.5(b) encircles the origin once in the clockwise direction.

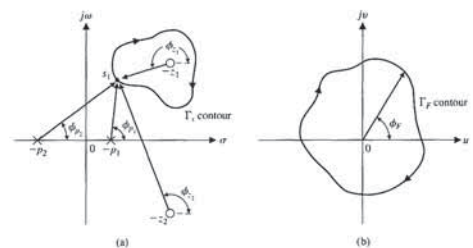


FIGURE 9.5 Evaluation of the net angle of Γ_F .

2. The magnitude of $L(s) = G_c(s)G(s)H(s)$ as $s = re^{j\phi}$ and $r \rightarrow \infty$ will normally approach zero or a constant. ■

EXAMPLE 9.3 System with three poles

Let us again consider the single-loop system shown in Figure 9.1 when

$$L(s) = G_c(s)G(s)H(s) = \frac{K}{s(\tau_1 s + 1)(\tau_2 s + 1)} \quad (9.23)$$

The Nyquist contour Γ_r is shown in Figure 9.10(a). Again, this mapping is symmetrical for $L(j\omega)$ and $L(-j\omega)$ so that it is sufficient to investigate the $L(j\omega)$ -locus. The small semicircle around the origin of the s -plane maps into a semicircle of infinite radius, as in Example 9.2. Also, the semicircle $re^{j\phi}$ in the s -plane as $r \rightarrow \infty$ maps into the point $L(s) = 0$, as we expect. Therefore, to investigate the stability of the system, it is sufficient to plot the portion of the contour Γ_r that is the real frequency polar plot $L(j\omega)$ for $0_+ < \omega < +\infty$. Thus, when $s = +j\omega$, we have

$$\begin{aligned} L(j\omega) &= \frac{K}{j\omega(j\omega\tau_1 + 1)(j\omega\tau_2 + 1)} \\ &= \frac{-K(\tau_1 + \tau_2) - jK(1/\omega)(1 - \omega^2\tau_1\tau_2)}{1 + \omega^2(\tau_1^2 + \tau_2^2) + \omega^4\tau_1^2\tau_2^2} \\ &= \frac{K}{[\omega^4(\tau_1 + \tau_2)^2 + \omega^2(1 - \omega^2\tau_1\tau_2)^2]^{1/2}} \\ &\quad \times \angle -\tan^{-1}(\omega\tau_1) - \tan^{-1}(\omega\tau_2) - (\pi/2). \end{aligned} \quad (9.24)$$

When $\omega = 0_+$, the magnitude of the locus is infinite at an angle of -90° in the $L(s)$ -plane. When ω approaches $+\infty$, we have

$$\begin{aligned} \lim_{\omega \rightarrow \infty} L(j\omega) &= \lim_{\omega \rightarrow \infty} \frac{1}{\omega^3\tau_1\tau_2} \angle -(\pi/2) - \tan^{-1}(\omega\tau_1) - \tan^{-1}(\omega\tau_2) \\ &= \lim_{\omega \rightarrow \infty} \frac{1}{\omega^3\tau_1\tau_2} \angle -3\pi/2. \end{aligned} \quad (9.25)$$

Therefore, $L(j\omega)$ approaches a magnitude of zero at an angle of -270° [29]. To approach at an angle of -270° , the locus must cross the u -axis in the $L(s)$ -plane, as shown in Figure 9.11. Thus, it is possible to encircle the -1 point. The number of encirclements when the -1 point lies within the locus, as shown in Figure 9.11, is equal to two, and the system is unstable with two roots in the right-hand s -plane. The point where the $L(s)$ -locus intersects the real axis can be found by setting the imaginary part of $L(j\omega) = u + jv$ equal to zero. We then have, from Equation (9.24),

plot because $s = j\omega$ and

$$L(s)|_{s=j\omega} = L(j\omega) \quad (9.19)$$

for this part of the contour. This results in the real frequency polar plot shown in Figure 9.10(b). When ω approaches $+\infty$, we have

$$\begin{aligned} \lim_{\omega \rightarrow +\infty} L(j\omega) &= \lim_{\omega \rightarrow +\infty} \frac{K}{j\omega(j\omega\tau + 1)} \\ &= \lim_{\omega \rightarrow +\infty} \frac{K}{\tau\omega^2} \angle -(\pi/2) - \tan^{-1}(\omega\tau). \end{aligned} \quad (9.20)$$

Therefore, the magnitude approaches zero at an angle of -180° .

(c) **The Portion from $\omega = +\infty$ to $\omega = -\infty$.** The portion of Γ_r from $\omega = +\infty$ to $\omega = -\infty$ is mapped into the point zero at the origin of the $L(s)$ -plane by the function $L(s)$. The mapping is represented by

$$\lim_{r \rightarrow \infty} L(s)|_{s=re^{j\phi}} = \lim_{r \rightarrow \infty} \frac{K}{r^2} \angle -2j\phi \quad (9.21)$$

as ϕ changes from $\phi = +90^\circ$ at $\omega = +\infty$ to $\phi = -90^\circ$ at $\omega = -\infty$. Thus, the contour moves from an angle of -180° at $\omega = +\infty$ to an angle of $+180^\circ$ at $\omega = -\infty$. The magnitude of the $L(s)$ contour when r is infinite is always zero or a constant.

(d) **The Portion from $\omega = -\infty$ to $\omega = 0_-$.** The portion of the contour Γ_r from $\omega = -\infty$ to $\omega = 0_-$ is mapped by the function $L(s)$ as

$$L(s)|_{s=-j\omega} = L(-j\omega). \quad (9.22)$$

Thus, we obtain the complex conjugate of $L(j\omega)$, and the plot for the portion of the polar plot from $\omega = -\infty$ to $\omega = 0_-$ is symmetrical to the polar plot from $\omega = +\infty$ to $\omega = 0_+$. This symmetrical polar plot is shown on the $L(s)$ -plane in Figure 9.10(b).

To investigate the stability of this second-order system, we first note that the number of poles, P , within the right-hand s -plane is zero. Therefore, for this system to be stable, we require $N = Z = 0$, and the contour Γ_r must not encircle the -1 point in the $L(s)$ -plane. Examining Figure 9.10(b), we find that irrespective of the value of the gain K and the time constant τ , the contour does not encircle the -1 point, and the system is always stable. As in Chapter 7, we are considering positive values of gain K . If negative values of gain are to be considered, we should use $-K$, where $K \geq 0$.

We may draw two general conclusions from this example:

1. The plot of the contour Γ_r for the range $-\infty < \omega < 0_-$ will be the complex conjugate of the plot for the range $0_+ < \omega < +\infty$, and the polar plot of $L(s) = G_c(s)G(s)H(s)$ will be symmetrical in the $L(s)$ -plane about the u -axis. Therefore, it is sufficient to construct the contour Γ_r for the frequency range $0_+ < \omega < +\infty$ in order to investigate the stability (keeping in mind the detour around the origin).

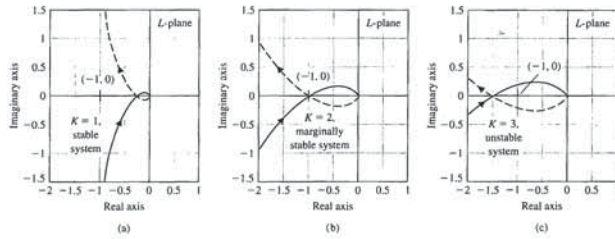


FIGURE 9.12 Nyquist plot for $L(s) = G_c(s)G(s)H(s) = \frac{K}{s(s+1)^2}$ when (a) $K = 1$, (b) $K = 2$, and (c) $K = 3$.

EXAMPLE 9.4 System with two poles at the origin

Again, let us determine the stability of the single-loop system shown in Figure 9.1 when

$$L(s) = G_c(s)G(s)H(s) = \frac{K}{s^2(\tau s + 1)} \quad (9.29)$$

The real frequency polar plot is obtained when $s = j\omega$, and we have

$$L(j\omega) = \frac{K}{-\omega^2(j\omega\tau + 1)} = \frac{K}{[\omega^4 + \tau^2\omega^6]^{1/2}} \angle -\pi - \tan^{-1}(\omega\tau). \quad (9.30)$$

We note that the angle of $L(j\omega)$ is always -180° or less, and the locus of $L(j\omega)$ is above the u -axis for all values of ω . As ω approaches 0_+ , we have

$$\lim_{\omega \rightarrow 0_+} L(j\omega) = \lim_{\omega \rightarrow 0_+} \frac{K}{\omega^2} \angle -\pi. \quad (9.31)$$

As ω approaches $+\infty$, we have

$$\lim_{\omega \rightarrow +\infty} L(j\omega) = \lim_{\omega \rightarrow +\infty} \frac{K}{\omega^3} \angle -3\pi/2. \quad (9.32)$$

At the small semicircular detour at the origin of the s -plane where $s = \epsilon e^{j\phi}$, we have

$$\lim_{\epsilon \rightarrow 0} L(s) = \lim_{\epsilon \rightarrow 0} \frac{K}{\epsilon^2} e^{-2j\phi}, \quad (9.33)$$

where $-\pi/2 \leq \phi \leq \pi/2$. Thus, the contour Γ_L ranges from an angle of $+\pi\omega = 0_-$ to $-\pi$ at $\omega = 0_+$, and passes through a full circle of 2π rad as ω changes from $\omega = 0_-$ to $\omega = 0_+$. The complete contour plot of Γ_L is shown in Figure 9.13. Because the

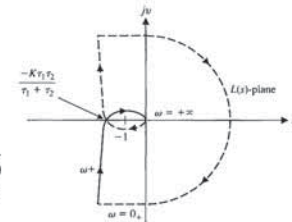


FIGURE 9.11 Nyquist diagram for $L(s) = K/(s(s+1)^2)$. The tick mark shown to the left of the origin is the -1 point.

$$v = \frac{-K(1/\omega)(1 - \omega^2\tau_1\tau_2)}{1 + \omega^2(\tau_1^2 + \tau_2^2) + \omega^4\tau_1^2\tau_2^2} = 0. \quad (9.26)$$

Thus, $v = 0$ when $1 - \omega^2\tau_1\tau_2 = 0$ or $\omega = 1/\sqrt{\tau_1\tau_2}$. The magnitude of the real part of $L(j\omega)$ at this frequency is

$$\begin{aligned} u &= \frac{-K(\tau_1 + \tau_2)}{1 + \omega^2(\tau_1^2 + \tau_2^2) + \omega^4\tau_1^2\tau_2^2} \Big|_{\omega=1/\sqrt{\tau_1\tau_2}} \\ &= \frac{-K(\tau_1 + \tau_2)\tau_1\tau_2}{\tau_1\tau_2 + (\tau_1^2 + \tau_2^2) + \tau_1\tau_2} = \frac{-K\tau_1\tau_2}{\tau_1 + \tau_2}. \end{aligned} \quad (9.27)$$

Therefore, the system is stable when

$$\frac{-K\tau_1\tau_2}{\tau_1 + \tau_2} \geq -1,$$

or

$$K \leq \frac{\tau_1 + \tau_2}{\tau_1\tau_2}. \quad (9.28)$$

Consider the case where $\tau_1 = \tau_2 = 1$, so that

$$L(s) = G_c(s)G(s)H(s) = \frac{K}{s(s+1)^2}.$$

Using Equation (9.28), we expect stability when

$$K \leq 2.$$

The Nyquist diagrams for three values of K are shown in Figure 9.12. ■

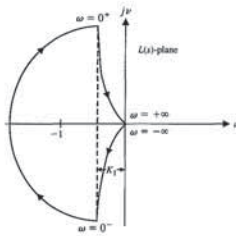


FIGURE 9.15 Nyquist diagram for $L(s) = K/(s(s-1))$.

of the s -plane, we let $s = \epsilon e^{j\phi}$ when $-\pi/2 \leq \phi \leq \pi/2$. Then, when $s = \epsilon e^{j\phi}$, we have

$$\lim_{\epsilon \rightarrow 0} L(s) = \lim_{\epsilon \rightarrow 0} \frac{K_1}{\epsilon - \epsilon e^{j\phi}} = \lim_{\epsilon \rightarrow 0} \left| \frac{K_1}{\epsilon} \right| \angle -180^\circ - \phi. \quad (9.35)$$

Therefore, this portion of the contour Γ_L is a semicircle of infinite magnitude in the left-hand $L(s)$ -plane, as shown in Figure 9.15. When $s = j\omega$, we have

$$\begin{aligned} L(j\omega) &= G_c(j\omega)G(j\omega)H(j\omega) = \frac{K_1}{j\omega(j\omega-1)} = \frac{K_1}{(\omega^2 + \omega^4)^{1/2}} \angle (-\pi/2) - \tan^{-1}(-\omega) \\ &= \frac{K_1}{(\omega^2 + \omega^4)^{1/2}} \angle +\pi/2 + \tan^{-1}\omega. \end{aligned} \quad (9.36)$$

Finally, for the semicircle of radius r as r approaches infinity, we have

$$\lim_{r \rightarrow \infty} L(s)|_{s=re^{j\phi}} = \lim_{r \rightarrow \infty} \left| \frac{K_1}{r^2} \right| e^{-2j\phi}, \quad (9.37)$$

where ϕ varies from $\pi/2$ to $-\pi/2$ in a clockwise direction. Therefore, the contour Γ_L , at the origin of the $L(s)$ -plane, varies 2π rad in a counterclockwise direction. Several important values of the $L(s)$ -locus are given in Table 9.3. The contour Γ_L in the $L(s)$ -plane encircles the -1 point once in the clockwise direction so $N = +1$.

Table 9.3 Values of $L(s) = G_c(s)G(s)H(s)$

s	$j0^-$	$j0^+$	$j1$	$+j\infty$	$-j\infty$
$ L /K_1$	∞	∞	$1/\sqrt{2}$	0	0
$\angle L$	-90°	$+90^\circ$	$+135^\circ$	$+180^\circ$	-180°

at this point, or $\omega^2 = 1/K_2$. The value of the real part of $L(j\omega)$ at the intersection is then

$$u|_{\omega^2=1/K_2} = \frac{-\omega^2 K_1(1+K_2)}{\omega^2 + \omega^4} \Big|_{\omega^2=1/K_2} = -K_1 K_2. \quad (9.42)$$

Therefore, when $-K_1 K_2 < -1$ or $K_1 K_2 > 1$, the contour Γ_L encircles the -1 point once in a counterclockwise direction, and therefore $N = -1$. Then the number of zeros of the system in the right-hand plane is

$$Z = N + P = -1 + 1 = 0.$$

Thus, the system is stable when $K_1 K_2 > 1$. Often, it may be useful to utilize a computer to plot the Nyquist diagram [5]. ■

EXAMPLE 9.6 System with a zero in the right-hand s -plane

Let us consider the feedback control system shown in Figure 9.1 as

$$L(s) = G_c(s)G(s)H(s) = \frac{K(s-2)}{(s+1)^2}.$$

We have

$$L(j\omega) = \frac{K(j\omega-2)}{(j\omega+1)^2} = \frac{K(j\omega-2)}{(1-\omega^2+j2\omega)}. \quad (9.43)$$

As ω approaches $+\infty$ on the $+j\omega$ axis, we have

$$\lim_{\omega \rightarrow +\infty} L(j\omega) = \lim_{\omega \rightarrow +\infty} \frac{K}{\omega} \angle -\pi/2.$$

When $\omega = \sqrt{5}$, we have $L(j\omega) = K/2$. At $\omega = 0$, we have $L(j\omega) = -2K$. The Nyquist diagram for $L(j\omega)/K$ is shown in Figure 9.17. $L(j\omega)$ intersects the $-1 + j0$ point when $K = 1/2$. Thus, the system is stable for the limited range of gain $0 < K \leq 1/2$. When $K > 1/2$, the number of encirclements of the -1 point is $N = 1$. The number of poles of $L(s)$ in the right half s -plane is $P = 0$. Therefore, we have

$$Z = N + P = 1,$$

and the system is unstable. Examining the Nyquist diagram of Figure 9.17, which is plotted for $L(j\omega)/K$, we conclude that the system is unstable for all $K > 1/2$. ■

9.4 RELATIVE STABILITY AND THE NYQUIST CRITERION

We discussed the relative stability of a system in terms of the s -plane in Section 6.3. For the s -plane, we defined the relative stability of a system as the property measured by the relative settling time of each root or pair of roots. Therefore, a system with a shorter settling time is considered more relatively stable. We would like to

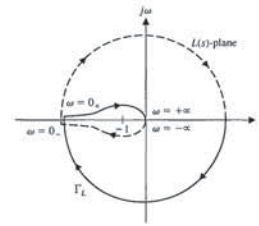


FIGURE 9.13 Nyquist contour plot for $L(s) = K/(s^2(rs+1))$.

contour encircles the -1 point twice, there are two roots of the closed-loop system in the right-hand plane, and the system, irrespective of the gain K , is unstable. ■

EXAMPLE 9.5 System with a pole in the right-hand s -plane

Let us consider the control system shown in Figure 9.14 and determine the stability of the system. First, let us consider the system without derivative feedback, so that $K_2 = 0$. We then have the loop transfer function

$$L(s) = G_c(s)G(s)H(s) = \frac{K_1}{s(s-1)}. \quad (9.34)$$

Thus, the loop transfer function has one pole in the right-hand s -plane, and therefore $P = 1$. For this system to be stable, we require $N = -P = -1$, one counterclockwise encirclement of the -1 point. At the semicircular detour at the origin

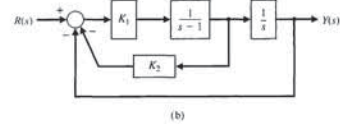
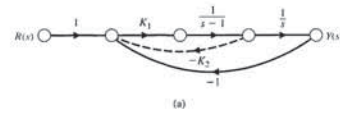


FIGURE 9.14 Second-order feedback control system. (a) Signal-flow graph. (b) Block diagram.

and there is one pole $s = 1$ in the right-hand plane so $P = 1$. Hence,

$$Z = N + P = 2, \quad (9.38)$$

and the system is unstable because two roots of the characteristic equation, irrespective of the value of the gain K_1 , lie in the right half of the s -plane.

Let us now consider again the system when the derivative feedback is included in the system shown in Figure 9.14 ($K_2 > 0$). Then the loop transfer function is

$$L(s) = G_c(s)G(s)H(s) = \frac{K_1(1+K_2s)}{s(s-1)}. \quad (9.39)$$

The portion of the contour Γ_L when $s = \epsilon e^{j\phi}$ is the same as the system without derivative feedback, as shown in Figure 9.16. However, when $s = re^{j\phi}$ as r approaches infinity, we have

$$\lim_{r \rightarrow \infty} L(s)|_{s=re^{j\phi}} = \lim_{r \rightarrow \infty} \left| \frac{K_1 K_2}{r} \right| e^{-j\phi}, \quad (9.40)$$

and the Γ_L -contour at the origin of the $L(s)$ -plane varies π rad in a counterclockwise direction. The frequency locus $L(j\omega)$ crosses the u -axis at a point determined by considering the real frequency transfer function

$$\begin{aligned} L(j\omega) &= G_c(j\omega)G(j\omega)H(j\omega) = \frac{K_1(1+K_2j\omega)}{-\omega^2 - j\omega} \\ &= \frac{-K_1(\omega^2 + \omega^2 K_2) + j(\omega - K_2\omega^3)K_1}{\omega^2 + \omega^4}. \end{aligned} \quad (9.41)$$

The $L(j\omega)$ -locus intersects the u -axis at a point where the imaginary part of $L(j\omega)$ is zero. Therefore,

$$\omega - K_2\omega^3 = 0$$

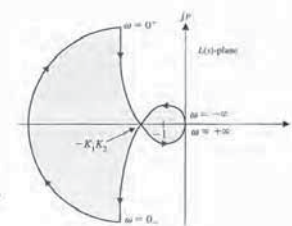


FIGURE 9.16 Nyquist diagram for $L(s) = K_1(1+K_2s)/(s(s-1))$.

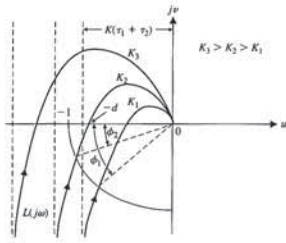


FIGURE 9.18 Polar plot for $L(j\omega)$ for three values of gain.

the relative stability. This measure of relative stability is called the **gain margin** and is defined as the **reciprocal of the gain** $|L(j\omega)|$ at the frequency at which the **phase angle reaches -180°** (that is, $v = 0$). The gain margin is a measure of the factor by which the system gain would have to be increased for the $L(j\omega)$ locus to pass through the $u = -1$ point. Thus, for a gain $K = K_2$ in Figure 9.18, the gain margin is equal to the reciprocal of $L(j\omega)$ when $v = 0$. Because $\omega = 1/\sqrt{\tau_1\tau_2}$ when the phase shift is -180° , we have a gain margin equal to

$$\frac{1}{|L(j\omega)|} = \left[\frac{K_2\tau_1\tau_2}{\tau_1 + \tau_2} \right]^{-1} = \frac{1}{d} \quad (9.46)$$

The gain margin can be defined in terms of a **logarithmic (decibel) measure** as

$$20 \log \frac{1}{d} = -20 \log d \text{ dB.} \quad (9.47)$$

For example, when $\tau_1 = \tau_2 = 1$, the system is stable when $K \leq 2$. Thus, when $K = K_2 = 0.5$, the gain margin is equal to

$$\frac{1}{d} = \left[\frac{K_2\tau_1\tau_2}{\tau_1 + \tau_2} \right]^{-1} = 4, \quad (9.48)$$

or, in logarithmic measure,

$$20 \log 4 = 12 \text{ dB.} \quad (9.49)$$

Therefore, the gain margin indicates that the system gain can be increased by a factor of four (12 dB) before the stability boundary is reached.

The gain margin is the increase in the system gain when phase = -180° that will result in a marginally stable system with intersection of the $-1 + j0$ point on the Nyquist diagram.

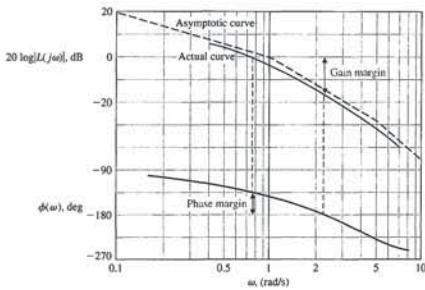


FIGURE 9.19 Bode diagram for $L(j\omega) = \frac{1}{j\omega(j\omega + 1)(0.2j\omega + 1)}$.

is shown in Figure 9.20. The indicated phase margin is 43° , and the gain margin is 15 dB. For comparison, the locus for

$$L_2(j\omega) = G_c(j\omega)G(j\omega)H_2(j\omega) = \frac{1}{j\omega(j\omega + 1)^2} \quad (9.52)$$

is also shown in Figure 9.20. The gain margin for L_2 is equal to 5.7 dB, and the phase margin for L_2 is equal to 20° . Clearly, the feedback system $L_2(j\omega)$ is relatively less stable than the system $L_1(j\omega)$. However, the question still remains: How much less stable is the system $L_2(j\omega)$ in comparison to the system $L_1(j\omega)$? In the following, we answer this question for a second-order system, and the general usefulness of the relation that we develop will depend on the presence of dominant roots.

Let us now determine the phase margin of a second-order system and relate the phase margin to the damping ratio ζ of an underdamped system. Consider the loop-transfer function of the system shown in Figure 9.1, where

$$L(s) = G_c(s)G(s)H(s) = \frac{\omega_n^2}{s(s + 2\zeta\omega_n)}. \quad (9.53)$$

The characteristic equation for this second-order system is

$$s^2 + 2\zeta\omega_n s + \omega_n^2 = 0.$$

Therefore, the closed-loop roots are

$$s = -\zeta\omega_n \pm j\omega_n\sqrt{1 - \zeta^2}.$$

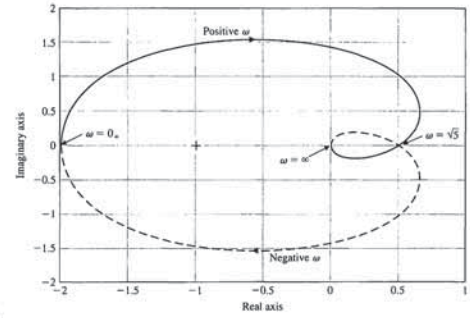


FIGURE 9.17 Nyquist diagram for Example 9.6 for $L(j\omega)/K$.

determine a similar measure of relative stability useful for the frequency response method. The Nyquist criterion provides us with suitable information concerning the absolute stability and, furthermore, can be utilized to define and ascertain the relative stability of a system.

The Nyquist stability criterion is defined in terms of the $(-1, 0)$ point on the polar plot or the 0-dB, -180° point on the Bode diagram or log-magnitude-phase diagram. Clearly, the proximity of the $L(j\omega)$ -locus to this stability point is a measure of the relative stability of a system. The polar plot for $L(j\omega)$ for several values of K and

$$L(j\omega) = G_c(j\omega)G(j\omega)H(j\omega) = \frac{K}{j\omega(j\omega\tau_1 + 1)(j\omega\tau_2 + 1)} \quad (9.44)$$

is shown in Figure 9.18. As K increases, the polar plot approaches the -1 point and eventually encircles the -1 point for a gain $K = K_3$. We determined in Section 9.3 that the locus intersects the u -axis at a point

$$u = \frac{-K\tau_1\tau_2}{\tau_1 + \tau_2}. \quad (9.45)$$

Therefore, the system has roots on the $j\omega$ -axis when

$$u = -1 \text{ or } K = \frac{\tau_1 + \tau_2}{\tau_1\tau_2}.$$

As K is decreased below this marginal value, the stability is increased, and the margin between the critical gain $K = (\tau_1 + \tau_2)/\tau_1\tau_2$ and a gain $K = K_2$ is a measure of

An alternative measure of relative stability can be defined in terms of the phase angle margin between a specific system and a system that is marginally stable. The **phase margin** is defined as the **phase angle through which the $L(j\omega)$ locus must be rotated so that the unity magnitude $|L(j\omega)| = 1$ point will pass through the $(-1, 0)$ point in the $L(j\omega)$ plane**. This measure of relative stability is equal to the additional phase lag required before the system becomes unstable. This information can be determined from the Nyquist diagram shown in Figure 9.18. For a gain $K = K_2$, an additional phase angle, ϕ_2 , may be added to the system before the system becomes unstable. Similarly, for the gain K_1 , the phase margin is equal to ϕ_1 , as shown in Figure 9.18.

The phase margin is the amount of phase shift of the $L(j\omega)$ at unity magnitude that will result in a marginally stable system with intersection of the $-1 + j0$ point on the Nyquist diagram.

The gain and phase margins are easily evaluated from the Bode diagram, and because it is preferable to draw the Bode diagram in contrast to the polar plot, it is worthwhile to illustrate the relative stability measures for the Bode diagram. The critical point for stability is $u = -1, v = 0$ in the $L(j\omega)$ -plane, which is equivalent to a logarithmic magnitude of 0 dB and a phase angle of 180° (or -180°) on the Bode diagram.

It is relatively straightforward to examine the Nyquist diagram of a minimum-phase system. Special care is required with a nonminimum-phase system, however, and the complete Nyquist diagram should be studied to determine stability.

The gain margin and phase margin can be readily calculated by utilizing a computer program, assuming the system is minimum phase. In contrast, for nonminimum-phase systems, the complete Nyquist diagram must be constructed.

The Bode diagram of

$$L(j\omega) = G_c(j\omega)G(j\omega)H(j\omega) = \frac{1}{j\omega(j\omega + 1)(0.2j\omega + 1)} \quad (9.50)$$

is shown in Figure 9.19. The phase angle when the logarithmic magnitude is 0 dB is equal to -137° . Thus, the phase margin is $180^\circ - 137^\circ = 43^\circ$, as shown in Figure 9.19. The logarithmic magnitude when the phase angle is -180° is -15 dB, and therefore the gain margin is equal to 15 dB, as shown in Figure 9.19.

The frequency response of a system can be graphically portrayed on the log-magnitude-phase-angle diagram. For the log-magnitude-phase diagram, the critical stability point is the 0-dB, -180° point, and the gain margin and phase margin can be easily determined and indicated on the diagram. The log-magnitude-phase locus of

$$L_1(j\omega) = G_c(j\omega)G(j\omega)H_1(j\omega) = \frac{1}{j\omega(j\omega + 1)(0.2j\omega + 1)} \quad (9.51)$$

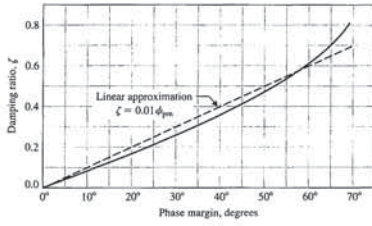


FIGURE 9.21 Damping ratio versus phase margin for a second-order system.

The phase margin for this system is

$$\begin{aligned} \phi_{pm} &= 180^\circ - 90^\circ - \tan^{-1} \frac{\omega_c}{2\zeta\omega_n} \\ &= 90^\circ - \tan^{-1} \left(\frac{1}{2\zeta} [(4\zeta^4 + 1)^{1/2} - 2\zeta^2]^{1/2} \right) \\ &= \tan^{-1} \frac{2}{[(4 + 1/\zeta^4)^{1/2} - 2]^{1/2}} \end{aligned} \quad (9.57)$$

Equation (9.57) is the relationship between the damping ratio ζ and the phase margin ϕ_{pm} , which provides a correlation between the frequency response and the time response. A plot of ζ versus ϕ_{pm} is shown in Figure 9.21. The actual curve of ζ versus ϕ_{pm} can be approximated by the dashed line shown in Figure 9.21. The slope of the linear approximation is equal to 0.01, and therefore an approximate linear relationship between the damping ratio and the phase margin is

$$\zeta = 0.01\phi_{pm} \quad (9.58)$$

where the phase margin is measured in degrees. This approximation is reasonably accurate for $\zeta \leq 0.7$ and is a useful index for correlating the frequency response with the transient performance of a system. Equation (9.58) is a suitable approximation for a second-order system and may be used for higher-order systems if we can assume that the transient response of the system is primarily due to a pair of dominant underdamped roots. The approximation of a higher-order system by a dominant second-order system is a useful approximation indeed! Although it must be used with care, control engineers find this approach to be a simple, yet fairly accurate, technique of setting the specifications of a control system.

Therefore, for the system with a loop transfer function

$$L(j\omega) = \frac{1}{j\omega(j\omega + 1)(0.2j\omega + 1)} \quad (9.59)$$

we found that the phase margin was 43°, as shown in Figure 9.19. Thus, the damping ratio is approximately

$$\zeta \approx 0.01\phi_{pm} = 0.43. \quad (9.60)$$

9.5 TIME-DOMAIN PERFORMANCE CRITERIA IN THE FREQUENCY DOMAIN

The transient performance of a feedback system can be estimated from the closed-loop frequency response. The **closed-loop frequency response** is the frequency response of the closed-loop transfer function $T(j\omega)$. The open- and closed-loop frequency responses for a single-loop system are related as follows:

$$\frac{Y(j\omega)}{R(j\omega)} = T(j\omega) = \frac{G_c(j\omega)G(j\omega)}{1 + G_c(j\omega)G(j\omega)H(j\omega)} \quad (9.62)$$

The Nyquist criterion and the phase margin index are defined for the loop transfer function $L(j\omega) = G_c(j\omega)G(j\omega)H(j\omega)$. However, as we found in Section 8.2, the maximum magnitude of the closed-loop frequency response can be related to the damping ratio of a second-order system of

$$M_{pw} = |T(\omega_c)| = (2\zeta\sqrt{1 - \zeta^2})^{-1}, \quad \zeta < 0.707. \quad (9.63)$$

This relation is graphically portrayed in Figure 8.11. Because this relationship between the closed-loop frequency response and the transient response is a useful one, we would like to be able to determine M_{pw} from the plots completed for the investigation of the Nyquist criterion. That is, we want to be able to obtain the closed-loop frequency response (Equation 9.62) from the open-loop frequency response. Of course, we could determine the closed-loop roots of $1 + L(s)$ and plot the closed-loop frequency response. However, once we have invested all the effort necessary to find the closed-loop roots of a characteristic equation, then a closed-loop frequency response is not necessary.

The relation between the closed-loop and open-loop frequency response is illuminated on the magnitude-phase plot when considering unity feedback systems, that is, when $H(s) = 1$ in Figure 9.1. In the unity feedback case, key performance indicators such as M_{pw} and ω_c can be determined from the magnitude-phase plot using circles of constant magnitude of the closed-loop transfer function. These circles are known as constant M -circles. If the system is not in fact a unity feedback system where $H(j\omega) = 1$, we can modify the system (see Section 5.6). For unity feedback systems, Equation (9.62) becomes

$$T(j\omega) = M(\omega)e^{j\theta(\omega)} = \frac{G_c(j\omega)G(j\omega)}{1 + G_c(j\omega)G(j\omega)} \quad (9.64)$$

The relationship between $T(j\omega)$ and $G_c(j\omega)G(j\omega)$ is readily obtained in terms of complex variables in the $G_c(j\omega)G(j\omega)$ -plane. The coordinates of the $G_c(j\omega)G(j\omega)$ -plane are u and v , and we have

$$G_c(j\omega)G(j\omega) = u + jv. \quad (9.65)$$

Therefore, the magnitude of the closed-loop transfer function is

$$M(\omega) = \left| \frac{G_c(j\omega)G(j\omega)}{1 + G_c(j\omega)G(j\omega)} \right| = \left| \frac{u + jv}{1 + u + jv} \right| = \frac{(u^2 + v^2)^{1/2}}{[(1 + u)^2 + v^2]^{1/2}} \quad (9.66)$$

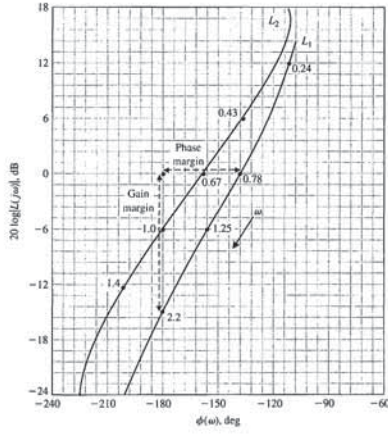


FIGURE 9.20 Log-magnitude-phase curve for L_1 and L_2 .

The frequency domain form of Equation (9.53) is

$$L(j\omega) = \frac{\omega_n^2}{j\omega(j\omega + 2\zeta\omega_n)} \quad (9.54)$$

The magnitude of the frequency response is equal to 1 at a frequency ω_c ; thus,

$$\frac{\omega_n^2}{\omega_c(\omega_c^2 + 4\zeta^2\omega_n^2)^{1/2}} = 1. \quad (9.55)$$

Rearranging Equation (9.55), we obtain

$$(\omega_c^2)^2 + 4\zeta^2\omega_n^2(\omega_c^2) - \omega_n^4 = 0. \quad (9.56)$$

Solving for ω_c , we find that

$$\frac{\omega_c^2}{\omega_n^2} = (4\zeta^4 + 1)^{1/2} - 2\zeta^2.$$

Then the percent overshoot to a step input for this system is approximately

$$P.O. = 22\%, \quad (9.61)$$

as obtained from Figure 5.8 for $\zeta = 0.43$.

It is feasible to develop a computer program to calculate and plot phase margin and gain margin versus the gain K for a specified $L(j\omega)$. Consider the system of Figure 9.1 with

$$L(s) = G_c(s)G(s)H(s) = \frac{K}{s(s + 4)^2}.$$

The gain for which the system is marginally stable is $K = K^* = 128$. The gain margin and the phase margin plotted versus K are shown in Figures 9.22(a) and (b), respectively. The gain margin is plotted versus the phase margin, as shown in Figure 9.22(c). Note that either the phase margin or the gain margin is a suitable measure of the performance of the system. We will normally emphasize phase margin as a frequency-domain specification.

The phase margin of a system is a quite suitable frequency response measure for indicating the expected transient performance of a system. Another useful index of performance in the frequency domain is M_{pw} , the maximum magnitude of the closed-loop frequency response, and we shall now consider this practical index.

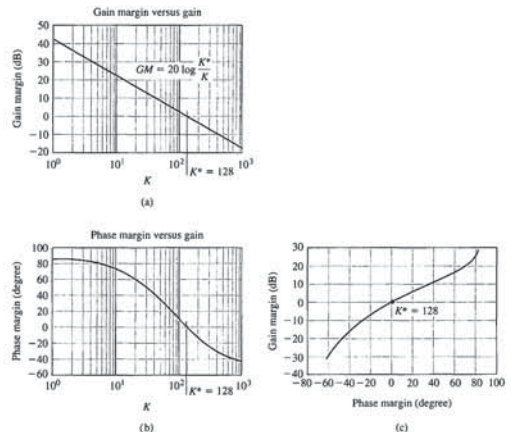


FIGURE 9.22 (a) Gain margin versus gain K . (b) Phase margin versus gain K . (c) Gain margin versus phase margin.

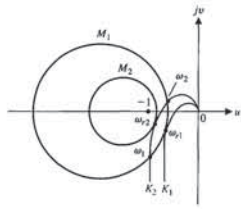


FIGURE 9.24 Polar plot of $G_c(j\omega)G(j\omega)$ for two values of a gain ($K_2 > K_1$).

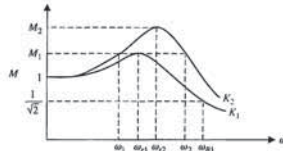


FIGURE 9.25 Closed-loop frequency response of $T(j\omega) = G_c(j\omega)G(j\omega)/(1 + G_c(j\omega)G(j\omega))$. Note that $K_2 > K_1$.

system from the $(u + jv)$ -plane. If the maximum magnitude, M_{pwr} , is the only information desired, then it is sufficient to read this value directly from the polar plot. The maximum magnitude of the closed-loop frequency response, M_{pwr} , is the value of the M circle that is tangent to the $G_c(j\omega)G(j\omega)$ -locus. The point of tangency occurs at the frequency ω_r , the resonant frequency. The complete closed-loop frequency response of a system can be obtained by reading the magnitude M of the circles that the $G_c(j\omega)G(j\omega)$ -locus intersects at several frequencies. Therefore, the system with a gain $K = K_2$ has a closed-loop magnitude M_1 at the frequencies ω_1 and ω_2 . This magnitude is read from Figure 9.24 and is shown on the closed-loop frequency response in Figure 9.25. The **bandwidth** for K_1 is shown as ω_{B1} .

It may be empirically shown that the crossover frequency ω_c on the open-loop Bode diagram is related to the closed-loop system bandwidth ω_B by the approximation $\omega_B = 1.6\omega_c$ for ξ in the range 0.2 to 0.8.

In a similar manner, we can obtain circles of constant closed-loop phase angles. Thus, for Equation (9.64), the angle relation is

$$\begin{aligned} \phi &= \angle T(j\omega) = \angle (u + jv)/(1 + u + jv) \\ &= \tan^{-1}\left(\frac{v}{u}\right) - \tan^{-1}\left(\frac{v}{1 + u}\right). \end{aligned} \quad (9.70)$$

Taking the tangent of both sides and rearranging, we have

$$u^2 + v^2 + u - \frac{v}{N} = 0, \quad (9.71)$$

Squaring Equation (9.66) and rearranging, we obtain

$$(1 - M^2)u^2 + (1 - M^2)v^2 - 2M^2u = M^2. \quad (9.67)$$

Dividing Equation (9.67) by $1 - M^2$ and adding the term $[M^2/(1 - M^2)]^2$ to both sides, we have

$$u^2 + v^2 - \frac{2M^2u}{1 - M^2} + \left(\frac{M^2}{1 - M^2}\right)^2 = \left(\frac{M^2}{1 - M^2}\right)^2 + \left(\frac{M^2}{1 - M^2}\right)^2. \quad (9.68)$$

Rearranging, we obtain

$$\left(u - \frac{M^2}{1 - M^2}\right)^2 + v^2 = \left(\frac{M}{1 - M^2}\right)^2, \quad (9.69)$$

which is the equation of a circle in the (u, v) -plane with the center at

$$u = \frac{M^2}{1 - M^2}, \quad v = 0.$$

The radius of the circle is equal to $|M/(1 - M^2)|$. Therefore, we can plot several circles of constant magnitude M in the $[G_c(j\omega)G(j\omega) = u + jv]$ -plane. Several constant M circles are shown in Figure 9.23. The circles to the left of $u = -1/2$ are for $M > 1$, and the circles to the right of $u = -1/2$ are for $M < 1$. When $M = 1$, the circle becomes the straight line $u = -1/2$, which is evident from inspection of Equation (9.67).

The open-loop frequency response for a system is shown in Figure 9.24 for two gain values where $K_2 > K_1$. The frequency response curve for the system with gain K_1 is tangent to magnitude circle M_1 at a frequency ω_{r1} . Similarly, the frequency response curve for gain K_2 is tangent to magnitude circle M_2 at the frequency ω_{r2} . Therefore, the closed-loop frequency response magnitude curves are estimated as shown in Figure 9.25. Hence, we can obtain the closed-loop frequency response of a

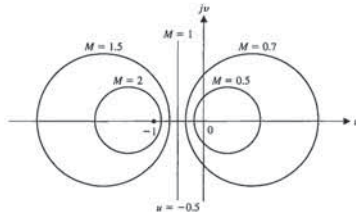


FIGURE 9.23 Constant M circles.

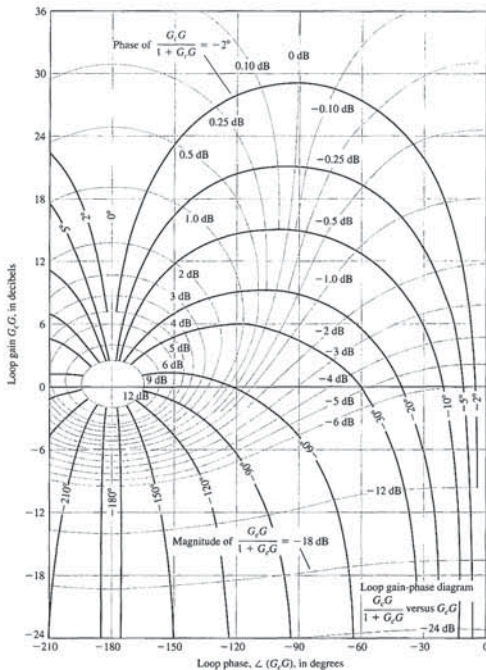


FIGURE 9.26 Nichols chart. The phase curves for the closed-loop system are shown as heavy curves.

where $N = \tan \phi$. Adding the term $1/4[1 + 1/N^2]$ to both sides of the equation and simplifying, we obtain

$$\left(u + \frac{1}{2}\right)^2 + \left(v - \frac{1}{2N}\right)^2 = \frac{1}{4}\left(1 + \frac{1}{N^2}\right), \quad (9.72)$$

which is the equation of a circle with its center at $u = -1/2$ and $v = +1/(2N)$. The radius of the circle is equal to $1/2[1 + 1/N^2]^{1/2}$. Therefore, the constant phase angle curves can be obtained for various values of N in a manner similar to the M circles.

The constant M and N circles can be used for analysis and design in the polar plane. However, it is much easier to obtain the Bode diagram for a system, and it would be preferable if the constant M and N circles were translated to a logarithmic gain phase. N. B. Nichols transformed the constant M and N circles to the log-magnitude-phase diagram, and the resulting chart is called the **Nichols chart** [3, 7]. The M and N circles appear as contours on the Nichols chart shown in Figure 9.26. The coordinates of the log-magnitude-phase diagram are the same as those used in Section 8.5. However, superimposed on the log-magnitude-phase plane we find constant M and N lines. The constant M lines are given in decibels and the N lines in degrees. An example will illustrate the use of the Nichols chart to determine the closed-loop frequency response.

EXAMPLE 9.7 Stability using the Nichols chart

Consider a unity feedback system with a loop transfer function

$$G_c(j\omega)G(j\omega) = \frac{1}{j\omega(j\omega + 1)(0.2j\omega + 1)}. \quad (9.73)$$

The $G_c(j\omega)G(j\omega)$ -locus is plotted on the Nichols chart and is shown in Figure 9.27. The maximum magnitude, M_{pwr} , is equal to +2.5 dB and occurs at a frequency $\omega_r = 0.8$. The closed-loop phase angle at ω_r is equal to -72° . The 3-dB closed-loop bandwidth, where the closed-loop magnitude is -3 dB, is equal to $\omega_B = 1.33$, as shown in Figure 9.27. The closed-loop phase angle at ω_B is equal to -142° . ■

EXAMPLE 9.8 Third-order system

Let us consider a unity feedback system with a loop transfer function

$$G_c(j\omega)G(j\omega) = \frac{0.64}{j\omega[(j\omega)^2 + j\omega + 1]} \quad (9.74)$$

where $\xi = 0.5$ for the complex poles. The Nichols diagram for this system is shown in Figure 9.28. The phase margin for this system as it is determined from the Nichols chart is 30° . On the basis of the phase, we use Equation (9.58) to estimate the system damping ratio as $\xi = 0.30$. The maximum magnitude is equal to +9 dB occurring at a frequency $\omega_r = 0.88$. Therefore,

$$20 \log M_{pwr} = 9 \text{ dB}, \quad \text{or} \quad M_{pwr} = 2.8.$$

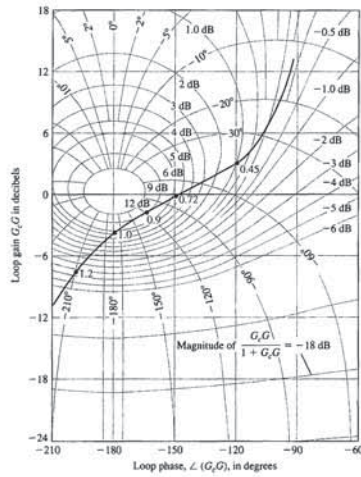


FIGURE 9.28 Nichols diagram for $G_c(j\omega)G(j\omega) = 0.64/(j\omega(j\omega^2 + j\omega + 1))$.

we are usually safe if the lower value of the damping ratio resulting from the phase margin and the M_{pw} relation is used for analysis and design purposes. ■

The Nichols chart can be used for design purposes by altering the $G_c G(j\omega)$ -locus so we can obtain a desirable phase margin and M_{pw} . The system gain K is readily adjusted to provide a suitable phase margin and M_{pw} by inspecting the Nichols chart. For example, let us consider again Example 9.8, where

$$G_c(j\omega)G(j\omega) = \frac{K}{j\omega(j\omega^2 + j\omega + 1)} \quad (9.76)$$

The $G_c G(j\omega)$ -locus on the Nichols chart for $K = 0.64$ is shown in Figure 9.28. Let us determine a suitable value for K so that the system damping ratio is greater than 0.30. Examining Figure 8.11, we find that it is required that M_{pw} be less than 1.75 (4.9 dB). From Figure 9.28, we find that the $G_c G(j\omega)$ -locus will be tangent to the 4.9-dB curve if the $G_c G(j\omega)$ -locus is lowered by a factor of 2.2 dB. Therefore, K should be

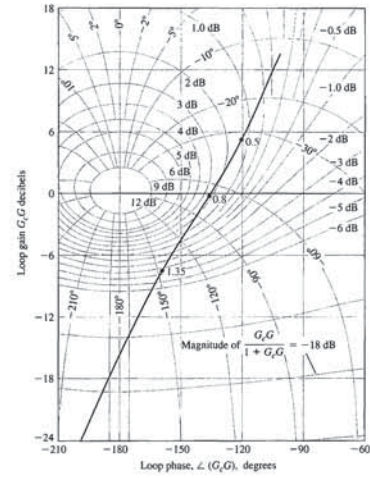


FIGURE 9.27 Nichols diagram for $G_c(j\omega)G(j\omega) = 1/(j\omega(j\omega + 1))$. Three points on curve are shown for $\omega = 0.5, 0.8,$ and $1.35,$ respectively.

Solving Equation (9.63), we find that $\zeta = 0.18$. We are confronted with two conflicting damping ratios, where one is obtained from a phase margin measure and another from a peak frequency response measure. In this case, we have discovered an example in which the correlation between the frequency domain and the time domain is unclear and uncertain. This apparent conflict is caused by the nature of the $G_c(j\omega)G(j\omega)$ -locus, which slopes rapidly toward the 180° line from the 0-dB axis. If we determine the roots of the characteristic equation for $1 + L(s)$, we obtain

$$q(s) = (s + 0.77)(s^2 + 0.225s + 0.826) = 0. \quad (9.75)$$

The damping ratio of the complex conjugate roots is equal to 0.124, where the complex roots do not dominate the response of the system. Therefore, the real root will add some damping to the system, and we might estimate the damping ratio to be approximately the value determined from the M_{pw} index; that is, $\zeta = 0.18$. A designer must use the frequency-domain-to-time-domain correlations with caution. However,

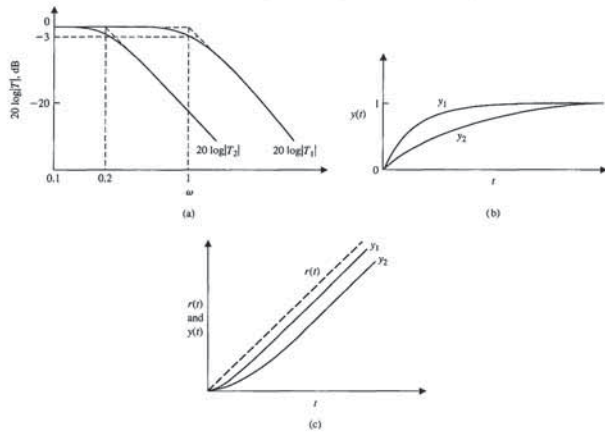


FIGURE 9.29 Response of two first-order systems.

the system. Fortunately, the Nyquist criterion can be utilized to determine the effect of the time delay on the relative stability of the feedback system. A pure time delay, without attenuation, is represented by the transfer function

$$G_d(s) = e^{-sT}, \quad (9.79)$$

where T is the delay time. The Nyquist criterion remains valid for a system with a time delay because the factor e^{-sT} does not introduce any additional poles or zeros within the contour. The factor adds a phase shift to the frequency response without altering the magnitude curve.

This type of time delay occurs in systems that have a movement of a material that requires a finite time to pass from an input or control point to an output or measured point [8, 9].

For example, a steel rolling mill control system is shown in Figure 9.31. The motor adjusts the separation of the rolls so that the thickness error is minimized. If the steel is traveling at a velocity v , then the time delay between the roll adjustment and the measurement is

$$T = \frac{d}{v}$$

reduced by 2.2 dB or the factor $\text{antilog}(2.2/20) = 1.28$. Thus, the gain K must be less than $0.64/1.28 = 0.50$ if the system damping ratio is to be greater than 0.30.

9.6 SYSTEM BANDWIDTH

The bandwidth of the closed-loop control system is an excellent measurement of the range of fidelity of response of the system. In systems where the low-frequency magnitude is 0 dB on the Bode diagram, the bandwidth is measured at the -3-dB frequency. The speed of response to a step input will be roughly proportional to ω_B , and the settling time is inversely proportional to ω_B . Thus, we seek a large bandwidth consistent with reasonable system components [12].

Consider the following two closed-loop system transfer functions:

$$T_1(s) = \frac{1}{s + 1}$$

and

$$T_2(s) = \frac{1}{5s + 1} \quad (9.77)$$

The frequency response of the two systems is contrasted in part (a) of Figure 9.29, and the step response of the systems is shown in part (b). Also the response to a ramp is shown in part (c) of that figure. The system with the larger bandwidth provides the faster step response and higher fidelity ramp response.

Now consider the two second-order systems with closed-loop transfer functions

$$T_3(s) = \frac{100}{s^2 + 10s + 100}$$

and

$$T_4(s) = \frac{900}{s^2 + 30s + 900} \quad (9.78)$$

Both systems have a ζ of 0.5. The frequency response of both closed-loop systems is shown in Figure 9.30(a). The natural frequency is 10 and 30 for systems T_3 and T_4 , respectively. The bandwidth is 12.7 and 38.1 for systems T_3 and T_4 , respectively. Both systems have a 16% overshoot, but T_4 has a peak time of 0.12 second compared to 0.36 for T_3 , as shown in Figure 9.30(b). Also, note that the settling time for T_4 is 0.27 second, while the settling time for T_3 is 0.8 second. The system with a larger bandwidth provides a faster response.

9.7 THE STABILITY OF CONTROL SYSTEMS WITH TIME DELAYS

The Nyquist stability criterion has been discussed and illustrated in the previous sections for control systems whose transfer functions are rational polynomials of $j\omega$. Many control systems have a time delay within the closed loop of the system that affects the stability of the system. A **time delay** is the time interval between the start of an event at one point in a system and its resulting action at another point in

$$L(j\omega) = G_c(j\omega)G(j\omega)e^{-j\omega T} \quad (9.81)$$

The usual loop transfer function is plotted on the $L(j\omega)$ -plane and the stability ascertained relative to the -1 point. Alternatively, we can plot the Bode diagram including the delay factor and investigate the stability relative to the 0-dB, -180° point. The delay factor $e^{-j\omega T}$ results in a phase shift

$$\phi(\omega) = -\omega T \quad (9.82)$$

and is readily added to the phase shift resulting from $G_c(j\omega)G(j\omega)$. Note that the angle is in radians in Equation (9.82). An example will show the simplicity of this approach on the Bode diagram.

EXAMPLE 9.9 Liquid level control system

A level control system is shown in Figure 9.32(a) and the block diagram in Figure 9.32(b) [11]. The time delay between the valve adjustment and the fluid output is $T = d/v$. Therefore, if the flow rate is $5 \text{ m}^3/\text{s}$, the cross-sectional area of the pipe is 1 m^2 , and the distance is equal to 5 m, then we have a time delay $T = 1 \text{ s}$. The loop transfer function is then

$$L(s) = G_d(s)G(s)G_f(s)e^{-sT} = \frac{31.5}{(s+1)(30s+1)(s^2/9 + (s/3) + 1)}e^{-sT} \quad (9.83)$$

The Bode diagram for this system is shown in Figure 9.33. The phase angle is shown both for the denominator factors alone and with the additional phase lag due to the time delay. The logarithmic gain curve crosses the 0-dB line at $\omega = 0.8$. Therefore, the phase margin of the system without the pure time delay would be 40° . However, with the time delay added, we find that the phase margin is equal to -3° , and the system is unstable. Consequently, the system gain must be reduced in order to provide a reasonable phase margin. To provide a phase margin of 30° , the gain would have to be decreased by a factor of 5 dB, to $K = 31.5/1.78 = 17.7$.

A time delay e^{-sT} in a feedback system introduces an additional phase lag and results in a less stable system. Therefore, as pure time delays are unavoidable in many systems, it is often necessary to reduce the loop gain in order to obtain a stable response. However, the cost of stability is the resulting increase in the steady-state error of the system as the loop gain is reduced. ■

The systems considered by most analytical tools are described by rational functions (that is, transfer functions) or by a finite set of ordinary constant coefficient differential equations. Since the time-delay is given by e^{-sT} , where T is the delay, we see that the time delay is nonrational. It would be helpful if we could obtain a rational function approximation of the time-delay. Then it would be more convenient to incorporate the delay into the block diagram for analysis and design purposes.

The Padé approximation uses a series expansion of the transcendental function e^{-sT} and matches as many coefficients as possible with a series expansion of a rational function of specified order. For example, to approximate the function e^{-sT} with a first-order rational function, we begin by expanding both functions in a series (actually a Maclaurin series),

$$e^{-sT} = f(0) + \frac{1}{1!}f'(0) + \frac{1}{2!}f''(0) + \dots$$

Section 9.8 Design Examples

$$e^{-sT} = 1 - sT + \frac{(sT)^2}{2!} - \frac{(sT)^3}{3!} + \frac{(sT)^4}{4!} - \frac{(sT)^5}{5!} + \dots \quad (9.84)$$

and

$$\frac{n_1s + n_0}{d_1s + d_0} = \frac{n_0}{d_0} + \left(\frac{d_0n_1 - n_0d_1}{d_0^2}\right)s + \left(\frac{d_0^2n_0 - d_1n_1}{d_0^3} - \frac{d_1n_1}{d_0^2}\right)s^2 + \dots$$

For a first-order approximation, we want to find n_0 , n_1 , d_0 , and d_1 such that

$$e^{-sT} \approx \frac{n_1s + n_0}{d_1s + d_0}$$

Equating the corresponding coefficients of the terms in s , we obtain the relationships

$$\frac{n_0}{d_0} = 1, \quad \frac{n_1}{d_0} - \frac{n_0d_1}{d_0^2} = -T, \quad \frac{d_0^2n_0 - d_1n_1}{d_0^3} - \frac{d_1n_1}{d_0^2} = \frac{T^2}{2}, \dots$$

Solving for n_0 , d_0 , n_1 , and d_1 yields

$$\begin{aligned} n_0 &= d_0, \\ d_1 &= \frac{d_0T}{2}, \\ n_1 &= -\frac{d_0T}{2}. \end{aligned}$$

Setting $d_0 = 1$, and solving yields

$$e^{-sT} \approx \frac{n_1s + n_0}{d_1s + d_0} = \frac{-\frac{T}{2}s + 1}{\frac{T}{2}s + 1} \quad (9.85)$$

A series expansion of Equation (9.85) yields

$$\frac{n_1s + n_0}{d_1s + d_0} = \frac{-\frac{T}{2}s + 1}{\frac{T}{2}s + 1} = 1 - Ts + \frac{T^2s^2}{2} - \frac{T^3s^3}{4} + \dots \quad (9.86)$$

Comparing Equation (9.86) to Equation (9.84), we verify that the first three terms match. So for small s , the Padé approximation is a reasonable representation of the time-delay. Higher-order rational functions can be obtained.

9.8 DESIGN EXAMPLES

In this example, we present three illustrative examples. The first example we consider is a design problem that supports green engineering and involves controlling the pitch angles of blades on large-scale wind turbines. The wind speeds are assumed to be high enough so that the pitch angle of the turbine blades can be prescribed properly to shed excess power to regulate the generated wind power at desired levels. The second example is a remotely controlled reconnaissance vehicle control design. The Nichols chart is illustrated as a key element of the design of a controller gain to meet time-domain specifications. The third example considers the control of a hot

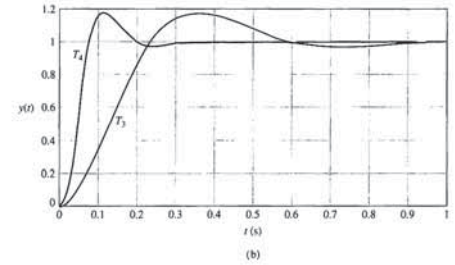
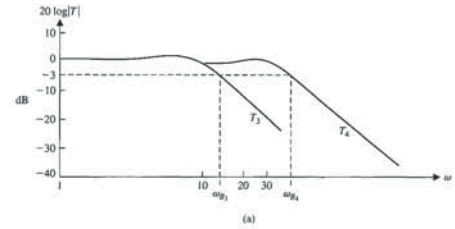


FIGURE 9.30 Response of two second-order systems.

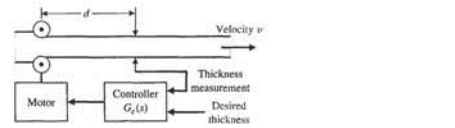


FIGURE 9.31 Steel rolling mill control system.

Therefore, to have a negligible time delay, we must decrease the distance to the measurement and increase the velocity of the flow of steel. Usually, we cannot eliminate the effect of time delay; thus, the loop transfer function is [10]

$$G_c(s)G(s)e^{-sT} \quad (9.80)$$

However, we note that the frequency response of this system is obtained from the loop transfer function

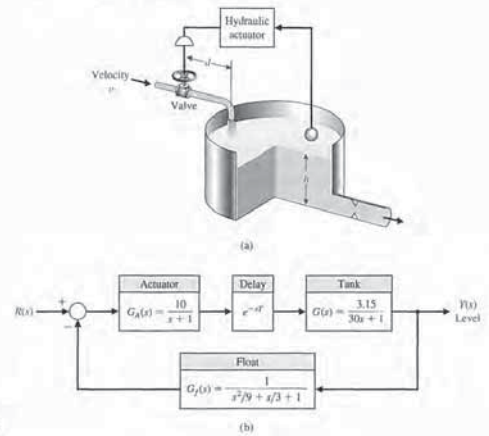


FIGURE 9.32 (a) Liquid level control system, (b) Block diagram.

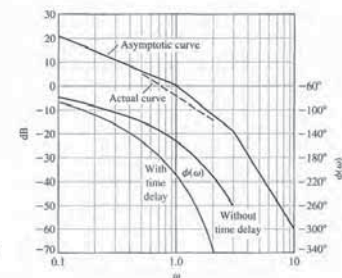


FIGURE 9.33 Bode diagram for level control system.

third-order transfer function of the turbine is given by

$$G(s) = \left[\frac{1}{\tau s + 1} \right] \left[\frac{K\omega_n^2}{s^2 + 2\zeta\omega_n s + \omega_n^2} \right] \quad (9.87)$$

where $K = -7000$, $\tau = 5$ seconds, $\zeta = 0.005$, and $\omega_n = 20$ rad/s. The input to the turbine model is the commanded pitch angle (in radians) plus disturbances and the output is the rotor speed (in rpm). For commercial wind turbines, pitch control is often achieved using a PID controller, as shown in Figure 9.35(b). Selecting a PID controller

$$G_c(s) = K_p + \frac{K_I}{s} + K_D s$$

requires selecting the coefficients of the controller K_p , K_I , and K_D . The objective is to design the PID system for fast and accurate control. The control specifications are gain margin $G.M. \geq 6$ dB and phase margin $30^\circ \leq P.M. \leq 60^\circ$. The specifications for the transient response are rise time $T_r < 4$ seconds and time to peak $T_p < 10$ seconds.

Remember that the output $\omega(s)$ shown in Figure 9.35 is actually the deviation from the rated speed of the turbine. At the rated speed, the pitch control of the blades is used to regulate the rotor speed. In the linear setting described by Figure 9.35, the input desired rotor speed $\omega_d(s) = 0$ and the goal is to regulate the output to zero in the presence of disturbances.

The loop transfer function is

$$L(s) = K\omega_n^2 K_D \frac{s^2 + (K_p/K_D)s + (K_I/K_D)}{s(\tau s + 1)(s^2 + 2\zeta\omega_n s + \omega_n^2)}$$

The objective is to determine the gains K_p , K_I , and K_D to meet the control design specifications. The phase margin specification can be used to determine a target damping of the dominant roots yielding

$$\zeta = \frac{P.M.}{100} = 0.3,$$

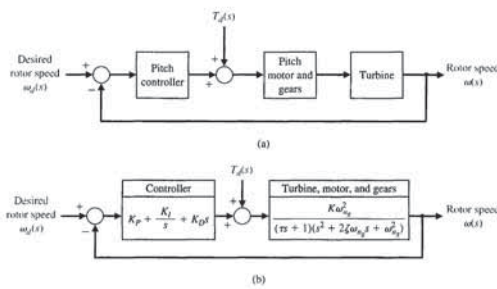


FIGURE 9.35 (a) Block diagram model of the wind turbine system. (b) Block diagram for control system design.

ingot robot used in manufacturing. The goal is to minimize the tracking error in the presence of disturbances and a known time-delay. The design process is illustrated, leading to a PI controller that meets a mixture of time-domain and frequency-domain performance specifications.

EXAMPLE 9.10 PID control of wind turbines for clean energy

Wind energy is currently the fastest-growing energy source in the world. It is a cost-effective, environmentally friendly solution to energy needs. Modern wind turbines are large, flexible structures operating in uncertain environments as wind direction and flow constantly changes. There are many controls challenges associated with efficient energy capture and delivery for wind turbines. In this design problem, we consider the so-called "above-rated" operational mode of the wind turbine. In this mode, the wind speeds are high enough that the pitch angle of the turbine blades needs to be prescribed properly to shed excess power so that the generated wind power is regulated at desired levels. This mode of operation readily permits the application of linear control theory.

Wind turbines are generally constructed in either a vertical axis configuration or a horizontal axis configuration, as shown in Figure 9.34. The horizontal axis configuration is the most common for energy production today. A horizontal axis wind turbine is mounted on a tower with two or three blades rotating placed atop a tall tower and driving an electric generator. The high placement of the blades takes advantage of the higher wind velocities. The vertical axis wind turbines are generally smaller and present a reduced noise footprint.

When there is sufficient wind, in order to regulate the rotor speed of the turbine shaft and thus the generator, the pitch of the wind turbine blades is collectively adjusted using a blade pitch motor, as illustrated in Figure 9.35(a). A simplified model of the turbine from the pitch command to the rotor speed is obtained by including a generator mode represented by a first-order transfer function in series with the drive train compliance represented by a second-order transfer function [32]. The

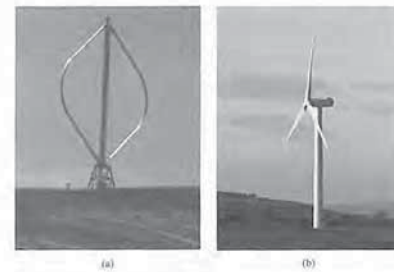


FIGURE 9.34 (a) Vertical axis wind turbine (Photo courtesy of SuperStock), and (b) Horizontal axis wind turbine (Photo courtesy of Alamy Images).

The dominant poles of the closed-loop feedback control system are $\omega_n = 0.41$ and $\zeta = 0.29$. This is very close to the design values which demonstrates the effectiveness of the design formulas even when the system under consideration is not a second-order system.

The response of the wind turbine to an impulsive disturbance is shown in Figure 9.38. In this numerical experiment, the disturbance (possibly a wind gust) imparts a step change in the wind turbine blade pitch angle. In practice, the disturbance would lead to varying pitch angle disturbances on the each blade, but for purposes of demonstration, we model this as a single step disturbance input. The result of the disturbance is a change on the rotor speed from the nominal that is brought back to zero in about 25 seconds. ■

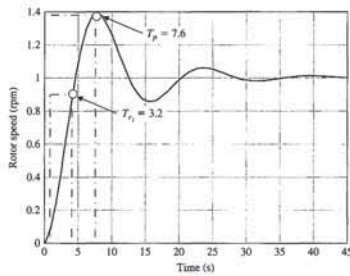


FIGURE 9.37 Closed-loop step response to a unit step showing rise time and time to peak specifications are satisfied.

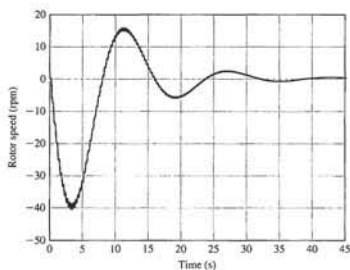


FIGURE 9.38 Disturbance response showing the rotor speed deviation from the rated speed.

where we target for a phase margin $P.M. = 30^\circ$. Then we utilize the rise time design formula to obtain a target natural frequency of the dominant roots. To this end, we use the design formula

$$T_r = \frac{2.16\zeta + 0.6}{\omega_n} < 4 \text{ seconds}$$

to obtain $\omega_n > 0.31$ when $\zeta = 0.3$. For design purposes, we choose $\omega_n = 0.4$ and $\zeta = 0.3$ for the dominant poles. As a final check on the target damping and natural frequency, we verify that the time to peak specification is reachable with $\omega_n = 0.4$ and $\zeta = 0.3$. The rise time and time to peak are estimated to be

$$T_r = \frac{2.16\zeta + 0.6}{\omega_n} = 3 \text{ seconds and } T_p = \frac{\pi}{\omega_n \sqrt{1 - \zeta^2}} = 8 \text{ seconds,}$$

which meet the design specification. First we locate the PID zeros in the left half-plane in the desired performance region defined by ω_n and ζ by specifying the ratios K_p/K_D and K_I/K_D and select the gain K_D to meet the phase margin and gain margin specifications using frequency response plots (that is, Bode plot).

The Bode plot is shown in Figure 9.36 where $K_p/K_D = 5$ and $K_I/K_D = 20$. The value of $K_D = -6.22 \times 10^{-6}$ was determined by observing the effects of varying the gain on the phase and gain margins and selecting the gain that satisfied the specifications as closely as possible. The PID controller is then given by

$$G_c(s) = -6.22 \times 10^{-6} \left[\frac{s^2 + 5s + 20}{s} \right]$$

The final design results in a phase margin of $P.M. = 32.9^\circ$ and a gain margin of $G.M. = 13.9$ dB. The step response is shown in Figure 9.37. The rise time $T_r = 3.2$ seconds and the time to peak $T_p = 7.6$ seconds. All the specifications are satisfied.

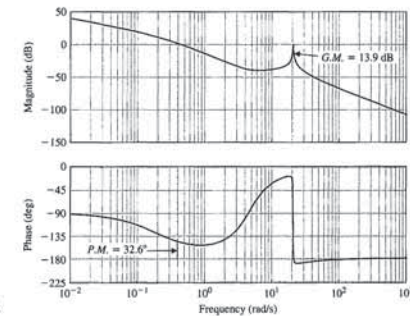


FIGURE 9.36 Bode plot with $K_p/K_D = 5$, $K_I/K_D = 20$, and $K_D = -6.22 \times 10^{-6}$.

Table 9.4 Frequency Response Data for Design Example

ω	0	1.2	1.6	2.0	2.8	4	6
dB	20	18.4	17.8	16.0	10.5	2.7	-5.2
Degrees	0	-65	-86	-108	-142	-161	-170

The calculations for $0 \leq \omega \leq 6$ provide the data summarized in Table 9.4. The Nichols diagram for $K = 20$ is shown in Figure 9.40. Examining the Nichols chart, we find that M_{pw} is 12 dB and the phase margin is 15 degrees. The step response of this system is underdamped, and we use Equation (9.58) and Figure 5.8 to predict an excessive overshoot of approximately 61%.

To reduce the overshoot to a step input, we can reduce the gain to achieve a predicted overshoot. To limit the overshoot to 25%, we select a desired ζ of the dominant roots as 0.4 (from Figure 5.8) and thus require $M_{pw} = 1.35$ (from Figure 8.11) or $20 \log M_{pw} = 2.6$ dB. To lower the gain, we will move the frequency response

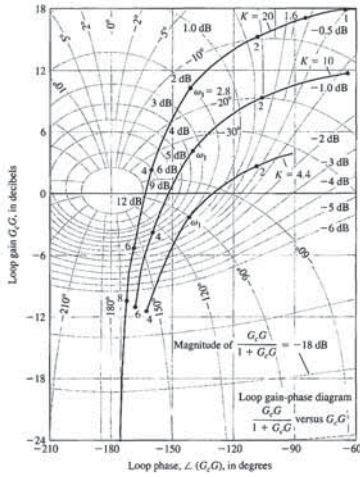


FIGURE 9.40 Nichols diagram for the design example when $K = 20$ and for two reduced gains.

EXAMPLE 9.11 Remotely controlled reconnaissance vehicle

The use of remotely controlled vehicles for reconnaissance for U.N. peacekeeping missions may be an idea whose time has come. One concept of a roving vehicle is shown in Figure 9.39(a), and a proposed speed control system is shown in Figure 9.39(b). The desired speed $R(s)$ is transmitted by radio to the vehicle; the disturbance $T_d(s)$ represents hills and rocks. The goal is to achieve good overall control with a low steady-state error and a low-overshoot response to step commands, $R(s)$ [13].

First, to achieve a low steady-state error for a unit step command, we calculate

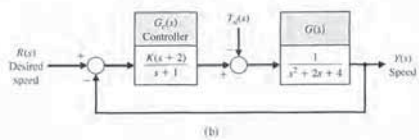
$$\begin{aligned} e_{ss} &= \lim_{s \rightarrow 0} sE(s) \\ &= \lim_{s \rightarrow 0} s \left[\frac{R(s)}{1 + L(s)} \right] \\ &= \frac{1}{1 + L(0)} = \frac{1}{1 + K/2} \end{aligned}$$

where $L(s) = G_c(s)G(s)$. If we select $K = 20$, we will obtain a steady-state error of 9% of the magnitude of the input command. Using $K = 20$, we reformulate $L(s) = G_c(s)G(s)$ for Bode diagram calculations, obtaining

$$L(s) = G_c(s)G(s) = \frac{10(1 + s/2)}{(1 + s)(1 + s/2 + s^2/4)}$$



FIGURE 9.39 (a) Remotely controlled reconnaissance vehicle. (b) Speed control system. This vehicle could be used for United Nations peacekeeping missions.



Examining the Nichols chart for $K = 10$, we have $M_{pw} = 7$ dB, and a phase margin of 26 degrees. Thus, we estimate a ζ for the dominant roots of 0.23 which should result in an overshoot to a step input of 23%. The actual response is recorded in Table 9.5. The bandwidth of the system is $\omega_B \approx 5$. Therefore, we predict a settling time (with a 2% criterion) of

$$T_s = \frac{4}{\zeta \omega_n} = \frac{4}{(0.34)(\omega_B/1.4)} = 3.3 \text{ s,}$$

since $\omega_B = 1.4\omega_n$ for $\zeta = 0.34$, using Figure 8.26. The actual settling time is approximately 5.4 seconds, as shown in Figure 9.41.

The steady-state effect of a unit step disturbance can be determined by using the final-value theorem with $R(s) = 0$, as follows:

$$y(\infty) = \lim_{s \rightarrow 0} s \left[\frac{G(s)}{1 + L(s)} \right] \left(\frac{1}{s} \right) = \frac{1}{4 + 2K} \quad (9.88)$$

Thus, the unit disturbance is reduced by the factor $4 + 2K$. For $K = 10$, we have $y(\infty) = 1/24$, or the steady-state disturbance is reduced to 4% of the disturbance magnitude. Thus we have achieved a reasonable result with $K = 10$.

The best compromise design would be $K = 10$, since we achieve a compromise steady-state error of 16.7%. If the overshoot and settling time are excessive, then we need to reshape the $L(j\omega)$ -locus on the Nichols chart by methods we will describe in Chapter 10. ■

EXAMPLE 9.12 Hot ingot robot control

The hot ingot robot mechanism is shown in Figure 9.42. The robot picks up hot ingots and sets them in a quenching tank. A vision sensor is in place to provide a measurement of the ingot position. The controller uses the sensed position information to orient the robot over the ingot (along the x-axis). The vision sensor provides the desired position input $R(s)$ to the controller. The block diagram depiction of the closed-loop

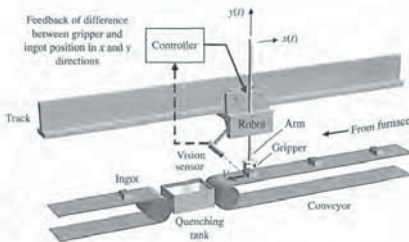


FIGURE 9.42 Artist's depiction of the hot ingot robot control system.

vertically down on the Nichols chart, as shown in Figure 9.40. At $\omega_n = 2.8$, we just intersect the 2.6-dB closed-loop curve. The reduction (vertical drop) in gain is equal to 13 dB, or a factor of 4.5. Thus, $K = 20/4.5 = 4.44$. For this reduced gain, the steady-state error is

$$e_{ss} = \frac{1}{1 + 4.4/2} = 0.31,$$

so that we have a 31% steady-state error.

The actual step response when $K = 4.44$, as shown in Figure 9.41, has an overshoot of 32%. If we use a gain of 10, we have an overshoot of 48% with a steady-state error of 17%. The performance of the system is summarized in Table 9.5. As a suitable compromise, we select $K = 10$ and draw the frequency response on the Nichols chart by moving the response for $K = 20$ down by $20 \log 2 = 6$ dB, as shown in Figure 9.40.

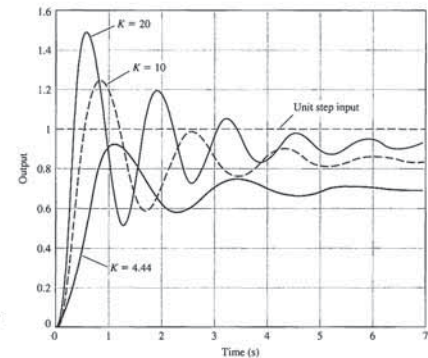


FIGURE 9.41 The response of the system for three values of K for a unit step input $r(t)$.

Table 9.5 Actual Response for Selected Gains

K	4.44	10	20
Percent overshoot	32.4	48.4	61.4
Settling time (seconds)	4.94	5.46	6.58
Peak time (seconds)	1.19	0.88	0.67
e_{ss}	31%	16.7%	9.1%

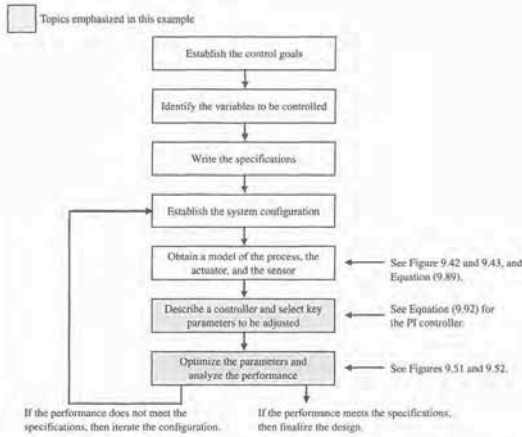
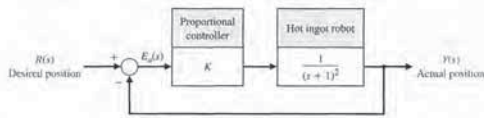


FIGURE 9.44 Elements of the control system design process emphasized in the hot ingot robot control example.

FIGURE 9.45 Hot ingot robot control system block diagram with the proportional controller and no time-delay.



The feedback control system is shown in Figure 9.45 with a proportional controller and no time-delay. The system is a type-zero system, so we expect a nonzero steady-state tracking error to a step input (see Section 5.6 for a review of system type). The closed-loop transfer function is

$$T(s) = \frac{K}{s^2 + 2s + 1 + K}$$

With the tracking error defined as

$$E(s) = R(s) - Y(s)$$

Solving for T yields $T = 0.24$ s. Thus for time-delays less than $T = 0.24$ s, our closed-loop system remains stable. However, the time-delay $T = \pi/4$ s will cause instability. Raising the gain only exacerbates matters, since the phase margin goes down further. Lowering the gain raises the phase margin, but the steady-state tracking error exceeds the 10% limit. A more complex controller is necessary. Before proceeding, let us consider the Nyquist plot and see how it changes with the addition of the time-delay. The Nyquist plot for the system (without the time-delay)

$$L(s) = G_c(s)G(s) = \frac{K}{(s+1)^2}$$

is shown in Figure 9.47, where we use $K = 9$. The number of open-loop poles of $G_c(s)G(s)$ in the right half-plane is $P = 0$. From Figure 9.47 we see that there are no encirclements of the -1 point, thus $N = 0$.

By the Nyquist theorem, we know that the net number of encirclements N equals the number of zeros Z (or closed-loop system poles) in the right half-plane minus the number of open-loop poles P in the right half-plane. Therefore,

$$Z = N + P = 0.$$

Since $Z = 0$, the closed-loop system is stable. More importantly, even when the gain K is increased (or decreased), the -1 point is never encircled—the gain margin is ∞ . Similarly when the time-delay is absent, the phase margin is always positive. The value of the $P.M.$ varies as K varies, but the $P.M.$ is always greater than zero.

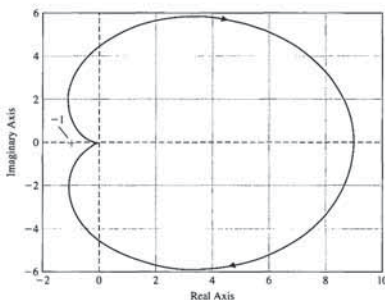
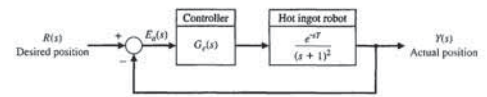


FIGURE 9.47 Nyquist plot with $K = 9$ and no time-delay showing no encirclements of the minus 1 point.

FIGURE 9.43 Hot ingot robot control system block diagram.



system is shown in Figure 9.43. More information on robots and robot vision systems can be found in [15, 30, 31].

The position of the robot along the track is also measured (by a sensor other than the vision sensor) and is available for feedback to the controller. We assume that the position measurement is noise free. This is not a restrictive assumption since many accurate position sensors are available today. For example some laser diode systems are self-contained (including the power supply, optics, and laser diode) and provide position accuracy of over 99.9%.

The robot dynamics are modeled as a second-order system with two poles at $s = -1$ and include a time delay of $T = \pi/4$ s. Therefore,

$$G(s) = \frac{e^{-sT}}{(s+1)^2}, \quad (9.89)$$

where $T = \pi/4$ s. The elements of the design process emphasized in this example are highlighted in Figure 9.44. The control goal is as follows:

Control Goal

Minimize the tracking error $E(s) = R(s) - Y(s)$ in the presence of external disturbances while accounting for the known time-delay.

To this end the following control specifications must be satisfied:

Design Specifications

- DS1 Achieve a steady-state tracking error less than 10% for a step input.
- DS2 Phase margin greater than 50° with the time-delay $T = \pi/4$ s.
- DS3 Percent overshoot less than 10% for a step input.

Our design method is first to consider a proportional controller. We will show that the design specifications cannot be simultaneously satisfied with a proportional controller; however, the feedback system with proportional control provides a useful vehicle to discuss in some detail the effects of the time-delay. In particular, we consider the effects of the time-delay on the Nyquist plot. The final design uses a PI controller, which is capable of providing adequate performance (that is, it satisfies all design specifications).

As a first try, we consider a simple proportional controller:

$$G_c(s) = K.$$

Then ignoring the time-delay for the moment, we have the loop gain

$$L(s) = G_c(s)G(s) = \frac{K}{(s+1)^2} = \frac{K}{s^2 + 2s + 1}$$

and with $R(s) = a/s$, where a is the input magnitude, we have

$$E(s) = \frac{s^2 + 2s + 1}{s^2 + 2s + 1 + K} \frac{a}{s}$$

Using the final value theorem (which is possible since the system is stable for all positive values of K) yields

$$e_{ss} = \lim_{s \rightarrow 0} sE(s) = \frac{a}{1 + K}.$$

Per specification DS1, we require the steady-state tracking error be less than 10%. Therefore,

$$e_{ss} \leq \frac{a}{10}$$

Solving for the appropriate gain K yields $K \geq 9$. With $K = 9$, we obtain the Bode plot shown in Figure 9.46.

If we raise the gain above $K = 9$, we find that the crossover moves to the right (that is, ω_c increases) and the corresponding phase margin ($P.M.$) decreases. Is a $P.M. = 38.9^\circ$ at $\omega = 2.8$ rad/s sufficient for stability in the presence of a time-delay of $T = \pi/4$ s? The addition of the time-delay term causes a phase lag without changing the magnitude plot. The amount of time-delay that our system can withstand while remaining stable is $\phi = -\omega T$ which implies that

$$-\frac{38.9\pi}{180} = -2.8T.$$

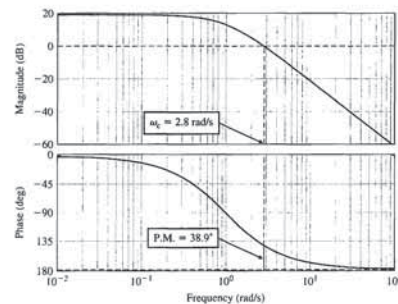


FIGURE 9.46 Bode plot with $K = 9$ and no time-delay showing gain margin $G.M. = \infty$ and phase margin $P.M. = 38.9^\circ$.

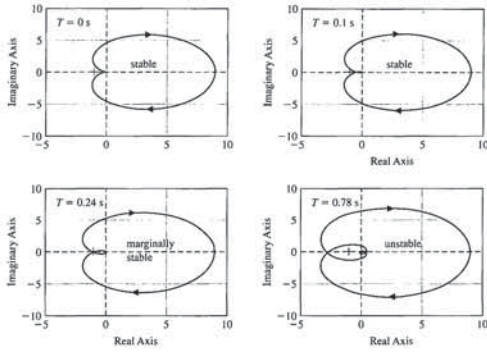


FIGURE 9.49 Nyquist plot with $K = 9$ and various time-delays.

Figure 9.49 shows the Nyquist plot for four values of time-delay: $T = 0, 0.1, 0.24$, and $\pi/4 = 0.78$ s. For $T = 0$ there is no possibility of an encirclement of the -1 point as K varies (see the upper left graph of Figure 9.49). We have stability (that is, $N = 0$) for $T = 0.1$ s (upper right graph), marginal stability for $T = 0.24$ s (lower left graph), and for $T = \pi/4 = 0.78$ s we have $N = 1$ (lower right graph), thus the closed-loop system is unstable.

Since we know that $T = \pi/4$ in this example, the proportional gain controller is not a viable controller. With it we cannot meet the steady-state error specifications and have a stable closed-loop system in the presence of the time-delay $T = \pi/4$. However, before proceeding with the design of a controller that meets all the specifications, let us take a closer look at the Nyquist plot with a time-delay.

Suppose we have the case where $K = 9$ and $T = 0.1$ s. The associated Nyquist plot is shown in the upper right of Figure 9.49. The Nyquist plot intersects (or crosses over) the real axis whenever the imaginary part of $G_c(j\omega)G(j\omega) = 0$ [see Equation (9.90)], or

$$(1 - \omega^2) \sin(0.1\omega) + 2\omega \cos(0.1\omega) = 0.$$

Thus we obtain the relation that describes the frequencies ω at which crossover occurs:

$$\frac{(1 - \omega^2) \tan(0.1\omega)}{2\omega} = -1. \quad (9.91)$$

Equation (9.91) has an infinite number of solutions. The first real-axis crossing (farthest in the left half-plane) occurs when $\omega = 4.43$ rad/s.

The magnitude of $|L(j4.43)|$ is equal to 0.0484 K. For stability we require that $|L(j\omega)| < 1$ when $\omega = 4.43$ (to avoid an encirclement of the -1 point). Thus, for

With the time-delay in the loop, we can rely on analytic methods to obtain the Nyquist plot. The loop transfer function with the time-delay is

$$L(s) = G_c(s)G(s) = \frac{K}{(s+1)^2} e^{-sT}.$$

Using the Euler identity

$$e^{-j\omega T} = \cos(\omega T) - j \sin(\omega T),$$

and substituting $s = j\omega$ into $L(s)$ yields

$$\begin{aligned} L(j\omega) &= \frac{K}{(j\omega+1)^2} e^{-j\omega T} \\ &= \frac{K}{\Delta} [(1 - \omega^2) \cos(\omega T) - 2\omega \sin(\omega T) - j[(1 - \omega^2) \sin(\omega T) + 2\omega \cos(\omega T)]], \end{aligned} \quad (9.90)$$

where

$$\Delta = (1 - \omega^2)^2 + 4\omega^2.$$

Generating a plot of $\text{Re}(L(j\omega))$ versus $\text{Im}(L(j\omega))$ for various values of ω leads to the plot shown in Figure 9.48. With $K = 9$, the number of encirclements of the -1 point is $N = 2$. Therefore, the system is unstable since $Z = N + P = 2$.

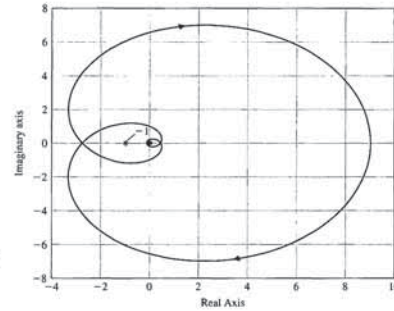


FIGURE 9.48 Nyquist plot with $K = 9$ and $T = \pi/4$ showing two encirclements of the -1 point, $N = 2$.

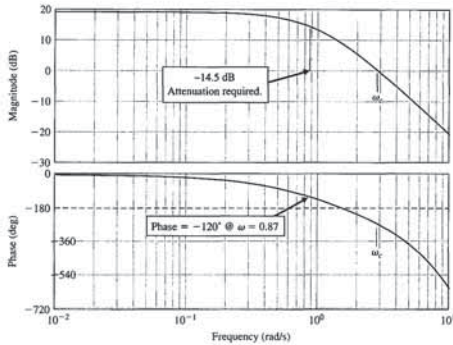


FIGURE 9.50 Uncompensated Bode plot with $K = 9$ and $T = \pi/4$.

design procedure. At $\omega = 0.87$ the magnitude is about 14.5 dB. If we want the crossover to be $\omega_c = 0.87$ rad/s, the controller needs to attenuate the system gain by 14.5 dB, so that the magnitude is 0 dB at $\omega_c = 0.87$. With

$$G_c(s) = K_p \frac{s + \frac{K_I}{K_p}}{s},$$

we can consider K_p to be the gain of the compensator (a good approximation for large ω). Therefore,

$$K_p = 10^{-(14.5/20)} = 0.188.$$

Finally we need to select K_I . Since we want the break frequency of the controller to be below the crossover frequency (so that the phase margin is not reduced significantly due to the presence of the PI zero), a good rule-of-thumb is to select $1/\tau = K_I/K_p = 0.1\omega_c$. To make the break frequency of the controller zero one decade below the crossover frequency. The final value of K_I is computed to be $K_I = 0.1\omega_c K_p = 0.0164$, where $\omega_c = 0.87$ rad/s. Thus the PI controller is

$$G_c(s) = \frac{0.188s + 0.0164}{s}. \quad (9.93)$$

The Bode plot of $G_c(s)G(s)$ is shown in Figure 9.51. The gain and phase margins are $G.M. = 5.3$ dB and $P.M. = 56.5^\circ$.

stability we find

$$K < \frac{1}{0.0484} = 20.67,$$

when $T = 0.1$. When $K = 9$, the closed-loop system is stable, as we already know. If the gain $K = 9$ increases by a factor of 2.3 to $K = 20.67$, we will be on the border of instability. This factor δ is the gain margin:

$$G.M. = 20 \log_{10} 2.3 = 7.2 \text{ dB}.$$

Consider the PI controller

$$G_c(s) = K_p + \frac{K_I}{s} = \frac{K_p s + K_I}{s}. \quad (9.92)$$

The loop system transfer function is

$$L(s) = G_c(s)G(s) = \frac{K_p s + K_I}{s} \frac{K}{(s+1)^2} e^{-sT}.$$

The system type is now equal to 1; thus we expect a zero steady-state error to a step input. The steady-state error specification DS1 is satisfied. We can now concentrate on meeting specification DS3, $P.O. < 10\%$ and DS2, the requirement for stability in the presence of the time-delay $T = \pi/4$ s.

From the percent overshoot specification we can determine a desired system damping ratio. Thus we determine for $P.O. \leq 10\%$ that $\zeta \geq 0.59$. Due to the PI controller, the system now has a zero at $s = -K_I/K_p$. The zero will not affect the closed-loop system stability, but it will affect the performance. Using the approximation (valid for small ζ , $P.M.$ expressed in degrees)

$$\zeta \approx \frac{P.M.}{100},$$

we determine a good target phase margin (since we want $\zeta \geq 0.59$) to be 60° . We can rewrite the PI controller as

$$G_c(s) = K_I \frac{1 + \tau s}{s},$$

where $1/\tau = K_I/K_p$ is the break frequency of the controller. The PI controller is essentially a low-pass filter and adds phase lag to the system below the break frequency. We would like to place the break frequency below the crossover frequency so that the phase margin is not reduced significantly due to the presence of the PI zero.

The uncompensated Bode plot is shown in Figure 9.50 for

$$G(s) = \frac{9}{(s+1)^2} e^{-sT},$$

where $T = \pi/4$. The uncompensated system phase margin is $P.M. = -88.34^\circ$ at $\omega_c = 2.83$ rad/s. Since we want $P.M. = 60^\circ$, we need the phase to be minus 120° at the crossover frequency. In Figure 9.50 we can estimate the phase $\phi = -120^\circ$ at $\omega \approx 0.87$ rad/s. This is an approximate value but is sufficiently accurate for the

We consider whether the design specifications have been met. The steady-state tracking specification (DS1) is certainly satisfied since our system is type one; the PI controller introduced an integrator. The phase margin (with the time-delay) is $P.M. = 56.5^\circ$, so the phase margin specification, DS2, is satisfied. The unit step response is shown in Figure 9.52. The percent overshoot is approximately $P.O. \approx 4.2\%$. The target percent overshoot was 10%, so DS3 is satisfied. Overall the design specifications are satisfied.

9.9 PID CONTROLLERS IN THE FREQUENCY DOMAIN

The PID controller provides a proportional term, an integral term, and a derivative term (see Section 7.6). We then have the PID controller transfer function as

$$G_c(s) = K_p + \frac{K_I}{s} + K_D s. \tag{9.94}$$

If we set $K_D = 0$, we have the PI controller

$$G_c(s) = K_p + \frac{K_I}{s}. \tag{9.95}$$

If we set $K_I = 0$, we have the PD controller

$$G_c(s) = K_p + K_D s. \tag{9.96}$$

In general, we note that PID controllers are particularly useful for reducing the steady-state error and improving the transient response when $G(s)$ has one or two poles (or may be approximated by a second-order process).

We may use frequency response methods to represent the addition of a PID controller. The PID controller, Equation (9.94), may be rewritten as

$$G_c(s) = \frac{K_I \left(\frac{K_D}{K_I} s^2 + \frac{K_p}{K_I} s + 1 \right)}{s} = \frac{K_I (\tau s + 1) \left(\frac{\tau}{\alpha} s + 1 \right)}{s}. \tag{9.97}$$

The Bode diagram of Equation (9.97) is shown in Figure 9.53 for $\omega\tau, K_I = 2$, and $\alpha = 10$. The PID controller is a form of a notch (or bandstop) compensator with a variable gain, K_I . Of course, it is possible that the controller will have complex zeros and a Bode diagram that will be dependent on the ζ of the complex zeros. The contribution by the zeros to the Bode chart may be visualized by reviewing Figure 8.10 for complex poles and noting that the phase and magnitude change as ζ changes. The PID controller with complex zeros is

$$G_c(\omega) = \frac{K_I [1 + (2\zeta/\omega_n)\omega - (\omega/\omega_n)^2]}{j\omega}. \tag{9.98}$$

Normally, we choose $0.9 > \zeta > 0.7$.

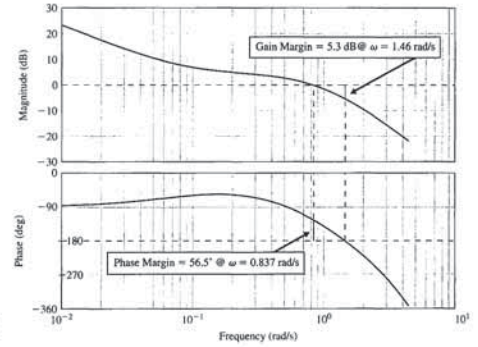


FIGURE 9.51 Compensated Bode plot with $K = 9$ and $T = \pi/4$.

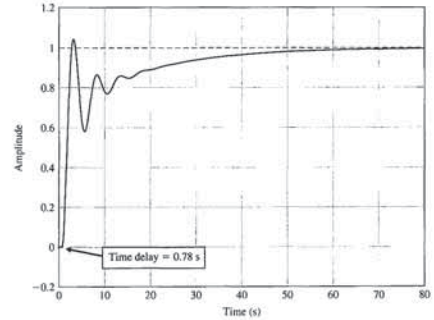


FIGURE 9.52 Hot ingot robot control step response.

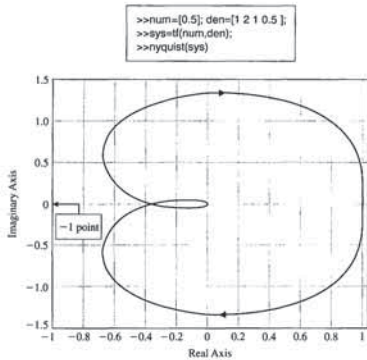


FIGURE 9.55 An example of the nyquist function.

automatically generated; otherwise, the real and imaginary parts of the frequency response (along with the frequency vector ω) is returned. An illustration of the nyquist function is given in Figure 9.55.

As discussed in Section 9.4, relative stability measures of **gain margin** and **phase margin** can be determined from both the Nyquist plot and the Bode diagram. The gain margin is a measure of how much the system gain would have to be increased for the $L(j\omega)$ locus to pass through the $-1 + j0$ point, thus resulting in an unstable system. The phase margin is a measure of the additional phase lag required before the system becomes unstable. Gain and phase margins can be determined from both the Nyquist plot and the Bode diagram.

Consider the system shown in Figure 9.56. Relative stability can be determined from the Bode diagram using the margin function, which is shown in Figure 9.57. If the margin function is invoked without left-hand arguments, the Bode diagram is automatically generated with the gain and phase margins labeled on the diagram. This is illustrated in Figure 9.58 for the system shown in Figure 9.56.

The script to generate the Nyquist plot for the system in Figure 9.56 is shown in Figure 9.59. In this case, the number of poles of $L(s) = G_c(s)G(s)H(s)$ with positive real parts is zero, and the number of counterclockwise encirclements of -1 is zero;

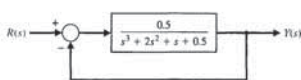


FIGURE 9.56 A closed-loop control system example for Nyquist and Bode with relative stability.

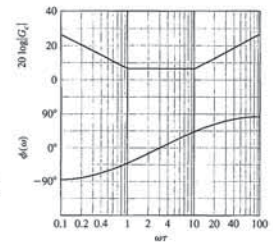


FIGURE 9.53 Bode diagram for a PID controller using the asymptotic approximation for the magnitude curve.

9.10 STABILITY IN THE FREQUENCY DOMAIN USING CONTROL DESIGN SOFTWARE

We now approach the issue of stability using the computer as a tool. This section revisits the Nyquist diagram, the Nichols chart, and the Bode diagram in our discussions on relative stability. Two examples will illustrate the frequency-domain design approach. We will make use of the frequency response of the closed-loop transfer function $T(j\omega)$ as well as the loop transfer function $L(j\omega)$. We also present an illustrative example that shows how to deal with a time delay in the system by utilizing a Padé approximation [6]. The functions covered in this section are nyquist, nichols, margin, padé, and ngrid.

It is generally more difficult to manually generate the Nyquist plot than the Bode diagram. However, we can use the control design software to generate the Nyquist plot. The Nyquist plot is generated with the nyquist function, as shown in Figure 9.54. When nyquist is used without left-hand arguments, the Nyquist plot is

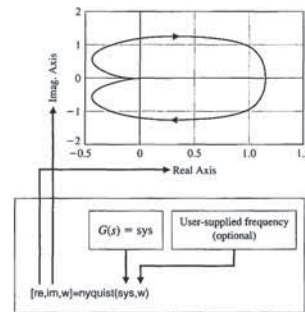


FIGURE 9.54 The Nyquist function.

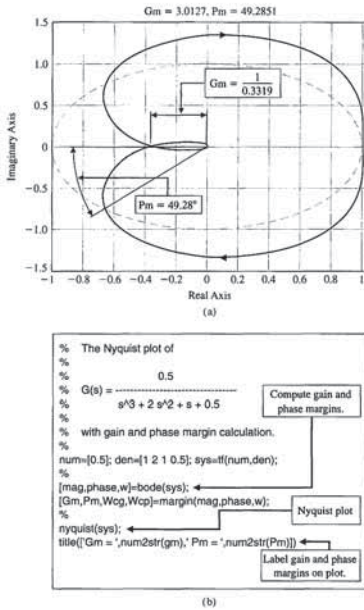


FIGURE 9.59 (a) The Nyquist plot for the system in Figure 9.56 with gain and phase margins. (b) m-file script.

hence, the closed-loop system is stable. We can also determine the gain margin and phase margin, as indicated in Figure 9.59.

Nichols Chart. Nichols charts can be generated using the nichols function, shown in Figure 9.60. If the nichols function is invoked without left-hand arguments, the Nichols chart is automatically generated; otherwise the nichols function returns the magnitude and phase in degrees (along with the frequency ω). A Nichols chart grid is drawn on the existing plot with the ngrid function. The Nichols chart, shown in

Figure 9.61, is for the system

$$G(j\omega) = \frac{1}{j\omega(j\omega + 1)(0.2j\omega + 1)} \quad (9.99)$$

EXAMPLE 9.13 Liquid level control system

Consider a liquid level control system described by the block diagram shown in Figure 9.32 (see Example 9.9). Note that this system has a time delay. The loop transfer function is given by

$$L(s) = \frac{31.5e^{-sT}}{(s + 1)(30s + 1)(s^2/9 + s/3 + 1)} \quad (9.100)$$

We first change Equation (9.100) in such a way that $L(s)$ has a transfer function form with polynomials in the numerator and the denominator. To do this, we can make an approximation to e^{-sT} with the padé function, shown in Figure 9.62. For example, suppose our time delay is $T = 1$ s, and we want a second-order approximation $n = 2$. Using the padé function, we find that

$$e^{-s} \approx \frac{s^2 - 6s + 12}{s^2 + 6s + 12} \quad (9.101)$$

Substituting Equation (9.101) into Equation (9.100), we have

$$L(s) \approx \frac{31.5(s^2 - 6s + 12)}{(s + 1)(30s + 1)(s^2/9 + s/3 + 1)(s^2 + 6s + 12)}$$

Now we can build a script to investigate the relative stability of the system using the Bode diagram. Our goal is to have a phase margin of 30° . The associated script is shown in Figure 9.63. To make the script interactive, we let the gain K (now set at $K = 31.5$) be adjustable and defined outside the script at the command level. Then we set K and run the script to check the phase margin and iterate if necessary. The final selected gain is $K = 16$. Remember that we have utilized a second-order Padé approximation of the time delay in our analysis. ■

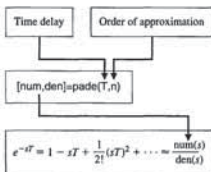


FIGURE 9.62 The padé function.

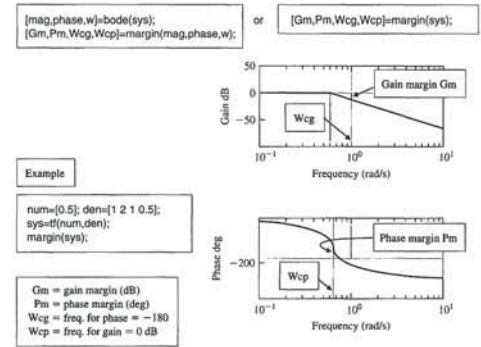


FIGURE 9.57 The margin function.

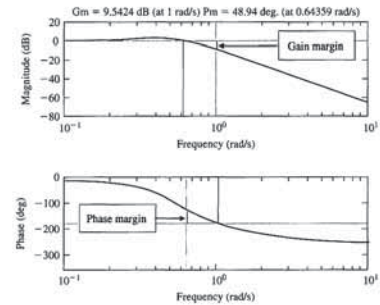


FIGURE 9.58 The Bode diagram for the system in Figure 9.56 with the gain margin and the phase margin indicated on the plots.

Figure 9.61, is for the system

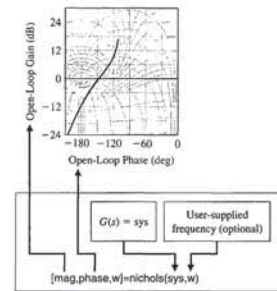


FIGURE 9.60 The nichols function.

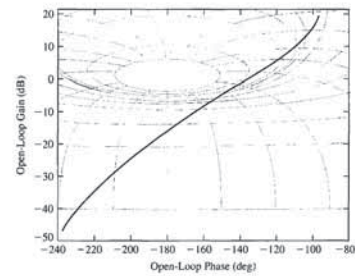


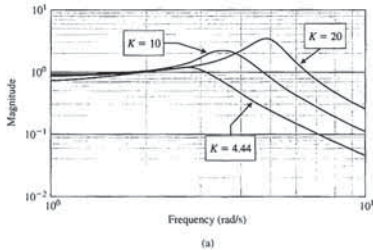
FIGURE 9.61 Nichols chart for the system of Equation (9.99).

The effect of the gain K on the steady-state error is clear from Equation (9.102): If $K = 20$, the error is 9% of the input magnitude; if $K = 10$, the error is 17% of the input magnitude.

Now we can investigate the overshoot specification in the frequency domain. Suppose we require that the percent overshoot is less than 50%. Solving

$$P.O. \approx 100 \exp^{-\zeta \pi / \sqrt{1-\zeta^2}} \leq 50$$

for ζ yields $\zeta \geq 0.215$. Referring to Figure 8.11, we find that $M_{pw} \leq 2.45$. We must keep in mind that the information in Figure 8.11 is for second-order systems only and can be used here only as a guideline. We now compute the closed-loop Bode diagram and check the values of M_{pw} . Any gain K for which $M_{pw} \leq 2.45$ may be a valid gain for our design, but we will have to investigate step responses further to check the actual overshoot. The script in Figure 9.64 aids us in this task. We further investigate the gains $K = 20, 10$, and 4.44 (even though $M_{pw} > 2.45$ for $K = 20$).

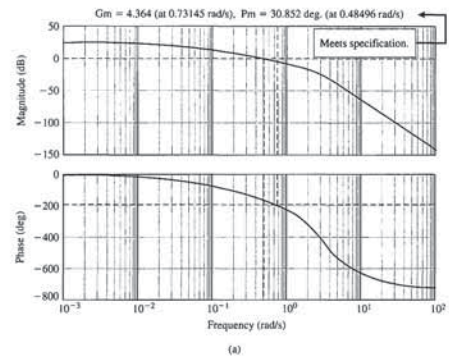


```

w=logspace(0,1,200); K=[20,10,4.44];
% Loop for three gains
% K = 20, 10, 4.44.
for i=1:3
    numgc=K(i)*[1 2]; dengc=[1 1]; sysgc=tf(numgc,dengc);
    numg=[1]; deng=[1 2 4]; sysg=tf(numg,deng);
    [sys]=series(sysgc,sysg); sys=feedback(sys,1);
    [mag_phase,w]=bode(sys,w);
    [mag_save(i,:),]=mag(:,1:); % Compute closed-loop
end
% Compute closed-loop
% frequency response
loglog(w,mag_save(1,:), w,mag_save(2,:), w,mag_save(3,:))
xlabel('Frequency (rad/s)'); ylabel('Magnitude'); grid on
    
```

FIGURE 9.64 Remotely controlled vehicle. (a) Closed-loop system Bode diagram. (b) m-file script.

(b)



```

>>K=16; liquid % Command level input.
liquid.m
% Liquid Control System Analysis
%
[np,dp]=pade(1,2);
sysp=tf(np,dp);
num=K;
d1=[1 1]; d2=[30 1]; d3=[1/9 1/3 1];
den=conv(d1,conv(d2,d3));
sysg=tf(num,den);
sys=series(sysp,sysg); % Compute LLs.
margin(sys); % Compute gain and
% phase margins.
    
```

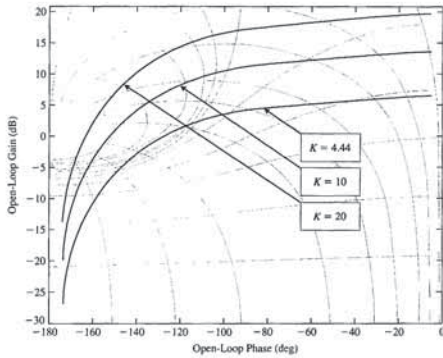
FIGURE 9.63 (a) Bode diagram for the liquid level control system. (b) m-file script.

(b)

EXAMPLE 9.14 Remotely controlled reconnaissance vehicle

Consider the speed control system for a remotely controlled reconnaissance vehicle shown in Figure 9.39. The design objective is to achieve good control with a low steady-state error and a low overshoot to a step command. Building a script will allow us to perform many design iterations quickly and efficiently. First, we investigate the steady-state error to a unit step command is

$$e_{ss} = \frac{1}{1 + K/2} \quad (9.102)$$



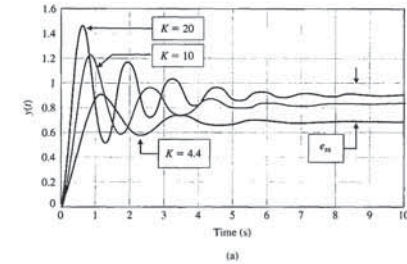
```

% Remotely Controlled Battlefield Vehicle
%
numgc=[1 2]; dengc=[1 1]; sysgc=tf(numgc,dengc);
numg=[1]; deng=[1 2 4]; sysg=tf(numg,deng);
[sys]=series(sysgc,sysg); % Compute GcG(s).
%
w=logspace(-1,1,200);
%
K=[20,10,4.44]; % Nichols chart for
hold off, clf % K = 20, 10, and 4.44.
for i=1:3
    nichols(K(i)*sys,w), ngrid
hold on
end
    
```

FIGURE 9.66 Remotely controlled vehicle. (a) Nichols chart. (b) m-file script.

(b)

and incorporates a PD controller with a zero at $s = -1$. We will determine the system gain margin and phase margin when $K = 400$. The Bode diagram for the system of Figure 8.52 when $K = 400$ is shown in Figure 9.68. The gain margin is 22.9 dB, and the phase margin is 37.2°. The plot of the step response of this system is shown in Figure 9.69. The settling time of this design is $T_s = 9.6$ ms.



```

t=[0:0.01:10]; K=[20,10,4.44];
y=zeros(length(t), length(K));
% Loop for three gains
% K = 20, 10, 4.44.
for i=1:3
    numgc=K(i)*[1 2]; dengc=[1 1]; sysgc=tf(numgc,dengc);
    numg=[1]; deng=[1 2 4]; sysg=tf(numg,deng);
    [sys]=series(sysgc,sysg);
    sys=feedback(sys,1);
    y(:,i)=step(sys,t); % Compute step response.
end
%
plot(t,y(:,1),t,y(:,2),t,y(:,3)),grid
xlabel('Time (s)'); ylabel('y(t)')
    
```

FIGURE 9.65 Remotely controlled vehicle. (a) Step response. (b) m-file script.

(b)

We can plot the step responses to quantify the overshoot as shown in Figure 9.65. Additionally, we could have used a Nichols chart to aid the design process, as shown in Figure 9.66.

The results of the analysis are summarized in Table 9.5 for $K = 20, 10$, and 4.44. We choose $K = 10$ as our design gain. Then we obtain the Nyquist plot and check relative stability, as shown in Figure 9.67. The gain margin is $G.M. = 49.56$ dB and the phase margin is $P.M. = 26.11^\circ$.

9.11 SEQUENTIAL DESIGN EXAMPLE: DISK DRIVE READ SYSTEM



In this chapter, we will examine the system described in Chapter 8, using the system represented by Figure 8.52. This system includes the effect of the flexure resonance

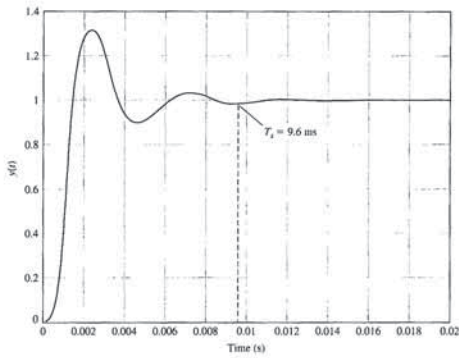
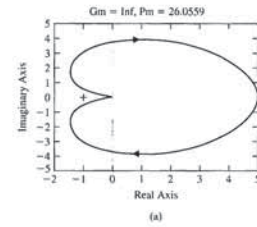


FIGURE 9.69 Response of the system to a step input.

9.12 SUMMARY

The stability of a feedback control system can be determined in the frequency domain by utilizing Nyquist's criterion. Furthermore, Nyquist's criterion provides us with two relative stability measures: (1) gain margin and (2) phase margin. These relative stability measures can be utilized as indices of the transient performance on the basis of correlations established between the frequency domain and the transient response. The magnitude and phase of the closed-loop system can be determined from the frequency response of the open-loop transfer function by utilizing constant magnitude and phase circles on the polar plot. Alternatively, we can utilize a log-magnitude-phase diagram with closed-loop magnitude and phase curves superimposed (called the Nichols chart) to obtain the closed-loop frequency response. A measure of relative stability, the maximum magnitude of the closed-loop frequency response, $M_{p_{max}}$ is available from the Nichols chart. The frequency response, $M_{p_{max}}$ can be correlated with the damping ratio of the time response and is a useful index of performance. Finally, a control system with a pure time delay can be investigated in a manner similar to that for systems without time delay. A summary of the Nyquist criterion, the relative stability measures, and the Nichols diagram is given in Table 9.6 for several transfer functions.

Table 9.6 is very useful and important to the designer and analyst of control systems. If we have the model of a process $G(s)$ and a controller $G_c(s)$, then we can determine $L(s) = G_c(s)G(s)$. With this loop transfer function, we can examine the transfer function table in column 1. This table contains fifteen typical transfer functions. For a selected transfer function, the table gives the Bode diagram, the Nichols diagram, and the root locus. With this information, the designer can determine or estimate the performance of the system and consider the addition or alteration of the controller $G_c(s)$.



```
% Remotely Controlled Vehicle
% Nyquist plot for K=10
%
numgc=10^1 2; dengc=1 1; sysgc=tf(numgc,dengc);
numg=1; deng=1 2 4; sysg=tf(numg,deng);
sys=series(sysgc,sysg);
%
[Gm,Pm,Wcg,Wcp]=margin(sys);
%
nyquist(sys);
title(['Gm = ',num2str(Gm), ' Pm = ',num2str(Pm)])
```

FIGURE 9.67 (a) Nyquist chart for the remotely controlled vehicle with $K = 10$. (b) m-file script.

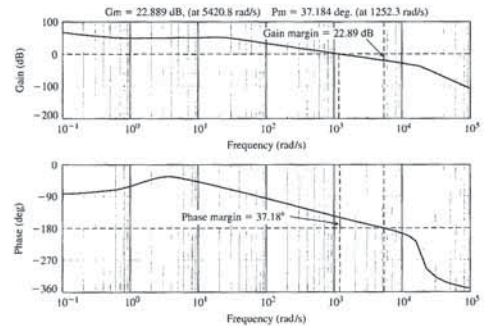


FIGURE 9.68 Bode diagram of the system shown in Figure 8.52.

Table 9.6 (continued)

Nichols Diagram	Root Locus	Comments
		Stable; gain margin = ∞
		Elementary regulator; stable; gain margin = ∞
		Regulator with additional energy-storage component; unstable, but can be made stable by reducing gain
		Ideal integrator; stable

Table 9.6 Transfer Function Plots for Typical Transfer Functions

$L(s)$	Polar Plot	Bode Diagram
1. $\frac{K}{s\tau_1 + 1}$		
2. $\frac{K}{(s\tau_1 + 1)(s\tau_2 + 1)}$		
3. $\frac{K}{(s\tau_1 + 1)(s\tau_2 + 1)(s\tau_3 + 1)}$		
4. $\frac{K}{s}$		

(continued)

Table 9.6 (continued)

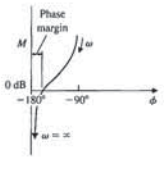
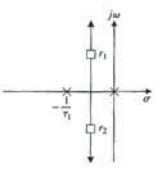
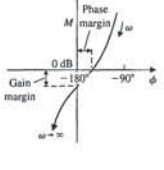
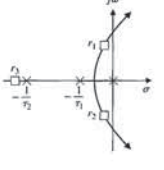
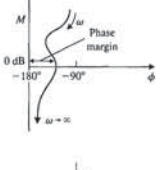
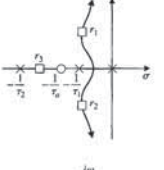
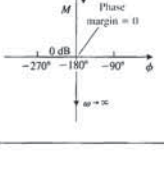
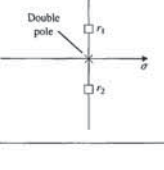
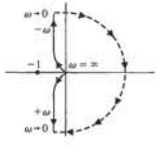
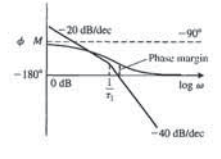
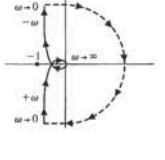
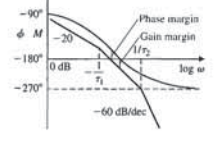
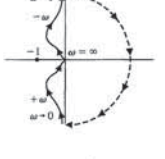
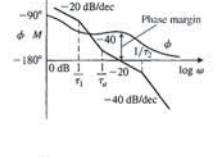
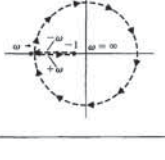
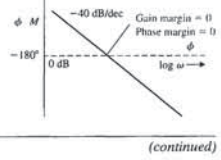
Nichols Diagram	Root Locus	Comments
		Elementary instrument servo; inherently stable; gain margin = ∞
		Instrument servo with field control motor or power servo with elementary Ward-Leonard drive; stable as shown, but may become unstable with increased gain
		Elementary instrument servo with phase-lead (derivative) compensator; stable
		Inherently marginally stable; must be compensated

Table 9.6 (continued)

$L(s)$	Polar Plot	Bode Diagram
5. $\frac{K}{s(\tau s_1 + 1)}$		
6. $\frac{K}{s(\tau s_1 + 1)(\tau s_2 + 1)}$		
7. $\frac{K(\tau s_2 + 1)}{(\tau s_1 + 1)(\tau s_2 + 1)}$		
8. $\frac{K}{s^2}$		

(continued)

Table 9.6 (continued)

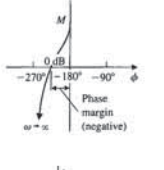
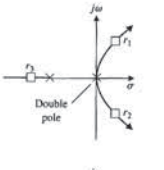
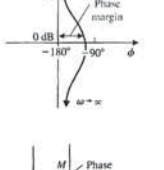
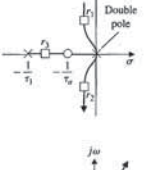
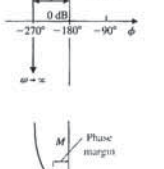
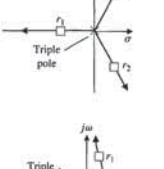
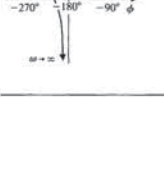
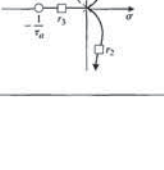
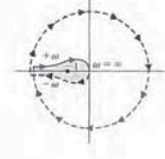
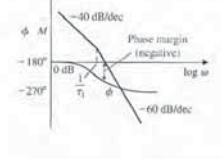

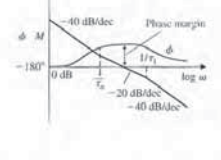
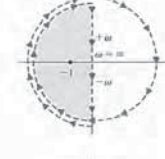
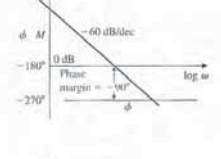
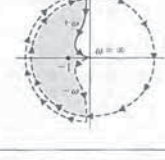
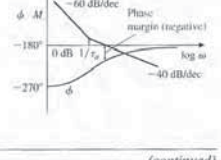
Nichols Diagram	Root Locus	Comments
		Inherently unstable; must be compensated
		Stable for all gains
		Inherently unstable
		Inherently unstable

Table 9.6 (continued)

$L(s)$	Polar Plot	Bode Diagram
9. $\frac{K}{s^2(\tau s_1 + 1)}$		
10. $\frac{K(\tau s_2 + 1)}{s^2(\tau s_1 + 1)}$ $\tau_2 > \tau_1$		
11. $\frac{K}{s^3}$		
12. $\frac{K(\tau s_2 + 1)}{s^3}$		

(continued)

Table 9.6 (continued)

Nichols Diagram	Root Locus	Comments
		Conditionally stable; becomes unstable if gain is too low
		Conditionally stable; stable at low gain, becomes unstable as gain is raised, again becomes stable as gain is further increased, and becomes unstable for very high gains
		Conditionally stable; becomes unstable at high gain

SKILLS CHECK

In this section, we provide three sets of problems to test your knowledge: True or False, Multiple Choice, and Word Match. To obtain direct feedback, check your answers with the answer key provided at the conclusion of the end-of-chapter problems. Use the block diagram in Figure 9.70 as specified in the various problem statements.

and the controller is the proportional-plus-derivative (PD) controller

$$G_c(s) = K(1 + T_d s)$$

- When $T_d = 0$, the PD controller reduces to a proportional controller, $G_c(s) = K$. In this case, use the Nyquist plot to determine the limiting value of K for closed-loop stability.
 - $K = 0.5$
 - $K = 1.6$
 - $K = 2.4$
 - $K = 4.3$
- Using the value of K in Problem 8, compute the gain and phase margins when $T_d = 0.2$.
 - $G.M. = 14 \text{ dB}$, $P.M. = 27^\circ$
 - $G.M. = 20 \text{ dB}$, $P.M. = 64.9^\circ$
 - $G.M. = \infty \text{ dB}$, $P.M. = 60^\circ$
 - Closed-loop system is unstable
- Determine whether the closed-loop system in Figure 9.70 is stable or not, given the loop transfer function

$$L(s) = G_c(s)G(s) = \frac{s+1}{s^2(4s+1)}$$

In addition, if the closed-loop system is stable, compute the gain and phase margins.

- Stable, $G.M. = 24 \text{ dB}$, $P.M. = 2.5^\circ$
 - Stable, $G.M. = 3 \text{ dB}$, $P.M. = 24^\circ$
 - Stable, $G.M. = \infty \text{ dB}$, $P.M. = 60^\circ$
 - Unstable
- Consider the closed-loop system in Figure 9.70, where the loop transfer function is

$$L(s) = G_c(s)G(s) = \frac{K(s+4)}{s^2}$$
 Determine the value of the gain K such that the phase margin is $P.M. = 40^\circ$.
 - $K = 1.64$
 - $K = 2.15$
 - $K = 2.63$
 - Closed-loop system is unstable for all $K > 0$
 - Consider the feedback system in Figure 9.70, where

$$G_c(s) = K \text{ and } G(s) = \frac{e^{-0.2s}}{s+5}$$

Notice that the plant contains a time-delay of $T = 0.2$ seconds. Determine the gain K such that the phase margin of the system is $P.M. = 50^\circ$. What is the gain margin for the same gain K ?

- $K = 8.35$, $G.M. = 2.6 \text{ dB}$
- $K = 2.15$, $G.M. = 10.7 \text{ dB}$

Table 9.6 (continued)

$L(s)$	Polar Plot	Bode Diagram
13. $\frac{K(st_{z_1} + 1)(st_{z_2} + 1)}{s^3}$		
14. $\frac{K(st_{z_1} + 1)(st_{z_2} + 1)}{s(st_{p_1} + 1)(st_{p_2} + 1)(st_{p_3} + 1)(st_{p_4} + 1)}$		
15. $\frac{K(st_{z_1} + 1)}{s^2(st_{p_1} + 1)(st_{p_2} + 1)}$		

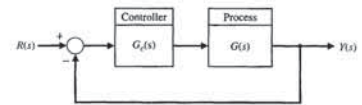


FIGURE 9.70 Block diagram for the Skills Check.

In the following True or False and Multiple Choice problems, circle the correct answers.

- The gain margin of a system is the increase in the system gain when the phase is -180° that will result in a marginally stable system. True or False
- A conformal mapping is a contour mapping that retains the angles on the s -plane on the transformed $F(s)$ -plane. True or False
- The gain and phase margin are readily evaluated on either a Bode plot or a Nyquist plot. True or False
- A Nichols chart displays curves describing the relationship between the open-loop and closed-loop frequency responses. True or False
- The phase margin of a second-order system (with no zeros) is a function of both the damping ratio ζ and the natural frequency, ω_n . True or False
- Consider the closed-loop system in Figure 9.70 where

$$L(s) = G_c(s)G(s) = \frac{3.25(1 + s/6)}{s(1 + s/3)(1 + s/8)}$$

The crossover frequency and the phase margin are:

- $\omega = 2.0 \text{ rad/s}$, $P.M. = 37.2^\circ$
- $\omega = 2.5 \text{ rad/s}$, $P.M. = 54.9^\circ$
- $\omega = 5.3 \text{ rad/s}$, $P.M. = 68.1^\circ$
- $\omega = 10.7 \text{ rad/s}$, $P.M. = 47.9^\circ$

- Consider the block diagram in Figure 9.70. The plant transfer function is

$$G(s) = \frac{1}{(1 + 0.25s)(0.5s + 1)}$$

and the controller is

$$G_c(s) = \frac{s + 0.2}{s + 5}$$

Utilize the Nyquist stability criterion to characterize the stability of the closed-loop system.

- The closed-loop system is stable.
- The closed-loop system is unstable.
- The closed-loop system is marginally stable.
- None of the above.

For Problems 8 and 9, consider the block diagram in Figure 9.70 where

$$G(s) = \frac{9}{(s+1)(s^2 + 3s + 9)}$$

c. Bandwidth	A contour mapping that retains the angles on the s -plane on the $F(s)$ -plane.	_____
d. Contour map	If a contour encircles Z zeros and P poles of $F(s)$ traversing clockwise, the corresponding contour in the $F(s)$ -plane encircles the origin of the $F(s)$ -plane $N = Z - P$ times clockwise.	_____
e. Nichols chart	The amount of phase shift of $G_c(j\omega)G(j\omega)$ at unity magnitude that will result in a marginally stable system with intersections of the point $-1 + j0$ on the Nyquist diagram.	_____
f. Closed-loop frequency response	Events occurring at time t at one point in the system occur at another point in the system at a later time, $t + T$.	_____
g. Logarithmic (decibel) measure	A feedback system is stable if and only if the contour in the $G(s)$ -plane does not encircle the $(-1, 0)$ point when the number of poles of $G(s)$ in the right-hand s -plane is zero. If $G(s)$ has P poles in the right-hand plane, then the number of counterclockwise encirclements of the $(-1, 0)$ point must be equal to P for a stable system.	_____
h. Gain margin	A contour or trajectory in one plane is mapped into another plane by a relation $F(s)$.	_____
i. Nyquist stability criterion	The increase in the system gain when phase = -180° that will result in a marginally stable system with intersection of the $-1 + j0$ point on the Nyquist diagram.	_____
j. Phase margin	The frequency at which the frequency response has declined 3 dB from its low-frequency value.	_____
k. Conformal mapping	A measure of the gain margin.	_____

EXERCISES

E9.1 A system has the loop transfer function

$$L(s) = G_c(s)G(s) = \frac{2(1 + s/10)}{s(1 + 5s)(1 + s/9 + s^2/81)}$$

Plot the Bode diagram. Show that the phase margin is approximately 17.5° and that the gain margin is approximately 26.2 dB.

E9.2 A system has the loop transfer function

$$L(s) = G_c(s)G(s) = \frac{K(1 + s/5)}{s(1 + s/2)(1 + s/10)}$$

where $K = 10.5$. Show that the system crossover (0 dB) frequency is 5 rad/s and that the phase margin is 40° .

E9.3 An integrated circuit is available to serve as a feedback system to regulate the output voltage of a power supply. The Bode diagram of the required loop transfer function $G_c(j\omega)G(j\omega)$ is shown in Figure E9.3. Estimate the gain and phase margins of the regulator.

Answer: $G.M. = 25$ dB, $P.M. = 75^\circ$

E9.4 Consider a system with a loop transfer function

$$G_c(s)G(s) = \frac{100}{s(s + 10)}$$

E9.13 A unity feedback system has a loop transfer function

$$L(s) = G_c(s)G(s) = \frac{150}{s(s + 5)}$$

(a) Find the maximum magnitude of the closed-loop frequency response using the Nichols chart. (b) Find the bandwidth and the resonant frequency of this system. (c) Use these frequency measures to estimate the overshoot of the system to a step response.

Answers: (a) 7.5 dB, (b) $\omega_B = 19$, $\omega_r = 12.6$

E9.14 A Nichols chart is given in Figure E9.14 for a system with $G_c(j\omega)G(j\omega)$. Using the following table, find (a) the peak resonance M_{pw} in dB; (b) the resonant frequency ω_r ; (c) the 3-dB bandwidth; and (d) the phase margin of the system.

ω_1	ω_2	ω_3	ω_4
rad/s	1	3	6
			10

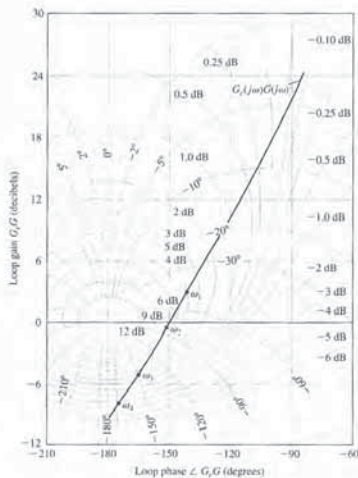


FIGURE E9.14 Nichols chart for $G_c(j\omega)G(j\omega)$.

E9.15 Consider a unity feedback system with the loop transfer function

$$L(s) = G_c(s)G(s) = \frac{100}{s(s + 20)}$$

Find the bandwidth of the closed-loop system.

Answer: $\omega_B = 6.4$ rad/sec

E9.16 The pure time delay e^{-sT} may be approximated by a transfer function as

$$e^{-sT} \approx \frac{1 - Ts/2}{1 + Ts/2}$$

for $0 < \omega < 2/T$. Obtain the Bode diagram for the actual transfer function and the approximation for $T = 0.2$ for $0 < \omega < 10$.

- c. $K = 5.22$, $G.M. = \infty$ dB
- d. $K = 1.22$, $G.M. = 14.7$ dB

13. Consider the control system in Figure 9.70, where the loop transfer function is

$$L(s) = G_c(s)G(s) = \frac{1}{s(s + 1)}$$

The value of the resonant peak, M_{pw} , and the damping factor, ζ , for the closed-loop system are:

- a. $M_{pw} = 0.37$, $\zeta = 0.707$
- b. $M_{pw} = 1.15$, $\zeta = 0.5$
- c. $M_{pw} = 2.55$, $\zeta = 0.5$
- d. $M_{pw} = 0.55$, $\zeta = 0.25$

14. A feedback model of human reaction time used in analysis of vehicle control can use the block diagram model in Figure 9.70 with

$$G_c(s) = e^{-sT} \text{ and } G(s) = \frac{1}{s(0.2s + 1)}$$

A typical driver has a reaction time of $T = 0.3$ seconds. Determine the bandwidth of the closed-loop system.

- a. $\omega_B = 0.5$ rad/s
- b. $\omega_B = 10.6$ rad/s
- c. $\omega_B = 1.97$ rad/s
- d. $\omega_B = 200.6$ rad/s

15. Consider a control system with unity feedback as in Figure 9.70 with loop transfer function

$$L(s) = G_c(s)G(s) = \frac{(s + 4)}{s(s + 1)(s + 5)}$$

The gain and phase margin are:

- a. $G.M. = \infty$ dB, $P.M. = 58.1^\circ$
- b. $G.M. = 20.4$ dB, $P.M. = 47.3^\circ$
- c. $G.M. = 6.6$ dB, $P.M. = 60.4^\circ$
- d. Closed-loop system is unstable

In the following Word Match problems, match the term with the definition by writing the correct letter in the space provided.

a. Time delay	The frequency response of the closed-loop transfer function $T(j\omega)$.	_____
b. Cauchy's theorem	A chart displaying the curves for the relationship between the open-loop and closed-loop frequency response.	_____

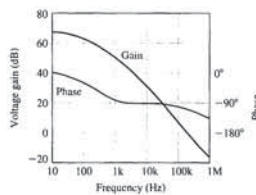


FIGURE E9.3 Power supply regulator.

We wish to obtain a resonant peak $M_{pw} = 3.0$ dB for the closed-loop system. The peak occurs between 6 and 9 rad/s and is only 1.25 dB. Plot the Nichols chart for the range of frequency from 6 to 15 rad/s. Show that the system gain needs to be raised by 4.6 dB to 171. Determine the resonant frequency for the adjusted system.

Answer: $\omega_r = 11$ rad/s

E9.5 An integrated CMOS digital circuit can be represented by the Bode diagram shown in Figure E9.5. (a) Find the gain and phase margins of the circuit. (b) Estimate how much we would need to reduce the system gain (dB) to obtain a phase margin of 60° .

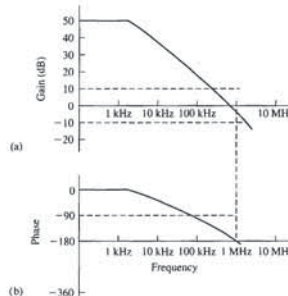


FIGURE E9.5 CMOS circuit.

E9.6 A system has a loop transfer function

$$L(s) = G_c(s)G(s) = \frac{K(s + 100)}{s(s + 10)(s + 40)}$$

When $K = 500$, the system is unstable. Show that if we reduce the gain to 50, the resonant peak is 3.5 dB. Find the phase margin of the system with $K = 50$.

E9.7 A unity feedback system has a loop transfer function

$$L(s) = G_c(s)G(s) = \frac{K}{s - 5}$$

Determine the range of K for which the system is stable using the Nyquist plot.

E9.8 Consider a unity feedback system with the loop transfer function

$$L(s) = G_c(s)G(s) = \frac{K}{s(s + 1)(s + 2)}$$

(a) For $K = 4$, show that the gain margin is 3.5 dB. (b) If we wish to achieve a gain margin equal to 16 dB, determine the value of the gain K .

Answer: (b) $K = 0.98$

E9.9 For the system of E9.8, find the phase margin of the system for $K = 5$.

E9.10 Consider the wind tunnel control system of Problem PT.31 for $K = 326$. Obtain the Bode diagram and show that the $PM = 25^\circ$ and that the $GM = 10$ dB. Also, show that the bandwidth of the closed-loop system is 6 rad/s.

E9.11 Consider a unity feedback system with the loop transfer function

$$G_c(s)G(s) = \frac{10(1 + 0.4s)}{s(1 + 2s)(1 + 0.24s + 0.04s^2)}$$

(a) Plot the Bode diagram. (b) Find the gain margin and the phase margin.

E9.12 A unity feedback system with the loop transfer function

$$L(s) = G_c(s)G(s) = \frac{K}{s(\tau_1 s + 1)(\tau_2 s + 1)}$$

where $\tau_1 = 0.02$ and $\tau_2 = 0.2$ s. (a) Select a gain K so that the steady-state error for a ramp input is 10% of the magnitude of the ramp function A , where $r(t) = At$, $t \geq 0$. (b) Plot the Bode plot of $G_c(s)G(s)$, and determine the phase and gain margins. (c) Using the Nichols chart, determine the bandwidth ω_B , the resonant peak M_{pw} , and the resonant frequency ω_r of the closed-loop system.

Answer:

- (a) $K = 10$
- (b) $PM = 32^\circ$, $GM = 15$ dB
- (c) $\omega_B = 10.3$, $M_{pw} = 1.84$, $\omega_r = 6.5$

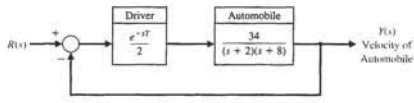


FIGURE E9.20 Automobile control system.

system, (b) estimate the bandwidth of the closed-loop system, and (c) estimate the settling time (with a 2% criterion) of the system.

E9.19 A unity feedback system with $G_c(s) = K$ has

$$G(s) = \frac{e^{-0.1s}}{s + 10}$$

Select a gain K so that the phase margin of the system is 50° . Determine the gain margin for the selected gain, K .

E9.20 Consider a simple model of an automobile driver following another car on the highway at high speed. The model shown in Figure E9.20 incorporates the driver's reaction time, T . One driver has $T = 1$ s, and another has $T = 1.5$ s. Determine the time response $y(t)$ of the system for both drivers for a step change in the command signal $R(s) = -1/s$, due to the braking of the lead car.

E9.21 A unity feedback control system has a loop transfer function

$$L(s) = G_c(s)G(s) = \frac{K}{s(s+2)(s+50)}$$

Determine the phase margin, the crossover frequency, and the gain margin when $K = 1300$.

Answers: $PM = 16.6^\circ$, $\omega_c = 4.9$, $GM = 4$ or 12 dB

E9.22 A unity feedback system has a loop transfer function

$$L(s) = G_c(s)G(s) = \frac{K}{(s+1)^2}$$

(a) Using a Bode diagram for $K = 10$, determine the system phase margin. (b) Select a gain K so that the phase margin is at least 60° .

E9.23 Consider again the system of E9.21 when $K = 438$. Determine the closed-loop system bandwidth, resonant frequency, and M_{pw} using the Nichols chart.

Answers: $\omega_B = 4.25$ rad/s, $\omega_r = 2.7$, $M_{pw} = 1.7$

E9.24 A unity feedback system has a loop transfer function

$$L(s) = G_c(s)G(s) = \frac{K}{-1 + \tau s}$$

where $K = \frac{1}{2}$ and $\tau = 1$. The polar plot for $G_c(j\omega)G(j\omega)$ is shown in Figure E9.24. Determine whether the system is stable by using the Nyquist criterion.

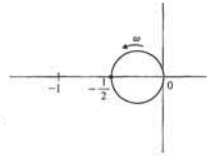


FIGURE E9.24 Polar plot for $G_c(s)G(s) = K/(-1 + \tau s)$.

E9.25 A unity feedback system has a loop transfer function

$$L(s) = G_c(s)G(s) = \frac{11.7}{s(1 + 0.05s)(1 + 0.1s)}$$

Determine the phase margin and the crossover frequency.

Answers: $PM = 27.7^\circ$, $\omega_c = 8.31$ rad/s

E9.26 For the system of E9.25, determine M_{pw} , ω_B , and ω_B for the closed-loop frequency response by using the Nichols chart.

E9.27 A unity feedback system has a loop transfer function

$$L(s) = G_c(s)G(s) = \frac{K}{s(s+6)^2}$$

PROBLEMS

P9.1 For the Nyquist plots of Problem P8.1, use the Nyquist criterion to ascertain the stability of the various systems. In each case, specify the values of N , P , and Z .

P9.2 Sketch the Nyquist plots of the following loop transfer functions $L(s) = G_c(s)G(s)$, and determine whether the system is stable by applying the Nyquist criterion:

(a) $L(s) = G_c(s)G(s) = \frac{K}{s(s^2 + s + 6)}$

(b) $L(s) = G_c(s)G(s) = \frac{K(s+1)}{s^2(s+6)}$

If the system is stable, find the maximum value for K by determining the point where the Nyquist plot crosses the u -axis.

P9.3 (a) Find a suitable contour Γ_r in the s -plane that can be used to determine whether all roots of the characteristic equation have damping ratios greater than $\zeta = 1$. (b) Find a suitable contour Γ_r in the s -plane that can be used to determine whether all the roots of the characteristic equation have real parts less than $s = -\sigma_1$. (c) Using the contour of part (b) and Cauchy's theorem, determine whether the following characteristic equation has roots with real parts less than $s = -1$: $\eta(s) = s^3 + 11s^2 + 56s + 96$.

P9.4 The Nyquist plot of a conditionally stable system is shown in Figure P9.4 for a specific gain K . (a) Determine

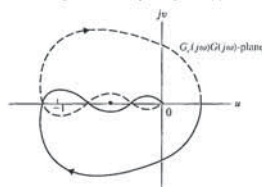


FIGURE P9.4 Nyquist plot of conditionally stable system.

whether the system is stable, and find the number of roots (if any) in the right-hand s -plane. The system has no poles of $G_c(s)G(s)$ in the right half-plane. (b) Determine whether the system is stable if the -1 point lies at the dot on the axis.

P9.5 A speed control for a gasoline engine is shown in Figure P9.5. Because of the restriction at the carburetor jets and the capacitance of the reduction manifold, the lag τ_r occurs and is equal to 1 second. The engine time constant τ_e is equal to $J/b = 3$ s. The speed measurement time constant is $\tau_m = 0.4$ s. (a) Determine the necessary gain K if the steady-state speed error is required to be less than 10% of the speed reference setting. (b) With the gain determined from part (a), apply the Nyquist criterion to investigate the stability of the system. (c) Determine the phase and gain margins of the system.

P9.6 A direct-drive arm is an innovative mechanical arm in which no reducers are used between motors and their loads. Because the motor rotors are directly coupled to the loads, the drive systems have no backlash, small friction, and high mechanical stiffness, which are all important features for fast and accurate positioning and dexterous handling using sophisticated torque control. The goal of the MIT direct-drive arm project is to achieve arm speeds of 10 m/s [15]. The arm has torques of up to 660 N m (475 ft lb). Feedback and a set of position and velocity sensors are used with each motor. The frequency response of one joint of the arm is shown in Figure P9.6(a). The two poles appear at 3.7 Hz and 68 Hz. Figure P9.6(b) shows the step response with position and velocity feedback used. The time constant of the closed-loop system is 82 ms. Develop the block diagram of the drive system and prove that 82 ms is a reasonable result.

P9.7 A vertical takeoff (VTOL) aircraft is an inherently unstable vehicle and requires an automatic stabilization system. An attitude stabilization system for the K-16B US Army VTOL aircraft has been designed and is shown in block diagram form in Figure P9.7 [16]. At 40 knots, the dynamics of the vehicle are approximately represented by the transfer function

$$G(s) = \frac{10}{s^2 + 0.36s}$$

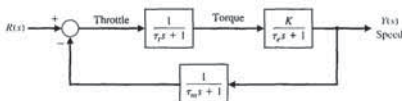


FIGURE P9.5 Engine speed control.

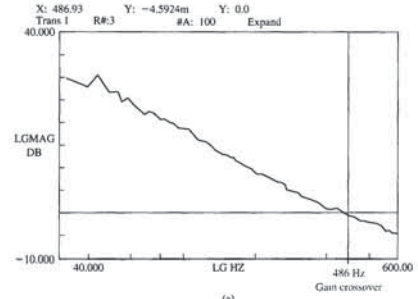
E9.17 A unity feedback system has a loop transfer function

$$L(s) = G_c(s)G(s) = \frac{K(s+2)}{s^3 + 2s^2 + 15s}$$

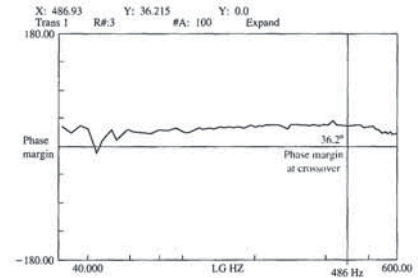
(a) Plot the Bode diagram and (b) determine the gain K required to obtain a phase margin of 30° . What is

the steady-state error for a ramp input for the gain of part (b)?

E9.18 An actuator for a disk drive uses a shock mount to absorb vibrational energy at approximately 60 Hz [14]. The Bode diagram of $G_c(s)G(s)$ of the control system is shown in Figure E9.18. (a) Find the expected percent overshoot for a step input for the closed-loop



(a)



(b)

FIGURE E9.18 Bode diagram of the disk drive, $G_c(s)G(s)$.

Determine the maximum gain K for which the phase margin is at least 40° and the gain margin is at least 6 dB. What are the gain margin and phase margin for this value of K ?

E9.28 A unity feedback system has the loop transfer function

$$L(s) = G_c(s)G(s) = \frac{K}{s(s+0.2)}$$

(a) Determine the phase margin of the system when $K = 0.16$. (b) Use the phase margin to estimate ζ and predict the overshoot. (c) Calculate the actual response for this second-order system, and compare the result with the part (b) estimate.

E9.29 A loop transfer function is

$$L(s) = G_c(s)G(s) = \frac{1}{s+2}$$

Using the contour in the s -plane shown in Figure E9.29, determine the corresponding contour in the $F(s)$ -plane ($B = -1 + j$).

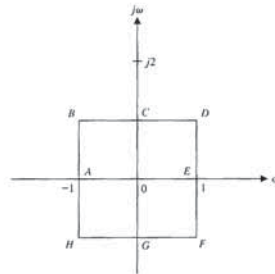


FIGURE E9.29 Contour in the s -plane.

E9.30 Consider the system represented in state variable form

$$\begin{aligned} \dot{\mathbf{x}} &= \mathbf{A}\mathbf{x} + \mathbf{B}u \\ y &= \mathbf{C}\mathbf{x} + \mathbf{D}u \end{aligned}$$

$$\mathbf{A} = \begin{bmatrix} 0 & 1 \\ -10 & -100 \end{bmatrix}, \mathbf{B} = \begin{bmatrix} 0 \\ 1 \end{bmatrix},$$

$$\mathbf{C} = [1000 \ 0], \text{ and } \mathbf{D} = [0].$$

Sketch the Bode plot.

E9.31 A closed-loop feedback system is shown in Figure E9.31. Sketch the Bode plot and determine the phase margin.

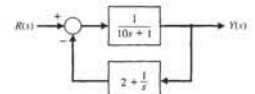


FIGURE E9.31 Nonunity feedback system.

E9.32 Consider the system described in state variable form by

$$\begin{aligned} \dot{\mathbf{x}}(t) &= \mathbf{A}\mathbf{x}(t) + \mathbf{B}u(t) \\ y(t) &= \mathbf{C}\mathbf{x}(t) \end{aligned}$$

where

$$\mathbf{A} = \begin{bmatrix} 0 & 1 \\ -4 & -1 \end{bmatrix}, \mathbf{B} = \begin{bmatrix} 0 \\ 3.2 \end{bmatrix}, \mathbf{C} = [2 \ 0].$$

Compute the phase margin.

E9.33 Consider the system shown in Figure E9.33. Compute the loop transfer function $L(s)$, and sketch the Bode plot. Determine the phase margin and gain margin when the controller gain $K = 5$.

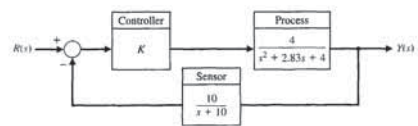


FIGURE E9.33 Nonunity feedback system with proportional controller K .

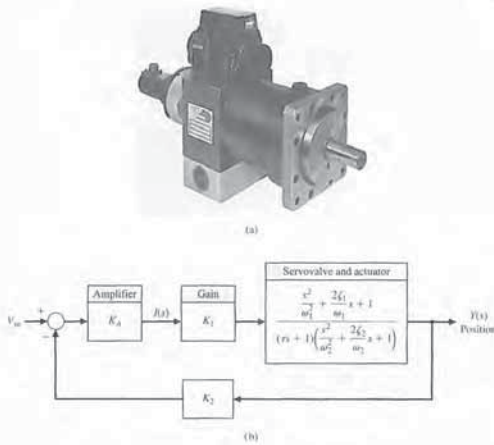


FIGURE P9.8 (a) A servovalve and actuator (courtesy of Moog, Inc., Industrial Division). (b) Block diagram.

edge of the wing and a brake on the tail to control the flight during entry. The block diagram of a pitch rate control system is shown in Figure P9.9(b). The sensor is represented by a gain, $H(s) = 0.5$, and the vehicle by the transfer function

$$G(s) = \frac{0.30(s + 0.05)(s^2 + 1600)}{(s^2 + 0.05s + 16)(s + 70)}$$

The controller $G_c(s)$ can be a gain or any suitable transfer function. (a) Sketch the Bode diagram of the system when $G_c(s) = 2$ and determine the stability margin. (b) Sketch the Bode diagram of the system when

$$G_c(s) = K_P + K_I/s \quad \text{and} \quad K_I/K_P = 0.5.$$

The gain K_P should be selected so that the gain margin is 10 dB.

P9.10 Machine tools are often automatically controlled as shown in Figure P9.10. These automatic systems are often called numerical machine controls [9]. On each axis, the desired position of the machine tool is

compared with the actual position and is used to actuate a solenoid coil and the shaft of a hydraulic actuator. The transfer function of the actuator (see Table 2.7) is

$$G_d(s) = \frac{X(s)}{Y(s)} = \frac{K_p}{s(\tau_p s + 1)}$$

where $K_p = 1$ and $\tau_p = 0.4$ s. The output voltage of the difference amplifier is

$$E_d(s) = K_1(X(s) - X_d(s)),$$

where $v_d(t)$ is the desired position input. The force on the shaft is proportional to the current i , so that $F = K_f i$, where $K_f = 3.0$. The spring constant K_s is equal to 1.5, $R = 0.1$, and $L = 0.2$.

(a) Determine the gain K_1 that results in a system with a phase margin of 30°. (b) For the gain K_1 of part (a), determine M_{pw} , ω_w , and the closed-loop system bandwidth. (c) Estimate the percent overshoot of the transient response to a step input $X_d(s) = 1/s$, and the settling time (to within 2% of the final value).

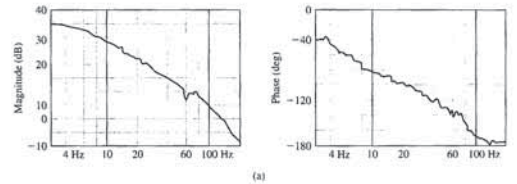


FIGURE P9.6 The MIT arm: (a) frequency response, and (b) position response.

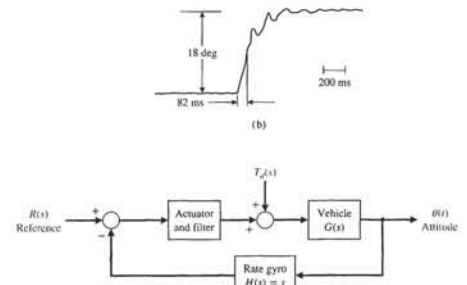


FIGURE P9.7 VTOL aircraft stabilization system.

The actuator and filter are represented by the transfer function

$$G_c(s) = \frac{K_1(s + 7)}{s + 3}$$

(a) Obtain the Bode diagram of the loop transfer function $L(s) = G_c(s)G(s)H(s)$ when the gain is $K_1 = 2$. (b) Determine the gain and phase margins of this system. (c) Determine the steady-state error for a wind disturbance of $T_d(s) = 1/s$. (d) Determine the maximum amplitude of the resonant peak of the closed-loop frequency response and the frequency of the resonance. (e) Estimate the damping ratio of the system from M_{pw} and the phase margin.

P9.8 Electrohydraulic servomechanisms are used in control systems requiring a rapid response for a large mass. An electrohydraulic servomechanism can provide an output of 100 kW or greater [17]. A photo of a servovalve and actuator is shown in Figure P9.8(a).

The output sensor yields a measurement of actuator position, which is compared with V_w . The error is amplified and controls the hydraulic valve position, thus controlling the hydraulic fluid flow to the actuator. The block diagram of a closed-loop electrohydraulic servomechanism using pressure feedback to obtain damping is shown in Figure P9.8(b) [17, 18]. Typical values for this system are $\tau = 0.02$ s for the hydraulic system they are $\omega_1 = 7(2\pi)$ and $\zeta_1 = 0.05$. The structural resonance ω_2 is equal to $10(2\pi)$, and the damping is $\zeta_2 = 0.05$. The loop gain is $K_A K_1 K_2 = 1.0$. (a) Sketch the Bode diagram and determine the phase margin of the system. (b) The damping of the system can be increased by drilling a small hole in the piston so that $\zeta_2 = 0.25$. Sketch the Bode diagram and determine the phase margin of this system.

P9.9 The space shuttle, shown in Figure P9.9(a), carries large payloads into space and returns them to earth for reuse [19]. The shuttle uses elevons at the trailing

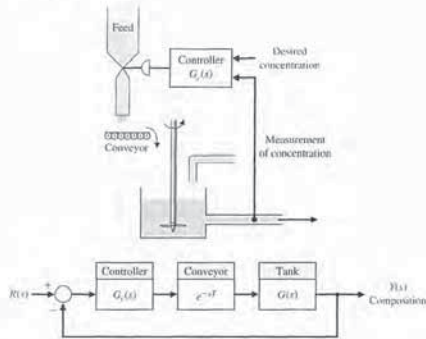


FIGURE P9.11 Chemical concentration control.

The transport of the feed along the conveyor requires a transport (or delay) time, $T = 1.5$ s. (a) Sketch the Bode diagram when $K_1 = K_2 = 1$, and investigate the stability of the system. (b) Sketch the Bode diagram when $K_1 = 0.1$ and $K_2 = 0.04$, and investigate the stability of the system. (c) When $K_1 = 0$, use the Nyquist criterion to calculate the maximum allowable gain K_2 for the system to remain stable.

P9.12 A simplified model of the control system for regulating the pupillary aperture in the human eye is shown in Figure P9.12 [20]. The gain K represents the pupillary gain, and τ is the pupil time constant, which is 0.5 s. The time delay T is equal to 0.5 s. The pupillary gain K_2 for the system to remain stable.

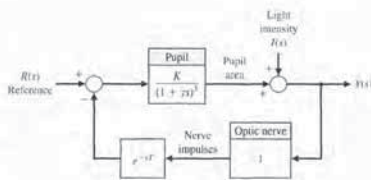


FIGURE P9.12 Human pupil aperture control.

(a) Assuming the time delay is negligible, sketch the Bode diagram for the system. Determine the phase margin of the system. (b) Include the effect of the time delay by adding the phase shift due to the delay. Determine the phase margin of the system with the time delay included.

P9.13 A controller is used to regulate the temperature of a mold for plastic part fabrication, as shown in Figure P9.13. The value of the delay time is estimated as 1.2 s. (a) Using the Nyquist criterion, determine the stability of the system for $K_p = K = 1$. (b) Determine a suitable value for K_p for a stable system that will yield a phase margin greater than 50° when $K = 1$.

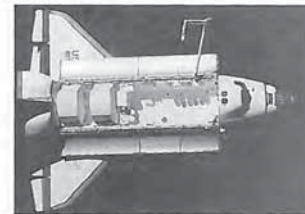


FIGURE P9.9

(a) The Earth-orbiting space shuttle against the blackness of space. The remote manipulator robot is shown with the cargo bay doors open in this top view, taken by a satellite. (b) Pitch rate control system. (Courtesy of NASA.)

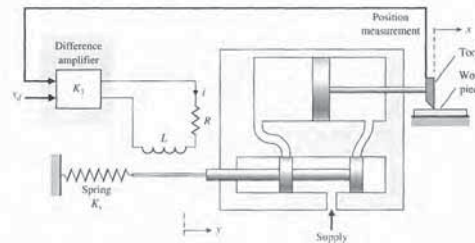
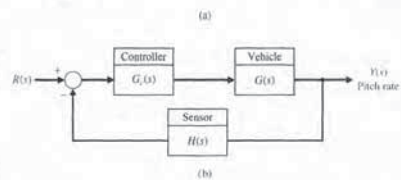


FIGURE P9.10 Machine tool control.

P9.11 A control system for a chemical concentration control system is shown in Figure P9.11. The system receives a granular feed of varying composition, and we want to maintain a constant composition of the output mixture by adjusting the feed-flow valve. The transfer function of the tank and output valve is

$$G(s) = \frac{5}{5s + 1}$$

and that of the controller is

$$G_c(s) = K_1 + \frac{K_2}{s}$$



FIGURE P9.16
(a) An electric carrier vehicle (photo courtesy of Control Engineering Corporation).
(b) Block diagram.

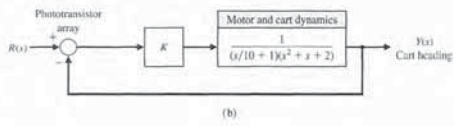
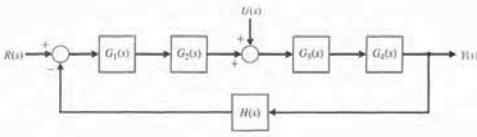


FIGURE P9.17
Chemical reactor control.



[22]. A typical chemical reactor control scheme is shown in Figure P9.17. The disturbance is represented by $U(s)$, and the chemical process by G_2 and G_4 . The controller is represented by G_1 and the valve by G_3 . The feedback sensor is $H(s)$ and will be assumed to be equal to 1. We will assume that G_2 , G_3 , and G_4 are all of the form

$$G_i(s) = \frac{K_i}{1 + \tau_i s}$$

where $\tau_1 = \tau_2 = 4$ s and $K_3 = K_4 = 0.1$. The valve constants are $K_2 = 20$ and $\tau_3 = 0.5$ s. We want to maintain a steady-state error less than 5% of the desired reference position.

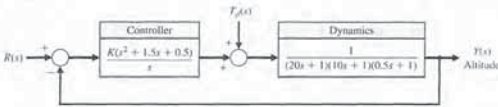


FIGURE P9.20
Tiltrotor aircraft control.

P9.21 Consider a unity feedback system with the loop transfer function $G_c(s)G(s) = \frac{K}{s(s+1)(s+4)}$.
(a) Sketch the Bode diagram for $K = 4$. Determine (b) the gain margin, (c) the value of K required to provide a gain margin equal to 12 dB, and (d) the value of K to yield a steady-state error of 25% of the magnitude A for the ramp input $r(t) = At, t > 0$. Can this gain be utilized and achieve acceptable performance?

P9.22 The Nichols diagram for $G_c(j\omega)G(j\omega)$ of a closed-loop system is shown in Figure P9.22. The frequency for each point on the graph is given in the following table:

Point	1	2	3	4	5	6	7	8	9
ω	1	2.0	2.6	3.4	4.2	5.2	6.0	7.0	8.0

Determine (a) the resonant frequency, (b) the bandwidth, (c) the phase margin, and (d) the gain margin. (e) Estimate the overshoot and settling time (with a 2% criterion) of the response to a step input.

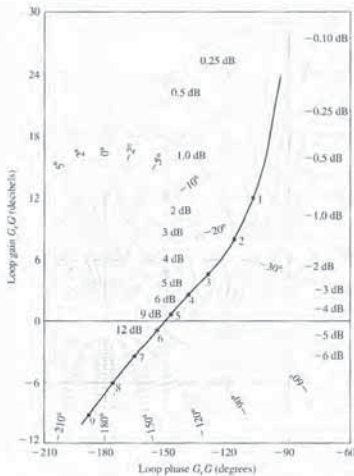


FIGURE P9.22
Nichols chart.

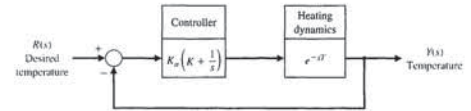


FIGURE P9.13
Temperature controller.

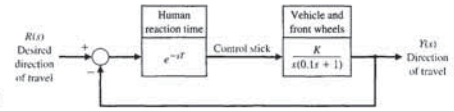


FIGURE P9.14
Automobile steering control.

P9.14 Electronics and computers are being used to control automobiles. Figure P9.14 is an example of an automobile control system, the steering control for a research automobile. The control stick is used for steering. A typical driver has a reaction time of $T = 0.2$ s.
(a) Using the Nichols chart, determine the magnitude of the gain K that will result in a system with a peak magnitude of the closed-loop frequency response M_{p_m} less than or equal to 2 dB.
(b) Estimate the damping ratio of the system based on (1) M_{p_m} and (2) the phase margin. Compare the results and explain the difference, if any.
(c) Determine the closed-loop 3-dB bandwidth of the system.

(d) Repeat parts (a), (b), and (c) when switch S is closed.

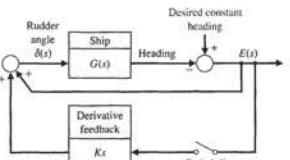


FIGURE P9.15 Automatic ship steering.

P9.15 Consider the automatic ship-steering system discussed in Problem P8.11. The frequency response of the open-loop portion of the ship steering control system is shown in Figure P8.11. The deviation of the tanker from the straight track is measured by radar and is used to generate the error signal, as shown in Figure P9.15. This error signal is used to control the rudder angle $\delta(s)$.
(a) Is this system stable? Discuss what an unstable ship-steering system indicates in terms of the transient response of the system. Recall that the system under consideration is a ship attempting to follow a straight track.
(b) Is it possible to stabilize this system by lowering the gain of the transfer function $G(s)$?
(c) Is it possible to stabilize this system? Suggest a suitable feedback compensator.

P9.16 An electric carrier that automatically follows a tape track laid out on a factory floor is shown in Figure P9.16(a) [15]. Closed-loop feedback systems are used to control the guidance and speed of the vehicle. The cart senses the tape path by means of an array of 16 phototransistors. The block diagram of the steering system is shown in Figure P9.16(b). Select a gain K so that the phase margin is approximately 30°.

P9.17 The primary objective of many control systems is to maintain the output variable at the desired or reference condition when the system is subjected to a disturbance

(a) When $G_c(s) = K_1$, find the necessary gain to satisfy the error-constant requirement. For this condition, determine the expected overshoot to a step change in the reference signal $r(t)$.
(b) If the controller has a proportional term plus an integral term so that $G_c(s) = K_1(1 + 1/s)$, determine a suitable gain to yield a system with an overshoot less than 30%, but greater than 5%. For parts (a) and (b), use the approximation of the damping ratio as a function of phase margin that yields $\zeta = 0.01 \phi_{pm}$. For these calculations, assume $\phi_{pm} = 0$.
(c) Estimate the settling time (with a 2% criterion) of the step response of the system for the controller of parts (a) and (b).
(d) The system is expected to be subjected to a step disturbance $U(s) = A/s$. For simplicity, assume that the desired reference is $r(t) = 0$ when the system has settled. Determine the response of the system of part (b) to the disturbance.

P9.19 In the United States, billions of dollars are spent annually for solid waste collection and disposal. One system, which uses a remote control pick-up arm for collecting waste bags, is shown in Figure P9.19. The loop transfer function of the remote pick-up arm is

$$L(s) = G_c(s)G(s) = \frac{0.5}{s(2s + 1)(s + 4)}$$

(a) Plot the Nichols chart and show that the gain margin is approximately 32 dB. (b) Determine the phase margin and the M_{p_m} for the closed loop. Also, determine the closed-loop bandwidth.

P9.20 The Bell-Boeing V-22 Osprey Tiltrotor is both an airplane and a helicopter. Its advantage is the ability to rotate its engines to a vertical position, as shown in Figure P7.33(a), for takeoffs and landings and then switch the engines to a horizontal position for cruising as an airplane. The altitude control system in the helicopter mode is shown in Figure P9.20. (a) Obtain the frequency response of the system for $K = 100$. (b) Find the gain margin and the phase margin for this system. (c) Select a suitable gain K so that the phase margin is 40°. (Decrease the gain above $K = 100$.) (d) Find the response $y(t)$ of the system for the gain selected in part (c).

P9.18 A model of an automobile driver attempting to steer a course is shown in Figure P9.18, where $K = 5.3$. (a) Find the frequency response and the gain and phase margins when the reaction time T is zero. (b) Find the phase margin when the reaction time is 0.1 s. (c) Find the reaction time that will cause the system to be borderline stable (phase margin = 0°).

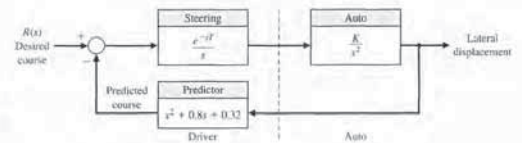


FIGURE P9.18
Automobile and driver control.



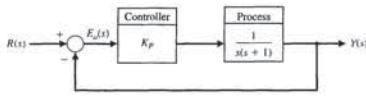
FIGURE P9.19
Waste collection system.

closed-loop system is stable. Plot the phase margin as a function of the gain $1 \leq K \leq K_{max}$. Explain what happens to the phase margin as K approaches K_{max} .

P9.28 Consider the feedback system shown in Figure P9.28 with the process transfer function given as

$$G(s) = \frac{1}{s(s+1)}$$

FIGURE P9.28
A unity feedback system with a proportional controller in the loop.



The controller is the proportional controller

$$G_c(s) = K_p$$

- (a) Determine a value of K_p such that the phase margin is approximately $P.M. = 45^\circ$.
- (b) Using the $P.M.$ obtained, predict the percent overshoot of the closed-loop system to a unit step input.
- (c) Plot the step response and compare the actual percent overshoot with the predicted percent overshoot.

ADVANCED PROBLEMS

AP9.1 Operational spacecraft undergo substantial mass property and configuration changes during their lifetime [25]. For example, the inertias change considerably during operations. Consider the orientation control system shown in Figure AP9.1.

- (a) Plot the Bode diagram, and determine the gain and phase margins when $\omega_n^2 = 15,267$.
- (b) Repeat part (a) when $\omega_n^2 = 9500$. Note the effect of changing ω_n^2 by 38%.

AP9.2 Anesthesia is used in surgery to induce unconsciousness. One problem with drug-induced unconsciousness is large differences in patient responsiveness. Furthermore, the patient response changes during an operation. A model of drug-induced anesthesia control is shown in Figure AP9.2. The proxy for unconsciousness is the arterial blood pressure.

- (a) Plot the Bode diagram and determine the gain margin and the phase margin when $T = 0.05$ s. (b) Repeat

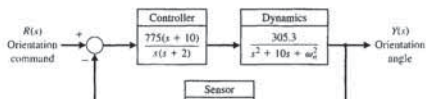


FIGURE AP9.1
Spacecraft orientation control.

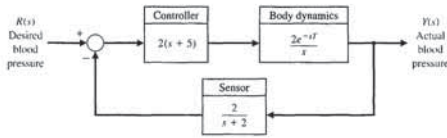


FIGURE AP9.2
Control of blood pressure with anesthesia.

P9.23 A closed-loop system has a loop transfer function

$$L(s) = G_c(s)G(s) = \frac{K}{s(s+8)(s+12)}$$

- (a) Determine the gain K so that the phase margin is 60° .
- (b) For the gain K selected in part (a), determine the gain margin of the system.

P9.24 A closed-loop system with unity feedback has a loop transfer function

$$L(s) = G_c(s)G(s) = \frac{K(s+20)}{s^2}$$

- (a) Determine the gain K so that the phase margin is 45° .
- (b) For the gain K selected in part (a), determine the gain margin.
- (c) Predict the bandwidth of the closed-loop system.

P9.25 A closed-loop system has the loop transfer function

$$L(s) = G_c(s)G(s) = \frac{K e^{-Ts}}{s}$$

- (a) Determine the gain K so that the phase margin is 60° when $T = 0.2$.
- (b) Plot the phase margin versus the time delay T for K as in part (a).

P9.26 A specialty machine shop is improving the efficiency of its surface-grinding process [21]. The existing machine is mechanically sound, but manually operated. Automating the machine will free the operator for other tasks and thus increase overall throughput of the machine shop. The grinding machine is shown in Figure P9.26(a) with all three axes automated with motors and feedback systems. The control system for the y -axis is shown in Figure P9.26(b). To achieve a low steady-state error to a ramp command, we choose $K = 10$. Sketch the Bode diagram of the open-loop system and obtain the Nichols chart plot. Determine the gain and phase margin of the system and the bandwidth of the closed-loop system. Estimate the ζ of the system and the predicted overshoot and settling time (with a 2% criterion).

P9.27 Consider the system shown in Figure P9.27. Determine the maximum value of $K = K_{max}$ for which the

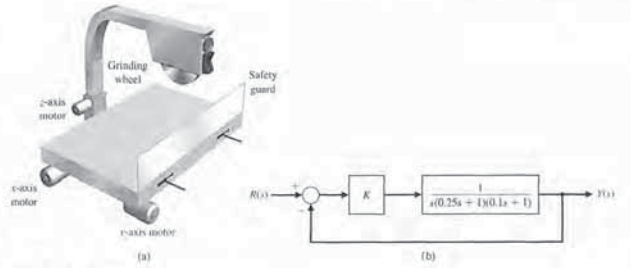


FIGURE P9.26 Surface-grinding wheel control system.

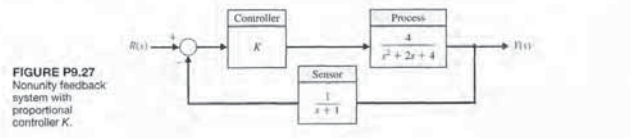


FIGURE P9.27
Nonunity feedback system with proportional controller K .

and too heavy for practical use. One solution is to eliminate the cable. The key to the cordless elevator is the linear motor technology now being applied to the development of magnetically levitated rail transportation systems. Under consideration is a linear synchronous motor that propels a passenger car along the tracklike guideway running the length of the elevator shaft. The motor works by the interaction of an electromagnetic field from electric coils on the guideway with magnets on the car [28].

If we assume that the motor has negligible friction, the system may be represented by the model shown in Figure AP9.7. Determine K so that the phase margin of the system is 45° . For the gain K selected, determine the system bandwidth. Also calculate the maximum value of the output for a unit step disturbance for the selected gain.

AP9.8 A control system is shown in Figure AP9.8. The gain K is greater than 500 and less than 3000. Select a gain that will cause the system step response to have an overshoot of less than 20%. Plot the Nichols diagram, and calculate the phase margin.

AP9.9 Consider the system shown in Figure AP7.12 which uses a PI controller. Let

$$\frac{K_I}{K_P} = 0.2,$$

and determine the gain K_P that provides the maximum phase margin.

AP9.10 A multiloop block diagram is shown in Figure AP9.10.

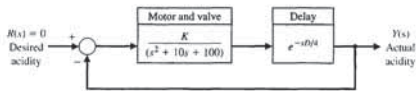


FIGURE AP9.6
Mine water acidity control.

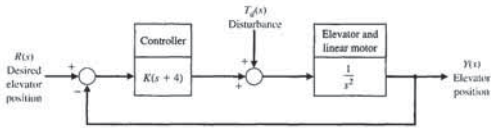


FIGURE AP9.7
Elevator position control.

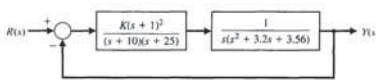


FIGURE AP9.8
Gain selection.

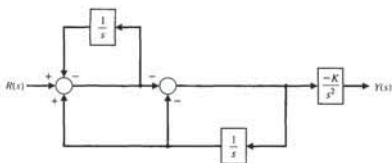


FIGURE AP9.10
Multiloop feedback control system.

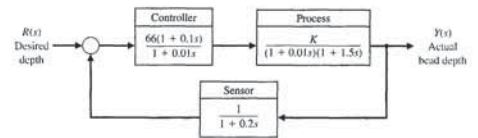


FIGURE AP9.3
Weld bead depth control.

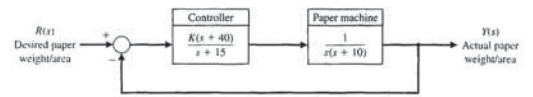


FIGURE AP9.4
Paper machine control.

- part (a) when $T = 0.1$ s. Describe the effect of the 100% increase in the time delay T .
- (c) Using the phase margin, predict the overshoot for a step input for parts (a) and (b).

AP9.3 Welding processes have been automated over the past decades. Weld quality features, such as final metallurgy and joint mechanics, typically are not measurable online for control. Therefore, some indirect way of controlling the weld quality is necessary. A comprehensive approach to in-process control of welding includes both geometric features of the bead (such as the cross-sectional features of width, depth, and height) and thermal characteristics (such as the heat-affected zone width and cooling rate). The weld bead depth, which is the key geometric attribute of a major class of welds, is very difficult to measure directly, but a method to estimate the depth using temperature measurement has been developed [26]. A model of the weld control system is shown in Figure AP9.3.

- (a) Determine the phase margin and gain margin for the system when $K = 1$.
- (b) Repeat part (a) when $K = 1.5$.
- (c) Determine the bandwidth of the system for $K = 1$ and $K = 1.5$ by using the Nichols chart.
- (d) Predict the settling time (with a 2% criterion) of a step response for $K = 1$ and $K = 1.5$.

gain. Determine the bandwidth of the closed-loop system.

AP9.5 NASA is planning many Mars missions with rover vehicles. A typical rover is a solar-powered vehicle which will see where it is going with TV cameras and will measure distance to objects with laser range finders. It will be able to climb a 30° slope in dry sand and will carry a spectrometer that can determine the chemical composition of surface rocks. It will be controlled remotely from Earth.

For the model of the position control system shown in Figure AP9.5, determine the gain K that maximizes the phase margin. Determine the overshoot for a step input with the selected gain.

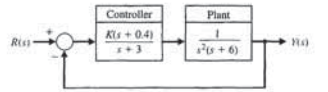


FIGURE AP9.5 Position control system of a Mars rover.

AP9.4 The control of a paper-making machine is quite complex [27]. The goal is to deposit the proper amount of fiber suspension (pulp) at the right speed and in a uniform way. Dewatering, fiber deposition, rolling, and drying then take place in sequence. Control of the paper weight per unit area is very important. For the control system shown in Figure AP9.4, select K so that the phase margin $P.M. \approx 45^\circ$ and the gain margin $G.M. \approx 10$ dB. Plot the step response for the selected

AP9.6 The acidity of water draining from a coal mine is often controlled by adding lime to the water. A valve controls the lime addition and a sensor is downstream. For the model of the system shown in Figure AP9.6, determine K and the distance D to maintain stability. We require $D > 2$ meters in order to allow full mixing before sensing.

AP9.7 Building elevators are limited to about 800 meters. Above that height, elevator cables become too thick

nominal time delay with $T = 1$ s. The goal is to achieve a step response with zero steady-state error and percent overshoot $P.O. \leq 10\%$.

Consider the controller

$$G_c(s) = \frac{5}{s(s+10)}$$

DESIGN PROBLEMS

CDP9.1 The system of Figure CDP4.1 uses a controller $G_c(s) = K_p$. Determine the value of K_p so that the phase margin is 70° . Plot the response of this system to a step input.

DP9.1 A mobile robot for toxic waste cleanup is shown in Figure DP9.1(a) [23]. The closed-loop speed control is represented by Figure 9.1 with $H(s) = 1$. The Nichols chart in Figure DP9.1(b) shows the plot of $G_c(j\omega)/K$ versus ω . The value of the frequency at the points indicated is recorded in the following table:

Point	1	2	3	4	5
ω	2	5	10	20	50

- (a) Determine the gain and phase margins of the closed-loop system when $K = 1$. (b) Determine the resonant peak in dB and the resonant frequency for $K = 1$. (c) Determine the system bandwidth and estimate the settling time (with a 2% criterion) and percent overshoot of this system for a step input. (d) Determine the appropriate gain K so that the overshoot to a step input is 30%, and estimate the settling time of the system.
- DP9.2** Flexible-joint robotic arms are constructed of lightweight materials and exhibit lightly damped open-loop dynamics [15]. A feedback control system for a flexible arm is shown in Figure DP9.2. Select K so that the system has maximum phase margin. Predict the overshoot for a step input based on the phase margin attained, and compare it to the actual overshoot for a step input. Determine the bandwidth of the closed-loop system. Predict the settling time (with a 2% criterion) of the system to a step input and compare it to the actual settling time. Discuss the suitability of this control system.
- DP9.3** An automatic drug delivery system is used in the regulation of critical care patients suffering from cardiac failure [24]. The goal is to maintain stable

patient status within narrow bounds. Consider the use of a drug delivery system for the regulation of blood pressure by the infusion of a drug. The feedback control system is shown in Figure DP9.3. Select an appropriate gain K that maintains narrow deviation for blood pressure while achieving a good dynamic response.

DP9.4 A robot tennis player is shown in Figure DP9.4(a), and a simplified control system for $\theta_2(t)$ is shown in Figure DP9.4(b). The goal of the control system is to attain the best step response while attaining a high K_p for the system. Select $K_{v1} = 0.4$ and $K_{v2} = 0.25$, and determine the phase margin, gain margin, bandwidth, percent overshoot, and settling time for each case. Obtain the step response for each case and select the best value for K .

DP9.5 An electrohydraulic actuator is used to actuate large loads for a robot manipulator, as shown in Figure DP9.5 [17]. The system is subjected to a step input, and we desire the steady-state error to be minimized. However, we wish to keep the overshoot less than 10%. Let $T = 0.8$ s.

(a) Select the gain K when $G_c(s) = K$, and determine the resulting overshoot, settling time (with a 2% criterion), and steady-state error. (b) Repeat part (a) when $G_c(s) = K_1 + K_2/s$ by selecting K_1 and K_2 . Sketch the Nichols chart for the selected gains K_1 and K_2 .

DP9.6 The physical representation of a steel strip-rolling mill is a damped-spring system [8]. The output thickness sensor is located a negligible distance from the output of the mill, and the objective is to keep the thickness as close to a reference value as possible. Any change of the input strip thickness is regarded as a disturbance. The system is a nonunity feedback system, as shown in Figure DP9.6. Depending on the maintenance of the mill, the parameter varies as $80 \leq b < 300$. Determine the phase margin and gain margin for the two extreme values of b when the normal value of

- (a) Compute the transfer function $T(s) = Y(s)/R(s)$.
- (b) Determine K such that the steady-state tracking error to a unit step input $R(s) = 1/s$ is zero. Plot the unit step response.
- (c) Using K from part (b), compute the system bandwidth ω_b .

AP9.11. Patients with a cardiological illness and less than normal heart muscle strength can benefit from an assistance device. An electric ventricular assist device (EVAD) converts electric power into blood flow by moving a pusher plate against a flexible blood sac. The pusher plate reciprocates to eject blood in systole and to allow the sac to fill in diastole. The EVAD will be implanted in tandem or in parallel with the intact natural heart as shown in Figure AP9.11(a). The EVAD is driven by rechargeable batteries, and the

electric power is transmitted inductively across the skin through a transmission system. The batteries and the transmission system limit the electric energy storage and the transmitted peak power. We desire to drive the EVAD in a fashion that minimizes its electric power consumption [33].

The EVAD has a single input, the applied motor voltage, and a single output, the blood flow rate. The control system of the EVAD performs two main tasks: It adjusts the motor voltage to drive the pusher plate through its desired stroke, and it varies the EVAD blood flow to meet the body's cardiac output demand. The blood flow controller adjusts the blood flow rate by varying the EVAD beat rate. A model of the feedback control system is shown in Figure AP9.11(b). The motor, pump, and blood sac can be modeled by a

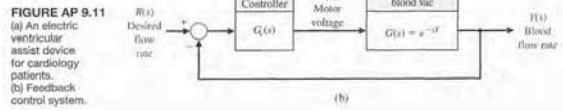
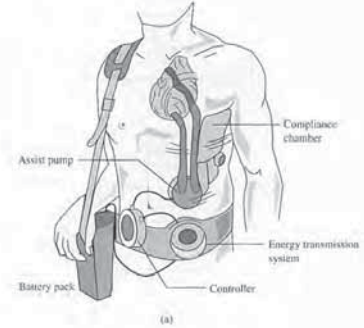


FIGURE AP 9.11 (a) An electric ventricular assist device for cardiology patients. (b) Feedback control system.

FIGURE DP9.2 Control of a flexible robot arm.

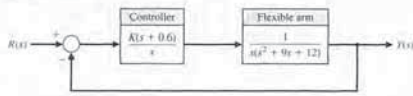


FIGURE DP9.3 Automatic drug delivery.

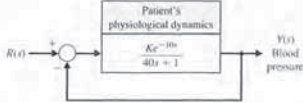


FIGURE DP9.4 (a) An articulated two-link tennis player robot. (b) Simplified control system.

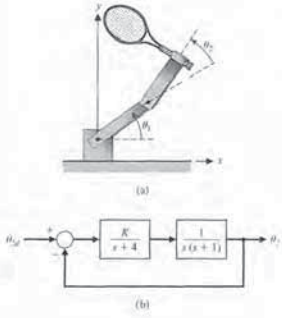


FIGURE DP9.5 Electrohydraulic actuator.

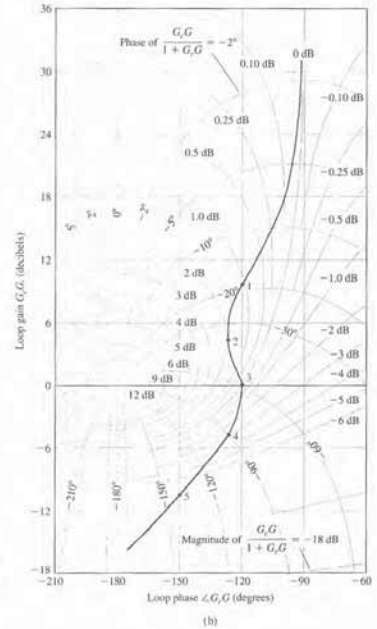
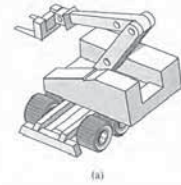
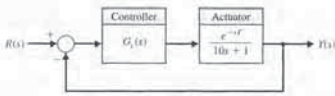


FIGURE DP9.1 (a) Mobile robot for toxic waste cleanup. (b) Nichols chart.

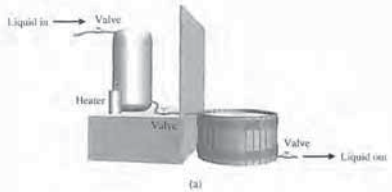


FIGURE DP9.9 Two-tank temperature control.

- (f) Prepare a table comparing the percent overshoot, settling time, and steady-state error for the designs of parts (b) through (c).
- DP9.10 Consider the system is described in state variable form by

$$\dot{x}(t) = Ax(t) + Bv(t)$$

$$y(t) = Cx(t)$$

where

$$A = \begin{bmatrix} 0 & 1 \\ 2 & 3 \end{bmatrix}, B = \begin{bmatrix} 0 \\ 1 \end{bmatrix}, C = [1 \quad 0]$$

Assume that the input is a linear combination of the states, that is,

$$v(t) = -Kx(t) + r(t)$$

where $r(t)$ is the reference input and the gain matrix is $K = [K_1 \quad K_2]$. Substituting $v(t)$ into the state variable equation yields the closed-loop system

$$\dot{x}(t) = [A - BK]x(t) + Br(t)$$

$$y(t) = Cx(t)$$

- (a) Obtain the characteristic equation associated with $A - BK$.

- (b) Design the gain matrix K to meet the following specifications: (i) the closed-loop system is stable; (ii) the system bandwidth $\omega_b \approx 1$ rad/s; and (iii) the steady-state error to a unit step input $R(s) = 1/s$ is zero.

DP9.11 The primary control loop of a nuclear power plant includes a time delay due to the need to transport the fluid from the reactor to the measurement point as shown in Figure DP9.11. The transfer function of the controller is

$$G_c(s) = K_p + \frac{K_I}{s}$$

The transfer function of the reactor and time delay is

$$G(s) = \frac{e^{-sT}}{Ts + 1}$$

where $T = 0.4$ s and $\tau = 0.2$ s. Using frequency response methods, design the controller so that the overshoot of the system is $P.O. \leq 10\%$. With this controller in the loop, estimate the percent overshoot and settling time (with a 2% criterion) to a unit step. Determine the actual overshoot and settling time and compare with the estimated values.

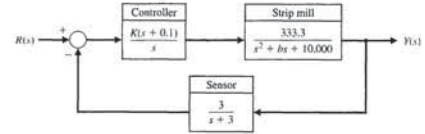


FIGURE DP9.6 Steel strip-rolling mill.

the gain is $K = 170$. Recommend a reduced value for K so that the phase margin is greater than 40° and the gain margin is greater than 8 dB for the range of b .

- DP9.7 Vehicles for lunar construction and exploration work will face conditions unlike anything found on Earth. Furthermore, they will be controlled via remote control. A block diagram of such a vehicle and the control are shown in Figure DP9.7. Select a suitable gain K when $T = 1.5$ s. The goal is to achieve a fast step response with an overshoot of less than 20%.

- DP9.8 The control of a high-speed steel-rolling mill is a challenging problem. The goal is to keep the strip thickness accurate and readily adjustable. The model of the control system is shown in Figure DP9.8. Design a control system by selecting K so that the step response of the system is as fast as possible with an overshoot less than 0.5% and a settling time (with a 2% criterion) less than 4 seconds. Use the root locus to select K , and calculate the roots for the selected K . Describe the dominant root(s) of the system.

DP9.9 A two-tank system containing a heated liquid has the model shown in Figure DP9.9(a), where T_1 is the temperature of the fluid flowing into the first tank and T_2 is the temperature of the liquid flowing

out of the second tank. The block diagram model is shown in Figure DP9.9(b). The system of the two tanks has a heater in tank 1 with a controllable heat input Q . The time constants are $\tau_1 = 10$ s and $\tau_2 = 50$ s.

- (a) Determine $T_2(s)$ in terms of $T_1(s)$ and $T_2(s)$. (b) If $T_2(s)$, the desired output temperature, is changed instantaneously from $T_2(s) = A/s$ to $T_2(s) = 2A/s$, determine the transient response of $T_2(t)$ when $G_c(s) = K/s$. Assume that, prior to the abrupt temperature change, the system is at steady state. (c) Find the steady-state error e_{ss} for the system of part (b), where $E(s) = T_2(s) - T_2(s)$. (d) Let $G_c(s) = K/s$ and repeat parts (b) and (c). Use a gain K such that the percent overshoot is less than 10%. (e) Design a controller that will result in a system with a settling time (with a 2% criterion) of $T_s < 150$ s and a percent overshoot of less than 10%, while maintaining a zero steady-state error when

$$G_c(s) = K_p + \frac{K_I}{s}$$

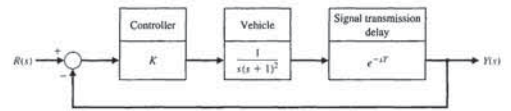


FIGURE DP9.7 Lunar vehicle control.

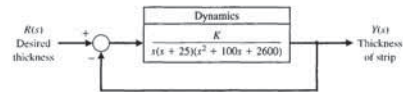


FIGURE DP9.8 Steel-rolling mill control.

FIGURE CP9.6 A feedback control system for the yaw acceleration control of a bank-to-turn missile.

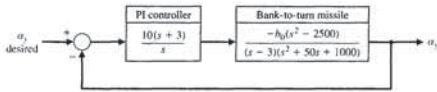
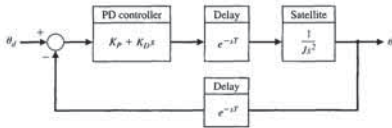


FIGURE CP9.7 A block diagram of a ground-controlled satellite.



- (a) Assume no transmission time delay (i.e., $T = 0$), and design the controller to the following specifications: (1) percent overshoot less than 20% to a unit step input and (2) time to peak less than 30 seconds.
- (b) Compute the phase margin with the controller in the loop but assuming a zero transmission time delay. Estimate the amount of allowable time delay for a stable system from the phase margin calculation.
- (c) Using a second-order Padé approximation to the time delay, determine the maximum allowable delay T_{max} for system stability by developing a m-file script that employs the padé function and computes the closed-loop system poles as a function of the time delay T . Compare your answer with the one obtained in part (b).

CP9.9 For the system in CP9.8, use the nichols function to obtain the Nichols chart and determine the phase margin and gain margin.

CP9.10 A closed-loop feedback system is shown in Figure CP9.10. (a) Obtain the Nyquist plot and determine the phase margin. Assume that the time delay $T = 0.5$ s. (b) Compute the phase margin when $T = 0.05$ s. (c) Determine the minimum time delay that destabilizes the closed-loop system.

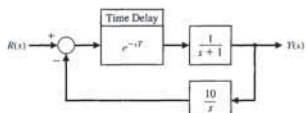


FIGURE CP9.10 Nonunity feedback system with a time delay.

CP9.8 Consider the system represented in state variable form

$$\dot{x} = \begin{bmatrix} 0 & 1 \\ -1 & -15 \end{bmatrix} x + \begin{bmatrix} 0 \\ 30 \end{bmatrix} u$$

$$y = [8 \quad 0] x + [0] u$$

Using the nyquist function, obtain the polar plot.

ANSWERS TO SKILLS CHECK

- True or False: (1) True; (2) True; (3) True; (4) True; (5) False
- Multiple Choice: (6) b; (7) a; (8) d; (9) a; (10) d; (11) b; (12) a; (13) b; (14) c; (15) a

Word Match (in order, top to bottom): f, e, k, b, j, a, i, d, h, c, g

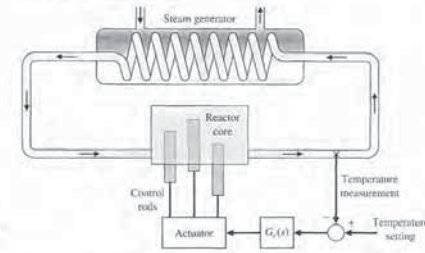


FIGURE DP9.10 Nuclear reactor control.

COMPUTER PROBLEMS

CP9.1 Consider a unity negative feedback control system with

$$L(s) = G_c(s)G(s) = \frac{141}{s^2 + 2s + 12}$$

Verify that the gain margin is ∞ and that the phase margin is 10° .

CP9.2 Using the nyquist function, obtain the polar plot for the following transfer functions:

- (a) $G(s) = \frac{5}{s + 5}$
- (b) $G(s) = \frac{50}{s^2 + 10s + 25}$
- (c) $G(s) = \frac{15}{s^3 + 3s^2 + 3s + 1}$

CP9.3 Using the nichols function, obtain the Nichols chart with a grid for the following transfer functions:

- (a) $G(s) = \frac{1}{s + 0.2}$
- (b) $G(s) = \frac{1}{s^2 + 2s + 1}$
- (c) $G(s) = \frac{6}{s^3 + 6s^2 + 11s + 6}$

Determine the approximate phase and gain margins from the Nichols charts and label the charts accordingly.

CP9.4 A negative feedback control system has the loop transfer function

$$L(s) = G_c(s)G(s) = \frac{K e^{-Ts}}{s + 12}$$

- (a) When $T = 0.2$ s, find K such that the phase margin is 40° using the margin function. (b) Obtain a plot of phase margin versus T for K as in part (a), with $0 \leq T \leq 0.3$ s.

CP9.5 Consider the paper machine control in Figure AP9.4. Develop an m-file to plot the bandwidth of the closed-loop system as K varies in the interval $1 \leq K \leq 50$.

CP9.6 A block diagram of the yaw acceleration control system for a bank-to-turn missile is shown in Figure CP9.6. The input is yaw acceleration command (in g 's), and the output is missile yaw acceleration (in g 's). The controller is specified to be a proportional, integral (PI) controller. The nominal value of b_0 is 0.5.

- (a) Using the margin function, compute the phase margin, gain margin, and system crossover frequency (0 dB), assuming the nominal value of b_0 . (b) Using the gain margin from part (a), determine the maximum value of b_0 for a stable system. Verify your answer with a Routh-Hurwitz analysis of the characteristic equation.

CP9.7 An engineering laboratory has presented a plan to operate an Earth-orbiting satellite that is to be controlled from a ground station. A block diagram of the proposed system is shown in Figure CP9.7. It takes T seconds for a signal to reach the spacecraft from the ground station and the identical delay for a return signal. The proposed ground-based controller is a proportional-derivative (PD) controller, where

$$G_c(s) = K_p + K_D s$$

TERMS AND CONCEPTS

Bandwidth The frequency at which the frequency response has declined 3 dB from its low-frequency value.

Cauchy's theorem If a contour encircles Z zeros and P poles of $F(s)$ traversing clockwise, the corresponding contour in the $F(s)$ -plane encircles the origin of the $F(s)$ -plane $N = Z - P$ times clockwise.

Closed-loop frequency response The frequency response of the closed-loop transfer function $T(j\omega)$.

Conformal mapping A contour mapping that retains the angles on the s -plane on the $F(s)$ -plane.

Contour map A contour or trajectory in one plane is mapped into another plane by a relation $F(s)$.

Gain margin The increase in the system gain when phase = -180° that will result in a marginally stable system with intersection of the $-1 + j0$ point on the Nyquist diagram.

Logarithmic (decibel) measure A measure of the gain margin defined as $20 \log_{10}(1/d)$, where $\frac{1}{d} = \frac{1}{|L(j\omega)|}$ when the phase shift is -180° .

Nichols chart A chart displaying the curves for the relationship between the open-loop and closed-loop frequency response.

Nyquist stability criterion A feedback system is stable if, and only if, the contour in the $L(s)$ -plane does not encircle the $(-1, 0)$ point when the number of poles of $L(s)$ in the right-hand s -plane is zero. If $L(s)$ has P poles in the right-hand plane, then the number of counterclockwise encirclements of the $(-1, 0)$ point must be equal to P for a stable system.

Phase margin The amount of phase shift of the $L(j\omega)$ at unity magnitude that will result in a marginally stable system with intersections of the $-1 + j0$ point on the Nyquist diagram.

Principle of the argument See Cauchy's theorem.

Time delay A time delay T , so that events occurring at time t at one point in the system occur at another point in the system at a later time $t + T$.